



**HOCHSCHULE OSNABRÜCK**  
UNIVERSITY OF APPLIED SCIENCES

**Fakultät Ingenieurwissenschaften und Informatik**

**Masterarbeit**

**über das Thema**

**Experimental and numerical analysis  
of passive cooling options  
for PV-Modules**

vorgelegt durch

Jesús Ignacio de Miguel Valencia

25 Juli 2019





**HOCHSCHULE OSNABRÜCK**  
UNIVERSITY OF APPLIED SCIENCES

**Fakultät Ingenieurwissenschaften und Informatik**  
Mechatronic Systems Engineering

## **Masterarbeit**

# **Experimental and numerical analysis of passive cooling options for PV-Modules**

Erstprüfer: Herr Prof. Dr.-Ing Markus Eck  
Zweitprüfer: Herr Prof.Dipl.-Ing. Peter Menger

Bearbeiter: Jesús Ignacio de Miguel Valencia  
Matrikelnummer: 888742

Geboren am 01.01.1994  
In: Pamplona (Spanien)

Ausgabedatum: 01.03.2019  
Abgabedatum: 25.07.2019

---

Erstprüfer

---

Master

---

Zweitprüfer

---

Eingereicht am:

Verlängerung    genehmigt    bis:





## Erklärung

Ich erkläre hiermit an Eides statt, dass ich die vorliegende Arbeit selbständig und ohne Benutzung anderer als der angegebenen Hilfsmittel angefertigt habe; die aus fremden Quellen direkt oder indirekt übernommenen Gedanken sind als solche kenntlich gemacht. Die Arbeit wurde bisher in gleicher oder ähnlicher Form keiner anderen Prüfungsbehörde vorgelegt und auch noch nicht veröffentlicht.

Ferner stimme ich zu, dass eine Software-Kopie meiner Arbeit für einen Plagiat- Test benutzt wird.

Ort, Datum:

---

---

(Unterschrift)

(Unterschrift)



# Table of Contents

ABSTRACT .....	
KEYWORDS .....	
1. Introduction .....	1
1.1. Frame and objectives of the Project .....	1
1.2. Scope and steps of the Project.....	8
2. Theoretical framework: heat transmission .....	10
2.1. Radiation .....	11
2.1.1. Calculations to adapt horizontal solar radiation to the panel tilt .....	12
2.1.2. Heat absorbed by the glass and solar cells .....	14
2.1.3. Radiation emitted by the sky .....	19
2.2. Conduction .....	19
2.3. Convection.....	20
2.3.1. Natural convection on an inclined plane .....	22
2.3.2. Forced convection on an inclined plane.....	23
2.3.3. Convection on the cooling fins .....	26
3. Description of the installation .....	27
3.1. Modules and cooling systems .....	27
3.1.1. Fins-cooled module .....	30
3.1.2. PCM-cooled module.....	31
3.2. Hardware and data collection.....	33
3.2.1. Temperature measurement .....	34
3.2.2. Solar radiation measurement .....	37
4. Optimization of the modules tilt .....	40
5. Design of the simulation model .....	43
5.1. Computing environment .....	43
5.2. Physical parameters .....	43
5.3. Model assumptions.....	46
5.4. Description of the three developed models .....	49
5.4.1. Standard module.....	49
5.4.2. Fins-cooled module .....	51
5.4.3. PCM-cooled module.....	53
5.5. Comparative study of the cooling methods.....	59

6.	Validation of the simulation model.....	64
6.1.	Source of errors in the simulation.....	64
6.2.	Comparison of the simulation output and real measurements.....	62
6.3.	Estimation of the simulation error.....	69
7.	Study of the economic viability.....	71
7.1.	Cost estimation for the three module options .....	71
7.2.	Choice of locations for the study .....	73
7.3.	Simulation results for each investment option.....	75
7.3.1.	Power generation.....	75
7.3.2.	Electricity cost .....	76
8.	Conclusions .....	79
	Bibliography .....	81

# **ABSTRACT**

This Master Thesis has been performed at Hochschule Osnabrück (Germany) on the basis of three previous projects carried out by Iñigo Cerro, Jon Ongay and Joel Höweler.

The main goal is the study of two passive cooling options for PV panels, fins and Phase Change Materials (PCM). The approach of the study is intended to achieve conclusions about their performance, as well as their economical viability, joining the calculation of annual expenditure and power generation in each case.

To this end, three numerical thermal models are built for the PV panel with and without cooling systems (fins and PCM). In this regard, a simulation program is developed in Matlab in order to calculate temperature and power generation functions, corresponding to the specified panel and input conditions (incident solar radiation, ambient temperature and wind speed).

The TSM-PD05 module is used as a reference for the study and the systems represented by the simulation models are arranged in a real scenario, as well as the required hardware for data collection. In this way, a validation of the simulation program reliability can be performed comparing simulated and real data.

Once the validation of the developed model is successful, the economical study is carried out, whose purpose is to calculate the cost of electricity for the three PV panel options and 15 chosen world locations that differ as for their input conditions.

# **KEYWORDS**

PV panel

Passive cooling system

Thermal modeling

Fins

PCM





HOCHSCHULE OSNABRÜCK  
UNIVERSITY OF APPLIED SCIENCES

## Themenblatt

Ausgabetermin des Themas für die Abschlussarbeit: 01.03.19

Für den Studierenden:

**Name:** de Miguel

**Vorname:** Jesús Ignacio

**Matrikel-Nr.:** 888742

**Studiengang:** Elektrotechnik (Master)

**Wird folgendes Thema gestellt:**

Numerical and experimental investigation of cooling methods for PV modules

**Erstprüfer(in):** Herr Prof. Dr. Markus Eck

**Zweitprüfer(in):** Herr Peter Menger

Bitte urschriftlich zurück an das

Studierendensekretariat

---

Das Thema der Abschlussarbeit wurde ausgegeben am: 01.03.19

Erklärung des Studierenden:

Ich habe zur Kenntnis genommen, dass die Abschlussarbeit in schriftlicher und elektronischer Form spätestens abzugeben ist am: **01.08.19** **August 01th, 2019**

Es ist mit den Prüfenden abzustimmen, in welcher Form und auf welchem Weg die Abgabe der elektronischen Fassung der Abschlussarbeit erfolgt. Schriftliche und elektronische Form müssen übereinstimmen.

---

Unterschrift des Prüflings





# 1. Introduction

## 1.1. Frame and objectives of the Project

Photovoltaic (PV) power is expected to play an important role in the near future of the power generation. This technology has experienced a substantial progress over the last decades, enabling it to be a competitive option in the current electricity market. Its renewable origin is not the only argument to support the use of PV panels, but it has numerous advantages in the current global framework, as for its low cost and the opportunities it offers:

- It is a renewable, clean, infinite and quiet source of energy.
- It does not need any kind of fuel.
- It requires little maintenance.
- Panels have a relatively long useful life (around 25 years) and resists adverse weather conditions.
- The plane geometry of the panels allows to integrate them into the buildings architecture, such as roofs, without taking up much useful space. This fact and their simple installation makes them suitable for an electricity grid with distributed generation, which seems to be a future trend due to its economical potential and lower grid losses in transmission.

The most remarkable barrier to overcome is the irregular availability of the generated power, which depends on the solar radiation. The logic solution to this inconvenient is the development of energy storage systems, which currently are experiencing a significant progress.

Nevertheless, the aspect which has definitely encouraged this technology is the huge and continuous costs drop of this power generation option. Thanks to the considerable recent improvements as for manufacturing and functioning, the cost of photovoltaic energy has decreased by around 75% in the last 10 years. This tendency is expected to continue in the coming years and the forecasts predict it will be the cheapest energy, as can be observed in Figure 1.1.1.

All these mentioned factors have already placed PV panels in an important position of the current electricity market and the growth of installed PV power is expected to keep steady in the near future. According to some sources, the global PV power capacity will be twice the present one in five years, as shown in Figure 1.1.2. (1)

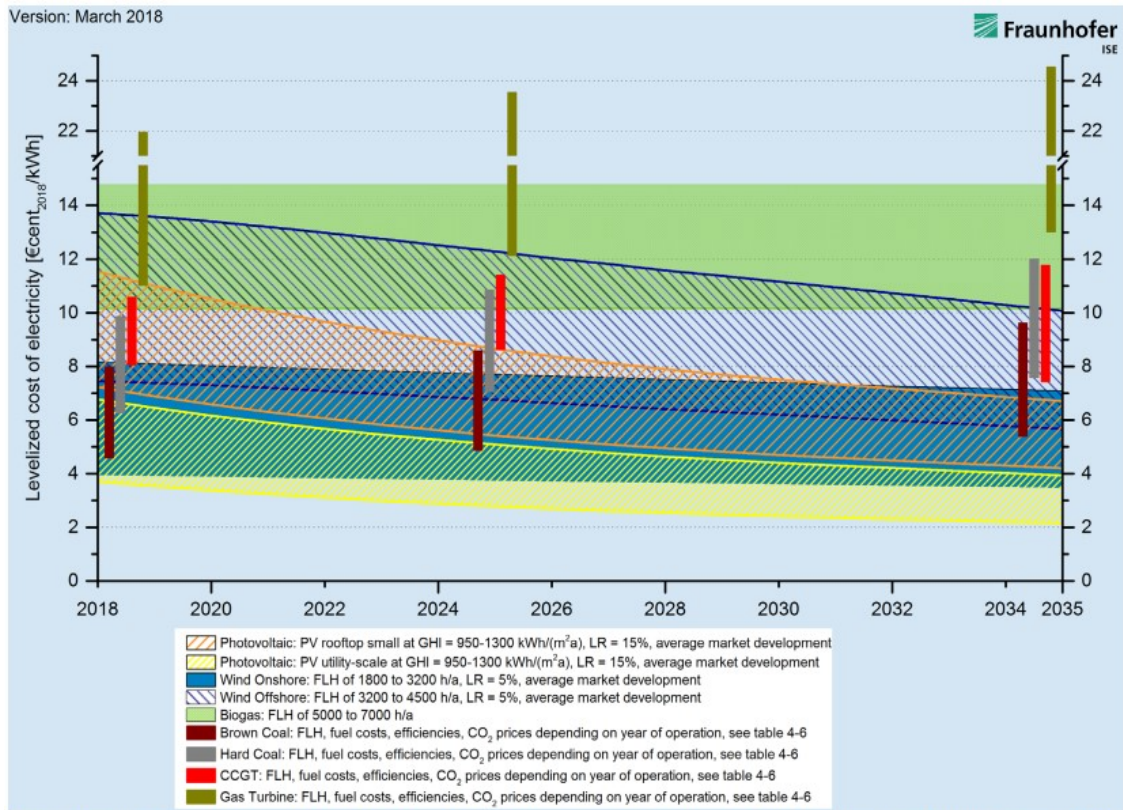
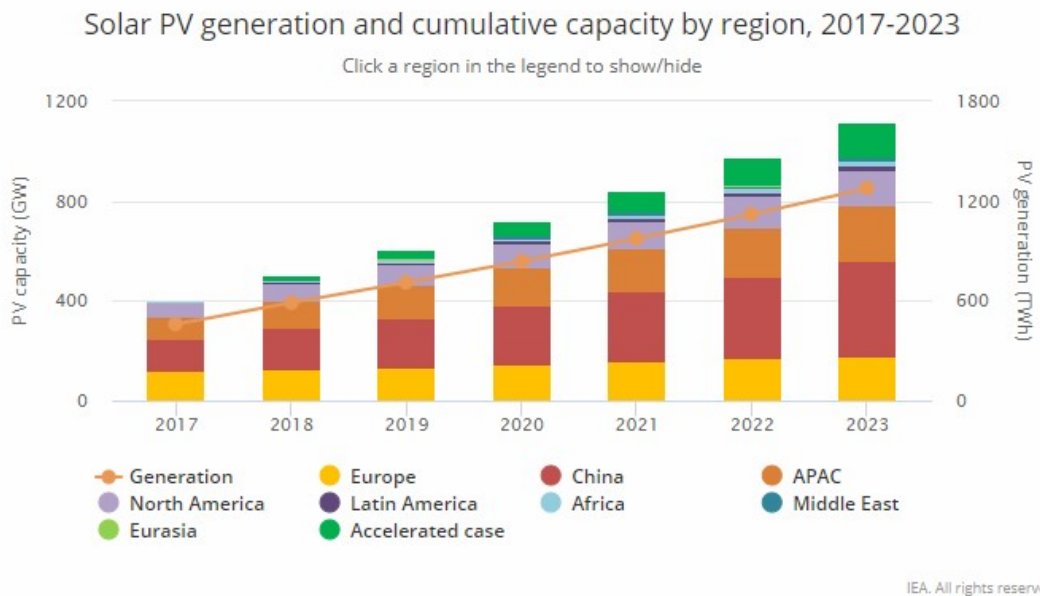


Figure 2 Learning-curve based predictions of the LCOE of renewable energy technologies and conventional power plants in Germany by 2035. Calculation parameters are listed in Tables 1 to 6. The LCOE value per reference year refers respectively to a new plant in that particular year.

Figure 1.1.1. Prediction of future electricity cost corresponding to different generation sources (1)



Source: Renewables 2018

Figure 1.1.2. Prediction of future global PV power capacity by region (2)

The presented arguments justify the efforts in the PV panels development, in order to achieve a better performance, a cost reduction and, in the end, an increasing economical viability. The low electrical efficiency of the PV generators in relation to the input energy coming from the sun through the top surface of the modules is an important weakness, which at present is the aim of numerous researches. The approach of this project is in this framework, specifically, it focuses on the existing solutions to an aspect that impacts negatively in the output efficiency of the PV panels, which is the **high cells temperature**.

However, an introduction to the photovoltaic power is necessary for a better understanding of this study. A PV panel is a type of electrical generator which converts energy coming from solar radiation, in particular from the wavelength interval around visible spectrum, into electricity. This conversion is based on **photoelectric effect**, which is a physical phenomenon whereby incident photons on a doped semiconductor material (which consists of elements of group IV of the periodic table, usually silicon, doped with elements of groups III and V), release electrons that gain enough energy for passing to the conduction band. These electrons, when a voltage is applied, are recirculated to the grid in the form of electrical power. The mentioned current and voltage are described by the **I-V characteristic curve of a PV cell**, given in Figure 1.1.3. It is required to state that a PV panel is formed by many cells wired together.

The I-V characteristic curve represents all the possible current-voltage working points (blue) of the cell under the specified irradiance and temperature conditions. The green function represents the electrical power extracted from the cell, which is the product of current and voltage, thus, it follows that a Maximum Power Point (MPP) exists. Usually, the converter coupled to the output of the PV panel, required to convert DC current to AC current for the grid, includes a Maximum Power Point Tracking (MPPT) system. This is the case of the panel used for the validation in this project, therefore, this working point is an assumption in the built model described in the following chapters.

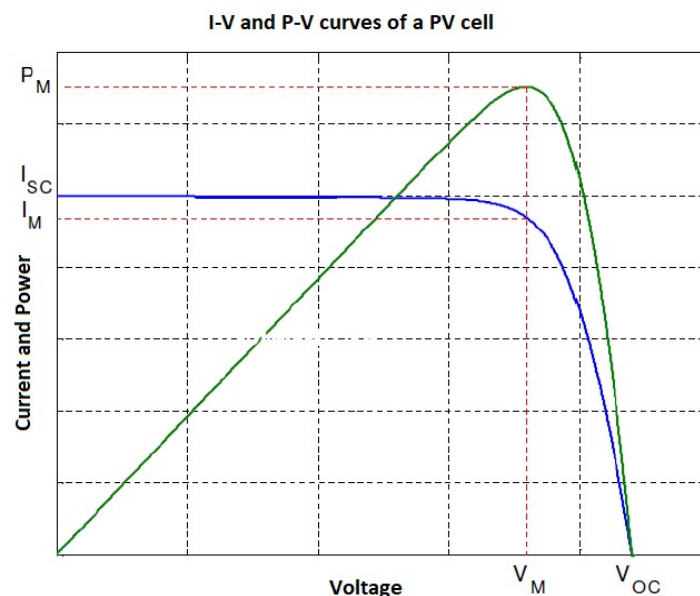


Figure 1.1.3. Current (I)-Voltage (V) characteristic curve of a PV cell

Predictably, the more incident photons, the higher the generated current, thus, the **output power grows with incident solar radiation**, as can be observed in Figure 1.1.4. But what most concerns the purpose of this project is the cells temperature impact in the characteristic curve. PV panels present an optimal working cell temperature, above which, the power drops, due to the **negative influence of the high temperatures** in the working voltages, as shown in Figure 1.1.5. Note that the highest cell temperatures are expected to coincide with the periods of highest solar radiation and, therefore, of highest power generation. This fact makes the influence of the temperature rise more negative.

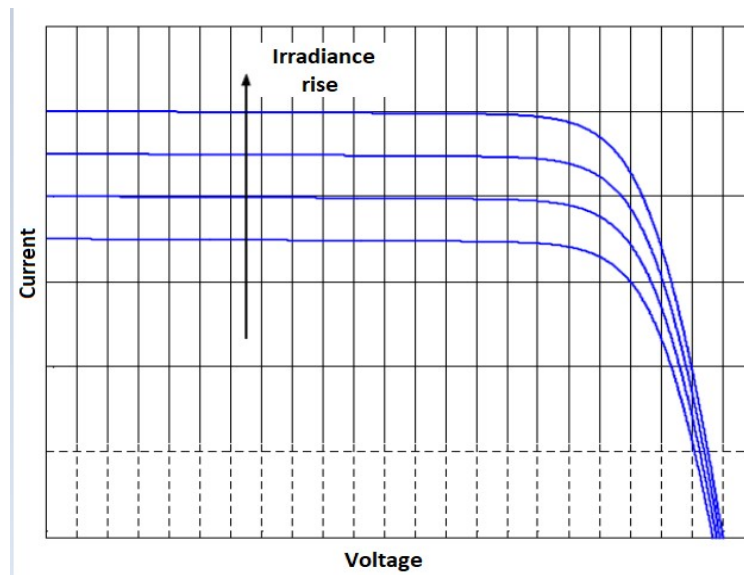


Figure 1.1.4. Impact of incident solar radiation on the I-V characteristic curve of a PV cell

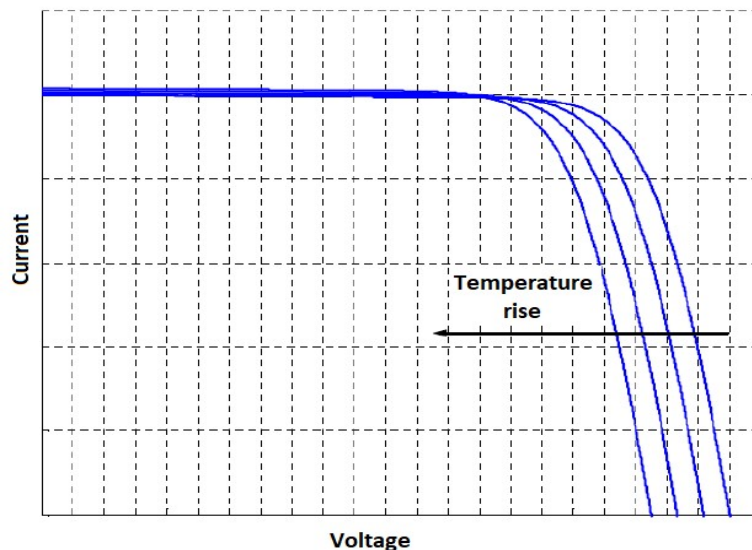


Figure 1.1.5. Impact of cell temperature on the I-V characteristic curve of a PV cell

The parameters that define the variation of short-circuit current  $I_{sc}$  and open-circuit voltage  $V_{oc}$  (see Figure 1.1.3.) with cells temperature are normally provided by the manufacturer in

the datasheet of the panel. These parameters define the variation of the characteristic curve with cells temperature.

$$\alpha = \frac{dI_{sc}}{dT} ; \beta = -\frac{dV_{oc}}{dT} \quad (1.1.1)$$

$\alpha$ : temperature coefficient of  $I_{sc}$

$\beta$ : temperature coefficient of  $V_{oc}$

The variable used in this project to test the impact of cells temperature in the output power is the **theoretical efficiency**. The theoretical efficiency of the PV panel is the ratio between the real power generation and the power generation measured in Standard Test Conditions (STC): a solar irradiance of  $1000 \text{ W/m}^2$  and a cell temperature of  $25 \text{ }^\circ\text{C}$ . The manufacturer provides the necessary parameters to calculate it for specific values of solar radiation and cell temperature. As will be explained in the following chapters, the module **TSM-PD05 of Trina Solar (3)** is used in this study to analyse the aspects which have been mentioned. For a better understanding of the temperature influence in the power generation the theoretical efficiency of the specified panel is given below, as a function of solar irradiance and cells temperature:

$$eff = \frac{P_g}{P_{g-st}} = \frac{G}{G_{st}} \cdot [1 - \gamma \cdot (T_c - T_{c-st})] = \frac{G}{1000 \text{ W/m}^2} \cdot [1 - 0.0041 \cdot (T_c - 25^\circ\text{C})] \quad (1.1.2)$$

$eff$ : theoretical electrical efficiency of the panel

$P_g$ : maximum power supply for the working conditions

$P_{g-st}$ : maximum power generation in STC

$G$ : global incident irradiance on the top of the PV panel

$G_{st}$ : irradiance in STC

$\gamma$ : coefficient of power variation as a function of cell temperature

$T_c$ : cell temperature

$T_{c-st}$ : cell temperature in STC

In Figure 1.1.6. the previous function is plotted. Note that the higher irradiance, the higher impact of temperature on the power loss.

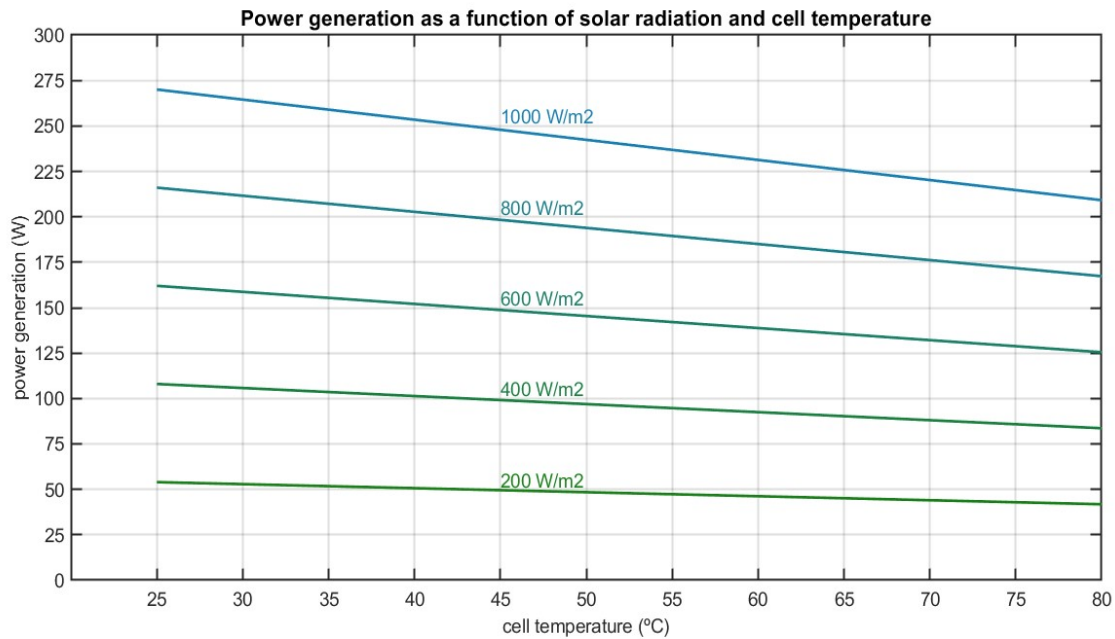


Figure 1.1.6. Variation of the output power of panel TSM-PD05 (Trina Solar) with incident irradiance and cells temperature

It must be stated that a PV panel is a device designed to capture solar radiation, which is not only converted into electricity power but, inevitably, a significant portion of it is converted into heat power, which cause a temperature rise in the material. This is due to the radiation absorption over the entire wavelength spectrum. In this regard, one important field of study is the spectral transmissivity of the solar glass on the top surface of the panel, in order to achieve a glass which reflects radiation in the non-useful wavelength range. Nevertheless, these kind of solutions are not able to completely eliminate the heat power absorption. This is why different **cooling systems** for the PV panels have appeared in recent years. The most remarkable cooling solutions are fins, forced air, water, heat pipes, Phase Change Material (PCM) cooling and thermoelectric cooling. This project focuses on the study of **cooling fins** and **PCM cooling**. Specifically, the main purpose is to analyse their economical viability in different locations around the world, where panels work under different climatic conditions.

**Cooling fins** are a widely used solution in numerous industrial and electronics applications when it is important to keep low values of temperature in some devices. It is based on increasing the fluid contact area, in this case the air, in order to enhance the convective heat flux evacuated to the ambient. There are many kinds of fins shapes, depending on the geometry of the convective surface and the fluid properties. The aluminum is a common material for the fins manufacturing, due to its high thermal conductivity and low cost. The simplicity of the fins usually makes them a cheap option.



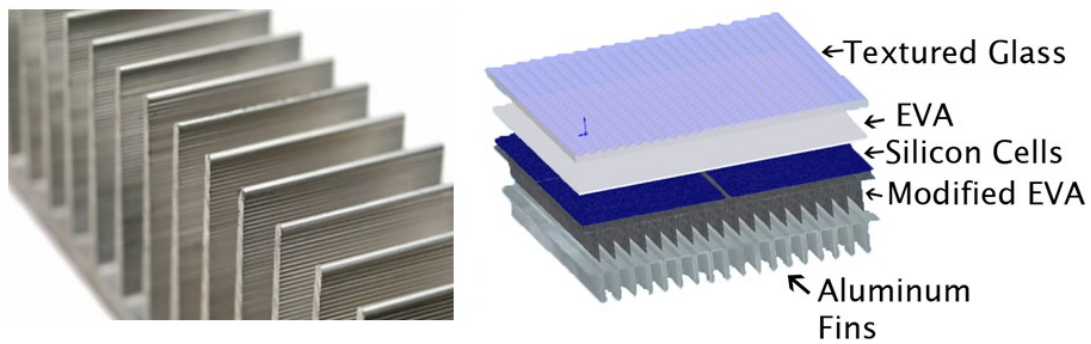


Figure 1.1.7. Cooling fins for PV panels

A **Phase Change Material (PCM)** is a substance able to store a large amount of heat in its melting interval. This is because its high value of latent heat, which allows the material absorb and release substantial amounts of heat energy without a significant temperature change in the phase change interval. This property makes PCM suitable for some cooling applications, since acts as a heat sink which delays temperature rise. The main inconvenient is that once the heat has been stored it has to be evacuated later, which also delays the temperature drop. Depending on the specific application, especially on the optimal working temperature of the device, some PCM thermal features are more desirable and an optimization study is advisable. In this respect, the melting temperature interval is an important aspect to consider.



Figure 1.1.8. Phase Change Materials (PCM) (4)

For the concepts covered in the following chapters, a brief explanation about the materials and the assembling of a PV panel is required. A complete scheme of the PV panel layers is shown in Figure 1.1.9. The **solar cells**, as explained before, are the responsible part for generating electricity but they need protection layers to ensure its integrity. Firstly, the top surface is covered by a **tempered glass**, which acts as a filter for incident radiation and as a barrier for humidity or elements that might damage the cells. Besides, there is an **Ethylene Vinyl Acetate (EVA) encapsulant layer** covering the cells, which also prevents humidity and dirt penetrating the solar panels and has a bonding function for the cells. Finally, a **back sheet layer** of a polymer material isolates the panel on the back surface.

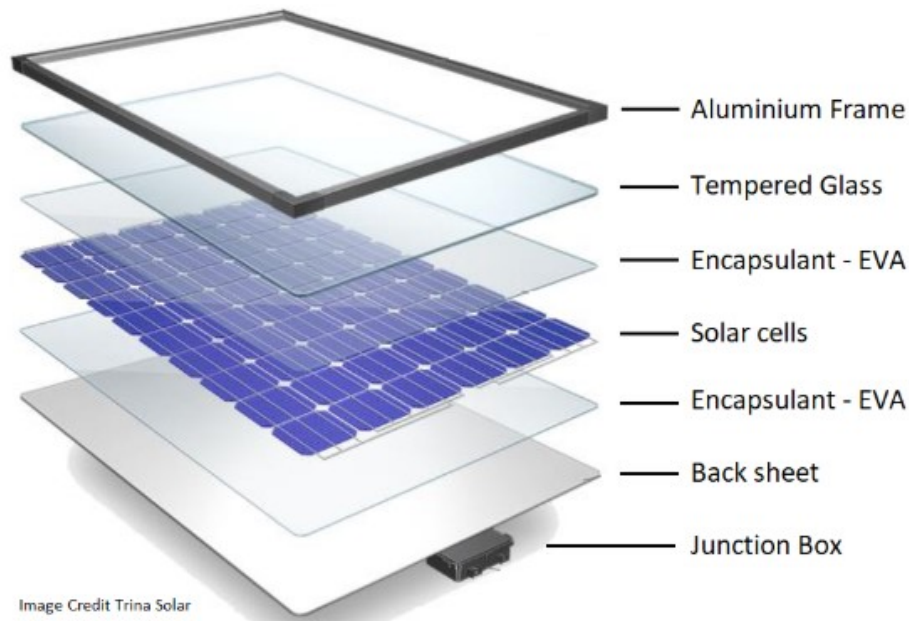


Figure 1.1.9. Scheme of the layers of a PV panel (5)

## 1.2. Scope and steps of the Project

The present project is carried out on the basis of three previous projects, performed by Iñigo Cerro (6), Jon Ongay (7) and Joel Höweler (8). The main goal of these works is to provide some conclusions about the **economical viability of PV panels cooling systems**, in particular fins and PCM cooling methods. To this end, a **simulation program** is developed, whose purpose is to calculate the **temperature function** of the PV panel layers, as well as the **output power generation**, from specified input data corresponding to **incident solar radiation, ambient temperature** and **wind speed**. The module **TSM-PD05 of Trina Solar** is used as a reference for the study. For the reliability of the simulation output, a **validation stage** is carried out by a comparative study of the temperature on the surface of **three real panels** of the mentioned model and the temperature function calculated by simulation. Each of the three panels uses a different cooling method, thus, it must be distinguished a **standard panel** (withouth a cooling system), a **fins-cooled panel** and a **PCM-cooled panel**. Once the validation stage is completed, the simulation program can be used for **input conditions of different locations around the world**. In this way, the **cost of PV energy** can be estimated in each case, from the simulation output corresponding to the annual power generation and the calculated annual expenditure.

The aim of this project is to improve the built model to ensure reliable conclusions as for the economical study. All the elements of the model and the installation were revised. For this reason and for a global understanding of the whole project, a complete review of all the stages is provided in this report. In this regard, the **steps** of this work and the three previous projects are listed below:



1. Choice of a **reference model for the PV panel** (TSM-PD05) and arrangement of all the necessary elements for the **modules functioning** and the **data collection** which is required for the validation. Iñigo Cerro and Jon Ongay designed a suitable support structure for the three panels and installed the cooling systems on the back of both cooled panels. Besides, a pyranometer and four thermocouples were placed for temperature and irradiance measurements, as well as the required hardware for the data record.
2. **Simulation model building**, which includes assumptions about the used thermal concepts that are explained in chapter 2. These thermal concepts correspond to radiation absorbed, heat transmission inside the mass elements of the panels and heat dissipation to ambient by free and forced convection. In chapter 5, a detailed description of the internal functioning of the models, as for the heat transfer and numerical aspects, is provided. The chosen software for the program development is Matlab.
3. **Validation of the models** by a comparative study of real temperature measurements and simulated temperatures. For this purpose, the same real conditions of the measured samples (irradiance, ambient temperature and wind speed) are used as input data for the simulation. In chapter 6, the accuracy and the error of the simulation program is analysed, as well as the source of the observed errors.
4. **Study of the economical viability of cooling options**. In chapter 7, the economical results are exposed, which join the estimation of the installation cost in the case of each option with the simulation output corresponding to the annual power generation of the three studied panels. First, the installation cost is estimated and an approximate confidence interval is provided for the annual expenditure, considering also the useful life of the installation, the interest rate and the operational cost. Then, the developed simulation will be used for calculating the annual power generation of 15 different locations around the world. In this simulation, typical input data of each location is used. Finally, with the mentioned terms, the cost of electricity can be calculated for each case (€/KWh). In this final result, both the installation cost variability and the possible error in the simulation are considered, therefore, an approximate interval for the cost is provided in all the cases.

## 2. Theoretical framework: heat transmission

The three existing thermal methods must be taken into account in the thermal modeling of the modules: **radiation**, **conduction** and **convection**.

Firstly, the module receive energy from the **sun radiation** entering through the top surface. A portion of this input energy is transformed into electricity thanks to the photoelectric effect in the solar cells but the remaining energy is absorbed by the panel as heat.

This heat absorption in the materials cause an increase in its temperature, which can be quantified as a function of the **specific heat** and the **mass** of the material, according to the following relation:

$$\frac{dQ}{dt} = m \cdot c_p \cdot \frac{dT}{dt} \quad (2.1)$$

$dQ/dt$ : power heat balance in the element

$m$ : mass of the element

$c_p$ : specific heat of the material

$dT/dt$ : temperature variation over time

Therefore, this heat absorption results in a temperature gradient inside the module material layers, which in turn cause a heat exchange by **conduction** between the mentioned layers.

Finally, the **convection** is the main way to dissipate the heat to the ambient through the top and the back surface, in contact with the air. It is not the only way if we consider the radiation emitted by both surfaces, phenomenon which have a lower impact in this case.

For understanding the thermal models dealt with in this project it is necessary to define the concept of **thermal resistance**, which is used to draw an analogy with Ohm's Law for electric circuits:

$$\dot{Q} = \frac{T_1 - T_2}{R} \quad (2.2)$$

$\dot{Q}$ : heat power transfer between elements 1 and 2 (W)

$T_1 - T_2$ : temperature difference between elements 1 and 2 (K)

$R$ : thermal resistance between elements 1 and 2 (K/W)

As can be seen heat power plays the role of current and temperature is analogue to voltage, comparing with Ohm's Law.

## 2.1. Radiation

Electromagnetic radiation is a form of energy transmission through electromagnetic waves. There are different types of electromagnetic radiation depending on its wavelength, defined as the quotient of the wave propagation speed by its frequency:

$$\lambda = \frac{c}{\nu} \quad (2.1.1)$$

$\lambda$ : wavelength

$c$ : wave propagation speed ( $2.988 \cdot 10^8$  m/s in vacuum)

$\nu$ : wave frequency

Thermal radiation is electromagnetic radiation generated by energy transitions of particles in matter, thus all matter emits thermal radiation above 0 K. Two important differences of this physical phenomenon compared to conduction and convection are the propagation in a vacuum without attenuation and the possibility of an energy transmission between two bodies separated by a medium colder than both. The thermal radiation emitted by a body as a function of its temperature is defined by Stefan-Boltzmann law:

$$Eb(T) = \sigma \cdot T^4 \quad (2.1.2)$$

$E_b(T)$ : radiant emittance of a black surface at temperature  $T$  ( $\text{W}/\text{m}^2$ )

$\sigma$ : Stefan-Boltzmann constant ( $5.67 \cdot 10^{-8} \text{ W}/\text{m}^2 \cdot \text{K}^4$ )

$T$ : Temperature of the black surface (K)

The radiant emittance of a surface ( $E$ ) is calculated by integration of the spectral radiant emittance ( $E_{b\lambda}$ ) in the whole wavelength spectrum and it depends on the spectral emissivity ( $\epsilon$ ) of the surface when it is not an ideal black body:

$$E(T) = \int \epsilon(\lambda) \cdot E_{b\lambda} d\lambda \quad (2.1.3)$$

For the purpose of the present project the thermal radiation which has most interest is the solar irradiance, since it is the input energy used by the solar cells to generate electricity. The solar irradiance is the power per unit area received from the Sun on a specific surface.

For the validation of the model this global solar irradiance is measured on the top surface of the panels and at the same tilt angle. Nevertheless, some additional calculations are necessary in the simulations for different geographical locations because the available irradiance data corresponds to measurements on a horizontal surface and, consequently, they must be adapted to the optimal tilt for each location.

### 2.1.1.1. Calculations to adapt horizontal solar radiation to the panel tilt

At this point, it is required to define the concepts of **direct radiation**, **diffuse radiation** and **reflected radiation**.

**Direct radiation** is the fraction of solar irradiance which arrives at the Earth's surface in a straight line from the Sun.

**Diffuse radiation** is the fraction of solar irradiance which suffers scattering due to molecules or particulates in the atmosphere and reaches the surface without a defined direction. It depends on the clearness index of the sky.

**Reflected radiation** is the fraction of solar irradiance which reaches the surface after being reflected by the Earth's surface. It depends on the albedo or reflection coefficient of the surroundings of the surface which is studied.

The incident total radiation on an inclined surface is given by the relation:

$$H_T = H_B + H_D + H_R \quad (2.1.1.1)$$

$H_T$ : global radiation on a tilted surface (Wh/m<sup>2</sup>)

$H_B$ : beam radiation on a tilted surface (Wh/m<sup>2</sup>)

$H_D$ : diffuse radiation on a tilted surface (Wh/m<sup>2</sup>)

$H_R$ : reflected radiation on a tilted surface (Wh/m<sup>2</sup>)

The radiation data that is usually available in weather historic record databases and which is used for the input data of the simulation corresponds to **global radiation incident on a horizontal surface ( $H_g$ )** and **diffuse radiation incident on a horizontal surface ( $H_d$ )**. Thus, some calculations are necessary to adapt these data to the geometric position of the module top surface. In this section, a methodology is given to this end. (9) (10) (11)

The next equation shows how to calculate **tilted beam radiation ( $H_B$ )** values from the horizontal ones:

$$H_B = (H_g - H_d) \cdot R_b \quad (2.1.1.2)$$

The  $R_b$  factor is a geometric variable to convert the horizontal beam radiation measured on the Earth surface to the effective beam radiation that arrives to the PV panel top surface. Therefore, in order to calculate it any time during a year it must be written as a function of the **hour angle ( $\omega$ )** and the **Earth's declination ( $\delta$ )** for the specified **latitude ( $\phi$ )** and **module tilt ( $\beta$ )**.  $R_b$  is given by:

$$R_b = \frac{\cos \theta}{\cos \theta_z} \quad (2.1.1.3)$$

where  $\theta$  is the **incidence angle**, the angle between the beam radiation on a surface and the normal to that surface, and it is calculated as follows for fixed panels facing the South (northern hemisphere):

$$\cos \theta = \sin \delta \cdot \sin(\phi - \beta) + \cos \delta \cdot \cos(\phi - \beta) \cdot \cos \omega \quad (2.1.1.4)$$

In the case of panels facing the North (southern hemisphere):

$$\cos \theta = \sin(-\delta) \cdot \sin(-\phi - \beta) + \cos(-\delta) \cdot \cos(-\phi - \beta) \cdot \cos \omega \quad (2.1.1.5)$$

$\delta$ : Earth's declination

$\phi$ : latitude

$\beta$ : panel tilt angle with the horizontal

$\omega$ : hour angle

The **Earth's declination ( $\delta$ )** is the angle between the normal to the plane of the Earth's orbit around the Sun and the Earth rotation axis. The relation for calculating it is shown below:

$$\delta = (23.45^\circ) \cdot \sin\left(360^\circ \cdot \frac{(284 + n)}{365}\right) \quad (2.1.1.6)$$

$n$ :  $n$ th day of the year.

The **hour angle ( $\omega$ )** is the angle between the celestial meridian of the panel location and the hour circle of the Sun, measured westward from the meridian. It is given by:

$$\omega = (AST - 12) \cdot 15^\circ \quad (2.1.1.7)$$

AST: Apparent Solar Time

Note that  $\omega=0^\circ$  at noon (AST=12).

As for  $\theta_z$  is the **solar zenith angle**, calculated by:

$$\cos \theta_z = \cos \phi \cdot \cos \delta \cdot \cos \omega + \sin \phi \cdot \sin \delta \quad (2.1.1.8)$$

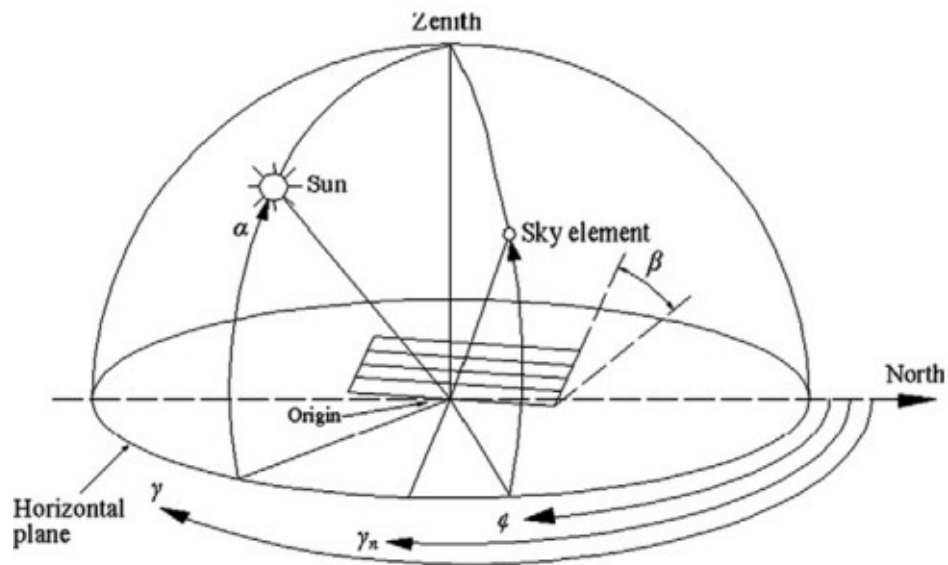


Figure 2.1.1.1. Geometric arrangement of the panel relative to the Sun position

On the other hand, the following formula is used for deducing the **reflected radiation on a tilted surface** ( $H_R$ ) from the global horizontal radiation, the ground albedo coefficient and the module tilt:

$$H_R = H_g \cdot \rho \cdot \frac{(1 - \cos \beta)}{2} \quad (2.1.1.9)$$

$\rho$ : ground albedo

For the simulation models is assumed a **ground albedo of  $\rho=0.25$** , approximately midway between asphalt and concrete.

Finally for the calculation of **diffuse radiation on a tilted surface** ( $H_D$ ) an isotropic model is assumed, which consider that the intensity of diffuse sky radiation is uniform over the sky dome. Considering that, the next relation is used:

$$H_D = \frac{1 + \cos \beta}{2} \cdot H_d \quad (2.1.1.10)$$

## 2.1.2. Heat absorbed by the glass and solar cells

Once it has been figured out the incident global radiation on the top surface of the module, the next step is to define how much of this radiation is reflected by the glass and the PV cells and how much is absorbed and, in turn, the proportion of absorbed radiation taking place in the glass and in the PV cells, considering that a part of the input radiation is transmitted through the glass. First, the concepts of **absorptivity ( $\alpha$ )**, **reflectivity ( $\rho$ )** and **transmissivity ( $\tau$ )** must be defined.

The **absorptivity** ( $\alpha$ ) is the fraction of irradiation absorbed by a surface:

$$\alpha = \frac{\text{absorbed radiation}}{\text{incident radiation}}, \quad 0 \leq \alpha \leq 1 \quad (2.1.2.1)$$

The **reflectivity** ( $\rho$ ) is the fraction of irradiation absorbed by a surface:

$$\rho = \frac{\text{absorbed radiation}}{\text{incident radiation}}, \quad 0 \leq \rho \leq 1 \quad (2.1.2.2)$$

The **transmissivity** ( $\tau$ ) is the fraction of irradiation absorbed by a surface:

$$\tau = \frac{\text{absorbed radiation}}{\text{incident radiation}}, \quad 0 \leq \tau \leq 1 \quad (2.1.2.3)$$

It is important to state that the sum of these three variables are equal to 1:

$$\alpha + \rho + \tau = 1 \quad (2.1.2.4)$$

The presented variables are obtained as a result of the integration in the wavelength spectrum of the analogous spectral variables ( $\alpha_\lambda, \rho_\lambda, \tau_\lambda$ ), so the general rule for a given wavelength ( $\lambda$ ) interval is as follows:

$$\alpha = \frac{\int_{\lambda_1}^{\lambda_2} \alpha_\lambda \cdot G_\lambda d\lambda}{\int_{\lambda_1}^{\lambda_2} G_\lambda d\lambda}, \quad \rho = \frac{\int_{\lambda_1}^{\lambda_2} \rho_\lambda \cdot G_\lambda d\lambda}{\int_{\lambda_1}^{\lambda_2} G_\lambda d\lambda}, \quad \tau = \frac{\int_{\lambda_1}^{\lambda_2} \tau_\lambda \cdot G_\lambda d\lambda}{\int_{\lambda_1}^{\lambda_2} G_\lambda d\lambda} \quad (2.1.2.5)$$

$G_\lambda$ : incident spectral radiation ( $\text{W}/\text{m}^2$ )

Note that the relation (2.1.2.4) can be applied in an infinitesimal wavelength interval, thus:

$$\alpha_\lambda + \rho_\lambda + \tau_\lambda = 1 \quad (2.1.2.6)$$

Considering that the available incident radiation data used in the simulation are total values integrated over the entire spectrum, their spectral distribution is unknown. For this reason, it is assumed that the total absorptivity, reflectivity and transmissivity are the same as if they were applied to the coming radiation from a black body at the Sun temperature (5778 K). This assumption does not differ much from the reality, since the form of the typical function of the spectral solar irradiation is similar to the black body function, as can be seen in Figure 2.1.2.1.

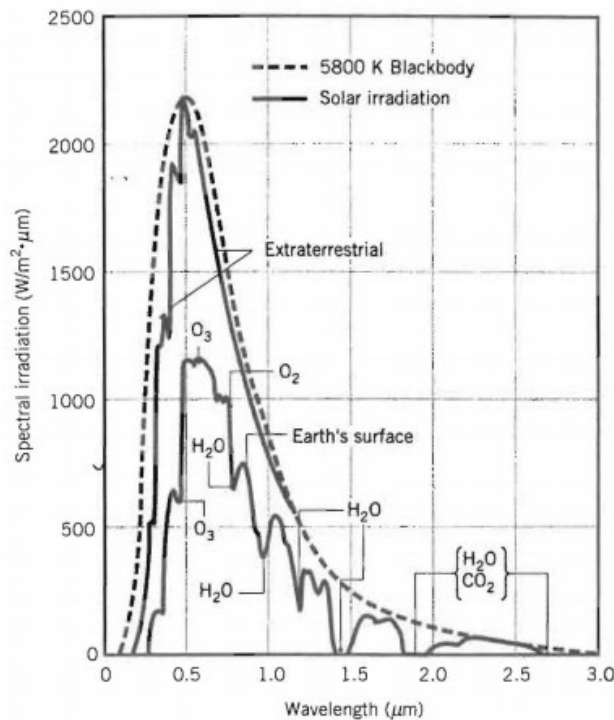


Figure 2.1.2.1. Typical spectral solar irradiation compared to the irradiation from a black body at the Sun temperature (5800 K) (12)

This last assumption allows to apply **Wien's displacement Law**, which states that the peak wavelength of the black body radiation curve can be calculated from the following relation:

$$\lambda_{max} \cdot T_{black\ body} = 2897.8\ \mu m \cdot K \quad (2.1.2.7)$$

$\lambda_{max}$ : peak black body radiation wavelength

$T_{black\ body}$ : black body temperature

This means that the black body radiation curve for a particular Temperature (T) keeps the same proportion in the wavelength emission interval (Figure 2.1.2.2.), which in turn, for a specified wavelength ( $\lambda$ ), knowing the product  $\lambda \cdot T$ , allows to calculate the **black body radiation function ( $f_\lambda$ )**, since their values are tabulated, as shown in Figure 2.1.2.3.

$$f_\lambda = \frac{\int_0^\lambda E_{b\lambda}(\lambda, T) d\lambda}{\sigma \cdot T^4} \quad (2.1.2.8)$$

$E_{b\lambda}(\lambda, T)$ : black body spectral radiation for the temperature T and the wavelength  $\lambda$



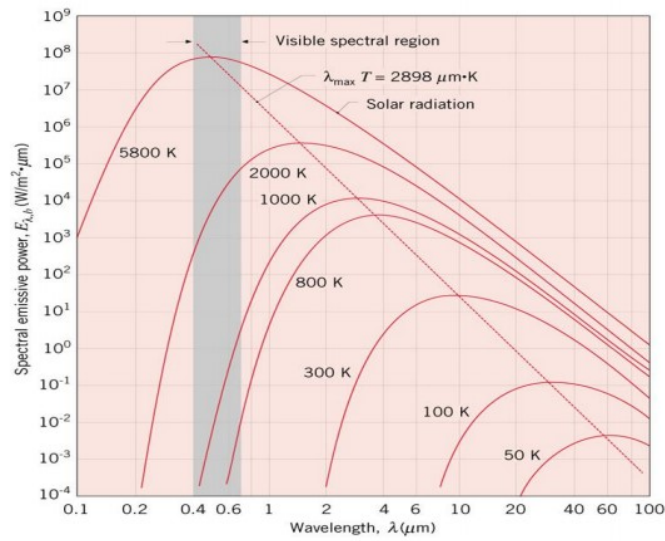


Figure 2.1.2.2. Spectral emissive blackbody power as a function of temperature (13)

$\lambda T,$ $\mu\text{m} \cdot \text{K}$	$f_{0\lambda}(T)$	$\lambda T,$ $\mu\text{m} \cdot \text{K}$	$f_{0\lambda}(T)$	$\lambda T,$ $\mu\text{m} \cdot \text{K}$	$f_{0\lambda}(T)$	$\lambda T,$ $\mu\text{m} \cdot \text{K}$	$f_{0\lambda}(T)$
555.6	0.00000	3,111.1	0.29825	5,777.8	0.71806	8,333.3	0.86880
666.7	0.00000	3,222.2	0.32300	5,888.9	0.72813	8,888.9	0.88677
777.8	0.00000	3,333.3	0.34734	6,000.0	0.73777	9,444.4	0.90168
888.9	0.00007	3,444.4	0.37118	6,111.1	0.74700	10,000.0	0.91414
1,000.0	0.00032	3,555.6	0.39445	6,222.2	0.75583	10,555.6	0.92462
1,111.1	0.00101	3,666.7	0.41708	6,333.3	0.76429	11,111.1	0.93349
1,222.2	0.00252	3,777.8	0.43905	6,444.4	0.77238	11,666.7	0.94104
1,333.3	0.00531	3,888.9	0.46031	6,555.6	0.78014	12,222.2	0.94751
1,444.4	0.00983	4,000.0	0.48085	6,666.7	0.78757	12,777.8	0.95307
1,555.6	0.01643	4,111.1	0.50066	6,777.8	0.79469	13,333.3	0.95788
1,666.7	0.02537	4,222.2	0.51974	6,888.9	0.80152	13,888.9	0.96207
1,777.8	0.03677	4,333.3	0.53809	7,000.0	0.80806	14,444.4	0.96572
1,888.9	0.05059	4,444.4	0.55573	7,111.1	0.81433	15,000.0	0.96892
2,000.0	0.06672	4,555.6	0.57267	7,222.2	0.82035	15,555.6	0.97174
2,111.1	0.08496	4,666.7	0.58891	7,333.3	0.82612	16,111.1	0.97423
2,222.2	0.10503	4,777.8	0.60449	7,444.4	0.83166	16,666.7	0.97644
2,333.3	0.12665	4,888.9	0.61941	7,555.6	0.83698	22,222.2	0.98915
2,444.4	0.14953	5,000.0	0.63371	7,666.7	0.84209	27,777.8	0.99414
2,555.6	0.17337	5,111.1	0.64740	7,777.8	0.84699	33,333.3	0.99649
2,666.7	0.19789	5,222.2	0.66051	7,888.9	0.85171	38,888.9	0.99773
2,777.8	0.22285	5,333.3	0.67305	8,000.0	0.85624	44,444.4	0.99845
2,888.9	0.24803	5,444.4	0.68506	8,111.1	0.86059	50,000.0	0.99889
3,000.0	0.27322	5,555.6	0.69655	8,222.2	0.86477	55,555.6	0.99918
		5,666.7	0.70754			$\infty$	1.00000

Figure 2.1.2.3. Tabulated blackbody radiation function ( $f_{\lambda}$ ) over the spectrum, as a function of the product of wavelength ( $\lambda$ ) and blackbody temperature ( $T$ )

The table above allows to calculate absorptivity ( $\alpha$ ), reflectivity ( $\rho$ ) and transmissivity ( $\tau$ ) by a discrete integration using the relations (2.1.2.5). If the spectral values of these variables are approximately constant in adjacent intervals of the spectrum ( $\lambda_i - \lambda_{i+1}$ ), discrete integration can be performed as follows:

$$\alpha = \alpha_0 \cdot f_{\lambda_1} + \alpha_1 \cdot (f_{\lambda_2} - f_{\lambda_1}) + \dots + \alpha_{n-1} \cdot (f_{\lambda_n} - f_{\lambda_{n-1}}) + \alpha_n \cdot (1 - f_{\lambda_n}) \quad (2.1.2.9)$$

$$\rho = \rho_0 \cdot f_{\lambda_1} + \rho_1 \cdot (f_{\lambda_2} - f_{\lambda_1}) + \dots + \rho_{n-1} \cdot (f_{\lambda_n} - f_{\lambda_{n-1}}) + \rho_n \cdot (1 - f_{\lambda_n}) \quad (2.1.2.10)$$

$$\tau = \tau_0 \cdot f_{\lambda_1} + \tau_1 \cdot (f_{\lambda_2} - f_{\lambda_1}) + \dots + \tau_{n-1} \cdot (f_{\lambda_n} - f_{\lambda_{n-1}}) + \tau_n \cdot (1 - f_{\lambda_n}) \quad (2.1.2.11)$$

For the purpose of this project, an approximate function is calculated for the spectral absorptivity, reflectivity and transmissivity of the glass+EVA layer and the PV cells layer, by considering constant values of the variables in discrete wavelength intervals. This data is provided in the next tables:

Glass + EVA					
Wavelength interval (nm)	0-320	320-370	370-1700	1700-2250	2250-
Transmissivity	0	0	0.87	0.77	0
Absorptivity	0.97	0.07	0.08	0.07	0
Reflectivity	0.03	0.93	0.05	0.16	1

Table 2.1.2.1. Approximate spectral transmissivity, absorptivity and reflectivity of Glass+EVA layer

PV cells				
Wavelength interval (nm)	0-200	200-400	400-1100	1100-
Transmissivity	0	0	0	0.27
Absorptivity	0.68	0.6	0.74	0.2
Reflectivity	0.32	0.4	0.26	0.53

Table 2.1.2.2. Approximate spectral transmissivity, absorptivity and reflectivity of PV cells layer

Figure 2.1.2.4. shows the complete path of the radiation, starting at the input through the glass surface. In the first stage, part of the radiation is directly reflected to the atmosphere and the remaining radiation is partly transmitted to the PV cells and partly absorbed by the glass. A significant part of the portion of the radiation which is transmitted to the cells is absorbed by them but a fraction is again reflected to the glass. This last fraction is partly absorbed in the glass and partly transmitted to the atmosphere. A small remaining radiation is still reflected in the glass but it is neglected. In the end, the two variables which matters for the goal of the problem are the **absorbed radiation in the glass (13.3%)** and the **absorbed radiation in the PV cells (46.5%)**. The full code for the calculation of the shown results (see Figure 2.1.2.4.) is given in Annex 6.

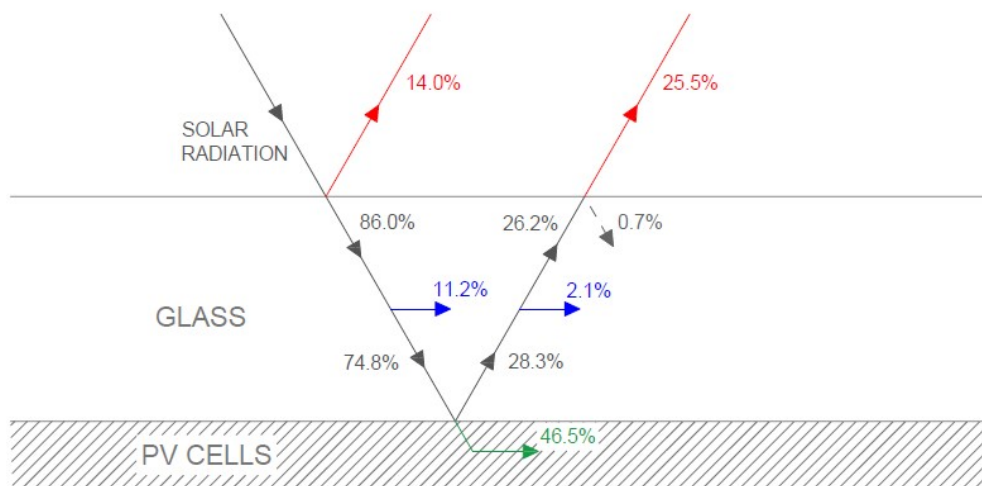


Figure 2.1.2.4. Complete path of the incoming radiation from the input through the top surface to its final target: absorbed by glass (13.3%), absorbed by PV cells (46.5%) or reflected to atmosphere (39.5%)

### 2.1.3. Radiation emitted by the sky

Suspended molecules and particles in the atmosphere also absorb and emit radiation. This is long wave emitted radiation, mainly between 5 and 8  $\mu\text{m}$  and above 13  $\mu\text{m}$ . Despite its significance is lower than the solar radiation it is convenient to include it in the total irradiance calculation. The models normally applied for the estimation of this long wave radiation use a fictitious temperature which is called **effective sky temperature ( $T_{\text{sky}}$ )**. It represents the temperature that emits the equivalent amount of energy radiation and it is calculated as follows:

$$T_{\text{sky}} = 0.0552 \cdot (T_{\text{amb}})^{1.5} \quad (2.1.3.1)$$

$T_{\text{amb}}$ : ambient temperature

Some authors recommend using the next relation for the radiation heat emission to the plane, instead of the general equation (14):

$$Q_{\text{rad sky-plane}} = \sigma \cdot \varepsilon_{\text{plane}} \cdot (T_{\text{sky}}^2 + T_{\text{surf}}^2) \cdot (T_{\text{sky}} + T_{\text{surf}}) \cdot (T_{\text{sky}} - T_{\text{surf}}) \quad (2.1.3.2)$$

$T_{\text{surf}}$ : temperature of the plane surface

$\varepsilon_{\text{plane}}$ : emissivity of the plane surface

## 2.2. Conduction

Conduction is the heat transfer mechanism inside a solid, liquid or gas material whereby most energetic particles transfer energy to the adjacent least energetic particles. This mechanism only needs a material medium and it is quantified by the following equation:

$$\frac{dQ_{\text{cond}}}{dt} = -k \cdot A \cdot \frac{dT}{dx} \quad (2.2.1)$$

$dQ_{\text{cond}}/dt$ : power heat exchange by conduction

$k$ : thermal conductivity of the material

$A$ : section normal to the power heat direction (x)

$dT/dx$ : temperature gradient in the x-direction

It is important to state that thermal conduction improves with a higher thermal conductivity, a larger section and a shorter length in the flux direction. According to the previous equation and following the electrical analogy, conductive thermal resistance is given by:

$$R_{cond} = \frac{L}{k \cdot A} \quad (2.2.2)$$

$R_{cond}$ : conductive thermal resistance

### 2.3. Convection

The heat transmission by convection appears when a moving fluid is in contact with a surface with which it exchanges heat. The movement of the mass particles promotes higher temperature differences between that particles and the surface and, therefore, improves the heat transmission. There are many factors that influence convection, especially the physical properties of the fluid (density, viscosity, thermal conductivity...), the fluid speed and geometric characteristics of the surface.

This form of heat transmission obeys Newton's law of cooling:

$$\frac{dQ_{conv}}{dt} = h \cdot A_s \cdot (T_s - T_\infty) \quad (2.3.1)$$

$dQ_{conv}/dt$ : power heat exchange by convection

$h$ : heat transfer coefficient of the convection process

$A_s$ : area in contact with the fluid

$T_s$ : temperature of the surface

$T_\infty$ : temperature of the fluid enough away from the fluid

The heat transfer coefficient by convection ( $h$ ) can be defined as the heat transfer speed between a solid surface and a fluid, per unit of surface area and per unit of temperature difference. The key for solving a convection problem is to figure out the  $h$  coefficient, which always depends on the fluid properties for system conditions. The present project only deal with air convection on the top and on the back surface of the panel and the heat transfer coefficient is calculated as a function of ambient temperature and the surface temperature, since they are the only significant variables in this case. Hence, other variables such as humidity or pressure are neglected. The temperature used to extract  $h$  of the table of dry air at atmospheric pressure (15) is calculated as follows:

$$T = \frac{T_s + T_\infty}{2} \quad (2.3.2)$$

The resolution method for any convection problem is based on calculating the Nusselt number, a dimensionless number which depends on the conditions of the fluid (temperature, pressure...) and on the geometry of the system. Nusselt number is calculated, in turn, as a function of other common dimensionless problems, as Prandtl, Grashof, Rayleigh or, in the case of forced convection, Reynolds. This last number includes the effect of the fluid speed. How the mentioned variables are related depends on the geometry of the specific problem. There is an extensive literature in this regard. The heat transfer coefficient is always calculated from the Nusselt number with the following relation:

$$Nu_L = \frac{h}{k} \cdot L \quad (2.3.3)$$

$h$ : heat transfer coefficient by convection

$k$ : thermal conductivity of the fluid

$L$ : characteristic length

It is required to distinguish two types of convection. On the one hand, **natural or free convection** occurs when the fluid motion is not generated by any external source, but by density gradients within the fluid volume. On the other hand, in **forced convection** the fluid motion is generated by an external source, such as a pump, a fan or, in the case of this project, the wind.

As explained later, with regard to this project, a distinction must be made between convection on the top of the panel and convection on the back of the panel. On both sides, natural convection is considered, but the wind only has a significant effect on the top, which implies that on this side a combined natural and forced convection occurs. The Nusselt number for a surface where there is a superimposed free and forced convection is calculated as following (16):

$$Nu = \sqrt[3]{Nu_{forced}^3 + Nu_{free}^3} \quad (2.3.4)$$

$Nu_{forced}$ : Nusselt number due to forced convection

$Nu_{free}$ : Nusselt number due to free convection

For a better understanding of the modeling, the formula to calculate the thermal resistance of the convective surface with the air is given by:

$$R_{conv} = \frac{1}{h \cdot A_s} \quad (2.3.5)$$

$R_{conv}$ : convective thermal resistance

### 2.3.1. Natural convection on an inclined plane

The natural convection problem on an inclined surface is solved by using the problem on a vertical surface as a starting point and making some modifications. For values of Rayleigh number between  $10^{-1}$  and  $10^{12}$ , the Nusselt number for natural convection on a vertical surface is defined by (16):

$$Nu = \{0.825 + 0.387 \cdot [Ra \cdot f_1(Pr)]^{1/6}\}^2 \quad (2.3.1.1)$$

$$f_1(Pr) = \left[1 + \left(\frac{0.492}{Pr}\right)^{9/16}\right]^{-16/9} \quad (2.3.1.2)$$

Nu: Nusselt number

Ra: Rayleigh number

Pr: Prandtl number

Rayleigh number is obtained by multiplying Prandtl number by Grashof number:

$$Ra = Pr \cdot Gr = Pr \cdot \frac{g \cdot \beta \cdot (T_s - T_\infty) \cdot L^3}{\nu^2} \quad (2.3.1.3)$$

Gr: Grashof number

g: acceleration due to Earth's gravity

$\beta$ : coefficient of thermal expansion, calculated as  $1/T$  (T in Kelvin)

$T_s$ : surface temperature

$T_\infty$ : ambient temperature

L: vertical length

$\nu$ : kinematic viscosity

A distinction must be made for the laminar and the turbulent case, which is determined by Rayleigh number (Ra). The upper limit  $Ra_c$  for the laminar range is given by (16):

$$Ra_c = 10^{(8.9 - \frac{\pi}{180} \cdot \alpha \cdot 1.82)} \quad (2.3.1.4)$$

$\alpha$ : angle of inclination to the vertical in ( $^\circ$ )

In the case of being in the laminar range, equation (2.3.1.1) is used, but the term Ra is replaced with  $Ra_\alpha$  (16):

$$Ra_\alpha = Ra \cdot \cos \alpha \quad (2.3.1.5)$$

However, in the turbulent range a new equation must be used (16):

$$Nu = 0.56 \cdot (Ra_c \cdot \cos \alpha)^{1/4} + 0.13 \cdot (Ra^{1/3} - Ra_c^{1/3}) \quad (2.3.1.6)$$

### 2.3.2. Forced convection on an inclined plane

In the present project it is impossible to avoid some uncertainty in the calculation of the forced convection impact, since the particularities of the surroundings in the hypothetical simulation emplacements are unknown and the wind direction is an uncontrolled variable. This variable is not considered because, anyway, its impact is changeable, depending on the elements of the surroundings.

Thus, some assumptions must be done to develop an approximate modeling. First, the wind effect on the back surface of the panel is neglected, considering that, usually, the panel frame, the arrangement of the installation and the own panel act as a barrier to the wind. As for the top surface of the panel, both natural convection and forced convection impact on the heat transfer. For the calculation of the heat transfer coefficient corresponding to forced convection, the following equation is used for the Nusselt number estimation as a function of the angle of attack (angle between flat plane surface and incoming uniform flow) (17):

$$Nu_L(\alpha) = A_f(\alpha) \cdot 1.2 \cdot (Re_L \cdot Pr)^{0.5} \quad (2.3.2.1)$$

$$A_f(\alpha) = \frac{1 + 1.36 \cdot m^{0.88}}{1 + m^{0.99}} \cdot (1 + m)^{-0.5} \quad ; \quad m = \frac{\alpha}{180^\circ - \alpha} \quad (2.3.2.2)$$

$Nu_L$ : Nusselt number

$Re_L$ : Reynolds number

Pr: Prandtl number

$\alpha$ : wind angle of attack to the plane

For this calculation, Prandtl number and kinematic viscosity are also required, which are drawn from dry air tables, as a function of the temperature (2.3.2). Besides, Reynolds number depends on the wind speed:

$$Re_L = \frac{u \cdot L}{\nu} \quad (2.3.2.3)$$

$u$ : wind speed

$L$ : characteristic length

$\nu$ : kinematic viscosity of the air

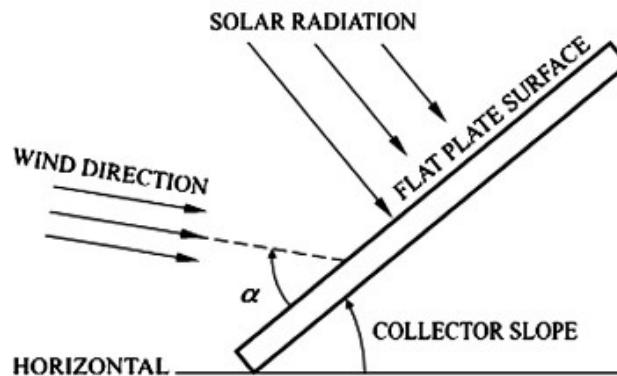


Figure 2.3.2.1. Wind angle of attack ( $\alpha$ ): angle between wind direction and flat plate surface (vertical component of the wind flow is neglected) (17)

Despite the simplicity of the presented equations, the calculation of the wind angle of attack is not a trivial matter, since it is too complicated to include its behavior in this project, as mentioned before. Note that the angle of attack depends on the panel tilt, which is a fixed value, but also on the wind direction, whose value is unknown in this case.

The proposed simplified solution is to consider a **mean angle of attack**, assuming the wind flows the same time in any direction. For this purpose, an integration over the wind direction interval must be performed. In order to simplify the analysis, vertical component of wind speed is neglected. For a better understanding, a scheme of the geometric arrangement of the elements is provided in Figure 2.3.2.2. It should be noted that, as is shown, when the wind flows against the back of the panel does not cause a forced convection on the top, therefore, Reynolds number is null in this case for the proposed equations. Following the assumption of considering the **mean impact of the wind** over the entire wind direction range, Reynolds number is divided by 2. According to the previous comments, the following equations are used:



$$\alpha_{MEAN} = \frac{1}{\pi} \int_{\frac{\pi}{2}}^{\frac{3\pi}{2}} \left( \arccos(\cos(\varphi) \cdot \sin(\beta)) - \frac{\pi}{2} \right) d\varphi \quad (2.3.2.4)$$

$$Re_{L-MEAN} = \frac{Re_L}{2}$$

$$Nu_{L-MEA}(\alpha) = A_f(\alpha_{MEAN}) \cdot 1.2 \cdot (Re_{L-MEAN} \cdot Pr)^{0.5} \quad (2.3.2.5)$$

$\alpha_{MEAN}$ : mean angle of attack

$\varphi$ : wind direction

$\beta$ : panel tilt angle

$Re_{L-MEA}$  : mean Reynolds number

$Nu_{L-MEAN}$ : mean Nusselt number

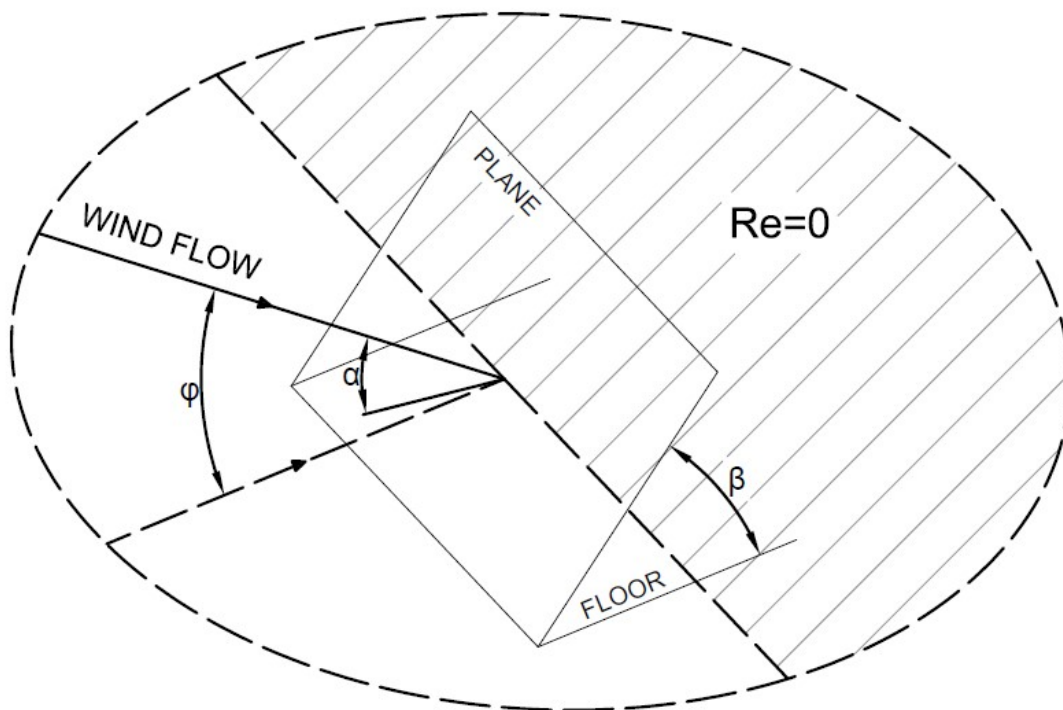


Figure 2.3.2.2. Scheme of the wind impact on the panel, depending on the wind direction ( $\varphi$ ), which in turn determine the wind angle of attack ( $\alpha$ )

### 2.3.3. Convection on the cooling fins

According to formula (2.3.5), in order to reduce the convective thermal resistance of a surface that dissipates heat, fins cooling methods seek to increase the contact area with the fluid ( $A_s$ ). In this project rectangular fins are used for testing their dissipation performance on a PV module.

Below is shown the rectangular cooling fin formula used in the model for simulating its convective thermal resistance. This formula is calculated by integration along the fin length of the heating balance in an infinitesimal volume, considering the temperature in the transverse section constant.

$$R_{conv\ fin} = \frac{1}{\tanh(a \cdot L) \sqrt{h \cdot p \cdot k \cdot A_c}} \quad (2.3.3.1)$$

$$a = \sqrt{\frac{h \cdot p}{k \cdot A_c}} \quad (2.3.3.2)$$

$R_{conv\ fin}$ : convective thermal resistance of the fins

$L$ : length of the fin

$p$ : perimeter of the fin

$k$ : thermal conductivity of the fin material

$A_c$ : cross section area of the fin

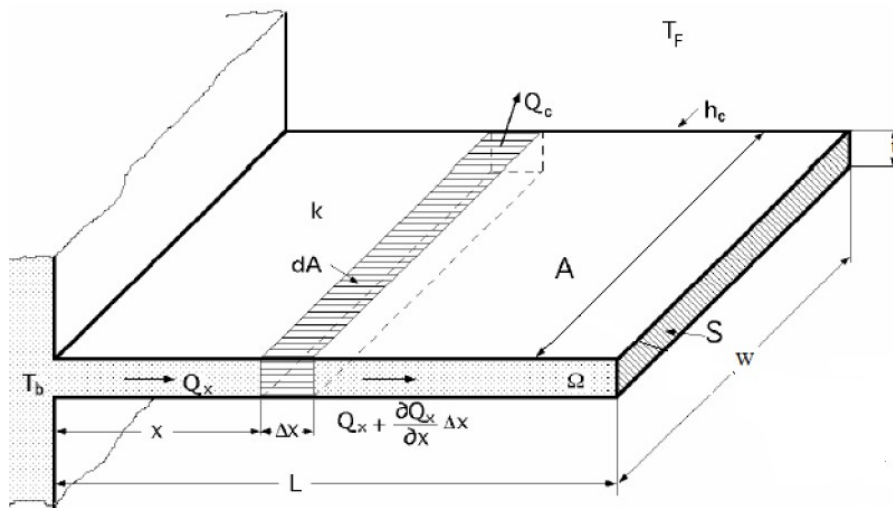


Figure 2.3.3.1. Thermal modeling of the heat transfer in a cooling fin

### 3. Description of the installation

The present chapter shows a description of the installation arranged for validating the designed simulation models by taking real measurements to compare with the simulated values. As explained in the introduction, the main purpose of this project is to study the performance of two cooling methods for PV panels: fins and a Phase Change Material (PCM). For this reason, three different type of panels were installed according to their cooling systems:

- **A standard PV panel without any cooling system**
- **A fins cooled PV panel**
- **A PCM cooled PV panel**

On the other hand, for the input data of the simulation program used for the validation, some data is necessary. Specifically, the next four variables are measured at the panels emplacement:

- **Temperature of the modules** ( $^{\circ}\text{C}$ ), measured using thermocouples on the back cover of them. This back temperature will be compared with the output back temperature of the simulation, for the ambient temperature, wind and radiation real input data of the specified day.
- **Ambient temperature** ( $^{\circ}\text{C}$ ) at the modules placement, measured every 5 minutes and obtained from a historical database record.
- **Solar global irradiation** ( $\text{W}/\text{m}^2$ ) measured by a pyranometer on the plane of the modules.
- **Wind speed** ( $\text{m}/\text{s}$ ), measured by an anemometer every 5 minutes and obtained from a historical database record.

#### 3.1. Modules and cooling systems

The installation is located at Hochschule Osnabrück (Germany), on the roof of a building, as can be seen in the Figure 3.1.1. It is important to state that they were installed facing the South, since they are located in the northern hemisphere and do not have a solar tracking system. The chosen model for the three arranged PV panels is the TSM-PD05 of Trina Solar, a multicrystalline module of a maximum power of 270 W. In the Annex 4 its detailed characteristics are given. The solar microinverter which can be seen in the Figure 3.1.2. is coupled on the back of the panels. It converts DC current of the PV panel to AC current for the grid and and controls the DC voltage to allow the panel working in the Maximum Power Point.



*Figure 3.1.1. Hochschule Osnabrück (Germany): emplacement of the installed panels on a roof (7)*



*Figure 3.1.2. Microinverter coupled on the back of TSM-PD05 panel:  
EVT248 model of ENVERTECH Corporation Ltd. (18)*

Jon Ongay and Iñigo Cerro developed a suitable support structure for the tilt requirements (7). Despite this support allows to adjust the panels to different tilt angles, as shown in Figure 3.1.3., for the experiments, they were fixed permanently to  $39^\circ$  with the horizontal. This angle is near  $36^\circ$ , which is the estimated optimal angle tilt for Osnabrück (see Chapter 4).



*Figure 3.1.3. Tilt angle adjustment of the PV panels (7)*

Some limitations of the panels emplacement must be mentioned. The most important one is the fact that the surrounding buildings and other elements act as a barrier to the wind, which has a non-negligible influence in the heat dissipation, but the wind sensor emplacement is not affected by these barriers. This adds some uncertainty in the validation, since the exact wind speed value on the panels surface is unknown.

The surrounding buildings also has a negative effect in the solar radiation because they impede its capture at certain times of day. This fact does not add uncertainty to the validation, since the irradiation is measured just on the plane of the panels, but for the simulations in different locations (chapter 7) it is assumed that there is no obstacles for the irradiation around the panels.

In Figure 3.1.4. is shown how both mentioned cooling systems, PCM and fins, are coupled on the back of the panels. As can be seen, the total back surface of the panel cannot be covered, due to the output electricity connection.



*Figure 3.1.4. Cooling fins and PCM profiles coupled on the back of two of the installed PV panels (7)*

### 3.1.1. Fins-cooled module

As was explained in section 2.3.3., the use of cooling fins is very common in order to improve the heat dissipation in all kinds of industrial systems. In this case, 56 aluminum fins were arranged on the back of the panel, as shown in Figure 3.1.1.1. They are 'L' profiles, which dimensions are shown in Figure 3.1.1.1.

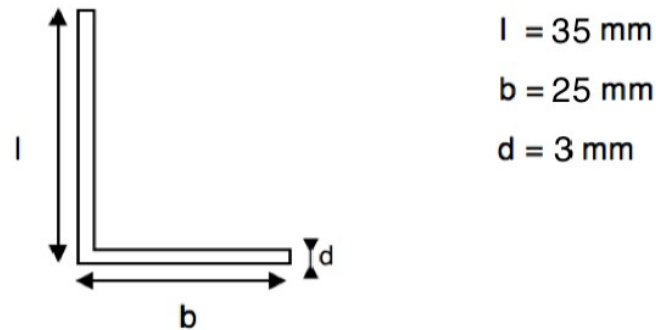


Figure 3.1.1.1. Dimensions of the aluminum fins 'L' section (8)



Figure 3.1.1.2. Aluminum fins arranged on the back of the panel (7)

With the aim of ensuring a suitable thermal conductivity to the aluminum fins a thin thermal paste layer was applied on the back surface of the module, as Figure 3.1.1.3. shows. In Figure 3.1.1.4. can be observed that a transversal aluminum profile was installed to fix the fins by pressing them against the back of the panel. An elastic material ensure a good fixing despite the deflection at the middle of the bar.





*Figure 3.1.1.3. Application of thermal paste for a good thermal conductivity between the back of the panel and the aluminum fins*

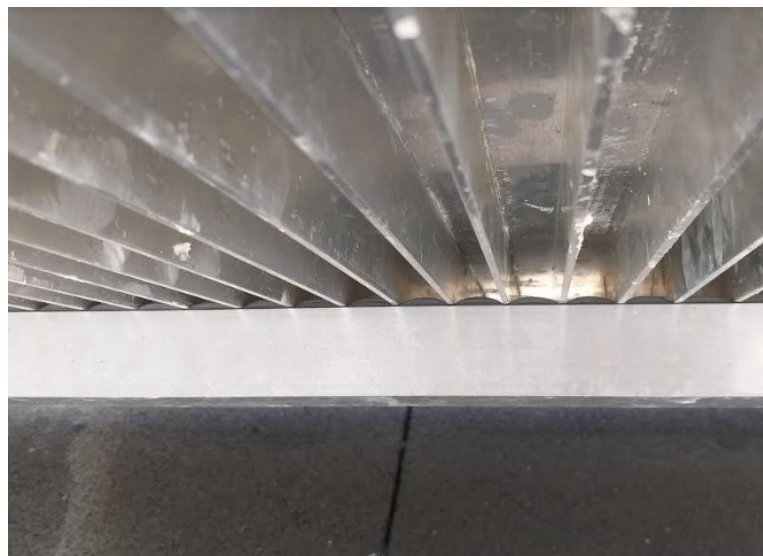


*Figure 3.1.1.4. Transversal aluminum profile to fix the fins*

### **3.1.2. PCM-cooled module**

When a Phase Change Material (PCM) must be chosen for a specific application, a wide variety of alternatives can be found in the market, depending on the system conditions. Iñigo Cerro carried out a study to find the most suitable PCM for Osnabrück conditions and found by simulation the optimal properties which this material should have, with respect to the

thickness, the melting point and other thermal aspects. According to this study, the chosen material closest to the optimal specifications is the RT44HC, whose datasheet is given in Annex 5. It is a material based on paraffins and waxes and its melting interval is 41-44 °C. It is important to state that, although the optimal PCM in the studied geographic locations probably does not differ much from the chosen in Osnabrück, for a more rigorous study a PCM optimization should be done in each case.

The PCM is introduced inside hollow aluminum profiles, which are sealed to avoid material leaks. In this way, aluminum profiles evacuate the heat both to the ambient and to the PCM. Figure 3.1.2.1. shows the dimensions of the mentioned aluminum profiles, which were chosen based on the thickness optimization study. In this case, there is a small air gap between the back of the panel and the aluminum profiles and its effect was included in the simulation.

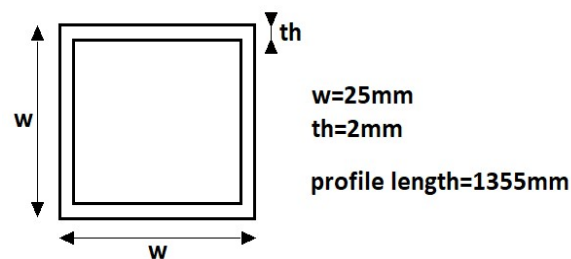


Figure 3.1.2.1. Dimensions of the aluminum PCM profiles



Figure 3.1.2.2. Aluminum PCM profiles arranged on the back of the panel (7)



### 3.2. Hardware and data collection

This section describes the electronic setting developed in order to collect the necessary data for the software validation. Specifically, the collected data corresponds to the temperature on the back of the studied panel, measured by **thermocouples**, and to the incident solar radiation on the plane of the panels, measured by a **pyranometer**. As mentioned previously, wind speed and ambient temperature data are collected from an external database.

The incoming signals from the thermocouples and the pyranometer must be adapted to suitable conditions for the Raspberry Pi, which reads the signals and converts them to the right values, which are displayed and recorded. The Raspberry Pi does not have Analog to Digital converter, so for reading analog inputs external hardware must be used. In this case the ADS1115 16-bit module is chosen, which can deal with four different analog input signals. This module uses I2C serial protocol, which allows communicating with Raspberry Pi only through two pins (SDA and SCL).

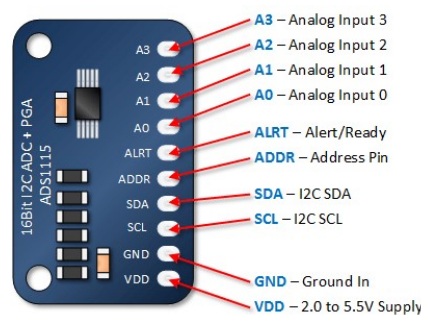


Figure 3.2.1. ADS1115: 16-bit, I2C compatible, Analog to Digital converter (19)

On the other hand, the output signal provided by thermocouples and the pyranometer are, in both cases, too small for the ADS1115 input range. For this reason, amplifier modules, which are shown in the following sections, are necessary.

Figure 3.2.2. shows a global scheme of the hardware arranged for the collection, processing and display of the mentioned data.

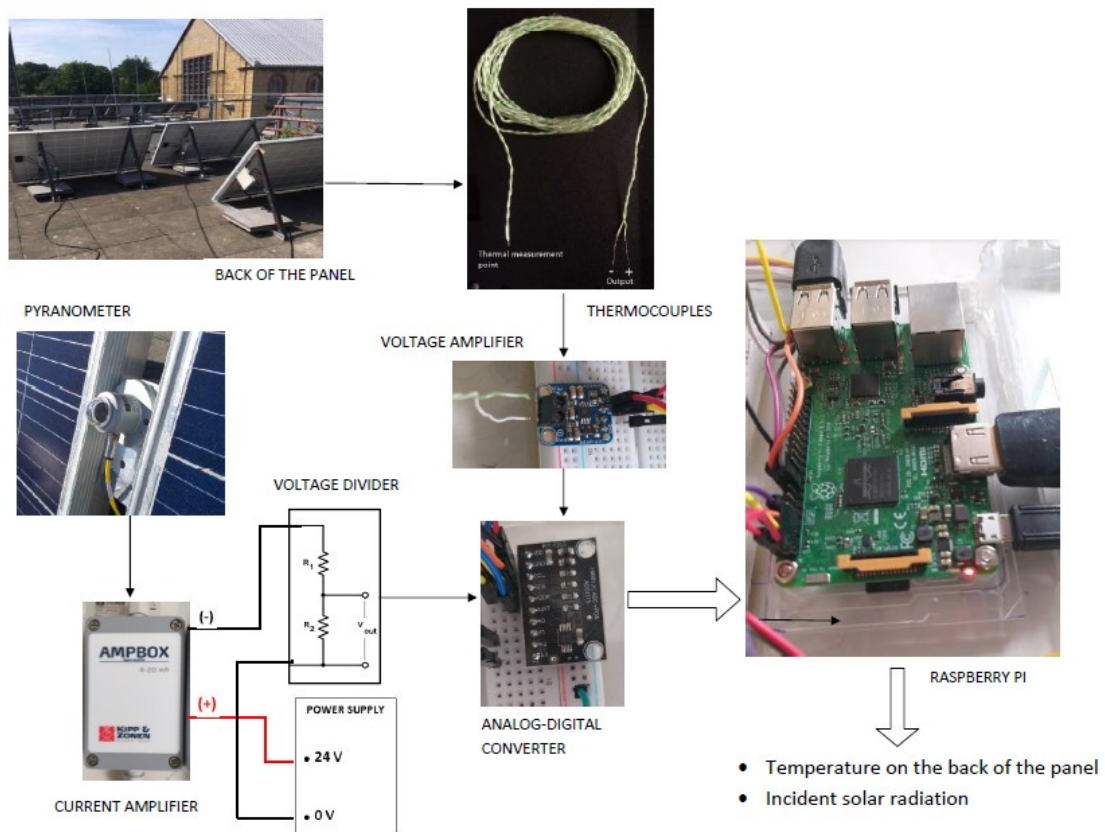


Figure 3.2.2. Global scheme of the data collection hardware

### 3.2.1. Temperature measurement

Temperature on the back of the three installed panels is the key variable to be studied. As will be explained in chapter 5, it is assumed a constant Temperature on this entire surface and in all the parallel sections of the panel. This back temperature will be compared with the back temperature function calculated by simulation. Although is the PV cells layer temperature which determines the electrical efficiency, the mentioned comparison is considered a reasonably accurate validation.

The chosen sensor for temperature measurements is the **thermocouple**. This is a wide used sensor in all kinds of industry applications, due to its low cost, the possibility of a direct contact with the measuring point or its wide range, among other benefits. In particular, **K-type** thermocouple is used in this case.<sup>7</sup>

Temperature measurement by a thermocouple is based on Seebeck effect, which says that if two conductors made of two different metals are joined at both ends and one end is at a different temperature relative to the other, a current is created.

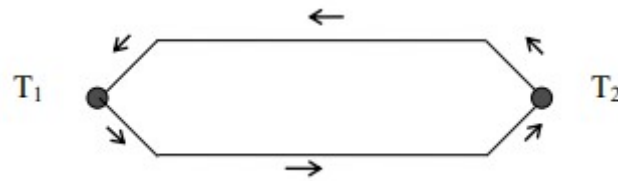


Figure 3.2.1.1. Seebeck effect between two different materials wires joined at both ends (20)

A K-type thermocouple is made of two twisted wires, of chrome and nickel alloys, respectively, and they are welded with each other at one of their tips, which is the terminal in contact with the temperature measuring point. At the other tip, a low voltage is generated between the two terminals when there is a difference between temperature at this end (cold) and the other end (hot).



Figure 3.2.1.2. K-type thermocouple

Because the signal proportional to the measured temperature is too weak for working with it directly in the Analog to Digital converter without an appropriate adaptation, an amplifying stage is necessary. For this purpose, the AD8495 precision amplifier is used, which is especially prepared for its use with K-type thermocouples. This module simplifies one of the main difficulties of measuring temperatures with thermocouples, which is the **cold junction compensation**. It must be taken into account that, as shown in relation (3.2.1.1), the output signal of the thermocouple in the 'cold' terminals (at the opposite end of the measuring point) is proportional to the temperature difference between both thermocouple ends, thus, for the temperature calculation at the 'hot' end, the temperature in the 'cold' end must be known. In this case, an integrated temperature sensor performs cold junction compensation, therefore the output signal can be considered directly proportional to the temperature at the measuring point.

$$V = \alpha \cdot (T - T_{ref}) \quad (3.2.1.1)$$

$V$ : voltage between terminals at the 'cold' end

$\alpha$ : proportionality factor, voltage increase with each Kelvin degree

$T$ : temperature to be measured

$T_{ref}$ : reference temperature, temperature at the 'cold' end

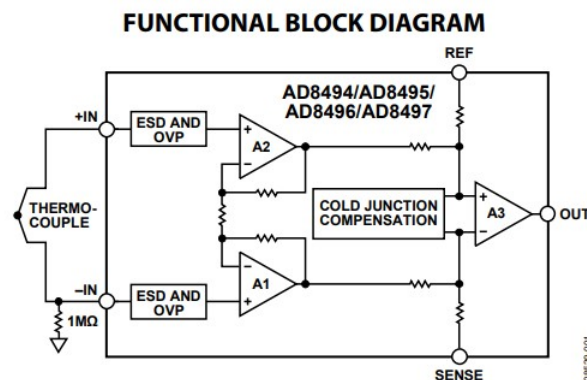


Figure 3.2.1.3. AD8495 functional block diagram (21)

Thanks to the amplifying stage, a suitable input signal reach Analog to Digital module and, at the last stage, a digital value in the 0 to  $2^{16}$  interval (16 bits) is obtained. The last step to get the real value of the temperature at the measuring point is the **calibration** from these digital values. To this end, the measuring junction is immersed in water, whose temperature is varied and measured at all times, in order to get correlated points of the measuring end temperature and its respective digital value. An example of this systematic process is shown below:

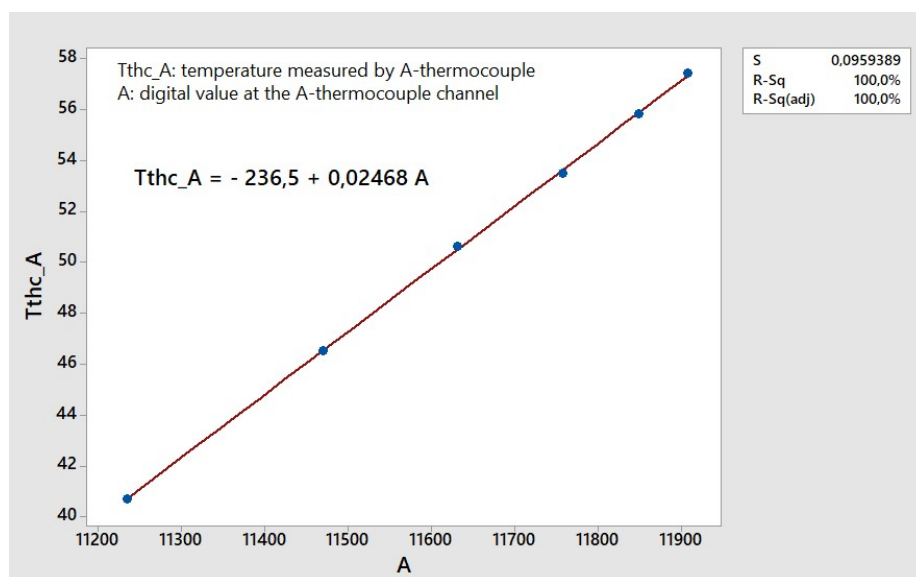


Figure 3.2.1.4. Thermocouple calibration

### 3.2.2. Solar radiation measurement

The instrument used for measuring the incoming solar radiation on the panels surface is the **pyranometer**. This sensor provides the value of the total input solar energy over the entire spectrum and the whole hemisphere for the set position, which must be the same plane as the PV panels (see Figure 3.2.2.2.). The output of the pyranometer is a voltage signal proportional to the irradiated power on the panels plane per unit area ( $\text{W}/\text{m}^2$  in SI units).



Figure 3.2.2.1. CMP3 Pyranometer of Kipp&Zonen (22)



Figure 3.2.2.2. Pyranometer coupled on the top surface of the PV panels

Figure 3.2.2.3. shows the pyranometer sensitivity, provided by the manufacturer ( $16.25 \mu\text{V}/\text{W}/\text{m}^2$ ). As can be seen, this output voltage signal is again too small. In this case, a current amplifier is used at the output of the sensor, thus, a resistors circuit is necessary to adapt this current to a suitable voltage for the Analog to Digital converter. For the choice of the resistances values, both the sensitivity of the pyranometer and of the current amplifier are considered. It should be noted that the wider the range of this last analog voltage, the higher the resolution of the digital signal, but the driver input limits must not be exceeded. In Figure 3.2.2.5. a scheme of the mentioned hardware is given, from the pyranometer to the Analog to Digital converter.



Figure 3.2.2.3. Pyranometer sensitivity provided by manufacturer



Figure 3.2.2.4. AMPBOX current loop amplifier of Kipp&Zonen adapted for pyranometer output (23)

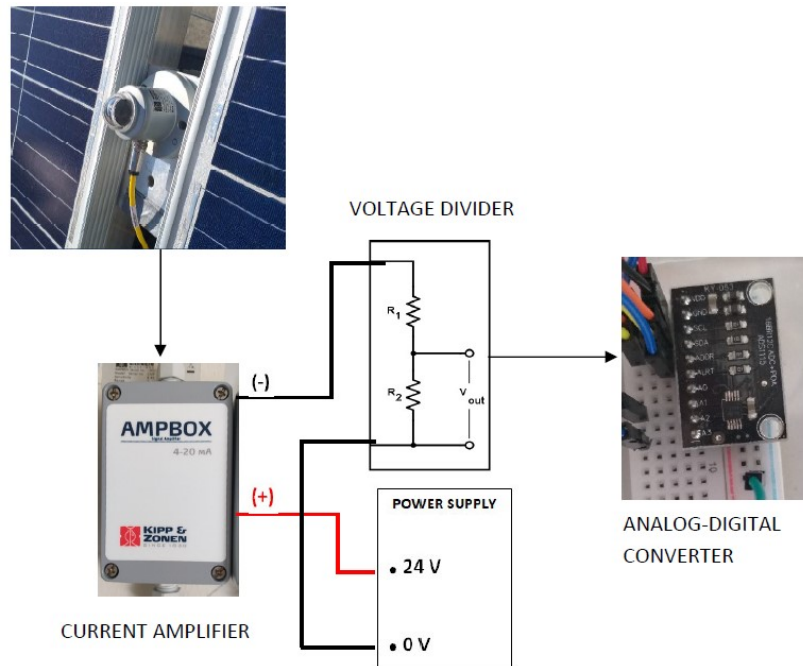


Figure 3.2.2.5. Hardware arranged for the pyranometer data collection

As in the case of thermocouples, a **calibration** must be done, considering in this case the linear correlation between pyranometer output voltage points, measured with a multimeter and proportional to the solar radiation as mentioned before, and the corresponding digital values.



## 4. Optimization of the modules tilt

The goal of this chapter is to establish a method for calculating the optimal tilt angle of a PV module in any geographic location, understanding the optimality as the angle which provides the maximum radiation input through the top surface of the panel over a year. For that purpose, equations listed in section 2.1.1 will be used to convert the available horizontal values of direct and diffuse radiation to corresponding values for incident radiation on an inclined surface. Taking into account that in the northern hemisphere PV modules are installed facing the South and facing the North in southern hemisphere (modules without solar trackers), a sweep is done for all the tilt angles from 0° to 90° in order to find the fixed year angle which provides a maximum radiation catchment.

To simplify calculations, daily values of solar radiation will be used in this chapter instead of hourly values as in the section 2.1.1., thus the conversion to tilted radiation values are analogous with the exception of the factor  $R_b$  for the estimation of the beam radiation on the tilted surface, whose formula is given below for surfaces in **northern hemisphere**:

$$R_b = \frac{\cos(\phi - \beta) \cdot \cos \delta \cdot \sin \omega_{ss} + \omega_{ss} \cdot \sin(\phi - \beta) \cdot \sin \delta}{\cos \phi \cdot \cos \delta \cdot \sin \omega_{ss} + \omega_{ss} \cdot \sin \phi \cdot \sin \delta} \quad (4.1)$$

For the **southern hemisphere**:

$$R_b = \frac{\cos(\phi + \beta) \cdot \cos \delta \cdot \sin \omega_{ss} + \omega_{ss} \cdot \sin(\phi + \beta) \cdot \sin \delta}{\cos \phi \cdot \cos \delta \cdot \sin \omega_{ss} + \omega_{ss} \cdot \sin \phi \cdot \sin \delta} \quad (4.2)$$

where  $\omega_{ss}$  is the **sunset hour angle**:

$$\omega_{ss} = 90^\circ - \arccos(-\tan(\phi) \cdot \tan(\delta)) \quad (4.3)$$

PV modules tilt optimization is not a trivial matter, not only because of its significance for the power generation but also because the variation of the Earth's declination substantially complicates the technical solution of the problem. This last fact makes the optimal tilt angle is not a fixed value over a year but it changes depending on the Earth's declination. A widely used solution to ensure at all times the optimal inclination of the module is a solar tracking system. Nevertheless, for the present study, a fixed tilt and a fixed orientation are assumed for the panels, which obviously have a lower cost.

Figure 4.1. and Figure 4.2. show daily, monthly and annual tilt angles for Osnabrück, which is used as a reference for the analysis. Note that in the central months the optimal tilt angle is lower due to the lower values of declination, which makes beam radiation reaches more directly the northern hemisphere surface. In addition to the declination, the other factor which influence the tilt optimization is the sky clearness. The lower sky clearness, the higher proportion of diffuse radiation, which is higher for lower tilt angles with the horizontal, as is stated by the relation (2.1.1.8). Therefore, with overcast skies, the declination impact is lower. On the other hand, annual optimal angle is not the mean of the optimal angle evolution over a



year, since the periods with higher solar irradiation have a higher influence for the total year calculation.

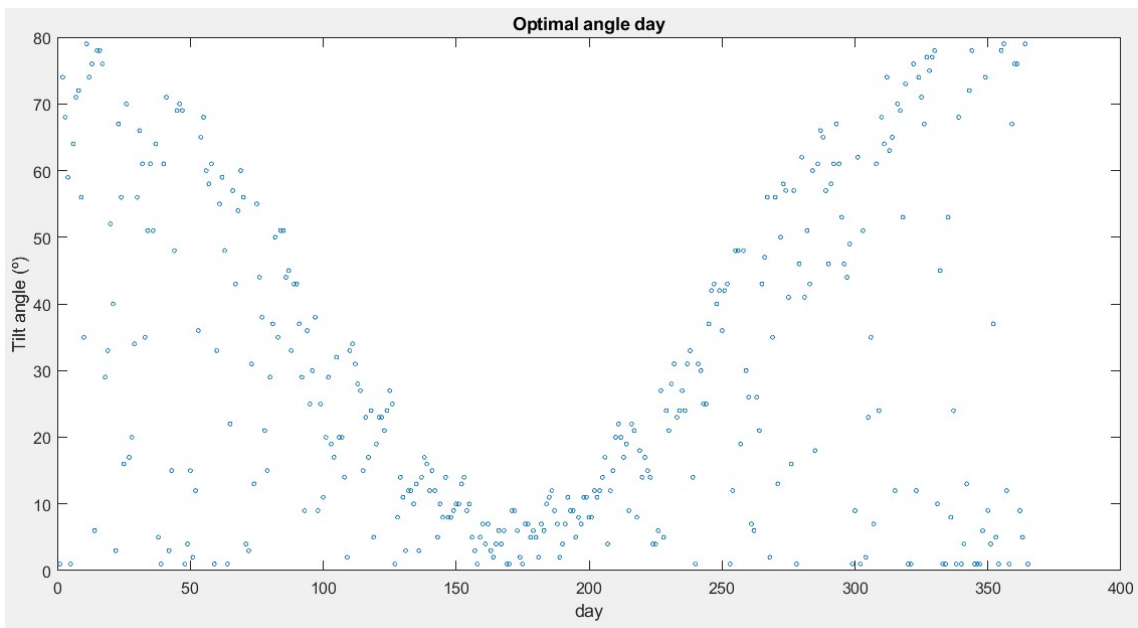


Figure 4.1. Daily optimal PV panels tilt angle for a typical year in Osnabrück

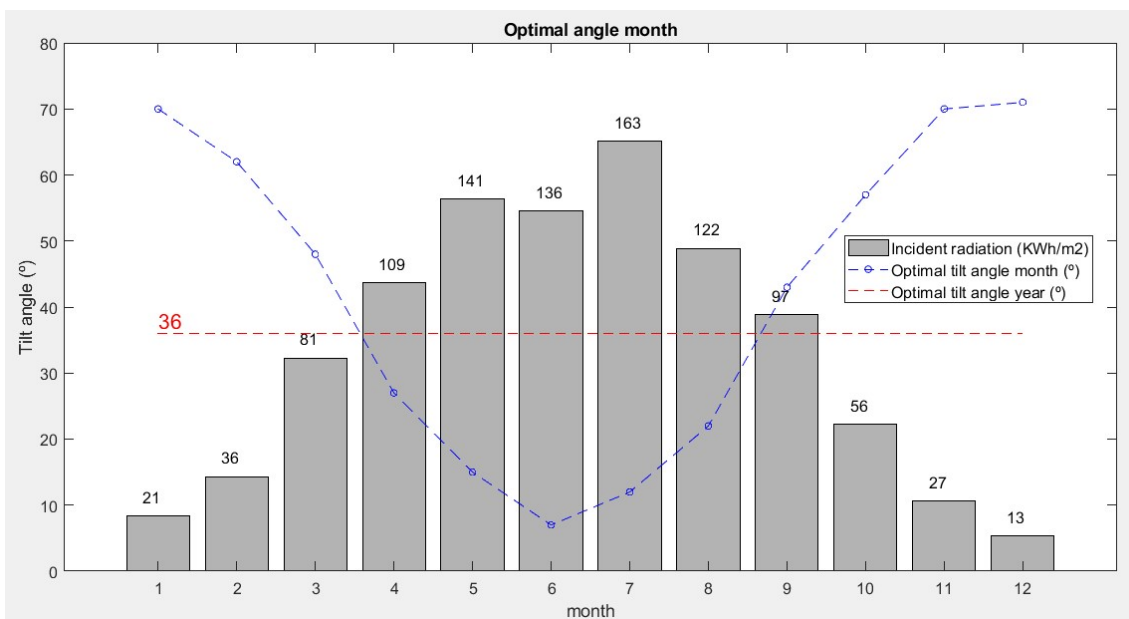


Figure 4.2. Monthly and annual optimal PV panels tilt angle for typical input conditions

As shown in Figure 4.2., the **optimal tilt angle of the PV panels for a fixed position in Osnabrück is 36°**. In order to provide a perception of the impact of the panel tilt on the input available radiation over one entire year, this last is plotted as a function of tilt angle in Figure 4.3. It can be observed that, approximately, the interval between 30° and 40° are suitable values for the case of Osnabrück.

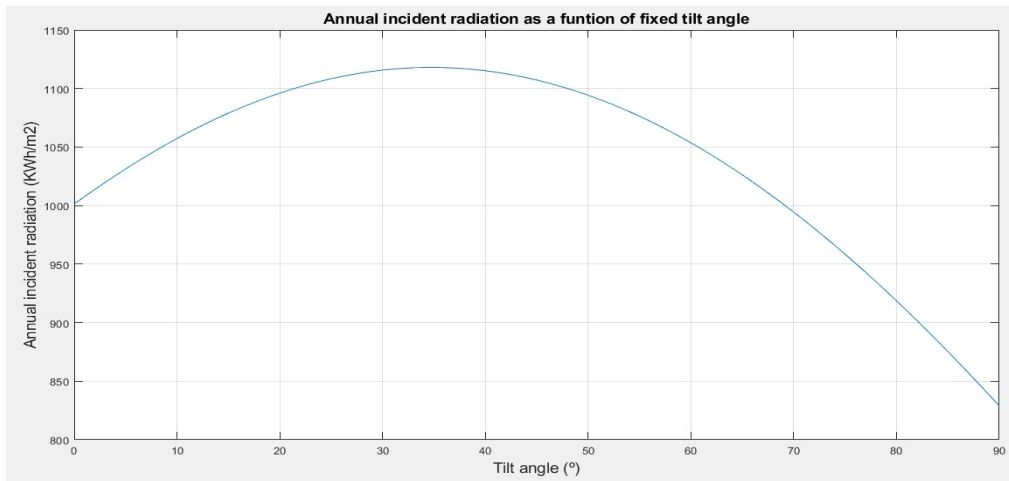


Figure 4.3. Annual incident radiation on the PV panels top surface as a function of tilt angle

In chapter 7, the performed study requires the optimal tilt angle for all the locations considered. To this end the same method which has been shown above is implemented for all of them. In each case, the corresponding daily data of direct and diffuse radiation and the latitude of the location are used as input data. As was mentioned before, it is assumed a fixed tilt for the panels, thus, in all cases, annual optimal tilt angle is the desired value. Table 4.1. lists the summarized obtained results corresponding to the 15 world locations. It is interesting to note in these results that the lower the latitude (location closer to the equator), the lower the optimal tilt and it is almost null in latitudes close to the equator.

Location	Latitude	Longitude	Optimal tilt angle (°)
Alice Springs (Australia)	-23.70	133.88	<b>18</b>
Antofagasta (Chile)	-23.65	-70.40	<b>17</b>
Bologna (Italy)	44.53	11.30	<b>24</b>
Cape Town (South Africa)	-33.92	18.42	<b>19</b>
Cox's Bazar (Bangladesh)	21.45	91.97	<b>27</b>
Harare (Zimbabwe)	-17.82	31.05	<b>18</b>
Jimma (Ethiopia)	7.68	36.84	<b>14</b>
Kuching (Malaysia)	1.55	110.33	<b>1</b>
Las Vegas (United States)	36.11	-115.17	<b>34</b>
Manaos (Brazil)	-3.12	-60.03	<b>5</b>
Mombasa (Kenya)	-4.04	39.67	<b>2</b>
Oslo (Norway)	59.91	10.76	<b>36</b>
Osnabrück (Germany)	52.27	8.05	<b>36</b>
Riyadh (Saudi Arabia)	24.77	46.74	<b>23</b>
Sevilla (Spain)	37.38	-5.97	<b>31</b>

Table 4.1. Optimal PV panels tilt angle for the considered locations in this project

## 5. Design of the simulation model

The present chapter provides a schematic and numerical description of the three models developed to estimate the cells temperature and, with it, the cells theoretical electrical efficiency. Besides, to study the performance of the model, some simulation outputs are shown, using artificial input data of the temperature, radiation and wind conditions. The full MATLAB code is given in Annex 6.

### 5.1. Computing environment

Building on the work performed in the previous projects, the computer environment is kept for the purpose of the thermal modeling carried out in this project. The workspace chosen by Iñigo Cerro and Jon Ongay (6) is **Matlab**, which is a multi-paradigm numerical computer environment and, for the aim of the present project, is an excellent tool to develop numerical simulations.

Matlab uses its own programming language, which allows, among other things, a simple definition of variables, multiple options as for matrix manipulations, many possibilities for plotting of functions and data, and a high flexibility in the use of available functions. Another benefit is the simple implementation of these functions, as well as the large user community, which makes the work with this computer environment easier.

### 5.2. Physical parameters

Since the used physical parameters in the developed model is quite large, all of them are listed and classified in the following tables:

Module dimensions			
Parameter	Description	Value	Unit
$w$	Module width	0.992	m
$l$	Module length	1.65	m
$a = w \cdot l$	Module surface	1.64	m <sup>2</sup>
$l_{Re} = \frac{4 \cdot a}{2 \cdot (l + w)}$	Characteristic length for Reynolds equation	1.24	m

Table 5.2.1. Physical parameters: module dimensions

Solar glass			
Parameter	Description	Value	Unit
$th_{SG}$	Thickness of the solar glass	3.2	mm
$\rho_{SG}$	Density of the solar glass	2500	Kg/m <sup>3</sup>
$m_{SG} = \rho_{SG} \cdot a \cdot th_{SG}$	Mass of the solar glass	13.12	Kg
$cp_{SG}$	Specific heat capacity of the solar glass	837	J/Kg·K
$k_{SG}$	Conductivity of the solar glass	0.9	W/m·K
$\alpha_{SG}$	Heat energy absorbed by the glass from incident radiation/ Total incident radiation	0.133	-
$\varepsilon_{SG}$	Emissivity of the solar glass	0.13	-
$a_{abs}$	Area of the panel which receive radiation (subtracting the area covered by the frame)	1.582	m <sup>2</sup>

Table 5.2.2. Physical parameters: solar glass

Silicon cells and aluminum conductors			
Parameter	Description	Value	Unit
$th_C$	Thickness of the cells	0.5	mm
$f_{CELLS}$	Area of the pannel covered by cells/total area of the pannel	0.9	-
$f_{SI}$	Area of the cell covered by silicon/total area of the cell	0.9	-
$\rho_{SI}$	Density of the silicon	2336	Kg/m <sup>3</sup>
$cp_{SI}$	Specific heat of the silicon	703	J/Kg·K
$k_{SI}$	Conductivity of the silicon	150	W/m·K
$\rho_{Al}$	Density of the aluminum	2700	Kg/m <sup>3</sup>
$cp_{Al}$	Specific heat of the aluminum	897	J/Kg·K
$k_{Al}$	Conductivity of the aluminum	235	W/m·K
$m_C = [\rho_{SI} \cdot f_{SI} + \rho_{Al} \cdot (1 - f_{SI})] \cdot a \cdot f_{CELLS} \cdot th_C$	Mass of the cell	1.75	Kg
$cp_C = f_{SI} \cdot cp_{SI} + (1 - f_{SI}) \cdot cp_{Al}$	Heat capacity of the cell	722.4	J/Kg·K
$k_C = f_{SI} \cdot k_{SI} + (1 - f_{SI}) \cdot k_{Al}$	Conductivity of the cell element	158.5	W/m·K

Table 5.2.3. Physical parameters: silicon cells and aluminum conductors

Back insulation			
Parameter	Description	Value	Unit
$th_{back}$	Thickness of the back insulation	0.4	mm
$\rho_{back}$	Density of the back insulation	1380	Kg/m <sup>3</sup>
$m_{back} = \rho_{back} \cdot a \cdot th_{back}$	Mass of the back insulation	0.905	Kg
$cp_{SG}$	Specific heat capacity of the back insulation	1050	J/Kg·K
$k_{SG}$	Conductivity of the back insulation	0.2	W/m·K

Table 5.2.4. Physical parameters: back insulation

Cooling fins			
Parameter	Description	Value	Unit
$th_{fin}$	Thickness of the fin	3	mm
$lg_{fin}$	Length of the fin	0.992	m
$w_{fin-long}$	Long width of the fin	35	mm
$w_{fin-short}$	Short width of the fin	25	mm
$\rho_{fin} = \rho_{Al}$	Density of the (aluminum) fins	2700	Kg/m <sup>3</sup>
$n_{fins}$	Number of fins	56	-
$m_{fins} = [th_{fin} \cdot (w_{fin-l} + w_{fin-s} - th_{fin})] \cdot lg_{fin} \cdot \rho_{Al} \cdot n_{fins}$	Total mass of the fins	25.65	Kg
$cp_{fin} = cp_{Al}$	Specific heat of the (aluminum) fins	897	J/Kg·K
$k_{fin} = k_{Al}$	Thermal conductivity of the (aluminum) fins	235	W/m·K
$a_{cover\ fins} = w_{fin-s} \cdot lg_{fin} \cdot n_{fins}$	Back area covered by the fins	1.389	m <sup>2</sup>

Table 5.2.5. Physical parameters: cooling fins

PCM + PCM profiles (square profiles)			
Parameter	Description	Value	Unit
$\rho_{PCM}$	Density of the PCM	800	Kg/m <sup>3</sup>
$cp_{PCM}$	Specific heat capacity of the PCM	2000	J/Kg·K
$k_{PCM}$	Conductivity of the PCM	0.2	W/m·K
$w_{prf}$	Width (external) of the profiles	25	mm
$th_{prf}$	Thickness of the profiles	2	mm
$lg_{prf}$	Length of the profiles	1.355	m
$\rho_{prf} = \rho_{Al}$	Density of the (aluminum) profiles	2700	Kg/m <sup>3</sup>
$n_{prfs}$	Number of profiles	34	-
$m_{prfs} = [w_{prf}^2 - (w_{prf} - 2 \cdot th_{prf})^2] \cdot lg_{prf} \cdot \rho_{prf} \cdot n_{prfs}$	Total mass of the (aluminum) profiles	22.89	Kg
$cp_{prf} = cp_{Al}$	Specific heat capacity of the (aluminum) profiles	897	J/Kg·K

Table 5.2.6. Physical parameters: PCM+PCM profiles (square aluminum profiles)

### 5.3. Model assumptions

This section lists all the assumptions considered in the model development. These assumptions are made taking into account a compromise between the output reliability and the model simplicity.

One of the most important premises is the **one-way heat flux**, which implies that the temperature is constant in a section parallel to the panel plane. This assumption is quite reasonable, due to the fact that the PV cells layer (basically composed of silicon and aluminum) has a high thermal conductivity and the external frame is isolated from the panel, so heat loss at the edges is neglectable. With this in mind, each different layer is considered as a single mass element whose temperature function is calculated at discrete time intervals. The temperatures are calculated in the middle point of the panel layers, in the transversal direction to the plane. A layer is understood as a mass element with homogeneous thermal properties in its entire volume. The temperature trend in a certain layer obeys the mentioned relation (2.1) but it is calculated only at discrete time points, with a small enough sample time step. The iterative calculation process is based on estimate the heat balance in the layer for a specific time step and use it to figure out the temperature at the next time step. Therefore, the next equation is repeated sequentially for each layer:

$$T_{i+1} = \frac{1}{m \cdot c_p} \cdot \left( \sum \dot{Q}_j \right) \cdot t_{step} + T_i$$

$T_{i+1}$ : temperature of the mass element at 'i+1' step

$m$ : mass of the element

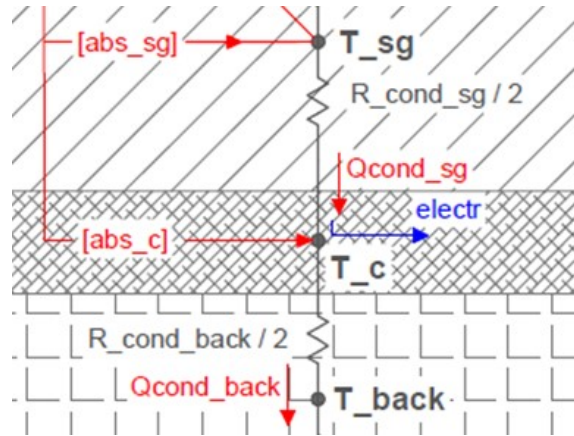
$c_p$ : specific heat of the mass element

$\sum \dot{Q}_j$ : heat balance in the mass element at the 'i' step

$t_{step}$ : time step

$T_i$ : temperature of the mass element at 'i' step

For a better understanding of this process an example is given below, for the calculation of the temperature in the PV cells layer (see Figure 5.3.1.):

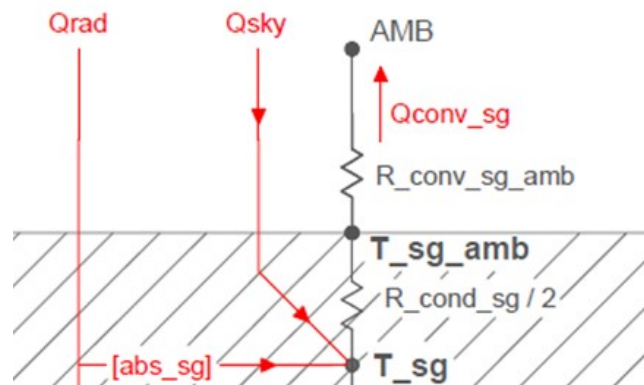


$$\dot{Q}_{cond\ sg} = \frac{T_{sg} - T_c}{R_{cond\ sg}/2} \quad \dot{Q}_{cond\ back} = \frac{T_c - T_{back}}{R_{cond\ back}/2}$$

$$T_{c_{i+1}} = \frac{1}{m_c \cdot c_{pc}} \cdot (\dot{Q}_{cond\ sg} + \dot{Q}_{rad} - electr - \dot{Q}_{cond\ back}) \cdot t_{step} + T_{c_i}$$

Figure 5.3.1. Example of the iterative calculation of temperature in the case of PV cells layer at successive simulation steps

As is shown in Figure 5.3.2., the temperature at the air contact border surface is calculated in the same way as in an analogous resistive electrical circuit:



$$T_{sg\ amb_{i+1}} = T_{amb_{i+1}} + \dot{Q}_{conv\ sg} \cdot R_{conv\ sg-amb}$$

Figure 5.3.2. Calculation of temperature at solar glass top surface

An analogy can be drawn by comparing the thermal model shown to an electrical circuit consisting of resistances and capacitors. In section 5.4., the electrical analogy is provided for the case of the three considered thermal models. The capacitors represent the heat (electric charge) storage of the mass elements, which implies a temperature (voltage) rise.

The imposed **simulation time step** is **0.5 s**. It was tested that too high time steps may lead to a destabilization of the program. Note that with each simulation step there is an error, since discrete values are used in the calculations, thus, the higher the sample time, the higher the error. It was noted how for a limit sample time the error increases after each iteration, which

finally leads to infinite values. This upper limit for the time step has a lot to do with the parameters used in the simulation, specifically the thermal resistances, the mass of the element and the specific heat of the mass element. Note that these terms are dividing in the presented formulas for the iterative calculation. For this reason, lower values amplify the error of the estimated temperature at the next step. Because of that, low values of thermal resistances are neglected, for example in the case of PV cells, which have a high thermal conductivity. In this way, total simulation time is reduced by eliminating terms with a lower impact in the final results.

Another important assumption is to consider that the **panel always works in the Maximum Power Point**, which is necessary to apply the theoretical formula for the electrical efficiency (1.1.2). This assumption is justified, since the microinverter connected to the panel has a Maximum Power Point Tracking (MPPT) system.

On the other hand, the **internal heat generation** in the panel, due to Joule effect, is **neglected**, since it has a minor effect in the heat balance.

In addition to the previous points, **other simplifications** were mentioned in chapter 2 as for the **angle of attack of the wind flow** and the **calculation of the absorptivity, transmissivity and reflectivity in the glass and the PV cells**.



## 5.4. Description of the three developed models

### 5.4.1. Standard module

Table 5.4.1.1 collects all the thermal resistances of the most basic standard module thermal model, without including any cooling system. Note that the cells layer conductive resistance has been neglected, due to its low thickness and to the high thermal conductivity of Silicon and Aluminum.

<b>Convective resistance solar glass – ambience</b>
$R_{conv\ sg} = \frac{1}{(h_{TOP} \cdot a_{abs})} = \frac{0.632}{h_{TOP}} \left( \frac{K}{W} \right); \quad h_{TOP} \ll \left[ \frac{W}{m^2} \cdot K \right]$
<b>Conductive resistance of the solar glass</b>
$R_{cond\ sg} = \frac{th_{sg}}{(k_{sg} \cdot a)} = 0.0022 \left( \frac{K}{W} \right)$
<b>Conductive resistance of the back insulation</b>
$R_{cond\ back} = \frac{th_{back}}{(k_{back} \cdot a)} = 0.0012 \left( \frac{K}{W} \right)$
<b>Convective resistance back insulation – ambience</b>
$R_{conv\ back} = \frac{1}{(h_{BACK} \cdot a)} = \frac{0.610}{h_{BACK}} \left( \frac{K}{W} \right); \quad h_{BACK} \ll \left[ \frac{W}{m^2} \cdot K \right]$

*Table 5.4.1.1. Thermal resistances of the standard module thermal model*

As explained in chapter 2.1.2, the input heat coming from the solar irradiance is absorbed in different proportions both in the glass and in the cells. As for the output power, the heat is dissipated by convection at both top and back air surfaces and the electricity generation must also be considered.

Figure 5.4.1.2. shows the model scheme, which includes all the considered thermal resistances and the power (heat and electricity) inputs and outputs.

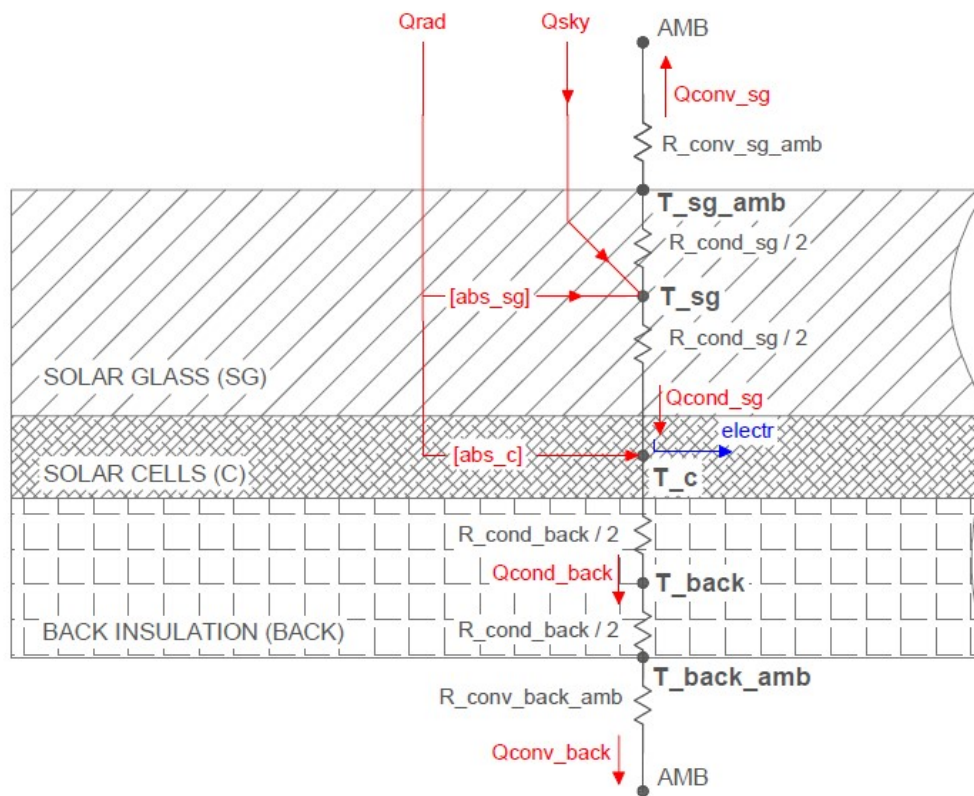


Figure 5.4.1.1. Scheme of the standard panel thermal model

Below, the analogous electrical circuit is shown, where the capacitors represent the thermal inertia of the three considered layers. The corresponding layers temperatures are calculated in the middle point, this is why conductive thermal resistance is divided into two halves at both sides of the capacitor terminal.

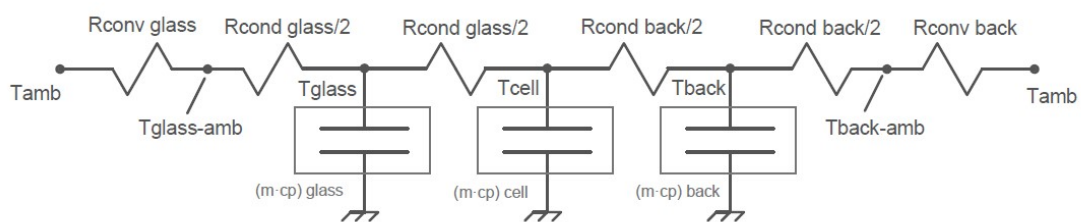


Figure 5.4.1.2. Electrical analogy of the standard panel thermal model

### 5.4.2. Fins-cooled module

The fins-cooled module model is developed on the base of the standard module model, including the back coupled cooling fins. As explained in section 2.3.1., the purpose of the fins is to reduce the convective thermal resistance through an increase of the air contact area and, thereby, to achieve an improvement in the heat dissipation.

<b>Convective resistance solar glass – ambiance</b>
$R_{conv\ sg} = \frac{1}{(h_{TOP} \cdot a_{abs})} = \frac{0.632}{h_{TOP}} \left( \frac{K}{W} \right); \quad h_{TOP} \ll \left[ \frac{W}{m^2} \cdot K \right]$
<b>Conductive resistance of the solar glass</b>
$R_{cond\ sg} = \frac{th_{sg}}{(k_{sg} \cdot a)} = 0.0022 \left( \frac{K}{W} \right)$
<b>Conductive resistance of the back insulation</b>
$R_{cond\ back} = \frac{th_{back}}{(k_{back} \cdot a)} = 0.0012 \left( \frac{K}{W} \right)$
<b>Convective resistance fins – ambiance</b>
$R_{conv\ fin} = \frac{1}{\tanh\left(\sqrt{\frac{h_{BACK} \cdot p}{k_{fin} \cdot A_c}} \cdot L\right) \cdot \sqrt{h_{BACK} \cdot p \cdot k_{fin} \cdot A_c}} = \frac{1}{\tanh(0.05 \cdot \sqrt{h_{BACK}}) \cdot \sqrt{1.39 \cdot h_{BACK}}} \left( \frac{K}{W} \right); \quad h_{BACK} \ll \left[ \frac{W}{m^2} \cdot K \right]$ $p = 2 \cdot (th_{fin} + lg_{fin}); \quad A_c = th_{fin} \cdot lg_{fin}; \quad L = w_{fin-l} - th_{fin}$
<b>Convective resistance cover fins – ambiance</b>
$R_{conv\ cover} = \frac{1}{h_{BACK} \cdot (a_{cover\ fins} - n_{fins} \cdot th_{fin} \cdot lg_{fin})} = \frac{0.818}{h_{BACK}} \left( \frac{K}{W} \right); \quad h_{BACK} \ll \left[ \frac{W}{m^2} \cdot K \right]$

Table 5.4.2.1. Thermal resistances of the fins-cooled module thermal model

As can be seen in Figure 5.4.2.1., the mentioned fins convective resistance is coupled in parallel to the back cover convective resistance and makes the equivalent resistance lower. Due to the high thermal conductivity of Aluminum, the conductive resistance of the fins is neglected.

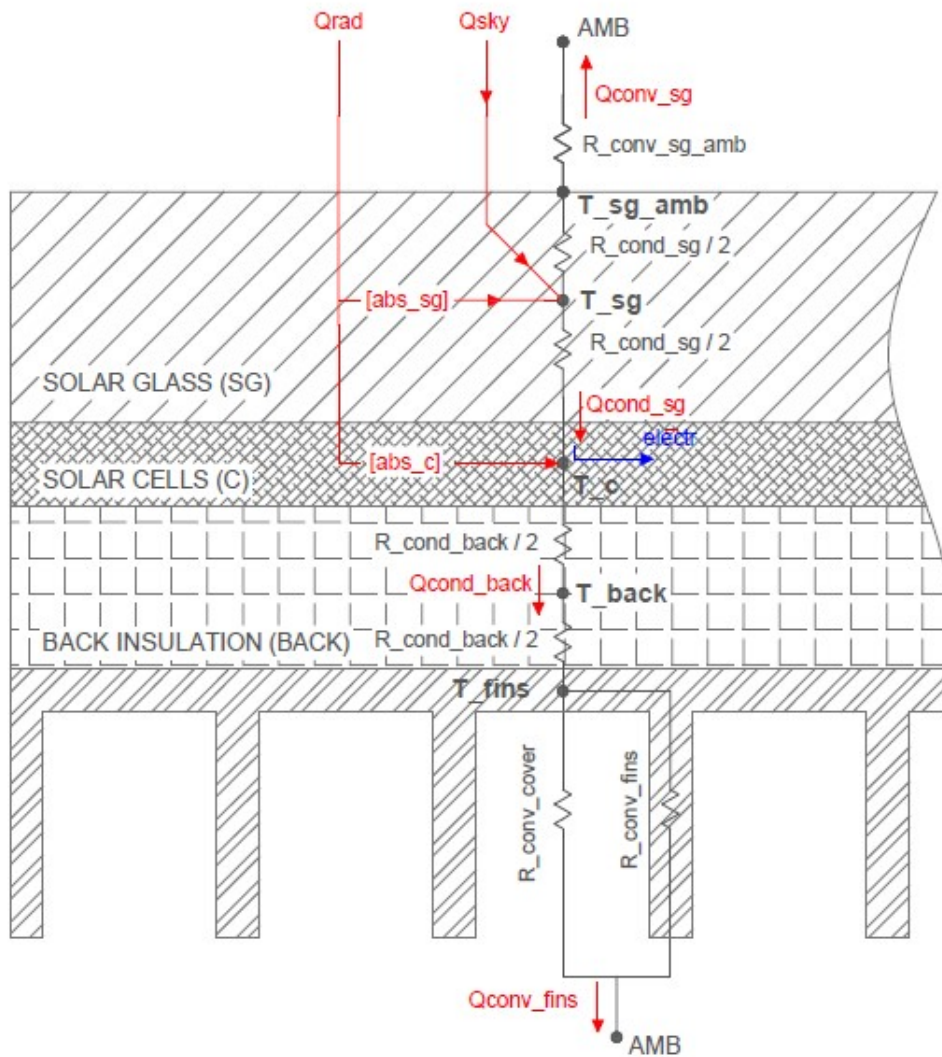


Figure 5.4.2.1. Scheme of the fins-cooled panel thermal model

The analogous electrical model of the system is included below. Note that the aluminum fins modifies the total convective resistance on the back and adds a new mass element to the system, which increases the total heat storage capacity.

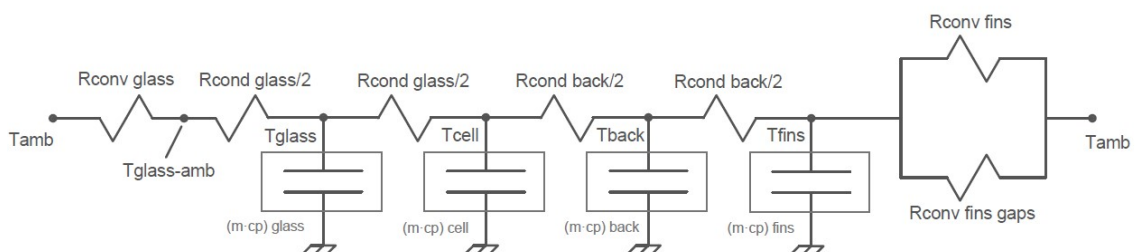


Figure 5.4.2.2. Electrical analogy of the fins-cooled panel thermal model

### 5.4.3. PCM-cooled module

The last shown model corresponds to PCM-cooled panel. The following table lists the thermal resistances which have been considered in this model:

<b>Convective resistance solar glass – ambience</b>
$R_{conv\ sg} = \frac{1}{(h_{TOP} \cdot a_{abs})} = \frac{0.632}{h_{TOP}} \left( \frac{K}{W} \right); \quad h_{TOP} \ll \left[ \frac{W}{m^2} \cdot K \right]$
<b>Conductive resistance of the solar glass</b>
$R_{cond\ sg} = \frac{th_{sg}}{(k_{sg} \cdot a)} = 0.0022 \left( \frac{K}{W} \right)$
<b>Conductive resistance of the back insulation</b>
$R_{cond\ back} = \frac{th_{back}}{(k_{back} \cdot a)} = 0.0012 \left( \frac{K}{W} \right)$
<b>Convective resistance back insulation – ambience</b>
$R_{conv\ back} = \frac{1}{(h_{BACK} \cdot a)} = \frac{0.610}{h_{BACK} (W/m^2 \cdot K)} \left( \frac{K}{W} \right); \quad h_{BACK} \ll \left[ \frac{W}{m^2} \cdot K \right]$
<b>Horizontal conductive resistance between mass differential elements of the PCM</b>
$R_{PCM-HORIZ} = \frac{n_{vert}}{n_{horiz} \cdot l_{gprf} \cdot n_{prf} \cdot k_{pcm}} = \frac{n_{horiz}}{n_{vert}} \cdot 0.1085 \left( \frac{K}{W} \right)$
<b>Vertical conductive resistance between mass differential elements of the PCM</b>
$R_{PCM-VERT} = \frac{n_{horiz}}{n_{vert} \cdot l_{gprf} \cdot n_{prf} \cdot k_{pcm}} = \frac{n_{vert}}{n_{horiz}} \cdot 0.1085 \left( \frac{K}{W} \right)$
$n_{horiz}$ : number of horizontal nodes in the matrix of PCM mass elements $n_{vert}$ : number of vertical nodes in the matrix of PCM mass elements

Table 5.4.3.1. Thermal resistances of the PCM-cooled module thermal model

The use of a Phase Change Material is a completely different solution for cooling, compared to thermal fins. In this last case, heat is dissipated to an infinite external sink, which is the ambient, but in the case of PCM-cooling an internal element is used as a heat sink, which is the PCM. This means that for a long enough period, the same heat which is ‘dissipated’ to the PCM returns in the end to the mass elements of the panel in contact with the material. Therefore, it is not correct to say that this transferred heat is dissipated, but is temporarily stored. The key point of the performance of this cooling method is the thermal inertia of the PCM, which delays the temperature rise during time periods of highest solar radiation by absorbing a significant heat energy, which is dissipated to the ambient during low radiation time periods. For this reason the main PCM downside is that a longer time is required for a temperature drop.

In Figure 5.4.3.1., the simulation model of the PCM-cooled panel can be seen, where the PCM square profiles are coupled on the back insulation. Again, to avoid instability in the simulation,

the conductive thermal resistance of the aluminum profiles is neglected, so the temperature in their entire volume is the same.

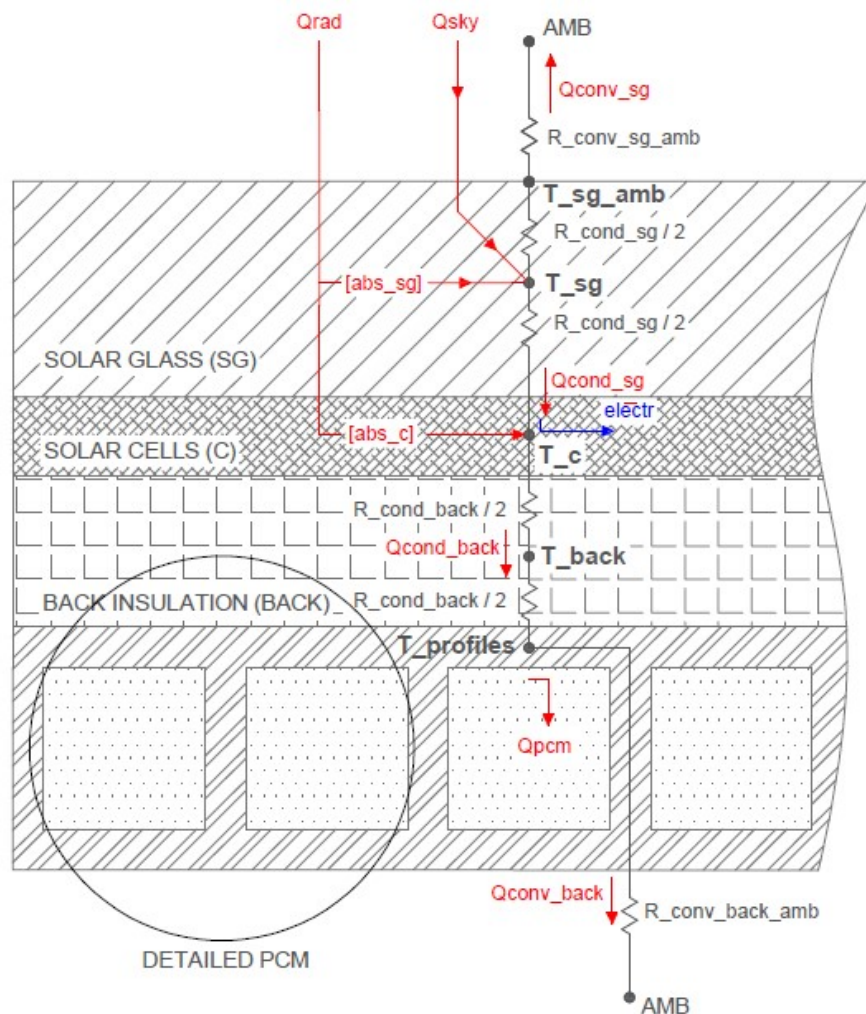


Figure 5.4.3.1. Scheme of the PCM-cooled panel thermal model

As for the internal thermal functioning of the PCM square profiles, a more detailed analysis must be done. The first key point to mention is that, due to the low heat conductivity, the high heat capacity and the significant thickness of PCM, it is unrealistic to assume a constant temperature in the entire PCM mass. In this respect, some authors recommend a **2-dimensional** approach to study the temperature of the PCM profiles section.

For this reason, as shown in Figure 5.4.3.2., the PCM section is divided in a matrix of discrete mass elements, joined by the corresponding thermal resistors in both horizontal and vertical direction. Firstly, to simplify the model development, a symmetry between individual profiles as for the thermal modeling should be noted, hence a global unique square section is set, including all the parallel thermal resistances and mass elements (see Figure 5.4.3.3.).



The calculation of the temperature function in each mass element of the PCM matrix obeys the same iterative process as in the other elements of the model. For the heat balance in all the section nodes, both a horizontal and a vertical heat flux matrix is calculated, and the corresponding sum is performed in each node.

### DETAILED PCM

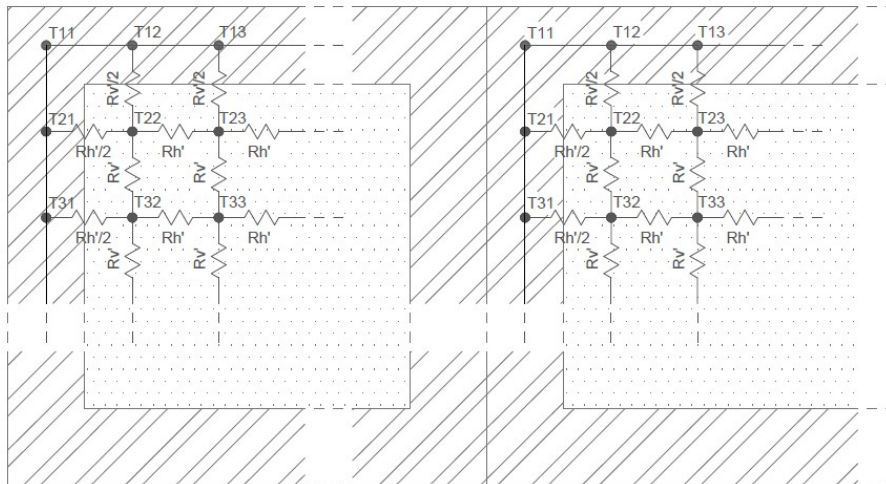


Figure 5.4.3.2. Array of PCM mass elements and thermal resistances (vertical and horizontal) of thermal modeling corresponding to the PCM profile section

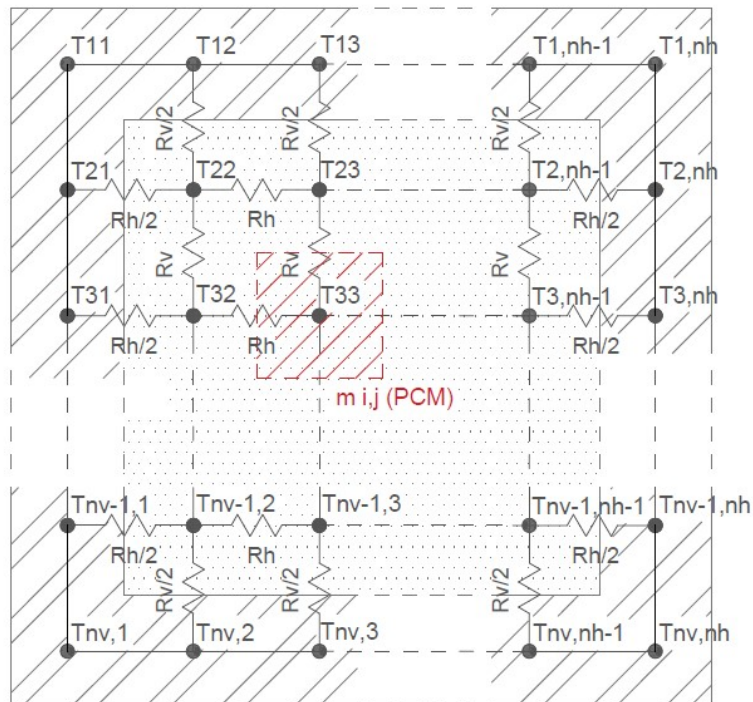


Figure 5.4.3.3. Global PCM square section, including all the parallel thermal resistances and mass elements of the PCM profiles

Another important aspect to impose is the behaviour of the PCM in the melting-solidification interval, as for the latent heat. The datasheet of RT44HC, provided by the manufacturer (24), was checked to determine the heat transferred to/from the material in each Kelvin degree rise/drop, in the phase change interval, approximately 40-44°C, as shown in Figure 5.4.3.4. Note that melting and solidification processes are asymmetric. For more details about RT44HC properties, see Annex 5.

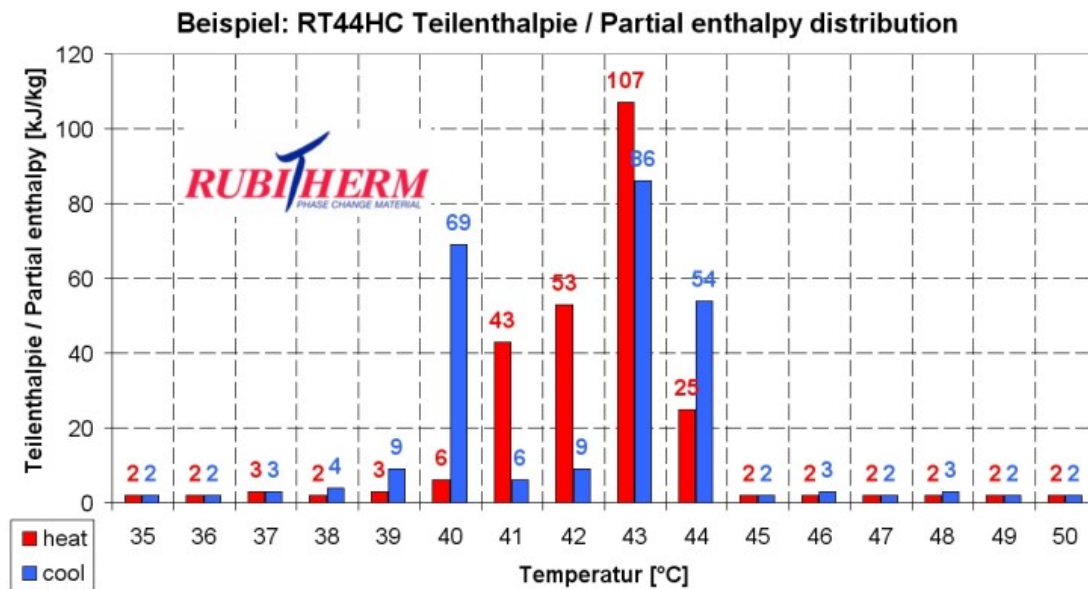


Figure 5.4.3.4. Partial enthalpy distribution of RT44HC material over the temperature interval from 35°C to 51°C

As for the code in the interval 35-51°C, the energy stored by each mass element is recorded in each iteration and the corresponding temperature is calculated by linear interpolation of this energy compared with the latent heat in the melting interval (heat entering PCM) or in the solidification interval (heat escaping PCM).

In order to test the validity and the necessity of the 2-dimensional model a study of the model output is carried out. On the other hand, the number of columns and rows of the PCM section matrix can be chosen by 2 variables in the code, corresponding to the horizontal and the vertical number of nodes, respectively. A matrix of **4x4 nodes** is considered a suitable size in this case, which is decided by making a comparison of temperature on the back of the panel for different matrix dimensions and for the same wind speed, ambient temperature and solar radiation conditions (see Figure 5.4.3.5 and Figure 5.5.1.). A square matrix is set, since the PCM section is also a square.



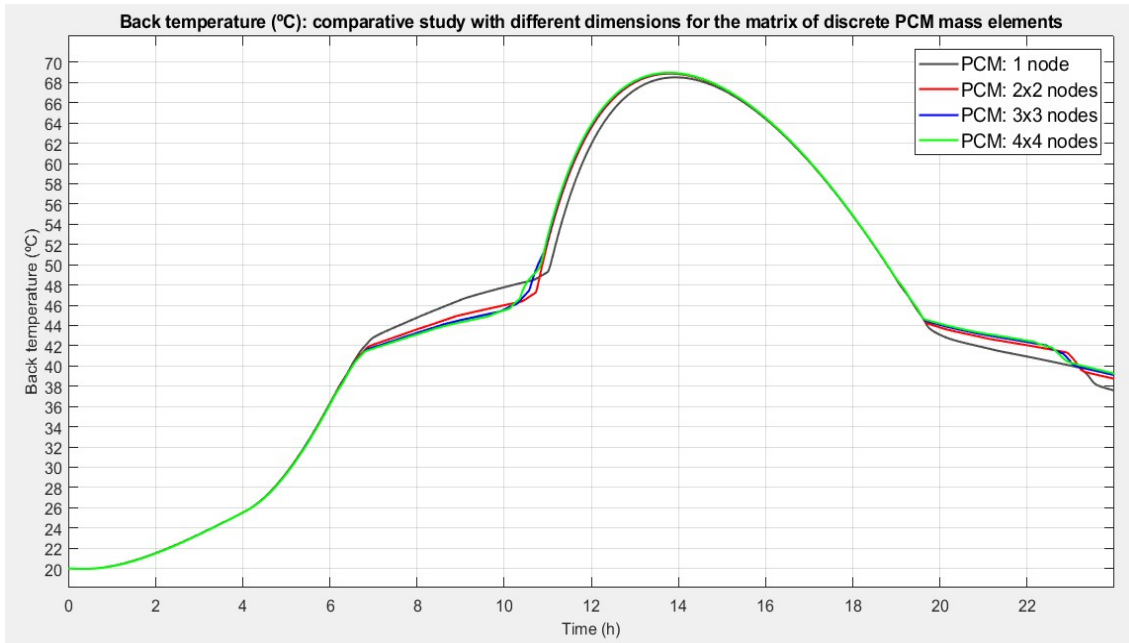


Figure 5.4.3.5. Back temperature (°C) comparative study with different dimensions for the matrix of discrete PCM mass elements (input conditions of Figure 5.5.1.)

As for the internal thermal functioning of the PCM, it is interesting to analyse it during the phase change process. To this end, a simulation of the temperature of the mass elements array at different stages during the melting process is shown below. A 10x10 matrix was set for a suitable display. The aim of this graphs is to demonstrate the difference in the temperature at different points of the section. The most external mass elements are warmer during the temperature rise, since they are in contact with the aluminum profile, so the heat power reach them firstly. Because of the low thermal conductivity of the material, a significant delay occurs in the heat flux to the center of the section.

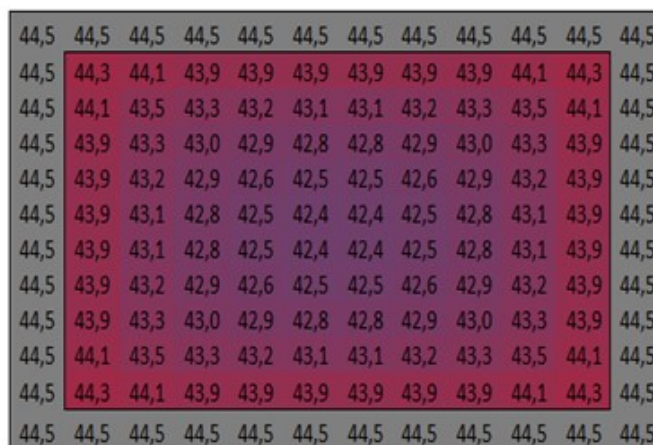


Figure 5.4.3.6. Temperatures (°C) of the discrete mass elements of the PCM section during melting process, 0 minutes (input conditions in Figure 5.5.1.)

45,4	45,4	45,4	45,4	45,4	45,4	45,4	45,4	45,4	45,4	45,4	45,4
45,4	45,3	45,1	44,8	44,8	44,8	44,8	44,8	44,8	45,1	45,3	45,4
45,4	45,1	44,4	43,8	43,7	43,6	43,6	43,7	43,8	44,4	45,1	45,4
45,4	44,8	43,8	43,4	43,2	43,1	43,1	43,2	43,4	43,8	44,8	45,4
45,4	44,8	43,7	43,2	43,0	42,9	42,9	43,0	43,2	43,7	44,8	45,4
45,4	44,8	43,6	43,1	42,9	42,8	42,8	42,9	43,1	43,6	44,8	45,4
45,4	44,8	43,6	43,1	42,9	42,8	42,8	42,9	43,1	43,6	44,8	45,4
45,4	44,8	43,7	43,2	43,0	42,9	42,9	43,0	43,2	43,7	44,8	45,4
45,4	44,8	43,8	43,4	43,2	43,1	43,1	43,2	43,4	43,8	44,8	45,4
45,4	45,1	44,4	43,8	43,7	43,6	43,6	43,7	43,8	44,4	45,1	45,4
45,4	45,3	45,1	44,8	44,8	44,8	44,8	44,8	44,8	45,1	45,3	45,4
45,4	45,4	45,4	45,4	45,4	45,4	45,4	45,4	45,4	45,4	45,4	45,4

Figure 5.4.3.7. Temperatures (°C) of the discrete mass elements of the PCM section during melting process, 25 minutes (input conditions in Figure 5.5.1.)

47,1	47,1	47,1	47,1	47,1	47,1	47,1	47,1	47,1	47,1	47,1	47,1
47,1	47,0	46,7	46,6	46,4	46,3	46,3	46,4	46,6	46,7	47,0	47,1
47,1	46,7	46,1	45,5	45,1	44,8	44,8	45,1	45,5	46,1	46,7	47,1
47,1	46,6	45,5	44,5	43,8	43,6	43,6	43,8	44,5	45,5	46,6	47,1
47,1	46,4	45,1	43,8	43,3	43,2	43,2	43,3	43,8	45,1	46,4	47,1
47,1	46,3	44,8	43,6	43,2	43,0	43,0	43,2	43,6	44,8	46,3	47,1
47,1	46,3	44,8	43,6	43,2	43,0	43,0	43,2	43,6	44,8	46,3	47,1
47,1	46,4	45,1	43,8	43,3	43,2	43,2	43,3	43,8	45,1	46,4	47,1
47,1	46,6	45,5	44,5	43,8	43,6	43,6	43,8	44,5	45,5	46,6	47,1
47,1	46,7	46,1	45,5	45,1	44,8	44,8	45,1	45,5	46,1	46,7	47,1
47,1	47,0	46,7	46,6	46,4	46,3	46,3	46,4	46,6	46,7	47,0	47,1
47,1	47,1	47,1	47,1	47,1	47,1	47,1	47,1	47,1	47,1	47,1	47,1

Figure 5.4.3.8. Temperatures (°C) of the discrete mass elements of the PCM section during melting process, 50 minutes (input conditions in Figure 5.5.1.)

49,7	49,7	49,7	49,7	49,7	49,7	49,7	49,7	49,7	49,7	49,7	49,7
49,7	49,6	49,5	49,3	49,2	49,1	49,1	49,2	49,3	49,5	49,6	49,7
49,7	49,5	49,0	48,5	48,1	47,9	47,9	48,1	48,5	49,0	49,5	49,7
49,7	49,3	48,5	47,7	47,0	46,5	46,5	47,0	47,7	48,5	49,3	49,7
49,7	49,2	48,1	47,0	45,8	44,7	44,7	45,8	47,0	48,1	49,2	49,7
49,7	49,1	47,9	46,5	44,7	43,6	43,6	44,7	46,5	47,9	49,1	49,7
49,7	49,1	47,9	46,5	44,7	43,6	43,6	44,7	46,5	47,9	49,1	49,7
49,7	49,2	48,1	47,0	45,8	44,7	44,7	45,8	47,0	48,1	49,2	49,7
49,7	49,3	48,5	47,7	47,0	46,5	46,5	47,0	47,7	48,5	49,3	49,7
49,7	49,5	49,0	48,5	48,1	47,9	47,9	48,1	48,5	49,0	49,5	49,7
49,7	49,6	49,5	49,3	49,2	49,1	49,1	49,2	49,3	49,5	49,6	49,7
49,7	49,7	49,7	49,7	49,7	49,7	49,7	49,7	49,7	49,7	49,7	49,7

Figure 5.4.3.9. Temperatures (°C) of the discrete mass elements of the PCM section during melting process, 75 minutes (input conditions in Figure 5.5.1.)

Finally, the corresponding electrical model is shown for a better understanding of the PCM model. It provides a clear idea of the PCM role as heat store. As explain before, it delays temperature rise, but in a long enough time interval the heat balance must be null for recovering the initial temperature.

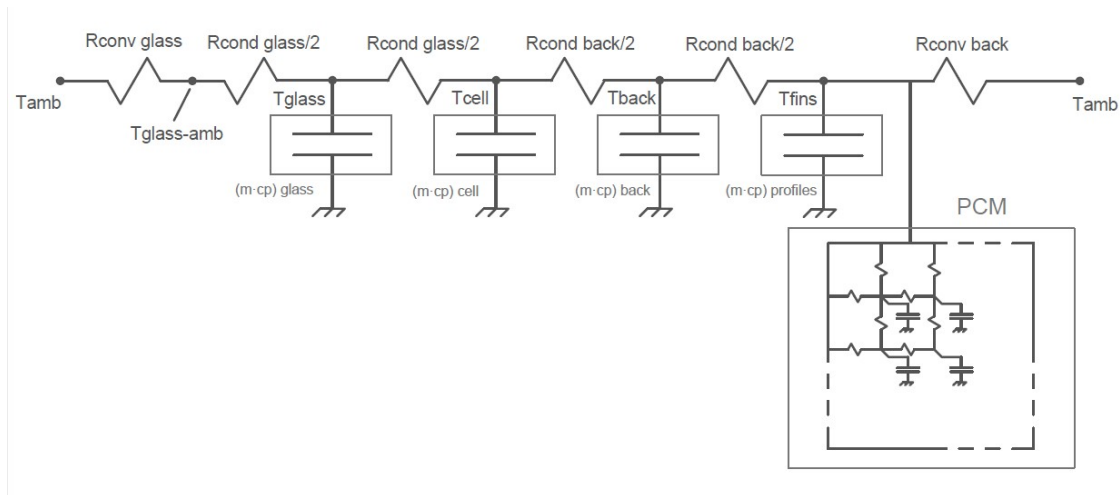


Figure 5.4.3.1. Electrical analogy of the PCM-cooled panel thermal model

## 5.5. Comparative study of the cooling methods

The aim of this chapter is to compare by simulation the performance of the three presented models, in order to analyse and understand the theoretical basis behind the thermal behavior of the three systems.

Firstly, the respective back temperature of the three panels is plotted for two different days. The results and the weather conditions (ambient temperature, wind speed and solar radiation) are shown in Figure 5.5.1. and Figure 5.5.3. As can be seen, both fins and PCM cooling methods keep the temperature substantially lower most of the time, specially at high irradiance periods. Nevertheless, functions tendency in the case of both cooled panels differs.

In the case of **fins panel**, temperature rise is slower than in standard panel, due to two reasons. First, heat dissipation is higher on the back thanks to larger air contact area and, second, aluminum fins adds an additional mass to be heated, so increases the total heat capacity of the system. As for the temperature drop period the slope of the function is lower in the case of the fins panel. On the one hand, the convective thermal resistance is lower due to the fins, which increase dissipation to ambient. However, on the other hand, the difference to the ambient temperature is smaller and the aluminum fins increase the thermal inertia, thus, might happen that the stored heat to be dissipated after temperature peak is higher.

As for the **PCM panel** function, the effect of the heat transferred to the PCM can be perfectly observed. It should be noted that in the melting interval (40-44 °C) temperature experience a drastic drop and keeps steady values even though the heat absorption by the system

continues, since this heat is stored in the PCM as latent heat in its phase change. In Figure 5.5.2. can be noted that, for days of high solar radiation, once the melting interval is exceeded, the temperature rise is again fast and can reach higher peaks than in the case of fins panel. Another important point to state is the slower drop of the temperature, due to dissipation of the significant heat energy stored in the PCM. In the solidification interval it keeps again steady values. In this respect, looking at the graphs, the main benefit and the main drawback of PCM-cooling is clear. The positive aspect are the low temperature values in the highest radiation interval, when most of the energy is generated. If the radiation is not too high, PCM-cooled panel may even present the lowest temperature peak, as shown in Figure 5.5.4. The inconvenient is the long time necessary to cool again the panel. During this cooling interval, although the incident radiation available to generate electricity is lower, the electrical efficiency is lower as well, compared to the other two options.

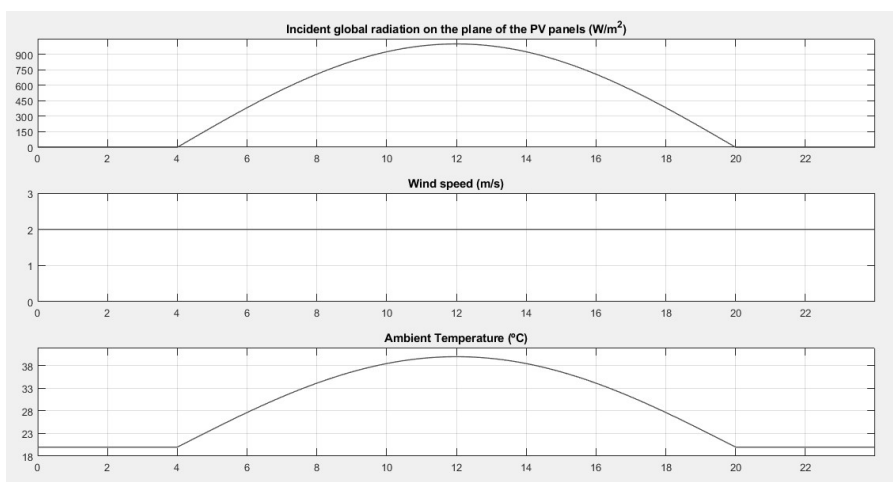


Figure 5.5.1. Input solar radiation, ambient temperature and wind speed conditions for comparing the performance of the three panels (see Figure 5.5.2.)

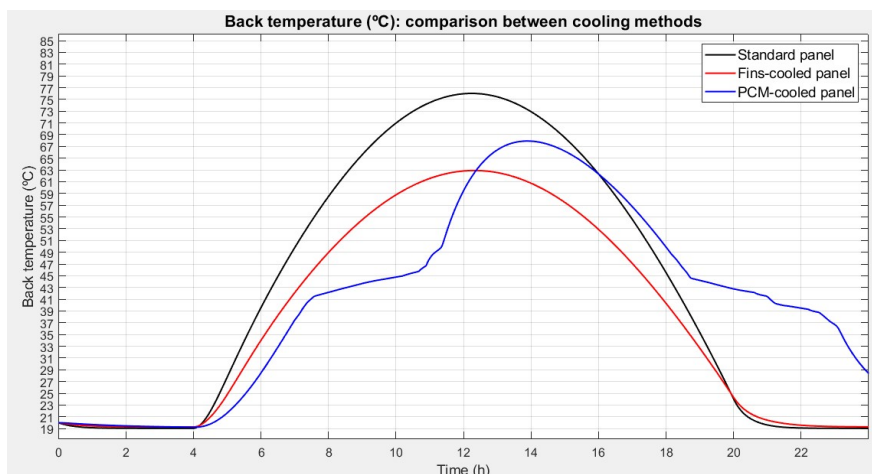


Figure 5.5.2. Comparison of back temperature function of the three panels (input conditions of Figure 5.5.1.)

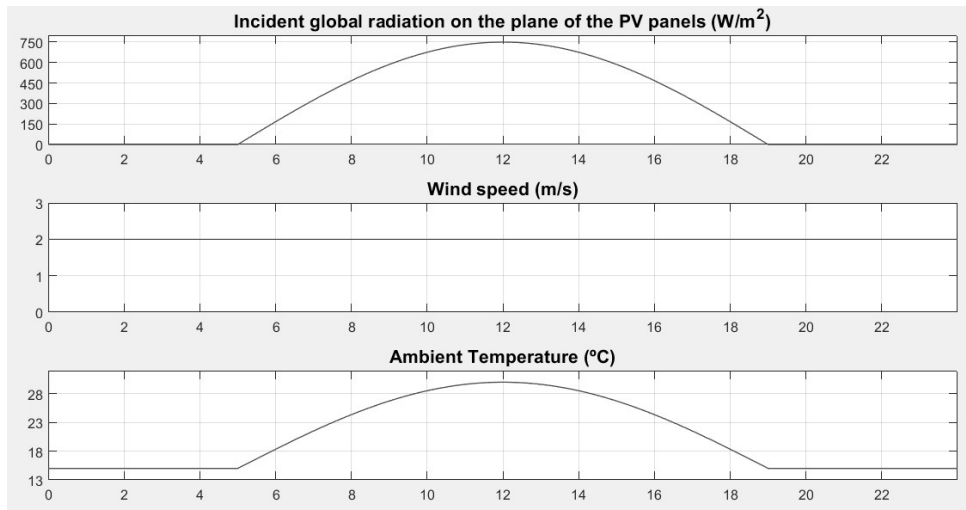


Figure 5.5.3. Input solar radiation, ambient temperature and wind speed conditions for comparing the performance of the three panels (see Figure 5.5.4.)

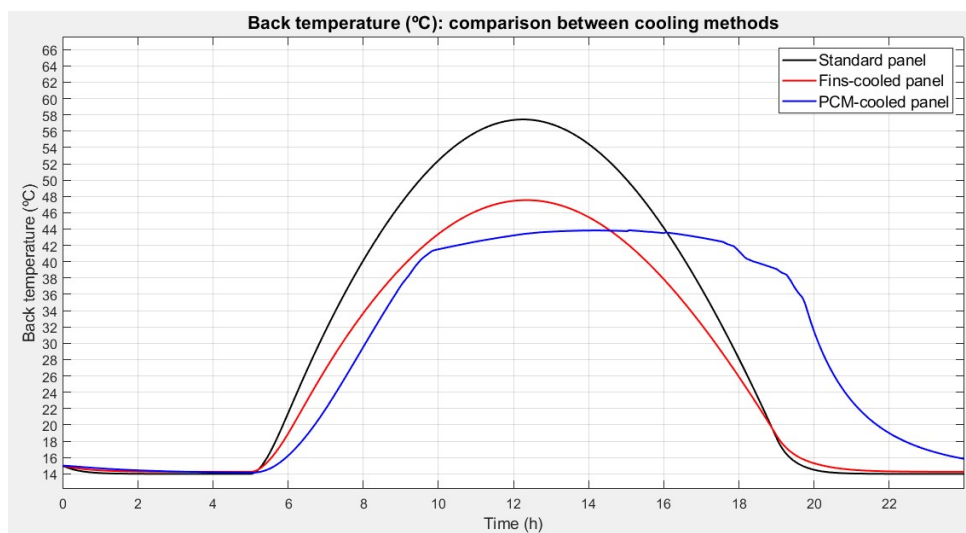


Figure 5.5.4. Comparison of back temperature function of the three panels (input conditions of Figure 5.5.3.)

Another interesting approach to analyse is the function of the **heat balance** in the panel over an entire simulated day. In Figures 5.5.5., 5.5.6 and 5.5.7. this function is plotted for the three panels and the input conditions given by Figure 5.5.3. As shown, the difference between the input heat energy (positive) and the output heat energy (negative) is the accumulated heat stored in the panel, which is responsible of the temperature variation. Note its clear correlation with the temperature function given by Figure 5.5.4. It must also be stated that this accumulated heat also has to be related with the total heat capacity of the specified panel. This is the reason why, despite the higher accumulated heat energy in the case of the fins panel, its temperature is lower compared to the standard panel, since the additional heat capacity of the aluminum fins must be taken into account. In Figure 5.5.7. can be observed how the accumulated heat remain during a longer time in the PCM panel, due to the internal

thermal properties of the PCM. It is for this reason that the temperature drop is slower in this case.

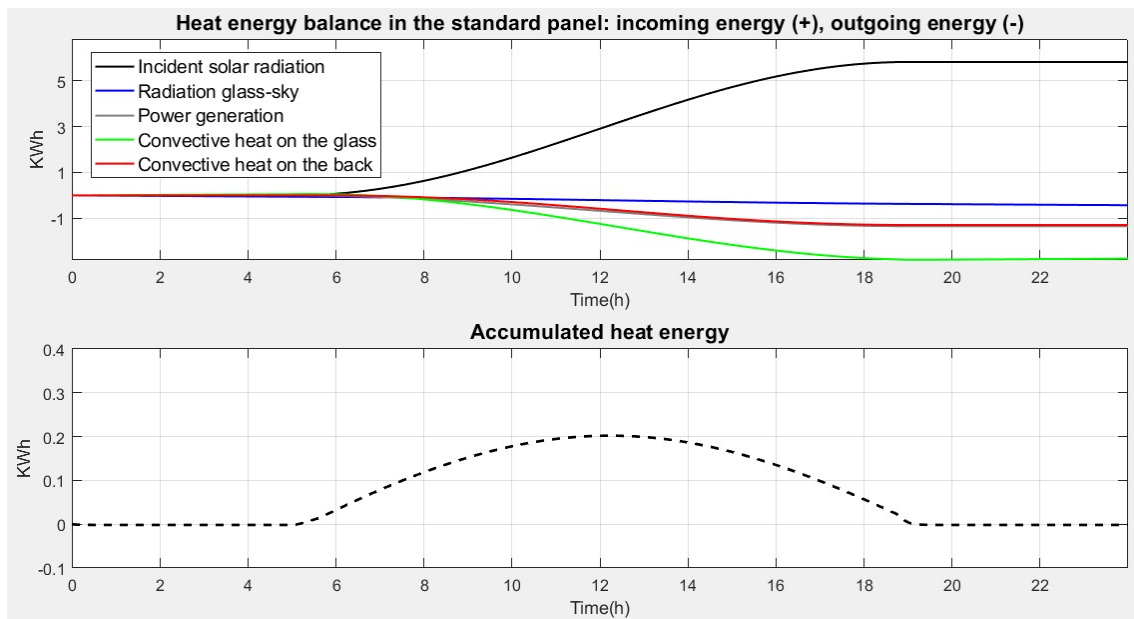


Figure 5.5.5. Standard panel: functions of the input (+) and the output (-) heat energy fluxes and accumulated net heat energy in the panel

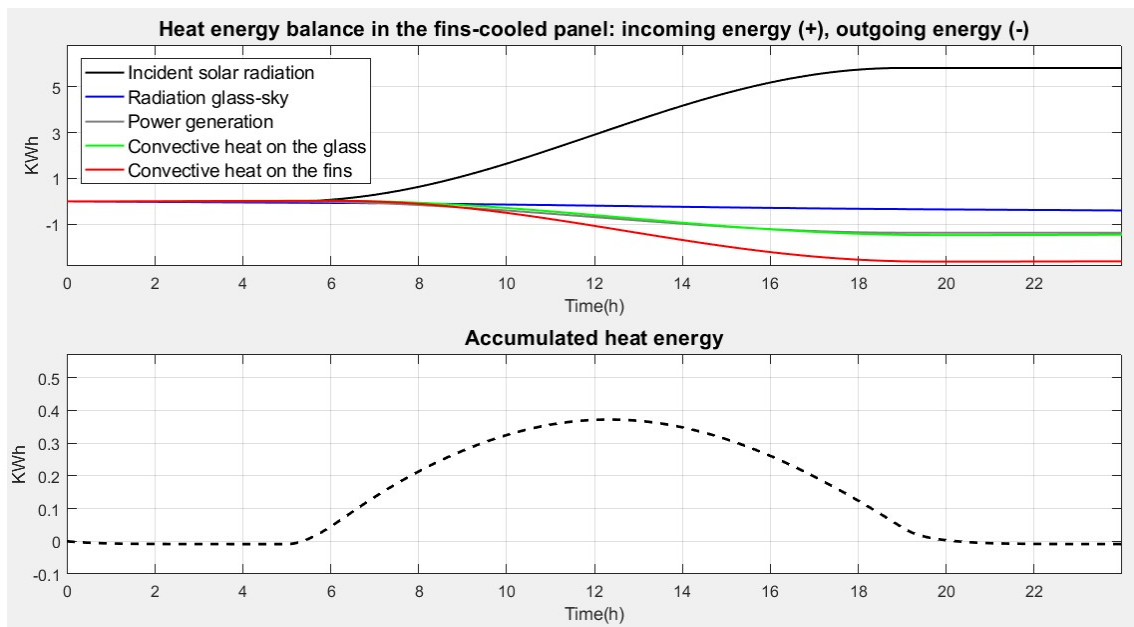


Figure 5.5.6. Fins panel: functions of the input (+) and the output (-) heat energy fluxes and accumulated net heat energy in the panel



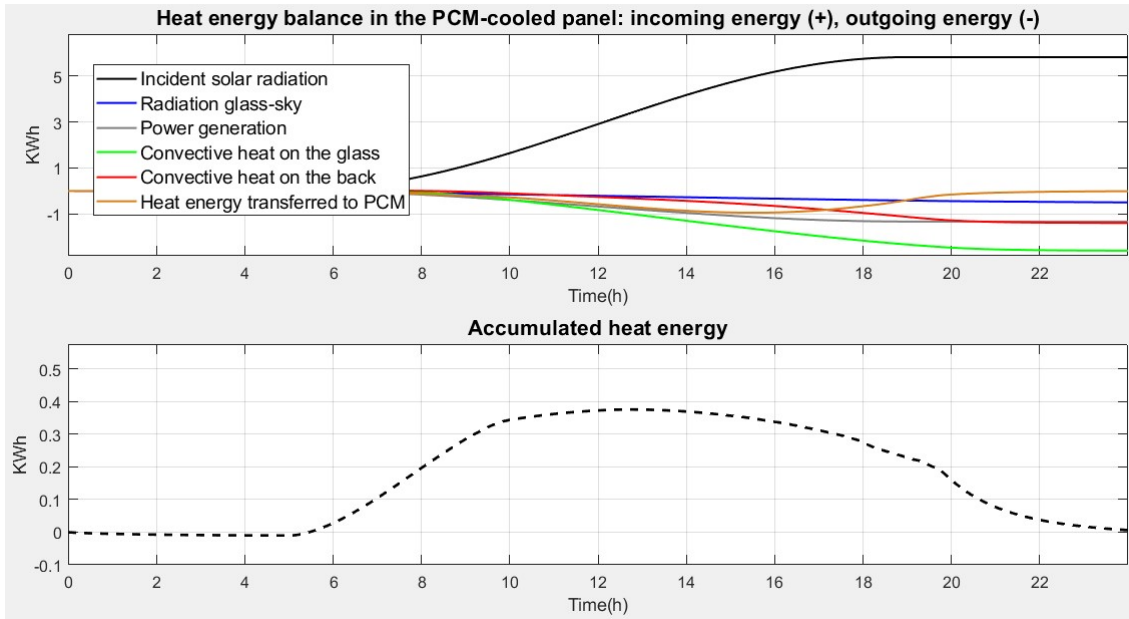


Figure 5.5.7. PCM panel: functions of the input (+) and the output (-) heat energy fluxes and accumulated net heat energy in the panel

On the other hand, it is important to understand the **impact of the wind** in the temperature function because it can be the source of the simulation error in some cases, as will be explained in chapter 6. In Figure 5.5.8. the same irradiance and ambient temperature conditions given by Figure 5.5.3. are simulated for the standard panel, but the constant wind speed is altered to analyse its effect in the change of the back temperature function. It is observed a difference of around 6 K in the peak temperature for a wind speed from 2 to 6 m/s, thus, the wind impact can be remarkable.

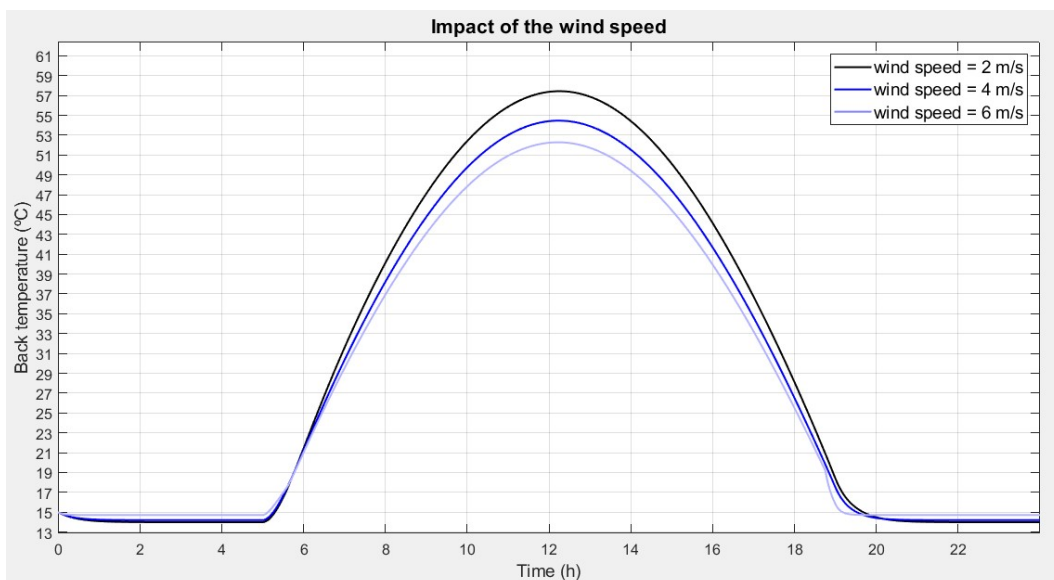


Figure 5.5.8. Wind speed impact on the temperature of the panel (input conditions of Figure 5.5.3.)

## 6. Validation of the simulation model

In this chapter, a comparative study between the simulated back temperature and the real measured data of this temperature is performed. The aim of this study is to analyse the accuracy and the error of the developed models as for the temperature, which is the key variable to be calculated, and the power generation, which is required for the conclusions of the economical study. For this purpose an error interval is estimated for both variables, according to the results of the validation.

### 6.1. Source of errors in the simulation

As explained in the previous chapters, some assumptions are made in the model construction. Some of them are inevitable due to the difficulty of controlling some external variables, like the wind direction, and others are made in order to find a compromise between a realistic model, the simplicity of it and an adequate simulation time. Besides these aspects, other external factors are a source of uncertainty for the results. Considering this, all the elements which can cause some error in the simulation output are listed below:

- **Wind impact** is a very difficult factor to predict in this case, due to its changing behavior and to the complex geometry of the system. When the wind flow has a specific direction it may change its influence on the convection due to some external elements which act as a barrier. However, this aspect is not reflected in the simulated temperature, since wind direction is not considered in the model. It must also be added that the sample time for the wind speed measurement is 5 minutes, which can be quite high, taking into account the constant changing behavior that the wind may have. These wind speed points correspond to mean values in the intervals and an interpolation is performed for the values inside these intervals.
- As explained before, the measurements of the wind speed and the ambient temperature are obtained from a database. These data correspond to a weather station, which is not exactly in the same emplacement as the installation. Besides the influence of this factor in the wind speed, which was commented on before, it can impact also in the accuracy of the **ambient temperature** of the system, which might differ slightly from the used temperature data.
- It must also be stated that **thermocouples** can cause some error in the measurements of the real back temperature, which also can impact in the difference with the simulated back temperature. The source of this error can be in the own scattering of the measurements, due to the noise coming from any part of the hardware. Besides, a good calibration is not easy to achieve because small changes in the thermocouples arrangement or in the probe position after the calibration process can affect to the calculated linear function. This function can also experiment small changes over time.



- Finally, as was stated in the previous chapters, **the used model is not ideal**, thus, some comments must be done as for its impact in the error:
  - The first point to state is the **thermal resistances calculation**. Conductive thermal resistances can present some error coming from the used parameters estimation but convective thermal resistances are more likely to present a higher error, due to the simplifications considered in the model as for the equations and the wind.
  - The **mass of the elements** may also have some impact in the output temperature, since errors in their calculation, due to deviations from the real elements dimensions or material density, change the thermal inertia of the system.
  - The estimation of the **radiated heat absorbed by the glass and the PV cells** must also be included in this analysis, since, as explained in chapter 2, some approximations were made.

## 6.2. Comparison of the simulation output and real measurements

This section shows the obtained output of the simulation for the studied days in the validation location. This **output** consists of the function of the **temperature on the back of the panel** and the variables related with the power generation: the **output power**, the **thermal efficiency** and the **electricity generation**. Besides, for a better understanding, the **input** variables are also plotted: **incident solar radiation**, **wind speed** and **ambient temperature**. In **Annex 1**, the detailed mentioned data is given for some simulated days, which are considered good references for the study of the model functioning.

The aim of this section is to validate the suitability of the developed program to achieve reliable results in the study. To this end, the magnitude of the error in the temperature function must be analysed and some reasons are provided for the difference between real temperature and simulated temperature. Besides, some aspects about the different behavior of the three panels are explained in order to check its concordance with the expected one.

Firstly, a typical function of the temperature on the back of the standard panel is shown in Figure 6.2.1. It should be noted that the simulated temperature in the starting time period is very similar to the ambient temperature. This is because, during this time, wind speed and solar radiation are null, thus, back temperature tends to ambient temperature. However, a discordance can be observed between real and simulated temperature in this period, which might either be due to a difference between the ambient temperature at the weather station and at the panels location or to an error in the thermocouples calibration. The inconvenient of this initial error is that it is transmitted to the following simulation steps but a good approximation is achieved in the period of highest temperatures, when most of the generated

energy is obtained and a good simulation performance is more important. Despite this error, a good matching is seen in the simulated function slope over the entire day

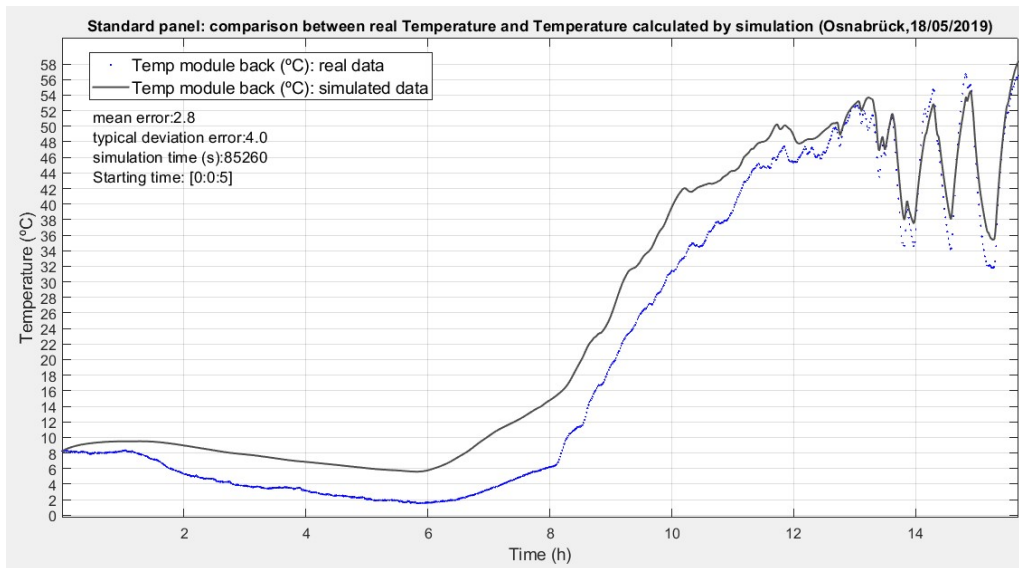


Figure 6.2.1. Standard panel: comparison between real temperature and temperature calculated by simulation (Osnabrück, 18/05/2019)

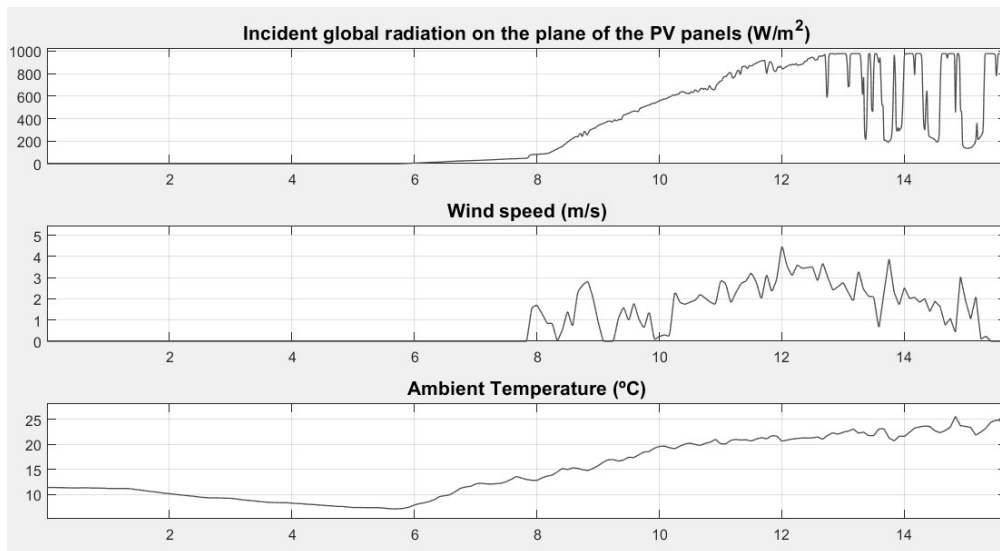


Figure 6.2.2. Input conditions for temperature plotted in Figure 6.2.1.

In Figure 6.2.3. it is interesting to note the difference of the error in two intervals apparently similar, as for the radiation, wind and ambient temperature conditions. This is probably because the uncontrolled impact of wind direction, taking into account the high wind conditions of the studied day and, therefore, its significant impact. As explained before, for some directions of the wind the elements of the surroundings act as a barrier for it, so, in these cases, the real impact of the wind is lower than expected considering the sensor measurements, which are not affected by these barriers. This aspect is reflected in the higher values of the real temperature compared with the output of the simulation.

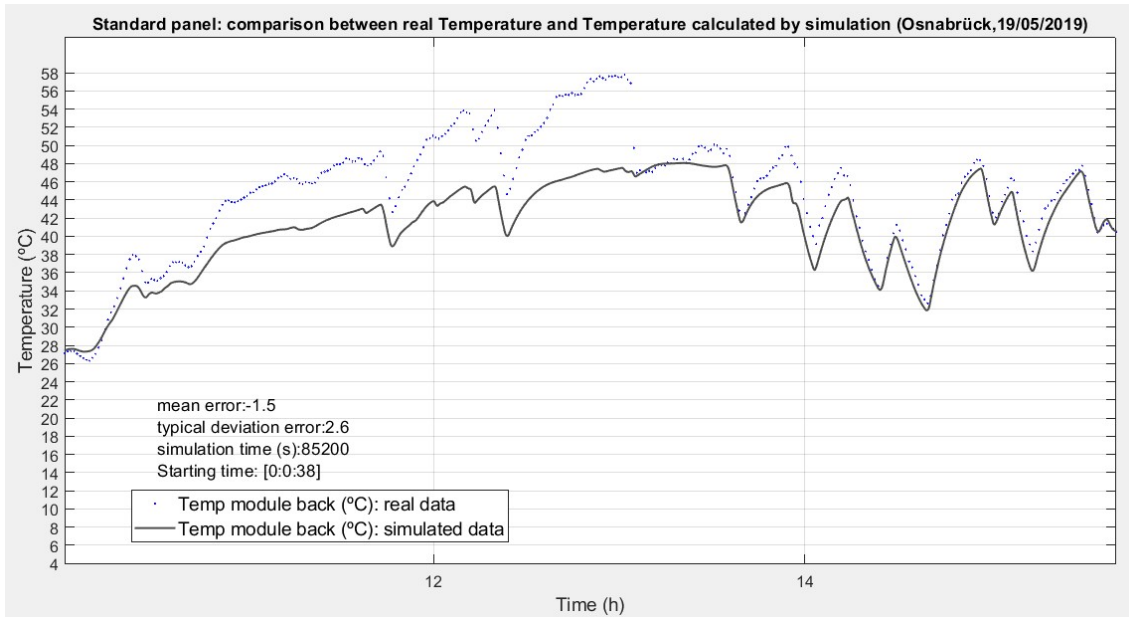


Figure 6.2.3. Standard panel: comparison between real temperature and temperature calculated by simulation (Osnabrück, 19/05/2019)

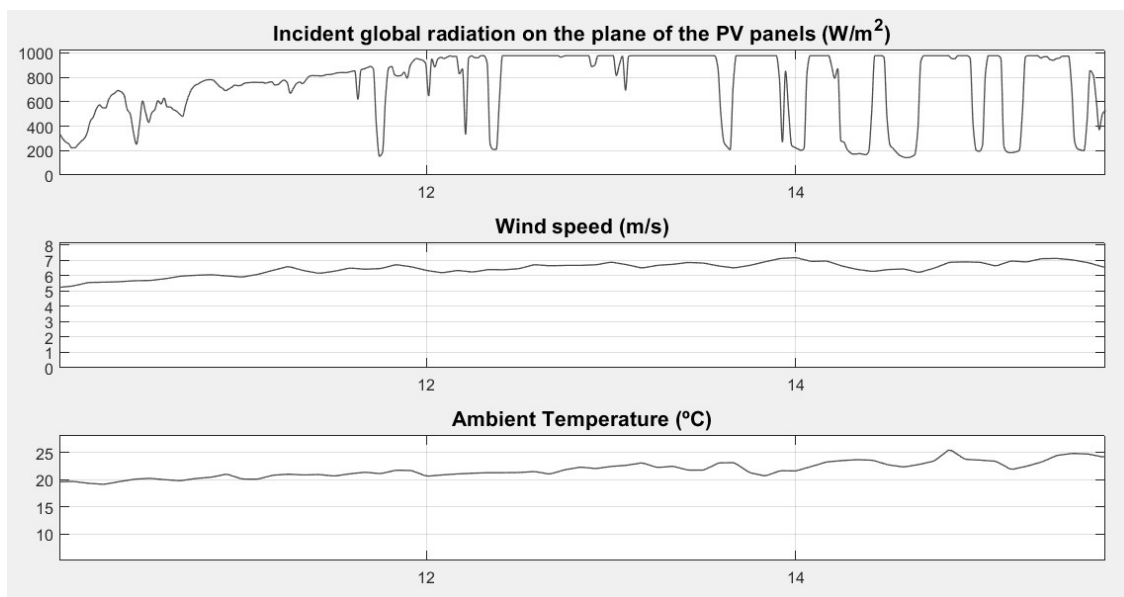


Figure 6.2.4. Input conditions for temperature plotted in Figure 6.2.3.

The purpose of Figure 6.2.5. is to provide an example of the different behavior of standard panel and fins panel, by showing the back temperature function of the mentioned panels over one entire day with similar weather conditions in both cases (see Annex 1). The main difference which can be observed is the lower temperatures in the interval around peak temperatures in the case of fins-cooled panel. In this panel, the temperature rise is substantially slower during the warm-up period. It is also important to state the slighter

fluctuation in the fins panel temperature, which is due to the higher global heat capacity of the panel, which, in turn, implies a lower function slope for the same power heat balance.

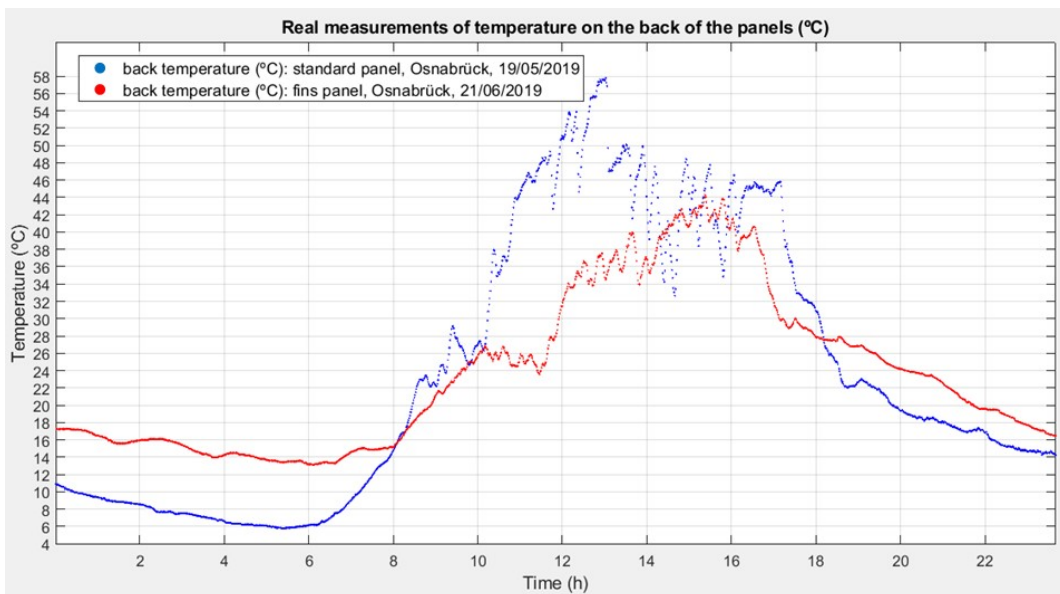


Figure 6.2.5. Comparison of real measurements of back temperature corresponding to standard panel and fins panel under similar input conditions

A typical daily temperature function for the PCM-cooled panel is given in Figure 6.2.6. The input conditions (see Annex 1) correspond to a day of high incident solar radiation. In these cases, a steady temperature interval is observed in the phase change period (40-45 °C), caused by the high latent heat absorption of the PCM. A good matching between real and simulated temperature is observed in this interval. The duration of this interval is slightly different in both cases, which is probably due to a non-ideal approximation of the total PCM mass.

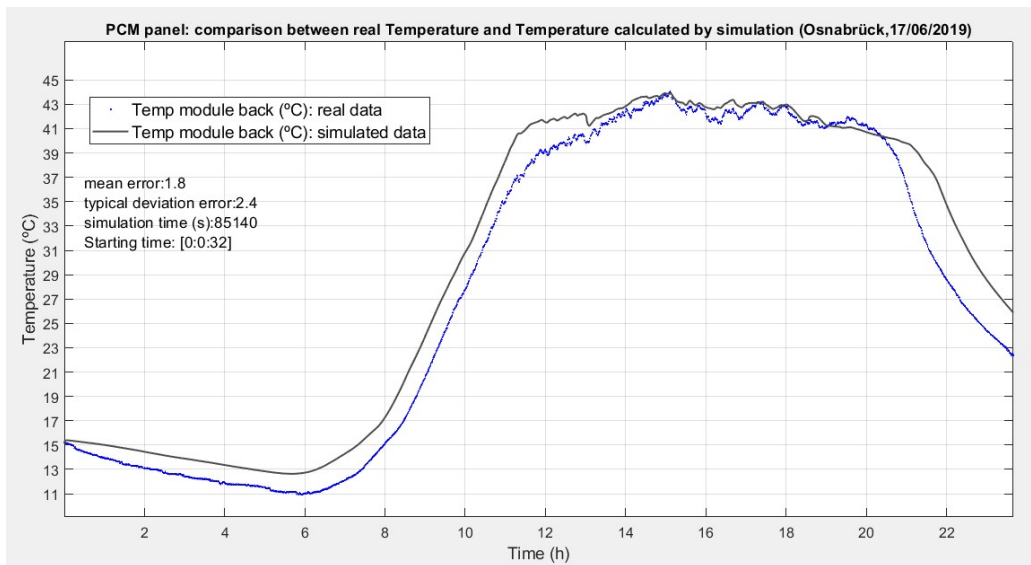


Figure 6.2.6. PCM panel: comparison between real temperature and temperature calculated by simulation (Osnabrück, 17/06/2019)

### 6.3. Estimation of the simulation error

The aim of this section is to analyse the accuracy of the simulation by calculating its error for the available data, corresponding to all the measured days in the validation location. In this way, a more realistic conception of the reliability of the simulation results is achieved. The reference term used to test the error is the **Root Mean Square Error (RMSE)**, calculated as follows:

$$\sqrt{\frac{\sum_n (\text{Simulated value} - \text{Real value})^2}{n}}$$

$n$ : number of comparisons

Note that RMSE gives the absolute error but, since this is an approximate estimation of the error, its sign is not considered. The following tables list the available data and the calculated error for each panel. The two variables whose error is calculated are the temperature on the back of the panel and the daily generation.

Date	Simulation time (s)	Simulated back temperature error (Temp back sim – Temp back real)	Electricity generation		
		RMSE (K)	Real (Wh)	Simulated (Wh)	Sim. error (%)
13/11/2018	14280	1.6	191	191	0.00
21/11/2018	11340	0.6	111	111	0.00
23/11/2018	10680	0.9	390	395	1.28
17/05/2019	28800	0.8	152	152	0.00
18/05/2019	85260	4.1	1192	1177	-1.26
19/05/2019	85200	2.7	1240	1255	1.21
20/05/2019	47400	4.5	125	128	2.40
28/06/2019	39180	2.3	933	924	-0.96

Table 6.3.1. Standard panel: estimation of Root Mean Square Error (RMSE) according to the simulations performed

Date	Simulation time (s)	Simulated back temperature error (Temp back sim – Temp back real)	Electricity generation		
		RMSE (K)	Real (Wh)	Simulated (Wh)	Sim. error (%)
28/05/2019	44520	1.5	247	250	1.21
30/05/2019	85200	1.0	450	448	-0.44
31/06/2019	85260	1.1	1088	1089	0.09
20/06/2019	85260	1.6	963	963	0.00
21/06/2019	85200	1.3	1350	1350	0.00
22/06/2019	85260	3.1	1545	1567	1.42
23/06/2019	85260	2.4	1496	1511	1.00
24/06/2019	85260	3.5	1486	1508	1.48
25/06/2019	85200	4.0	1418	1438	1.41

Table 6.3.2. Fins panel: estimation of Root Mean Square Error (RMSE) according to the simulations performed

Date	Simulation time (s)	Simulated back temperature error (Temp back sim – Temp back real)	Electricity generation		
		RMSE (K)	Real (Wh)	Simulated (Wh)	Sim. error (%)
22/05/2019	85380	1.6	767	767	0
23/05/2019	85200	2.2	1260	1246	0.00
24/05/2019	63840	2.1	1037	1031	-1.11
07/06/2019	85260	2.5	1486	1473	-0.58
08/06/2019	85260	4.4	703	689	-0.87
10/06/2019	85200	4.5	981	965	-1.99
11/06/2019	85200	3.2	939	929	-1.63
12/06/2019	86040	3.4	436	431	-1.06
13/06/2019	85200	5.4	1319	1286	-1.15
15/06/2019	85140	1.3	947	941	-2.50
16/06/2019	85140	1.3	1005	1003	-0.63
17/06/2019	85140	2.4	1326	1316	-0.20

Table 6.3.3. PCM panel: estimation of Root Mean Square Error (RMSE) according to the simulations performed

Taking into account the shown data, the error is calculated for the whole simulated time (see Table 6.3.4.), joining all the simulations. In the case of the daily generation error, it is calculated by weighing each simulated day according to the corresponding simulation time. Because this is a rough estimation, since the number of comparisons carried out is small, an **error of 2%** is considered a proper value in the case of the power generation for the simulations performed in the economical study, which is exposed in chapter 7.

Estimated RMSE (Root Mean Square Error)		
	Back Temperature (K)	Daily power generation (%)
<b>Standard panel</b>	3.20	1.35
<b>Fins-cooled panel</b>	2.45	0.98
<b>PCM-cooled panel</b>	3.15	1.26

Table 6.3.4. Estimation of the total RMSE corresponding to the back temperature and the error percentage of the daily power generation in the case of the three studied panels

## 7. Study of the economic viability

### 7.1. Cost estimation for the three module options

The goal of this section is to calculate the total initial investment for the three mentioned alternatives and the annual expenditure. The Table 7.1.3. presents the detailed budget of the standard panel, the fins-cooled panel and the PCM-cooled panel. Different suppliers were consulted for the price estimation of each component. For a more realistic analysis, taking into account that there are many factors which can affect the price of the component, an approximate confidence range is provided, thus, the minimum, the maximum and the mean value is shown in the table in each case.

In the case of the aluminum profiles used in the cooling systems, it is difficult to find a good reference for the price, since it is very changing depending on the specific features of the product. For this reason, an approximation is performed, based on the material cost and in the indirect costs (manufacturing, logistics...). This last term is calculated as a percentage of the direct costs. The calculated costs are shown in Table 7.1.1. and Table 7.1.2.

Cost estimation for 'L' aluminum profiles			
	Min	Mean	Max
Material cost (€/Kg)	1.20	1.50	1.80
Mass per unit (Kg)	-	0.462	-
Direct costs per unit (€/unit)	0.55	0.69	0.82
Indirect costs per unit: 150-200% direct cost (€/unit)	0.83	1.24	1.65
Total manufacturing cost per unit (€/unit)	1.38	1.93	2.47
Profit margin: 30-60% total manufacturing cost (€/unit)	0.41	0.95	1.48
Installation costs: 15% total manufacturing cost (€/unit)	0.21	0.30	0.38
<b>Total price per unit (€/unit)</b>	<b>2.00</b>	<b>3.17</b>	<b>4.33</b>

Table 7.1.1. Cost estimation for 'L' aluminum profiles

Cost estimation for square aluminum profiles			
	Min	Mean	Max
Material cost (€/Kg)	1.20	1.50	1.80
Mass per unit (Kg)	-	0.673	-
Direct costs per unit (€/unit)	0.81	1.01	1.21
Indirect costs per unit: 150-200% direct cost (€/unit)	1.21	1.82	2.42
Total manufacturing cost per unit (€/unit)	2.02	2.83	3.63
Profit margin: 30-60% total manufacturing cost (€/unit)	0.61	1.40	2.18
Installation costs: 15% total manufacturing cost (€/unit)	0.30	0.47	0.54
<b>Total price per unit (€/unit)</b>	<b>2.93</b>	<b>4.70</b>	<b>6.35</b>

Table 7.1.2. Cost estimation for square aluminum profiles

Standard panel								
Element	Unit cost (€)				Qty.	Total cost (€)		
	min	mean	max	unit		min	mean	max
PV panel + microinverter	220	270	320	ud.	1	220	270	320
Support structure	10	20	30	ud.	1	10	20	30
Installation cost (5%)	-	-	-	-	-	12	15	18
						<b>242</b>	<b>305</b>	<b>368</b>
Fins-cooled panel								
Element	Unit cost (€)				Qty.	Total cost (€)		
	min	mean	max	unit		min	mean	Max
PV panel + microinverter	220	270	320	ud.	1	220	270	320
Support structure	10	20	30	ud.	1	10	20	30
Aluminum fins	2	3.2	4.4	ud.	56	112	179	246
Installation cost (5%)	-	-	-	-	-	23	27	32
						<b>365</b>	<b>496</b>	<b>628</b>
PCM-cooled panel								
Element	Unit cost (€)				Qty.	Total cost (€)		
	min	mean	max	unit		min	mean	Max
PV panel + microinverter	220	270	320	ud.	1	220	270	320
Support structure	10	20	30	ud.	1	10	20	30
PCM Aluminum profiles	2.9	4.7	6.4	ud.	34	99	160	218
PCM (RT44HC)	3	5.50	8	Kg	16	48	88	128
Installation cost (5%)	-	-	-	-	-	24	30	36
						<b>401</b>	<b>568</b>	<b>732</b>

Table 7.1.3. Calculated budget of the three PV panel options

The next step is to calculate the annual cost of the energy generation for each option. Considering, in addition to the **initial investment**, the **interest rate** and the **operational cost**. This last includes the permanent maintenance and inspection cost associated to the panel. The following relation is used:

$$C_{annual} = Inv \cdot (a + k_{op}) \quad (7.1.1)$$

$$a = \frac{p}{1 - (1 + p)^{-n}} \quad (7.1.2)$$

$C_{annual}$ : annual electricity generation cost

$Inv$ : initial investment

$k_{op}$ : operational cost factor

$a$ : annuity factor

$p$ : interest rate

$n$ : lifetime of the panel

In this case, an **operational cost factor** between **1.5** and **3%** and a an **interest rate** between **2** and **8%** are considered realistic values. On the other hand, most authors agree that **25 years** is a good estimate of the **mean lifetime** of crystalline PV panels. Taking all this into consideration, Table 7.1.4. lists the annual expenditure for each cooling alternative:



<b>Operational cost factor. <math>k_{op}</math></b>									1.5 – 3 %		
<b>Interest rate. <math>p</math></b>									2 – 8 %		
<b>Annuity factor. <math>a</math></b>									5.1 – 9.4 %		
<b>Standard panel</b>											
Initial investment (€)			Annuity (€)			Operational annual cost (€)			annual installation cost (€)		
min	mean	max	min	mean	max	min	mean	max	min	mean	Max
242	305	368	12.3	23.5	34.6	3.6	7.3	11.0	15.9	30.8	45.6
<b>Fins-cooled panel</b>											
Initial investment (€)			Annuity (€)			Operational annual cost (€)			annual installation cost (€)		
min	mean	max	min	mean	max	min	mean	max	min	mean	max
365	496	628	18.6	38.8	59.0	5.5	12.2	18.8	24.1	51.0	77.8
<b>PCM-cooled panel</b>											
Initial investment (€)			Annuity (€)			Operational annual cost (€)			annual installation cost (€)		
min	mean	max	min	mean	max	min	mean	max	min	mean	max
401	568	732	20.5	44.7	68.8	6.0	14.7	22.0	26.5	58.7	90.8

Table 7.1.4. Estimation of the annual expenditure corresponding to the three PV panel options

As shown in the previous table a wide range is obtained in the estimation of the annual cost in each case, which represents the uncertainty of the economical factor. However, in the study of the viability presented in the section 7.3.2. it is important to pay attention to the mean values for the comparison.

## 7.2. Choice of locations for the study

For a complete evaluation of the studied cooling options, its performance is studied in **15 different locations** around the world. These locations differ in their climatic conditions and their latitude, which have a critical impact on the annual power generation and, therefore, on the economic viability of the installation. In this sense, the choice of the locations pretend to provide a variety of conditions in the study and it is because of this that each location has its own particularities. This is shown in Figure 7.2.1. and Table 7.2.1., where the 15 locations are listed, as well as a summary of their climatic conditions, that correspond to the typical annual data which is used in the simulation.

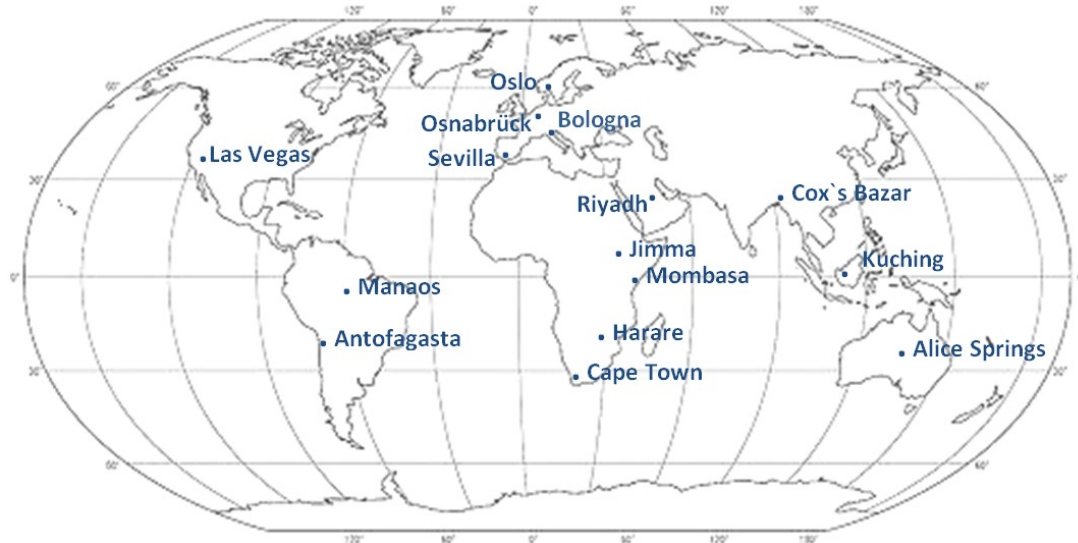


Figure 7.2.1. World locations chosen for the economical study

Location	Lat.	Long.	Incident radiation (KWh/m <sup>2</sup> )			Ambient temperature (°C)			Wind speed (m/s)		
			Min. total month	Total year	Max. total month	Min. mean month	Mean year	Max. mean month	Min. mean month	Mean year	Max. mean month
Alice Springs (Australia)	-24.30	134.9	164	2397	225	11.5	21.2	29.3	1.2	2.4	3.9
Antofagasta (Chile)	-24.35	70.60	129	2237	229	14.0	17.0	20.5	2.9	4.0	4.9
Bologna (Italy)	45.53	11.30	28	1216	181	1.1	12.9	23.9	1.1	1.7	2.1
Cape Town (Sth. Africa)	-34.80	18.42	92	2043	244	12.3	16.5	20.9	4.0	5.2	7.7
Cox's Bazar (Bangladesh)	21.45	92.97	116	1932	194	20.8	26.0	29.0	0.9	2.1	3.1
Harare (Zimbabwe)	-18.18	31.50	144	2066	201	14.3	18.9	21.7	2.3	3.4	4.5
Jimma (Ethiopia)	8.68	37.84	130	1956	187	17.2	18.2	19.4	0.3	0.7	1.2
Kuching (Malaysia)	2.55	110.33	110	1538	139	25.4	26.2	27.0	0.8	1.0	1.3
Las Vegas (U. S. A.)	36.11	-115.83	145	2306	224	7.8	19.8	33.1	3.1	4.5	6.0
Manaos (Brazil)	-3.88	-60.97	121	1747	169	25.8	26.8	27.9	0.7	1.0	1.3
Mombasa (Kenya)	-4.96	40.67	141	1977	181	23.7	25.9	28.1	2.7	3.5	4.3
Oslo (Norway)	60.91	11.76	9	1002	165	-3.8	6.6	17.5	1.2	2.3	2.8
Osnabrück (Germany)	52.27	8.5	22	1126	140	2.4	10.3	18.4	2.4	3.1	3.8
Riyadh (S. Arabia)	25.77	47.74	143	2361	226	14.0	26.2	36.4	1.1	3.0	4.3
Sevilla (Spain)	37.38	-6.3	101	1971	223	10.4	18.4	27.4	2.1	2.7	3.4

Table 7.2.1. Comparison of input conditions corresponding to the world locations for the study

The first aspect to note as for the input conditions is that, logically, the more irradiance over an entire year, the higher annual power generation and, in this regard, the factors with a more remarkable influence are the latitude and the sky clearness. The annual solar irradiance is expected to be higher in locations near the equator, since the extraterrestrial global irradiance is higher in these cases. However, in Table 7.2.1. can be observed that some locations has higher irradiance values than others closer to the equator, for example, in the case of Las Vegas and Manaus, which is due to the clearer skies in Las Vegas. Therefore, the latitude is not the only variable to consider as for the solar radiation. Latitude is neither the only variable to consider in the case of ambient temperature, since other factors also affect it, such as sky clearness, wind, humidity, rains or altitude.

It is also important to state that the locations with higher absolute latitudes show more contrast between maximum and minimum mean monthly values of radiation and ambient temperature. This is because the higher impact of the declination change over a year in these latitudes, which cause more fluctuations in weather conditions.

### 7.3. Simulation results for each investment option

The aim of this section is to join the calculations of the costs shown in section 7.1. with the energy output of the developed simulation, which is run for the input data of all the studied locations, corresponding to the weather conditions of one entire typical year. The desired final term is the cost of the electricity in each case. On the basis of the results obtained, a final conclusion about the economical viability of each installation in the different locations can be provided.

#### 7.3.1. Power generation

The main purpose of the built model is to provide a tool able to figure out the **power generation of the three studied PV modules during one year**, using as input data the hourly values of the solar irradiation on the specified location, as well as the corresponding data of the ambient temperature and the wind speed. To simulate realistic conditions, typical data of the entire year is used in each location. (25)

It is important to state that these results do not consider any **degradation** in the electrical performance. but the panels in the same conditions as in the validation. In the final calculation of the cost of energy. a conversion is made to take into account this factor.

A summarized table is shown below. with the annual output of the electricity generation for each location and for each panel option. A more detailed report. with the monthly results of all the locations is given in Annex 2.

LOCATION	Standard panel annual generation		Fins panel annual generation		PCM panel annual generation	
	KWh	%impr. cooling	KWh	%impr. cooling	KWh	%impr. cooling
Alice Springs (Australia)	463.2	0	484.4	+4.6	468.0	+1.0
Antofagasta (Chile)	451.1	0	468.5	+3.9	450.0	-0.2
Bologna (Italy)	251.4	0	258.6	+2.9	252.2	+0.3
Cape Town (South Africa)	412.3	0	426.7	+3.5	412.8	+0.1
Cox's Bazar (Bangladesh)	377.2	0	391.4	+3.8	380.8	+1.0
Harare (Zimbabwe)	413.7	0	429.2	+3.8	415.0	+0.3
Jimma (Ethiopia)	388.9	0	405.0	+4.1	391.2	+0.6
Kuching (Malaysia)	302.3	0	312.9	+3.5	305.0	+0.9
Las Vegas (United States)	455.8	0	472.5	+3.7	458.9	+0.7
Manaos (Brazil)	339.0	0	352.6	+4.0	342.8	+1.1
Mombasa (Kenya)	381.6	0	398.2	+4.4	385.9	+1.1
Oslo (Norway)	215.2	0	220.2	+2.3	214.8	-0.2
Osnabrück (Germany)	240.1	0	245.5	+2.3	240.0	0.0
Riyadh (Saudi Arabia)	448.7	0	468.9	+4.5	454.1	+1.2
Sevilla (Spain)	391.8	0	406.3	+3.7	394.5	+0.7

Table 7.3.1.1. Comparison of the power generation results for the three PV panel options

Two important conclusions are given below. based on the results shown in the previous table and in the tables of Annex 2:

- In the case of the fins-cooled panel. an improvement in the annual power generation is achieved for all the locations. This additional generation is in the range of **2.3 – 4.6 %**. The best performance of the fins are observed in the locations with the highest values of incident solar radiation. as Alice Springs or Mombasa. for example. This is because the higher impact of the fins cooling in the periods of high irradiance levels and. in turn. high temperatures of the cells.
- The PCM-cooled panel also provides a higher power generation but this is a more slight increase. in the range of **0 – 1.2 %**. Again. the more incident radiation. the better is the performance of the cooling method but in the cases of the lowest levels of radiation. as Antofagasta or Oslo. the impact can be even negative.

### 7.3.2. Electricity cost

Once it is known both the power generation of each alternative and its corresponding annual expenditure. the electricity cost can be calculated for each location and for each panel option. Since the electrical efficiency decrease in the panels over their lifetime. due to the degradation of the materials. an additional term is added to the power generation. which consider the mean panel performance in its entire lifetime. as for the degradation. Considering a **useful life**

of **25 years** and an **annual degradation rate of 0.8%** as realistic estimations. the following integration is calculated:

$$MLD = \frac{1}{N} \cdot \int_0^N (1 - SDR)^y dy = \frac{1}{25} \cdot \int_0^{25} (1 - 0.008)^y dy = 0.906 \quad (7.3.2.1)$$

*SDR*: system degradation rate

*MLD*: mean lifetime degradation

It should be noted that in a real installation. the shown degradation factor is not a fixed term. since the degradation is higher with more extreme weather conditions. In a more detailed study. a correlation between these two factors could be included.

For the calculation of the electricity cost. an **error of 2%** is included in the **power generation**. which is considered a realistic approach. taking into account the error calculated in section 6.3. during the validation stage. This error and the estimation interval for the annual cost of the installation are considered to calculate a minimum. maximum and mean cost of electricity for each case. The following table shows the summarized economical results for all the locations. A more detailed presentation of the results is given in Annex 3.

LOCATION	Standard panel electricity cost (€/KWh)			Fins panel electricity cost (€/KWh)			PCM panel electricity cost (€/KWh)		
	min	mean	max	min	mean	max	min	mean	max
Alice Springs (Australia)	0.037	<b>0.073</b>	0.111	0.054	<b>0.116</b>	0.181	0.061	<b>0.138</b>	0.219
Antofagasta (Chile)	0.038	<b>0.075</b>	0.114	0.056	<b>0.120</b>	0.187	0.064	<b>0.144</b>	0.227
Bologna (Italy)	0.068	<b>0.135</b>	0.204	0.101	<b>0.218</b>	0.339	0.114	<b>0.257</b>	0.406
Cape Town (South Africa)	0.042	<b>0.082</b>	0.125	0.061	<b>0.132</b>	0.205	0.069	<b>0.157</b>	0.248
Cox's Bazar (Bangladesh)	0.046	<b>0.090</b>	0.136	0.067	<b>0.144</b>	0.224	0.075	<b>0.170</b>	0.269
Harare (Zimbabwe)	0.042	<b>0.082</b>	0.124	0.061	<b>0.131</b>	0.204	0.069	<b>0.156</b>	0.246
Jimma (Ethiopia)	0.044	<b>0.087</b>	0.132	0.064	<b>0.139</b>	0.216	0.073	<b>0.166</b>	0.261
Kuching (Malaysia)	0.057	<b>0.112</b>	0.170	0.083	<b>0.180</b>	0.280	0.094	<b>0.212</b>	0.335
Las Vegas (United States)	0.038	<b>0.075</b>	0.113	0.055	<b>0.119</b>	0.185	0.062	<b>0.141</b>	0.223
Manaos (Brazil)	0.051	<b>0.100</b>	0.151	0.074	<b>0.160</b>	0.248	0.084	<b>0.189</b>	0.298
Mombasa (Kenya)	0.045	<b>0.089</b>	0.135	0.065	<b>0.141</b>	0.220	0.074	<b>0.168</b>	0.265
Oslo (Norway)	0.080	<b>0.158</b>	0.239	0.118	<b>0.256</b>	0.398	0.134	<b>0.302</b>	0.476
Osnabrück (Germany)	0.072	<b>0.142</b>	0.214	0.106	<b>0.229</b>	0.357	0.120	<b>0.270</b>	0.426
Riyadh (Saudi Arabia)	0.038	<b>0.076</b>	0.114	0.056	<b>0.120</b>	0.187	0.063	<b>0.143</b>	0.225
Sevilla (Spain)	0.044	<b>0.087</b>	0.131	0.064	<b>0.139</b>	0.216	0.073	<b>0.164</b>	0.259

Table 7.3.2.1. Comparison of the electricity cost (€/KWh) results for the three PV panel options in the 15 locations

Because the installation cost is the same in all the locations. the more annual power generation. the lower is the electricity cost. In the following graph a more visual comparison between locations and cooling options can be observed:

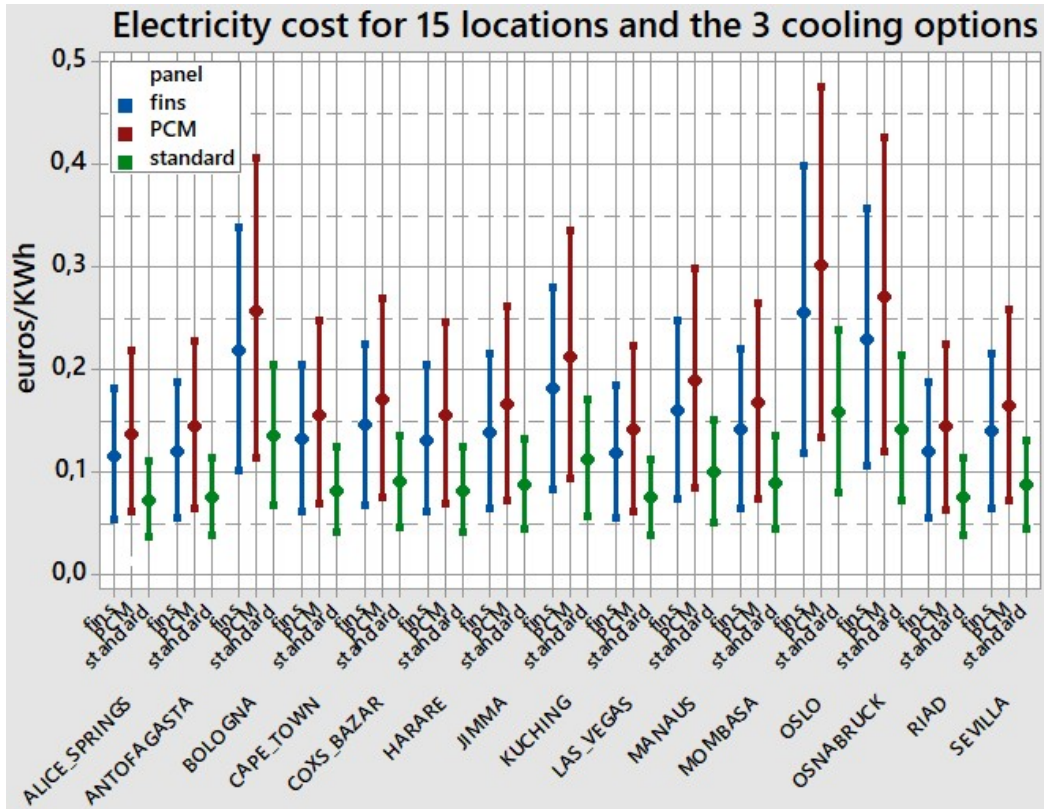


Figure 7.3.2.1. Comparative graph of the electricity cost (€/KWh) results for the three PV panel options in the 15 locations

In order to give a different approach as for the economical study, Table 7.3.2.2. provides for each location the maximum cost of the cooling system to achieve a cost reduction. In this way, the influence of the changing cost of the cooling options is eliminated of the analysis. In this case, as it is an approximate estimation, only the mean value is considered as for the standard panel cost. Note that higher cost savings correspond to locations with higher annual power generation, where the cooling systems have a greater influence.

LOCATION	Maximum cost of fins cooling system	Maximum cost of PCM cooling system
Alice Springs (Australia)	13,96	3,16
Antofagasta (Chile)	11,76	-0,74
Bologna (Italy)	8,73	0,97
Cape Town (South Africa)	10,65	0,37
Cox's Bazar (Bangladesh)	11,48	2,91
Harare (Zimbabwe)	11,43	0,96
Jimma (Ethiopia)	12,62	1,80
Kuching (Malaysia)	10,69	2,72
Las Vegas (United States)	11,17	2,07
Manaus (Brazil)	12,23	3,42
Mombasa (Kenya)	13,27	3,44
Oslo (Norway)	7,09	-0,57
Osnabrück (Germany)	6,86	-0,13
Riyadh (Saudi Arabia)	13,73	3,67
Sevilla (Spain)	11,29	2,10

Table 7.3.2.2. Estimation of the maximum cost of the cooling system installation to achieve a cost reduction

## 8. Conclusions

The achievement of the initial proposed goals is commented in this chapter, as well as the main conclusions of the economical study performed in chapter 7.

As for the simulation model development, all the thermal concepts that impact on it were analysed and the assumptions made were justified. Some of these assumptions imply a non ideal approach but they are necessary to simplify the model by approximations or because of the own uncertainty of the problem conditions. Despite the simplifications, the thermal model was intended to be as close as possible to the reality.

On the other hand, the aim of chapter 6 was the validation of the simulation model, understood as a study of the accuracy and the reliability of the simulation output. To this end, a comparative study was made, through a review of the simulated temperature on the back of the studied panels and the respective real temperatures measured at the installed panels in the validation emplacement. The evaluation of the simulation model was successful but it was concluded that a changing error in the temperature function is inevitable and, for this reason, an approximate error range was estimated. Nevertheless, it was proved that the error of the simulated power generation is small, which is positive for the reliability of the economical study.

Once it was validated the simulation, it was used for the study about the economical viability of the fins and PCM cooling options, for which 15 locations around the world were chosen. These locations present different input conditions due to their specific latitude and climate, with the aim of provide more variety to the obtained panels performance results. As expected, an improvement is achieved in the annual power generation in the case of the two cooling options, but the **fins-cooled PV panel** demonstrated to be substantially more effective (**energy gain between 2.3 and 4.6%**) than the **PCM panel (energy gain between 0 and 1.2%)**. This improvement is more remarkable in the locations with higher generation potential as for the available solar radiation.

Despite this greater generation thanks to cooling systems, the conclusions about cost of electricity in each case do not support the investment in these additional accessories for the PV panel. This is because the electricity gain due to the higher thermal efficiency is small compared to the required investment. Although the cost calculations are changing and relative, which impede to provide a definitive conclusion, the results suggest that for a justified investment in the studied cooling options, they must be pretty cheap. Otherwise, for the considered expenditure in each alternative, the estimated mean cost of electricity is **0.092 €/KWh** for the **standard panel** (no cooling), **0.174 €/KWh** for the **fins-cooled panel** and **0.194 €/KWh** for the **PCM-cooled panel**.





## Bibliography

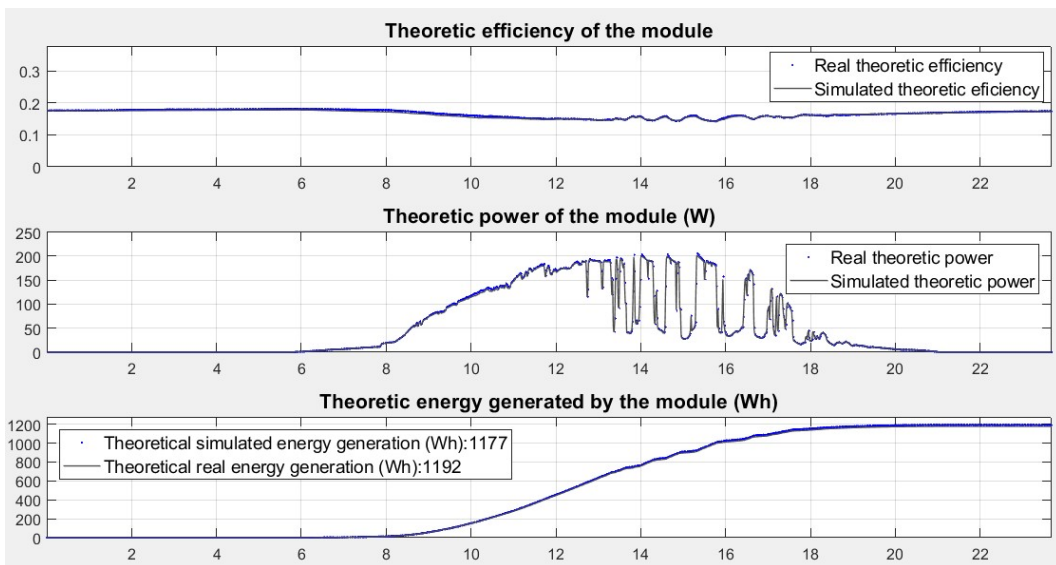
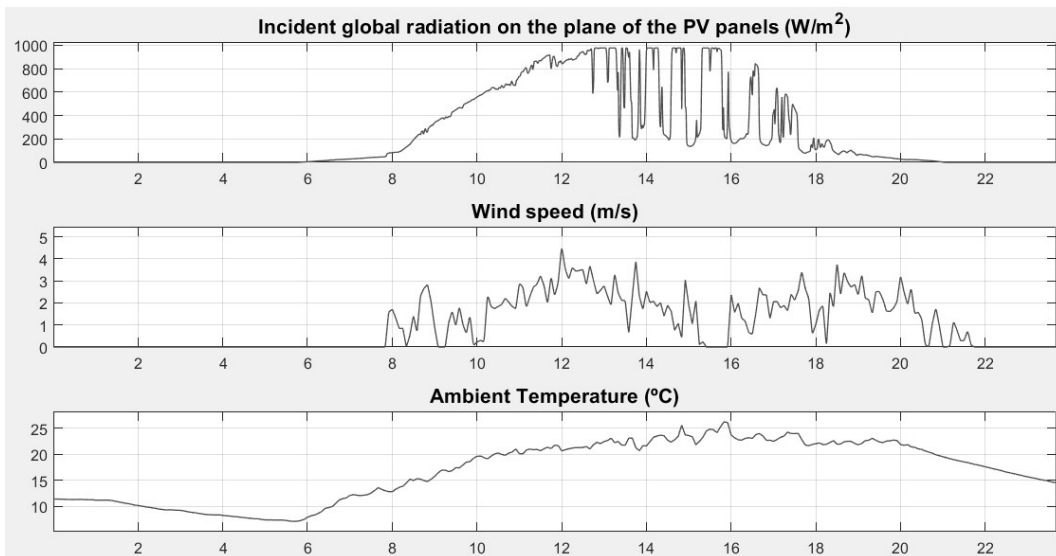
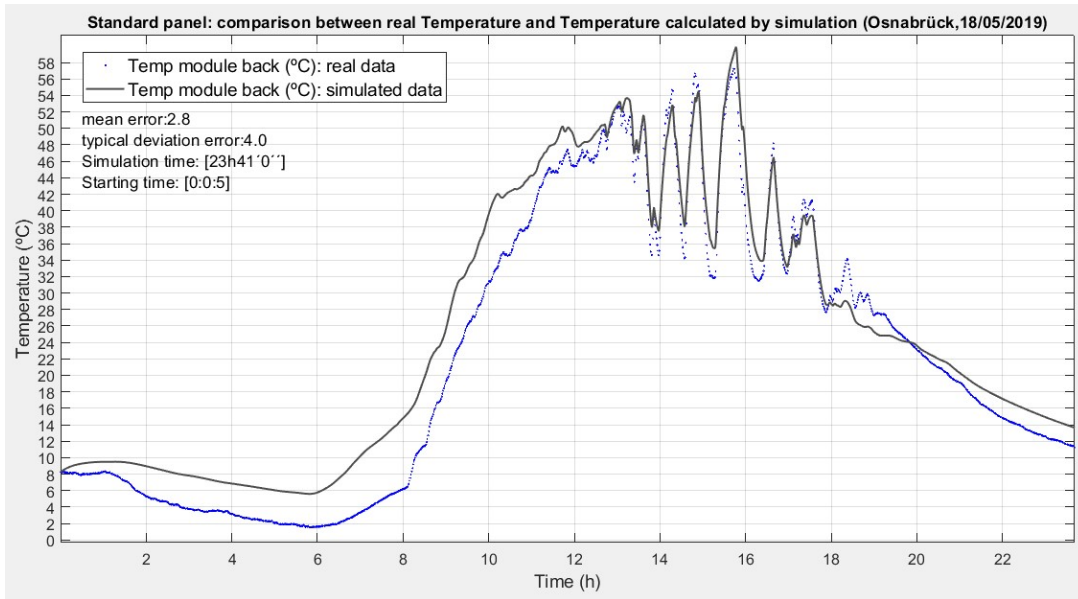
1. **FRAUNHOFER INSTITUTE FOR SOLAR ENERGY SYSTEMS ISE.** *LEVELIZED COST OF ELECTRICITY RENEWABLE ENERGY TECHNOLOGIES.* 2018.
2. **International Energy Agency.** [Online] <https://www.iea.org/topics/renewables/solar/>.
3. **datasheet TSM-PD05, Trina Solar.** [Online] [https://static.trinasolar.com/sites/default/files/EN\\_TSM\\_PD05\\_datasheet\\_B\\_2017\\_web.pdf](https://static.trinasolar.com/sites/default/files/EN_TSM_PD05_datasheet_B_2017_web.pdf).
4. **Rubitherm Phase Change Material.** [Online] <https://www.rubitherm.eu/index.php/produktkategorie/organische-pcm-rt>.
5. **Solar energy.** [Online] <http://vpmp.ac.in/wp-content/uploads/2017/01/STUDY-material.pdf>.
6. **Belzuz, Iñigo Cerro.** *Simulation of PV-modules and passive cooling systems using MATLAB.* 2018.
7. **Ibáñez, Jon Ongay.** *Setup and experimental analysis of passive cooling systems for PV modules.* 2018.
8. **Höweler, Joel.** *Experimentelle und numerische Untersuchung von passiven Kühlmethode von PV-Modulen.* 2019.
9. **Benghanem, M.** *Optimization of tilt angle for solar panel: Case study for Madinah, Saudi Arabia.* 2011.
10. **Aggarwal, R K.** *Estimation of Total Solar Radiation on Tilted Surface.* 2013.
11. **Liu, B. and Jordan, R.** *Daily insolation on surfaces tilted towards equator.* 1961.
12. **Theodore L. Bergman, Adrienne S. Lavine, Frank P. Incropera, David P. Dewitt.** *Fundamentals of Heat and Mass Transfer.*
13. **Singer, Farah.** *Influence of the nonlocal effects on the near-field radiative heat transfer.* 2015.
14. **Fuentes, Martin K.** *A Simplified Thermal Model for Flat-Plate Photovoltaic Arrays .* 1987.
15. **Chapman, Alan J.** *Heat Transfer, Appendix.*
16. **Verein Deutscher Ingenieure.** *VDI Heat Atlas, chapter F2.* s.l. : Springer.
17. **C. Mahboub, N. Moumami, A. Moumami, S. Youcef-Ali.** *Effect of the angle of attack on the wind convection coefficient.* 2011.
18. **Envertech.** *EVT248 Microinverter, User Manual.*
19. **Texas Instruments.** *ADS111x datasheet.*

20. **Pyromation, Inc.** Thermocouple theory. [Online]  
[https://www.pyromation.com/Downloads/Doc/Training\\_TC\\_Theory.pdf](https://www.pyromation.com/Downloads/Doc/Training_TC_Theory.pdf).
21. **Devices, Analog.** *datasheet, AD849X Precision Thermocouple Amplifiers with Cold Junction Compensation.*
22. **Kipp&Zonen.** CMP3 Pyranometer. [Online]  
<https://www.kippzonen.com/Product/11/CMP3-Pyranometer#.XTeBSegzblU>.
23. —. AMPBOX Amplifier. [Online] <https://www.kippzonen.com/Product/37/AMPBOX-Amplifier#.XTeDK-gzblU>.
24. **Rubitherm.** RT44HC datasheet. [Online]  
[https://www.rubitherm.eu/media/products/datasheets/Techdata\\_-RT44HC\\_EN\\_06082018.PDF](https://www.rubitherm.eu/media/products/datasheets/Techdata_-RT44HC_EN_06082018.PDF).
25. **EnergyPlus.** [Online] <https://energyplus.net/>.

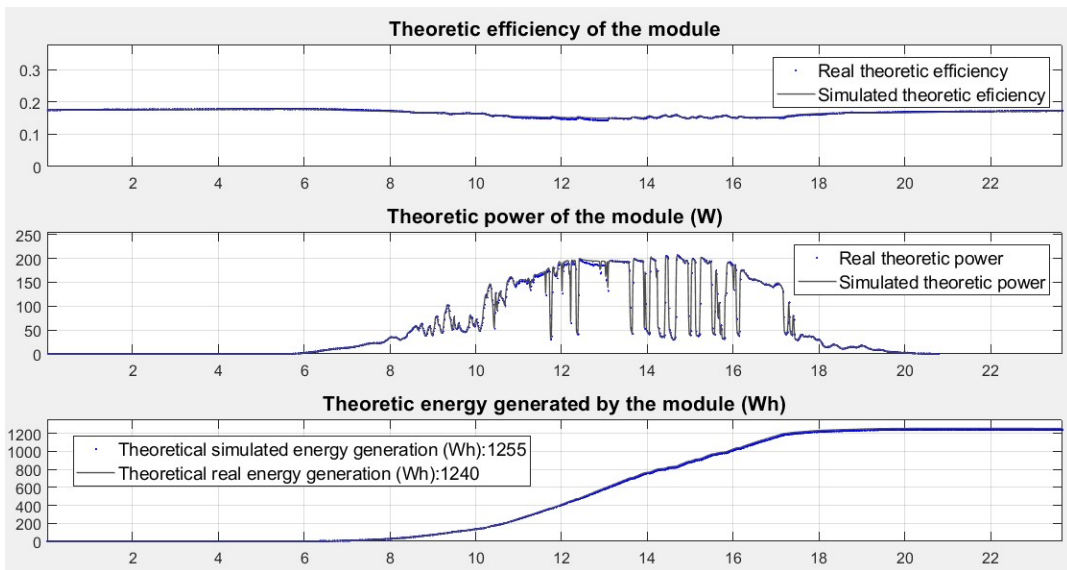
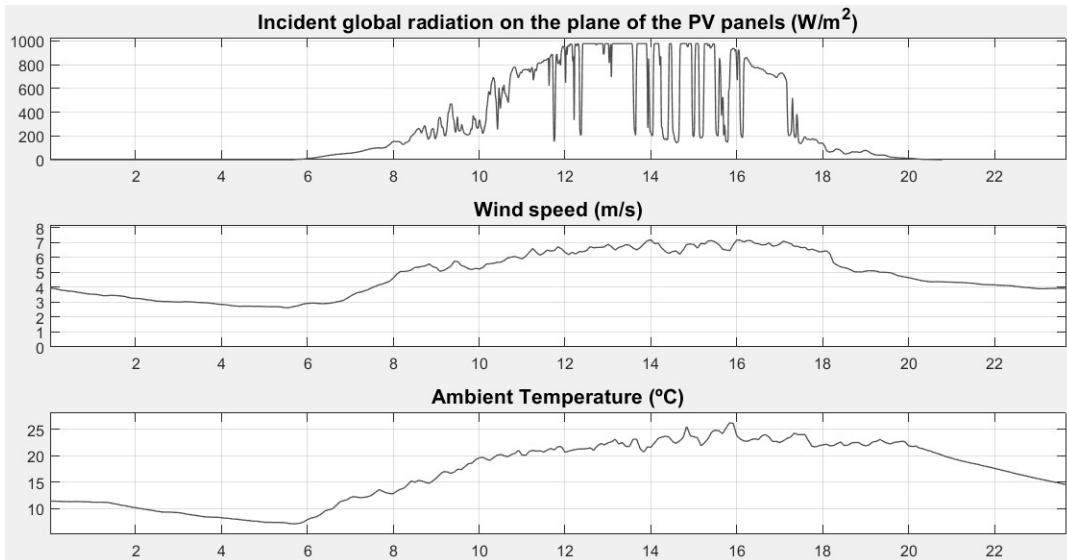
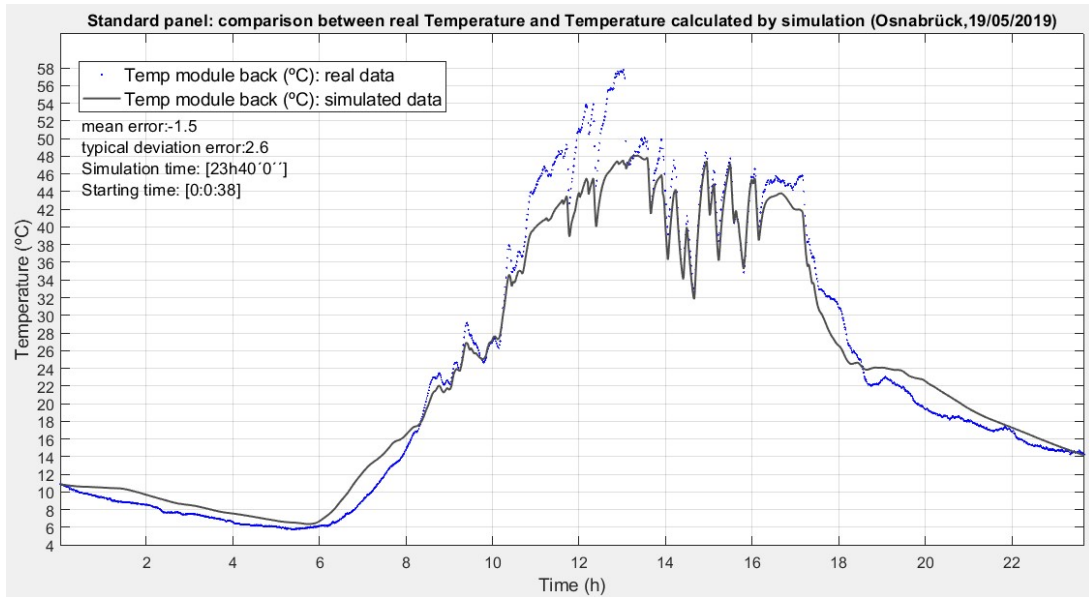


20. **Pyromation, Inc.** Thermocouple theory. [Online]  
[https://www.pyromation.com/Downloads/Doc/Training\\_TC\\_Theory.pdf](https://www.pyromation.com/Downloads/Doc/Training_TC_Theory.pdf).
21. **Devices, Analog.** *datasheet, AD849X Precision Thermocouple Amplifiers with Cold Junction Compensation.*
22. **Kipp&Zonen.** CMP3 Pyranometer. [Online]  
<https://www.kippzonen.com/Product/11/CMP3-Pyranometer#.XTeBSegzblU>.
23. —. AMPBOX Amplifier. [Online] <https://www.kippzonen.com/Product/37/AMPBOX-Amplifier#.XTeDK-gzblU>.
24. **Rubitherm.** RT44HC datasheet. [Online]  
[https://www.rubitherm.eu/media/products/datasheets/Techdata\\_-RT44HC\\_EN\\_06082018.PDF](https://www.rubitherm.eu/media/products/datasheets/Techdata_-RT44HC_EN_06082018.PDF).
25. **EnergyPlus.** [Online] <https://energyplus.net/>.

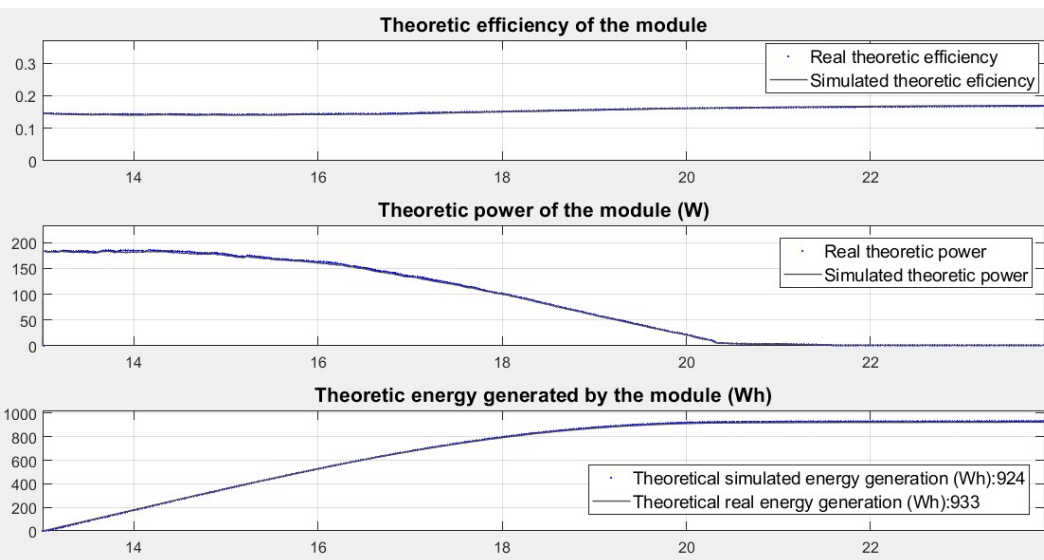
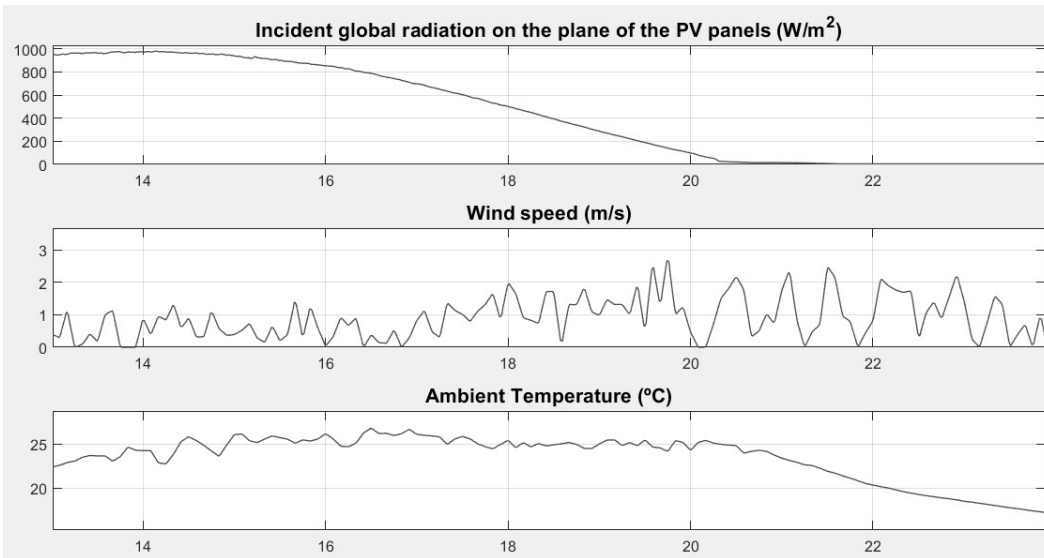
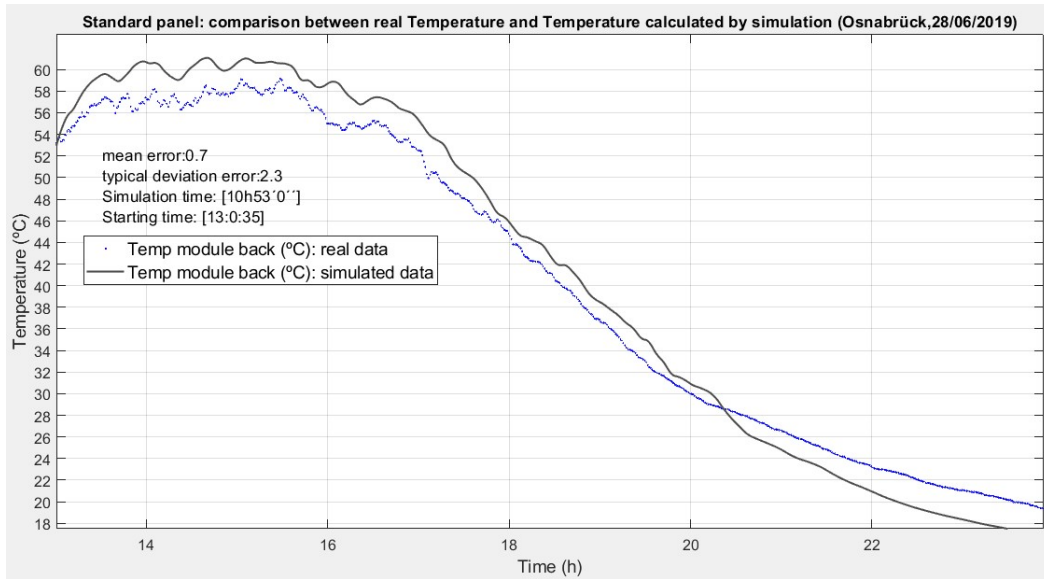
## **Annex 1. Validation of simulation models by comparison with real data**



Validation of standard panel. 18/05/2019

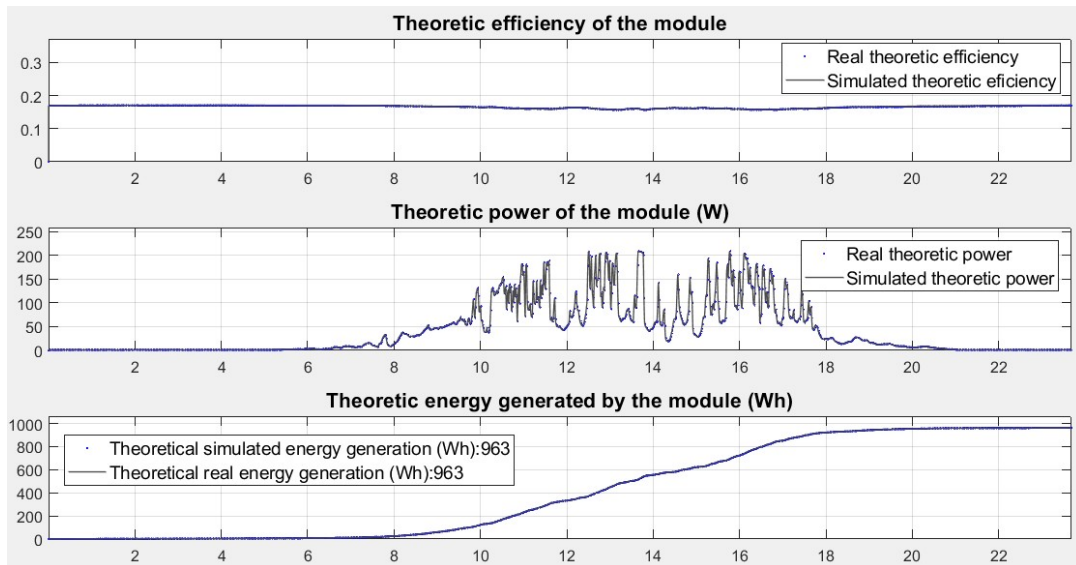
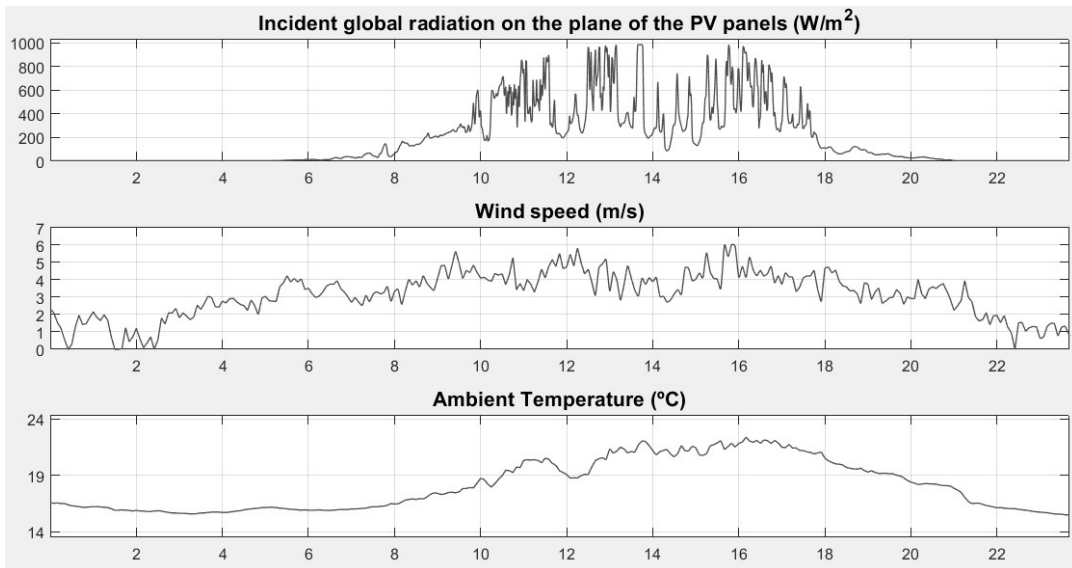
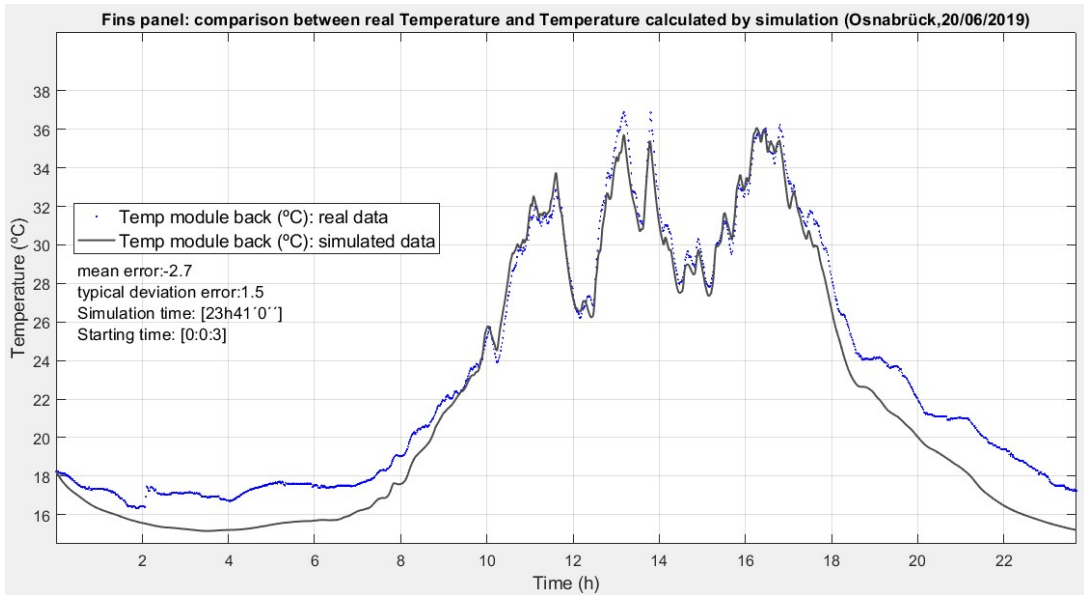


Validation of standard panel. 19/05/2019

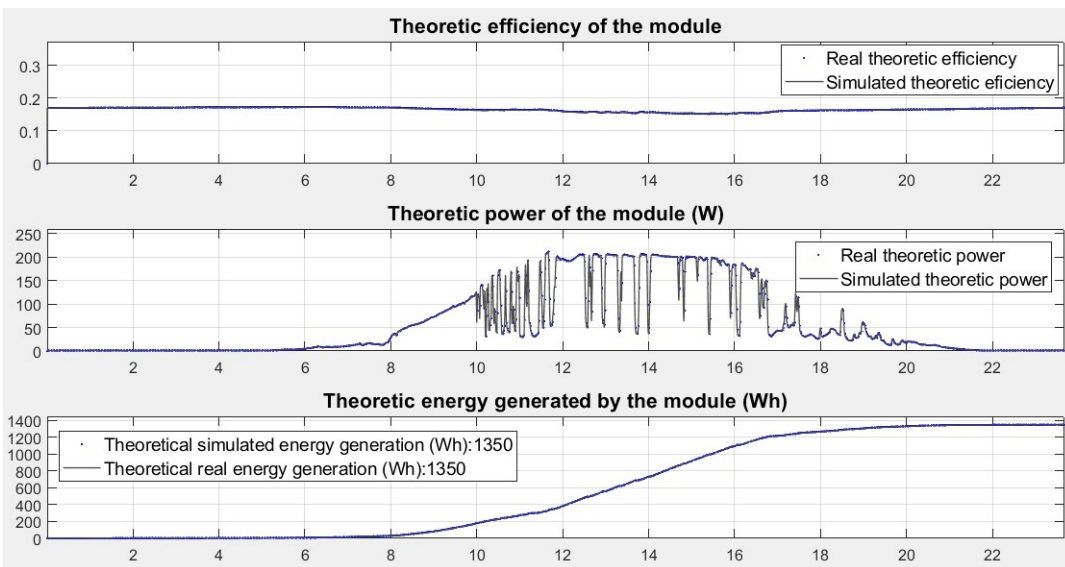
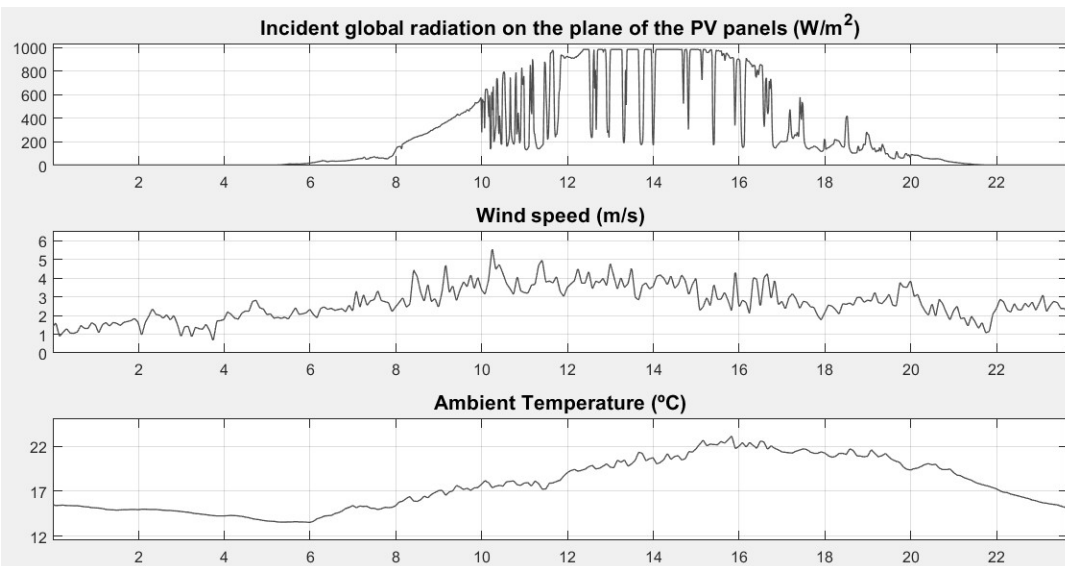
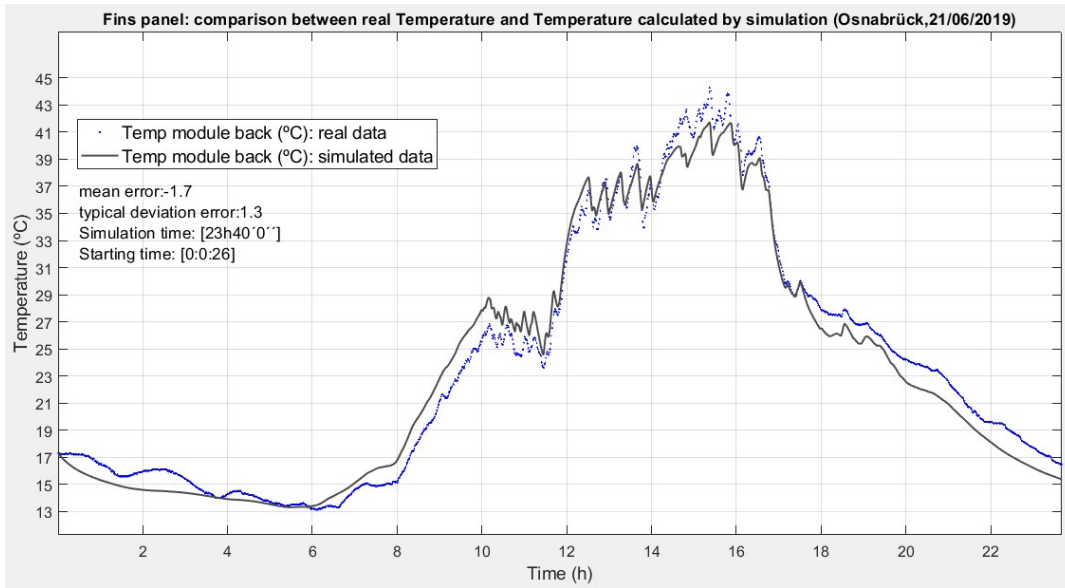


Validation of standard panel. 28/06/2019

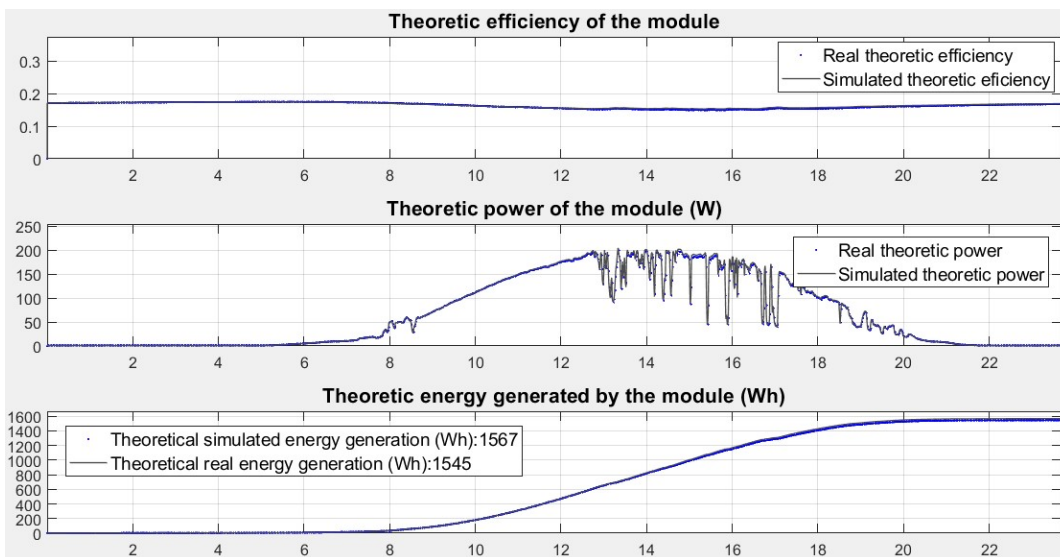
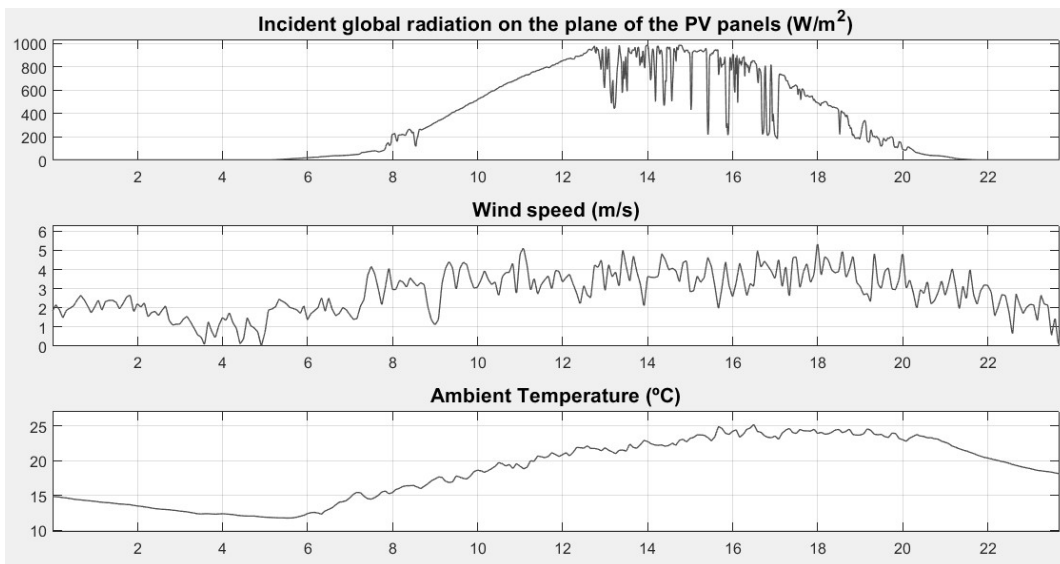
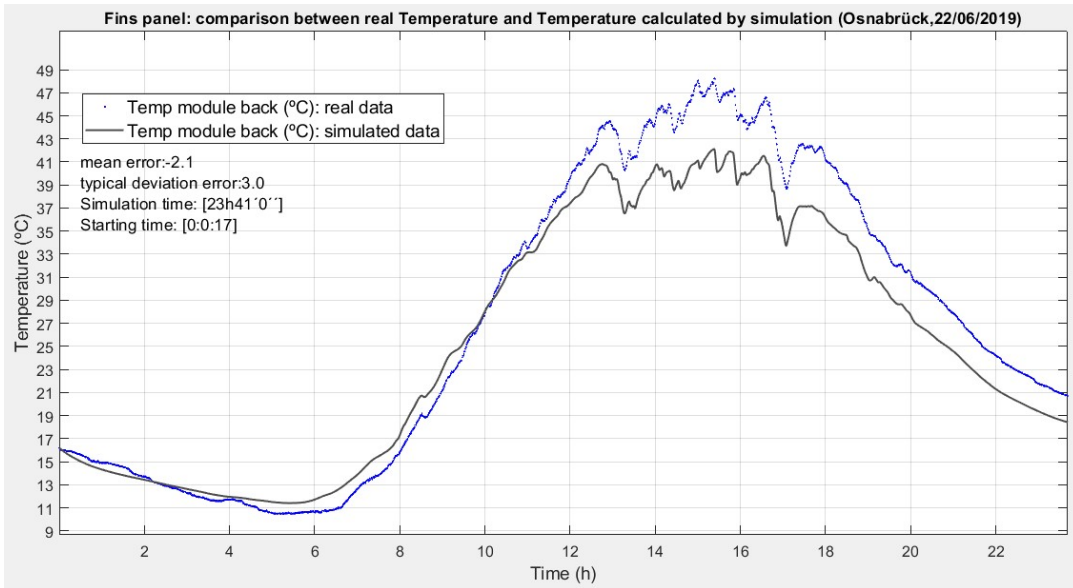




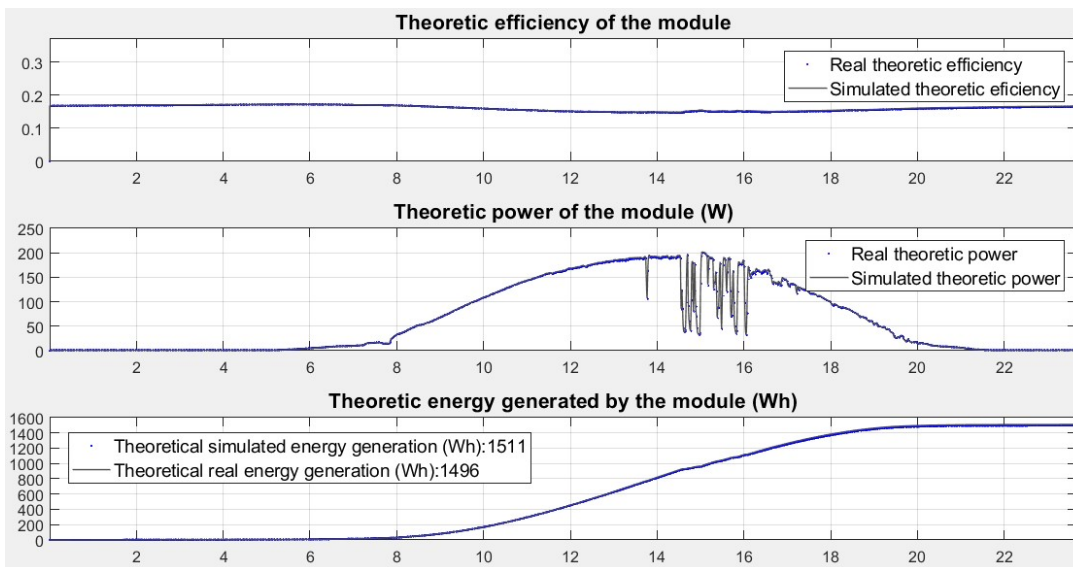
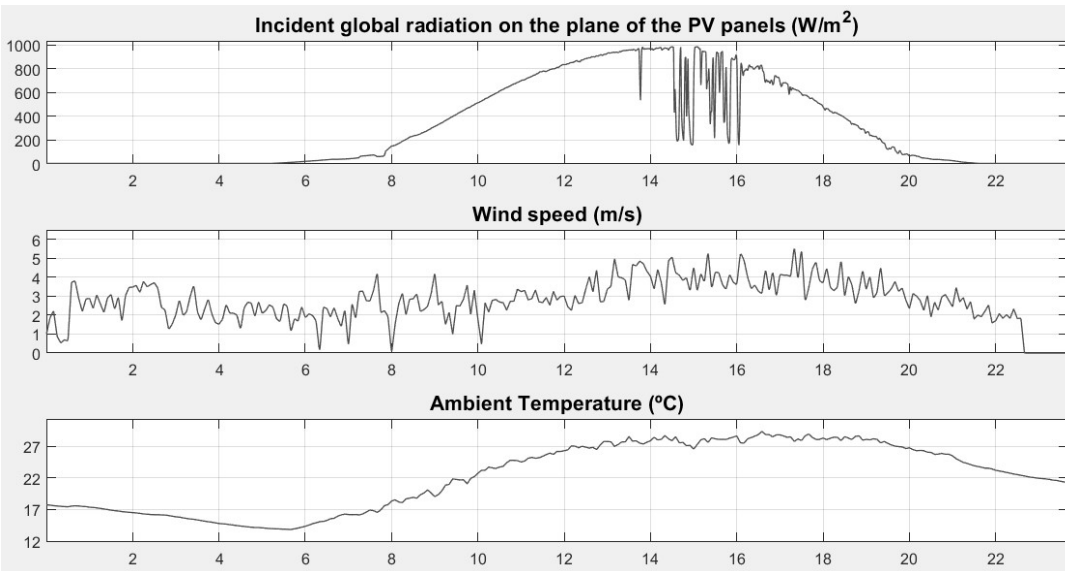
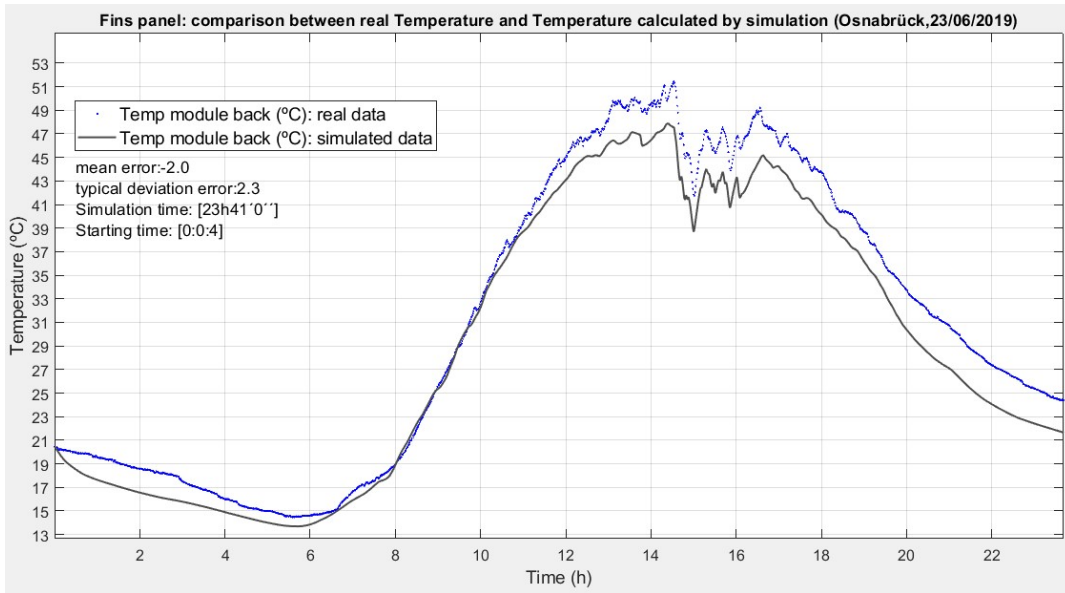
Validation of fins panel. 20/06/2019



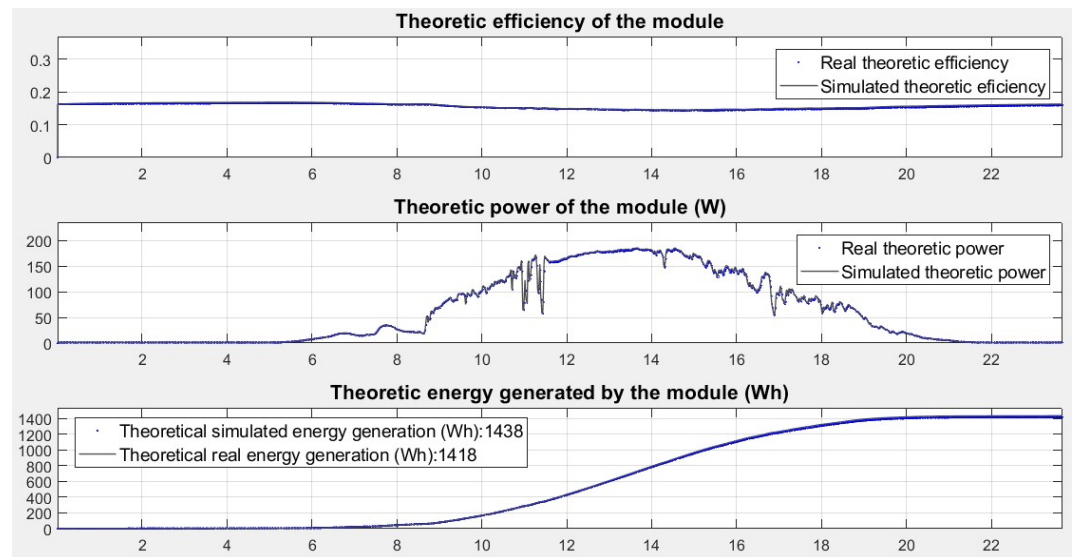
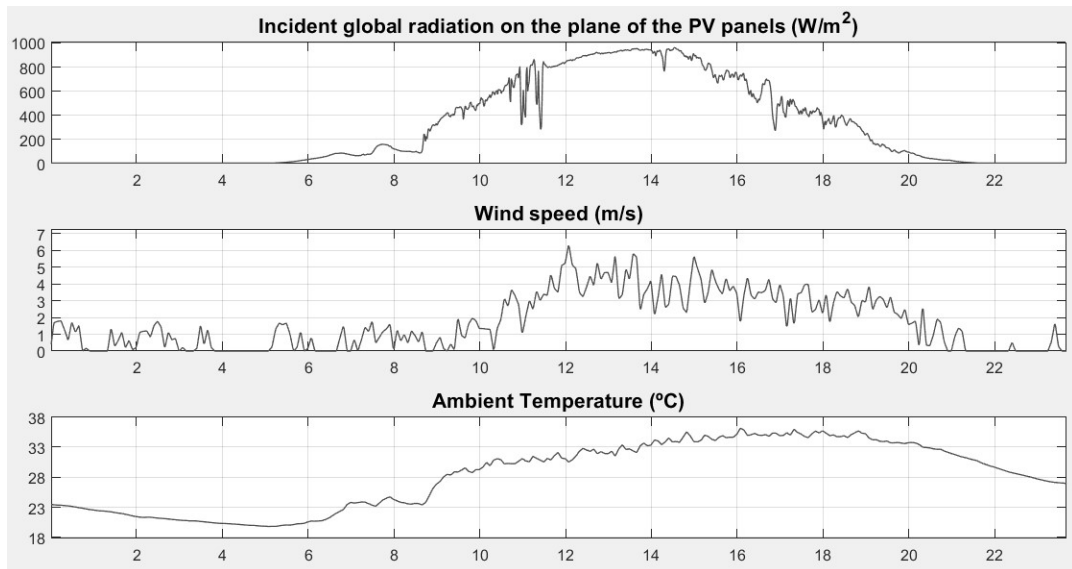
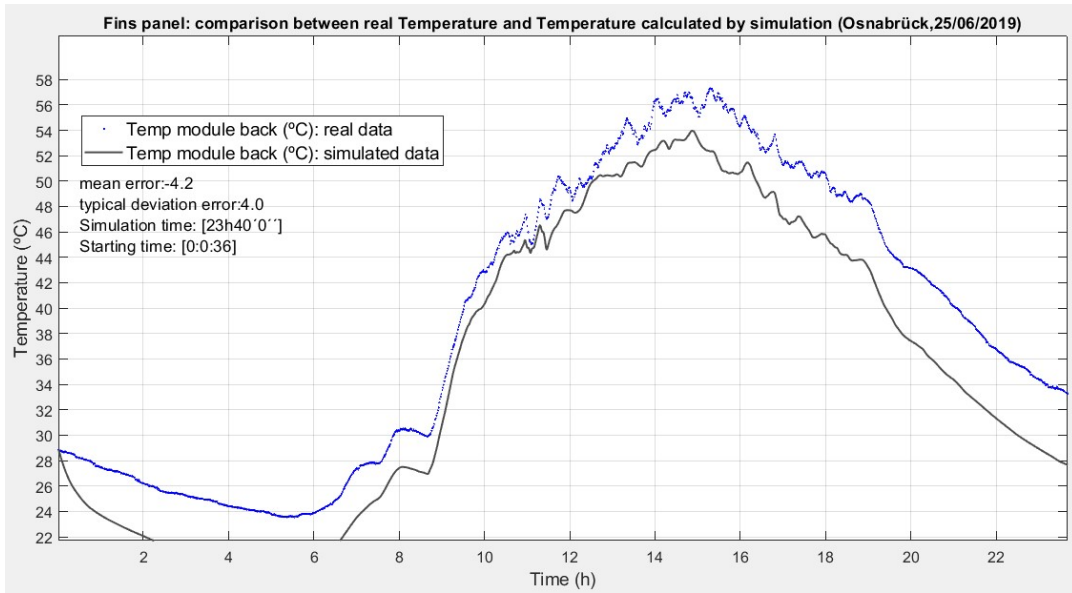
Validation of fins panel. 21/06/2019



Validation of fins panel. 22/06/2019

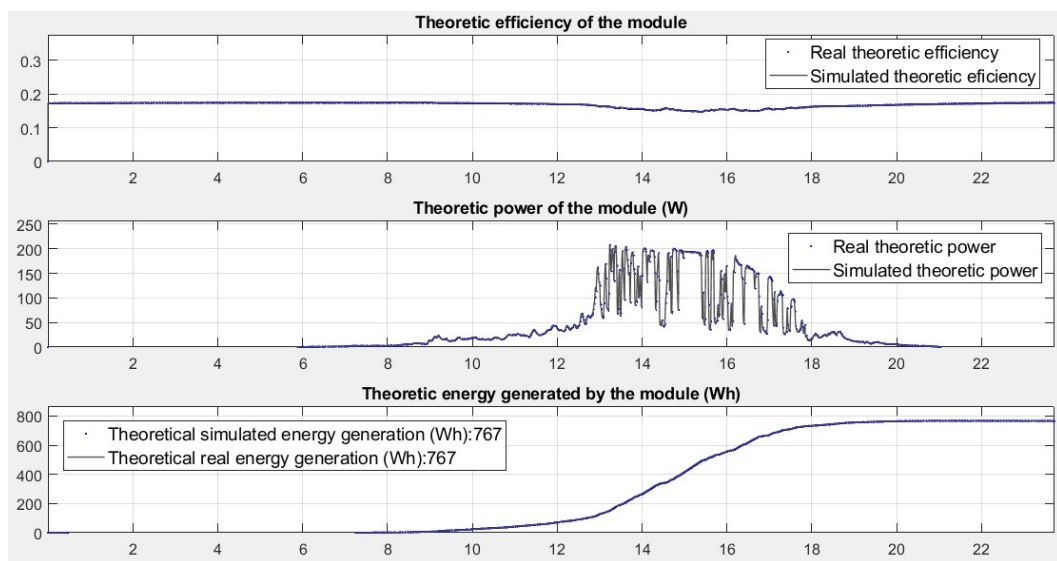
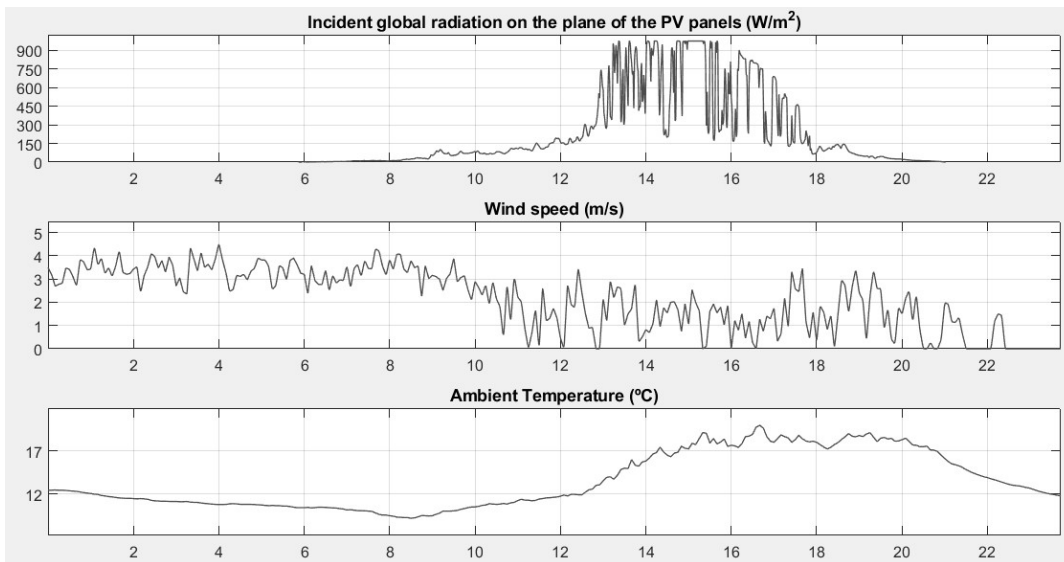
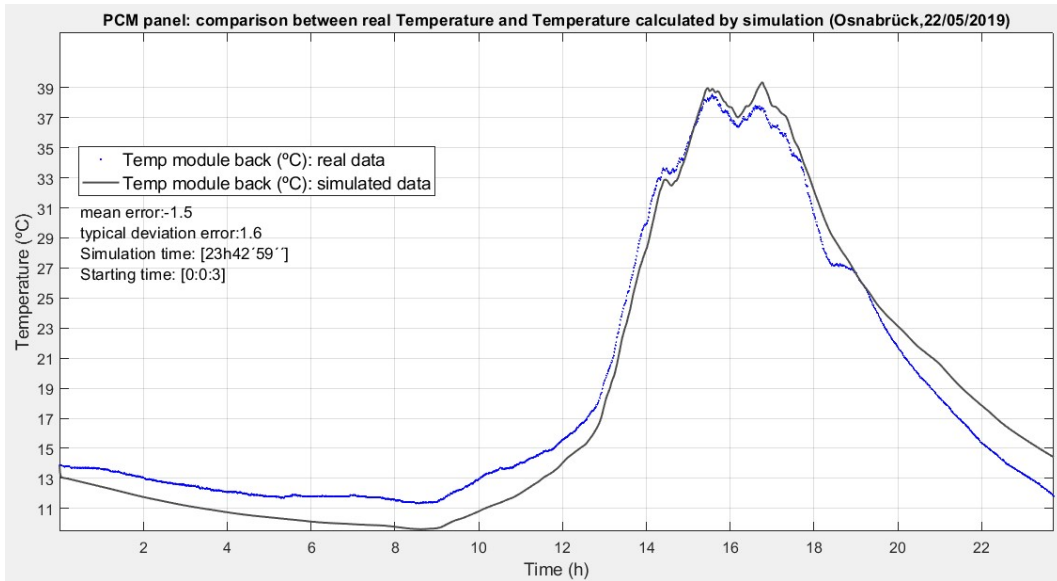


Validation of fins panel. 23/06/2019

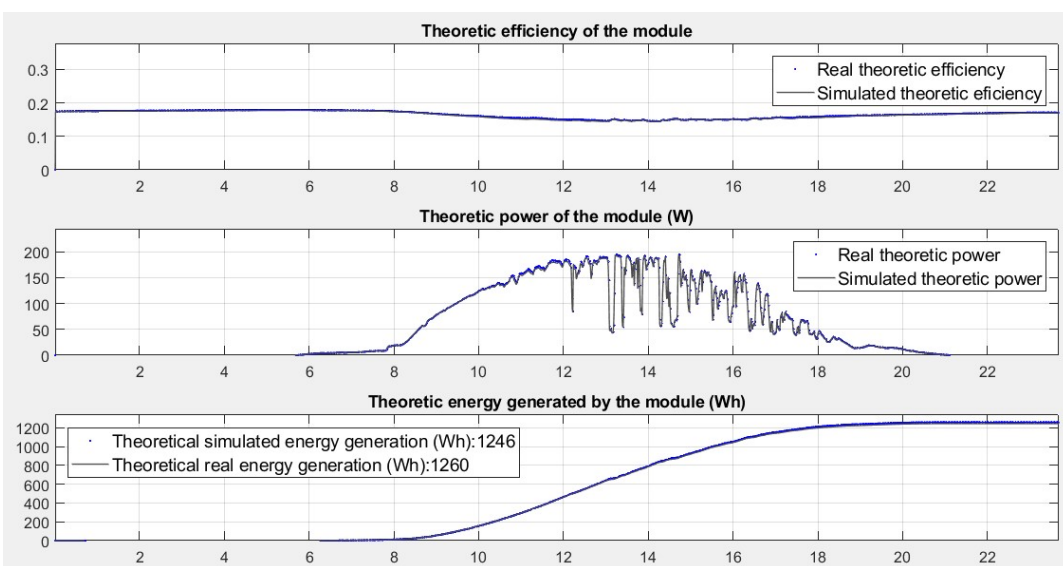
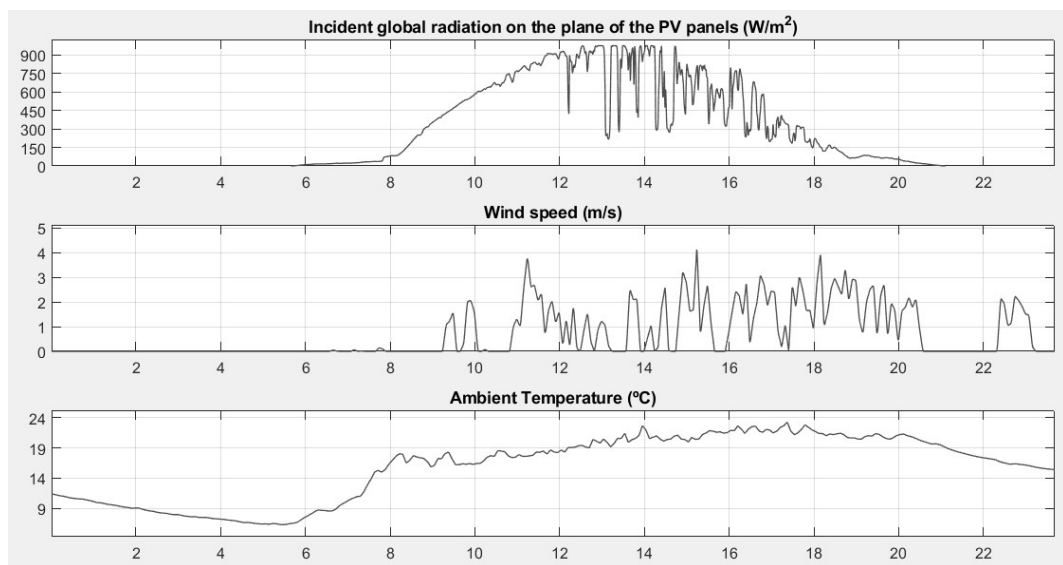
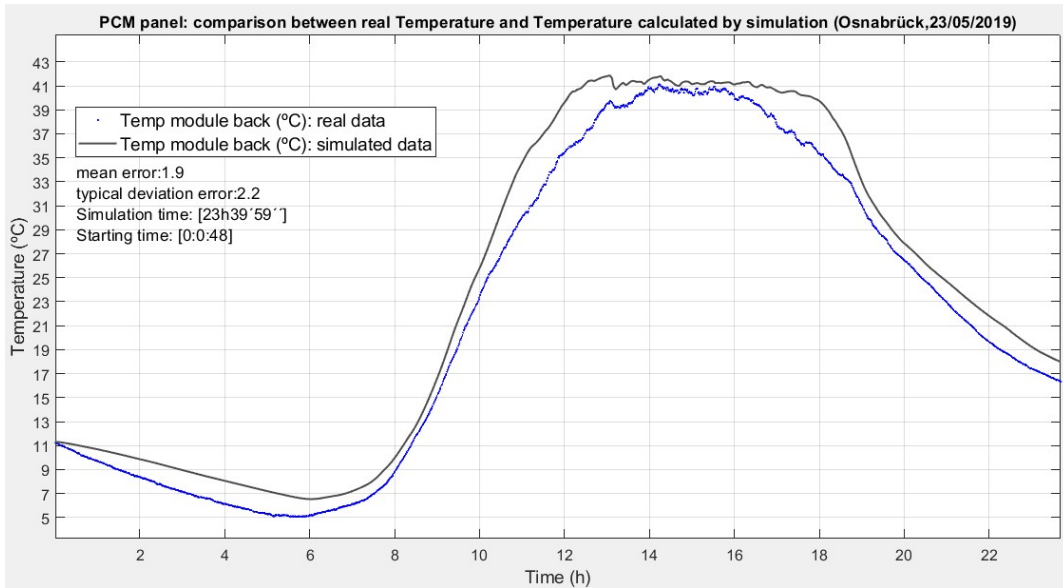


Validation of fins panel. 25/06/2019

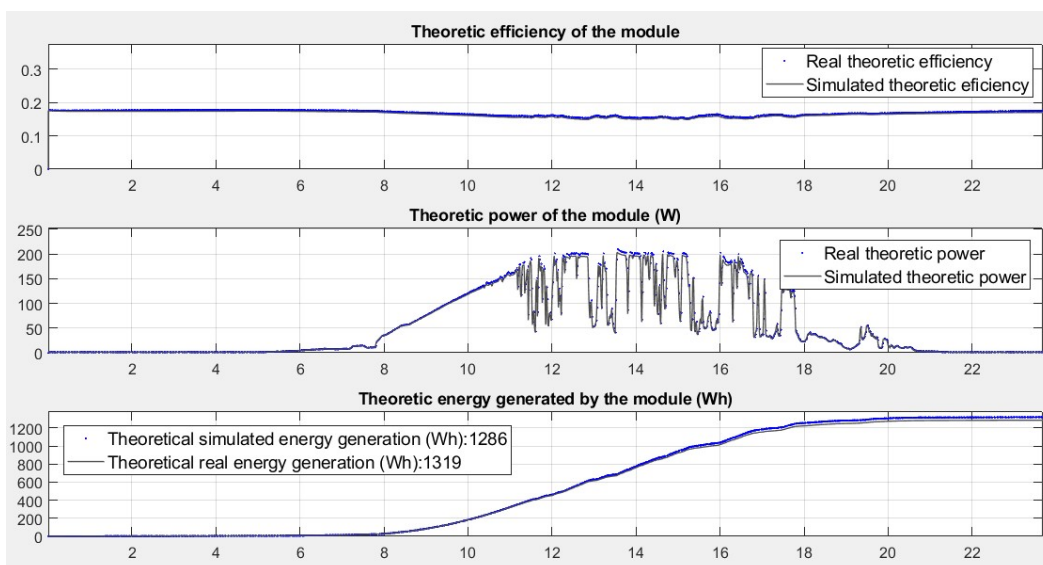
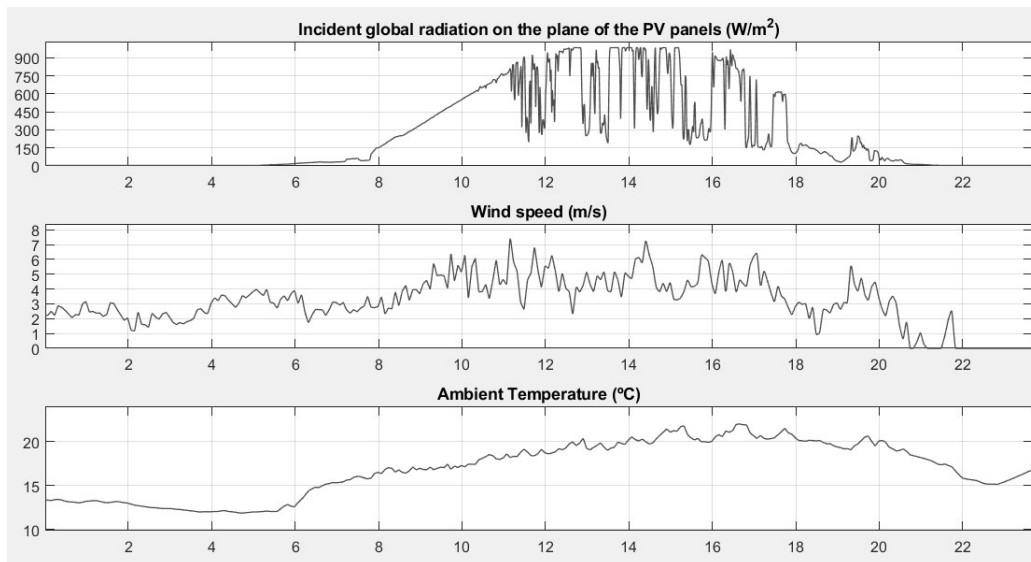
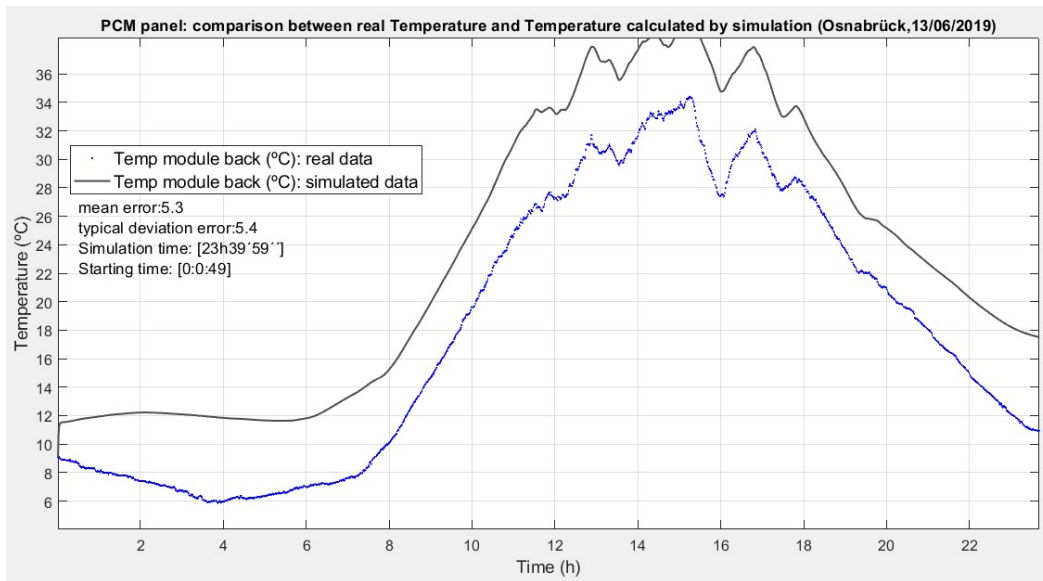




Validation of PCM panel. 22/05/2019

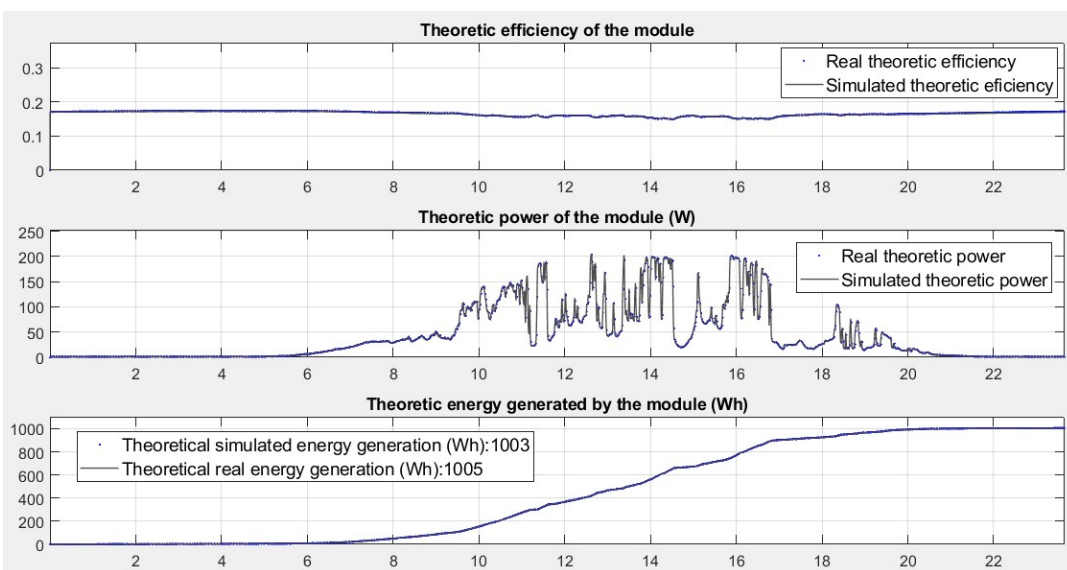
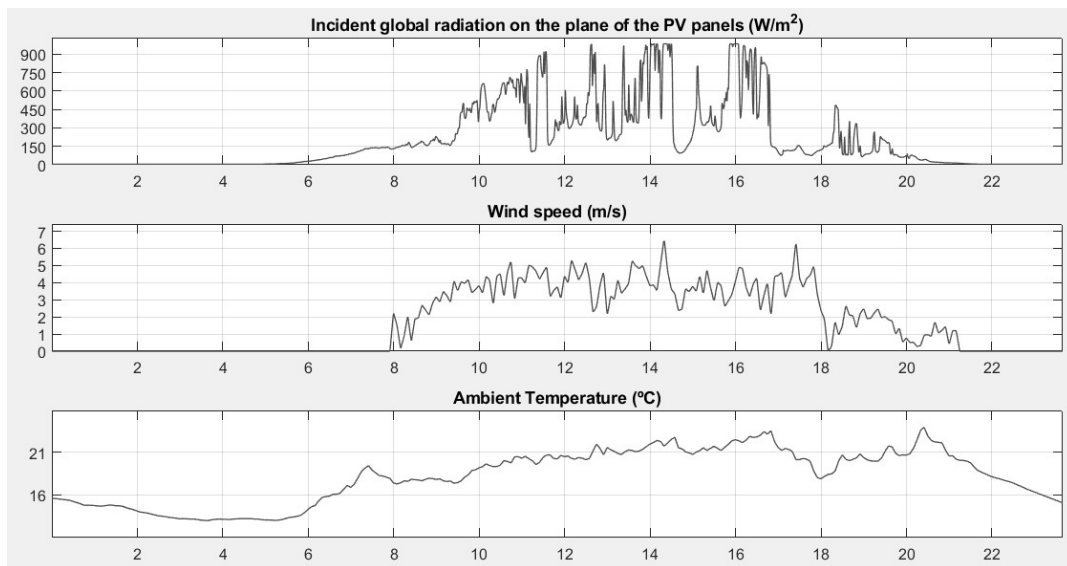
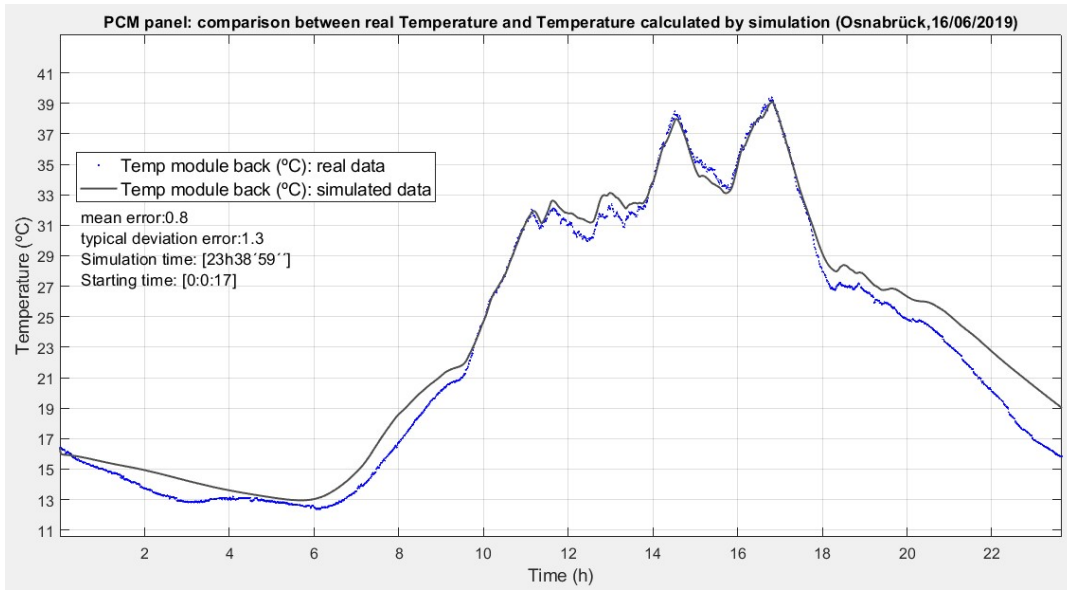


Validation of PCM panel. 23/05/2019

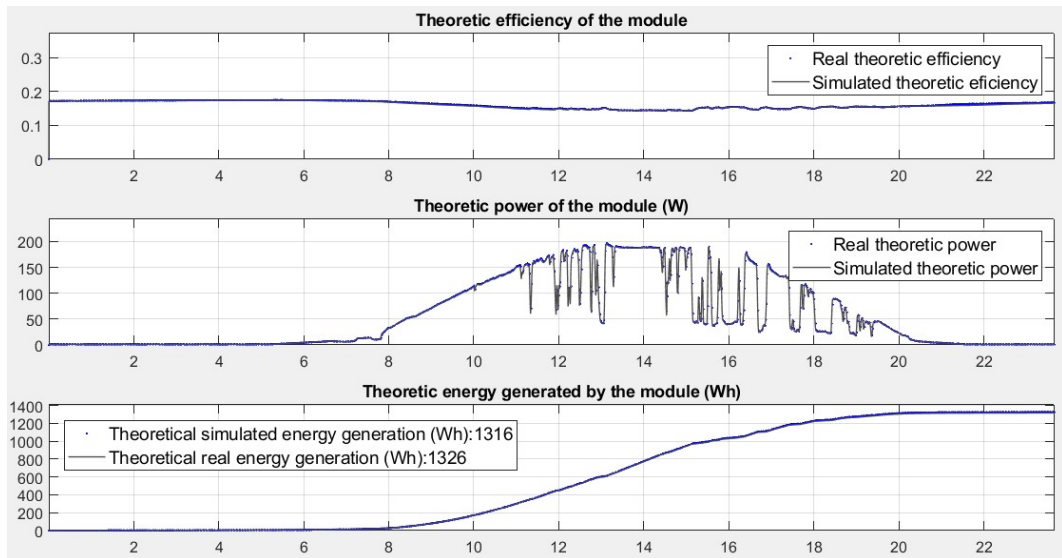
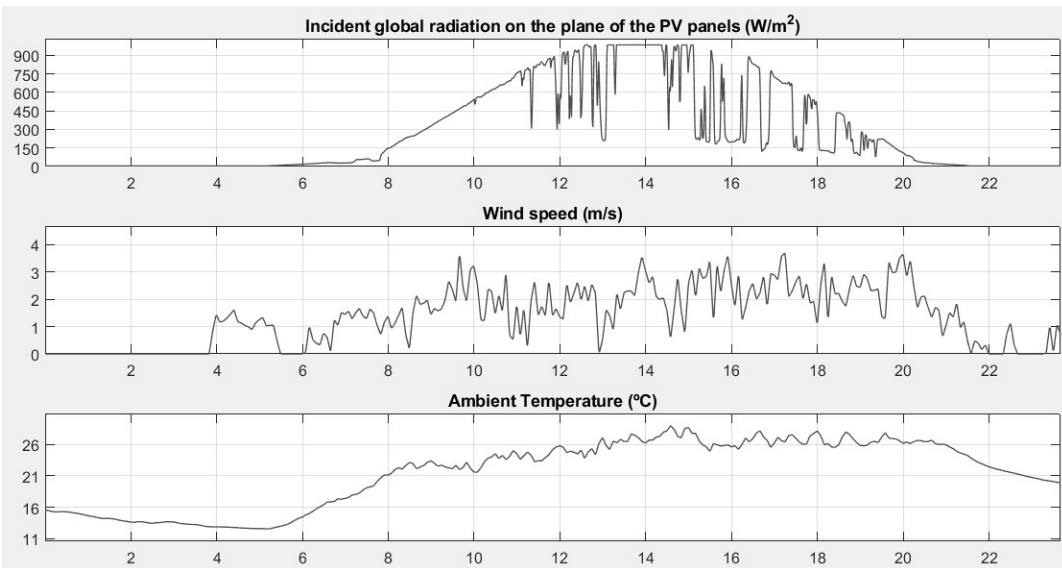
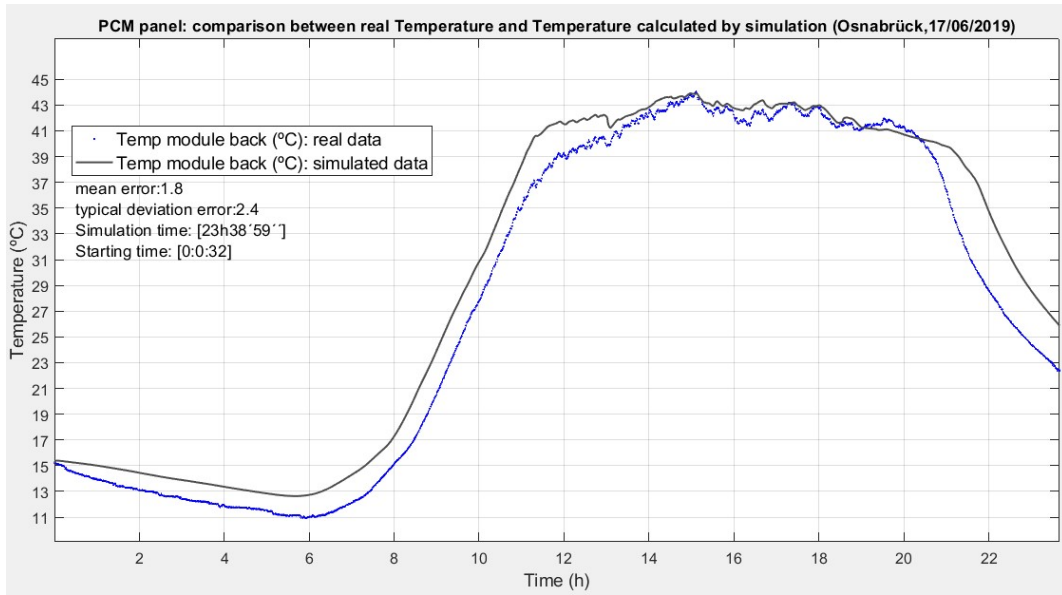


*Validation of PCM panel. 13/06/2019*





Validation of PCM panel. 16/06/2019



Validation of PCM panel. 17/06/2019

## Annex 2. Monthly and annual simulation results for all the locations and the three cooling options

ALICE SPRINGS													
LAT(°)   LONG(°)	-24.30   134.88												
Optimum tilt (°)	18												
Month	Jan	Feb	Mar	Apr	May	Jun	Jul	Aug	Sep	Oct	Nov	Dec	TOTAL YEAR
mean ambient Temperature (°C)	27,9	27,9	25,3	20,4	16,8	11,5	12,0	13,1	20,4	22,4	27,4	29,3	<b>21,2</b>
total incident rad. (KWh/m <sup>2</sup> )	225,4	203,6	220,5	195,5	170,1	164,0	165,5	192,8	210,0	210,5	214,7	223,9	<b>2396,7</b>
mean wind speed (m/s)	2,4	3,4	2,2	1,2	1,5	2,6	1,4	1,7	3,5	2,5	3,9	1,9	<b>2,4</b>
St. panel: mean cell Temp. (°C)	39,2	38,8	36,2	30,6	25,1	19,4	20,0	22,4	30,7	32,8	38,0	40,8	<b>31,2</b>
St. panel: mean theoretical eff.	0,155	0,156	0,157	0,161	0,165	0,169	0,168	0,167	0,161	0,160	0,156	0,154	<b>0,161</b>
Standard panel: mean power (W)	56,6	56,6	55,7	52,8	45,8	46,9	45,5	52,2	56,7	54,4	56,0	55,7	<b>52,9</b>
St. panel: total energy gen. (KWh)	42,1	38,0	41,5	38,0	34,1	33,8	33,9	38,8	40,8	40,5	40,3	41,4	<b><u>463,2</u></b>
Fins panel: mean cell Temp. (°C)	35,4	35,1	32,6	27,1	22,3	16,7	17,3	19,3	27,3	29,3	34,5	36,9	<b>27,8</b>
Fins panel: mean theoretical eff.	0,158	0,158	0,160	0,164	0,167	0,171	0,170	0,169	0,163	0,162	0,159	0,157	<b>0,163</b>
Fins panel: mean power (W)	59,4	59,4	58,5	55,3	47,6	48,6	47,4	54,4	59,3	57,0	58,6	58,5	<b>55,3</b>
Fins panel: total energy gen. (KWh)	44,2	39,9	43,5	39,8	35,4	35,0	35,2	40,5	42,7	42,4	42,2	43,5	<b><u>484,4</u></b>
PCM panel: mean cell Temp. (°C)	41,2	40,7	38,5	33,0	27,0	20,9	21,7	24,4	32,6	35,0	39,8	42,7	<b>33,1</b>
PCM panel: mean theoretical eff.	0,154	0,154	0,156	0,160	0,164	0,168	0,167	0,165	0,160	0,158	0,155	0,153	<b>0,160</b>
PCM panel: mean power (W)	57,5	57,5	56,7	53,3	46,0	46,8	45,5	52,3	57,2	55,1	56,9	56,6	<b>53,5</b>
PCM panel: total energy gen. (KWh)	42,8	38,6	42,2	38,4	34,2	33,7	33,8	38,9	41,2	41,0	41,0	42,1	<b><u>468,0</u></b>

<b>ANTOFAGASTA</b>													
LAT(°)   LONG(°)	-24.35   70.60												
Optimum tilt (°)	17												
Month	Jan	Feb	Mar	Apr	May	Jun	Jul	Aug	Sep	Oct	Nov	Dec	TOTAL YEAR
mean ambient Temperature (°C)	20,5	20,3	19,6	17,6	16	14,6	14	14,3	15,2	15,9	17,3	19	<b>17,0</b>
total incident rad. (KWh/m <sup>2</sup> )	228,6	212,0	218,7	185,2	149,4	129,3	136,5	162,0	180,4	208,5	202,4	224,6	<b>2237,5</b>
mean wind speed (m/s)	4,4	3,7	3,8	3,7	2,9	3,6	3,8	3,5	4,4	4,7	4,9	4,4	<b>4,0</b>
St. panel: mean cell Temp. (°C)	30,6	31	29,3	26,2	22,9	20,7	20,2	21,6	23,6	25,1	26,5	29	<b>25,6</b>
St. panel: mean theoretical eff.	0,161	0,161	0,162	0,164	0,166	0,168	0,168	0,167	0,166	0,165	0,164	0,162	<b>0,165</b>
Standard panel: mean power (W)	60,7	61,8	58,1	51,7	41,1	37,4	38,2	44,8	51,1	56,8	56,7	60,1	<b>51,5</b>
St. panel: total energy gen. (KWh)	45,2	41,5	43,2	37,2	30,6	26,9	28,4	33,3	36,8	42,2	40,8	44,7	<b><u>451,1</u></b>
Fins panel: mean cell Temp. (°C)	27,2	27,3	26	23,3	20,5	18,6	18,1	19,1	20,7	22	23,4	25,6	<b>22,7</b>
Fins panel: mean theoretical eff.	0,164	0,163	0,164	0,166	0,168	0,169	0,170	0,169	0,168	0,167	0,166	0,165	<b>0,167</b>
Fins panel: mean power (W)	63,2	64,6	60,6	53,8	42,6	38,6	39,5	46,4	53,1	59	58,9	62,6	<b>53,6</b>
Fins panel: total energy gen. (KWh)	47,0	43,4	45,1	38,7	31,7	27,8	29,4	34,5	38,2	43,9	42,4	46,5	<b><u>468,5</u></b>
PCM panel: mean cell Temp. (°C)	32,2	32,8	31	27,6	24	21,6	21,1	22,7	24,8	26,4	27,8	30,6	<b>26,9</b>
PCM panel: mean theoretical eff.	0,160	0,160	0,161	0,163	0,166	0,167	0,168	0,167	0,165	0,164	0,163	0,161	<b>0,164</b>
PCM panel: mean power (W)	60,8	62	58,2	51,6	41	37,3	38,1	44,6	50,9	56,4	56,5	60	<b>51,5</b>
PCM panel: total energy gen. (KWh)	45,2	41,6	43,3	37,1	30,5	26,8	28,3	33,2	36,6	42,0	40,7	44,7	<b><u>450,0</u></b>

<b>BOLOGNA</b>													
LAT(°)   LONG(°)	45.53   11.30												
Optimum tilt (°)	24												
Month	Jan	Feb	Mar	Apr	May	Jun	Jul	Aug	Sep	Oct	Nov	Dec	TOTAL YEAR
mean ambient Temperature (°C)	1,1	3,3	8,1	12,7	17,5	21,4	23,9	23,6	19,7	13,7	7,2	2,6	<b>12,9</b>
total incident rad. (KWh/m <sup>2</sup> )	35,9	49,8	85,1	123,2	163,3	170,8	181,2	155,9	115,1	73,3	33,9	28,1	<b>1215,6</b>
mean wind speed (m/s)	1,1	1,6	1,8	2,1	2	2	2	1,8	1,6	1,3	1,3	1,2	<b>1,7</b>
St. panel: mean cell Temp. (°C)	2,4	5,6	12,1	18,9	25,7	30,5	33,1	31,6	25,7	17,2	8,4	3,4	<b>17,9</b>
St. panel: mean theoretical eff.	0,180	0,178	0,174	0,169	0,165	0,161	0,159	0,161	0,165	0,170	0,176	0,180	<b>0,170</b>
Standard panel: mean power (W)	11,2	16,8	24,9	35,7	44,9	47,3	47,9	41,5	32,7	21,1	10,7	8,7	<b>28,6</b>
St. panel: total energy gen. (KWh)	8,4	11,3	18,6	25,7	33,4	34,1	35,7	30,8	23,6	15,7	7,7	6,5	<b><u>251,4</u></b>
Fins panel: mean cell Temp. (°C)	2	4,9	10,8	16,8	22,9	27,4	30	28,9	23,7	16,1	8	3,2	<b>16,2</b>
Fins panel: mean theoretical eff.	0,181	0,179	0,175	0,171	0,166	0,163	0,162	0,162	0,166	0,171	0,176	0,180	<b>0,171</b>
Fins panel: mean power (W)	11,3	17	25,5	36,8	46,3	49	49,7	42,9	33,7	21,6	10,8	8,8	<b>29,5</b>
Fins panel: total energy gen. (KWh)	8,4	11,5	19,0	26,5	34,5	35,3	37,0	31,9	24,2	16,0	7,8	6,6	<b><u>258,6</u></b>
PCM panel: mean cell Temp. (°C)	2,8	6,2	12,8	20	27	32	34,8	33,2	26,9	17,9	8,8	3,7	<b>18,8</b>
PCM panel: mean theoretical eff.	0,180	0,178	0,173	0,168	0,164	0,160	0,158	0,159	0,164	0,170	0,176	0,179	<b>0,169</b>
PCM panel: mean power (W)	11,3	16,8	25	35,7	44,9	47,5	48,3	41,8	32,8	21,2	10,7	8,8	<b>28,7</b>
PCM panel: total energy gen. (KWh)	8,4	11,3	18,6	25,7	33,4	34,2	36,0	31,1	23,6	15,8	7,7	6,5	<b><u>252,2</u></b>

CAPE TOWN													
LAT(°)   LONG(°)	-34.80   18.42												
Optimum tilt (°)	19												
Month	Jan	Feb	Mar	Apr	May	Jun	Jul	Aug	Sep	Oct	Nov	Dec	TOTAL YEAR
mean ambient Temperature (°C)	20,8	20,9	19,1	16,5	14,8	12,8	12,3	12,9	14,3	16	18,3	19,8	<b>16,5</b>
total incident rad. (KWh/m <sup>2</sup> )	244,0	207,3	195,1	145,2	120,0	91,6	95,7	130,3	155,6	197,3	224,3	236,9	<b>2043,5</b>
mean wind speed (m/s)	7,2	5,3	5,1	4	4,1	5,6	4,2	4,3	5,4	4,6	7,7	4,3	<b>5,2</b>
St. panel: mean cell Temp. (°C)	31,3	31	27,6	23,2	20,2	16,9	16,5	18,6	21,4	24,9	28	30,7	<b>24,2</b>
St. panel: mean theoretical eff.	0,161	0,161	0,163	0,166	0,168	0,170	0,171	0,169	0,167	0,165	0,163	0,161	<b>0,165</b>
Standard panel: mean power (W)	64,4	60,5	52,4	41,2	33,4	26,9	27,2	36,5	44,5	53,5	62,4	62,6	<b>47,1</b>
St. panel: total energy gen. (KWh)	47,9	40,6	39,0	29,6	24,8	19,4	20,3	27,2	32,1	39,8	44,9	46,6	<b><u>412,2</u></b>
Fins panel: mean cell Temp. (°C)	27,9	27,7	24,8	21	18,4	15,6	15,1	16,7	19	21,9	24,9	27	<b>21,7</b>
Fins panel: mean theoretical eff.	0,163	0,163	0,165	0,168	0,169	0,171	0,172	0,171	0,169	0,167	0,165	0,164	<b>0,167</b>
Fins panel: mean power (W)	66,9	62,9	54,3	42,5	34,4	27,6	27,9	37,6	45,9	55,5	64,6	65,3	<b>48,8</b>
Fins panel: total energy gen. (KWh)	49,8	42,3	40,4	30,6	25,6	19,9	20,8	28,0	33,1	41,3	46,5	48,6	<b><u>426,7</u></b>
PCM panel: mean cell Temp. (°C)	32,7	32,6	29	24,3	21	17,6	17,3	19,5	22,4	26,2	29,3	32,4	<b>25,4</b>
PCM panel: mean theoretical eff.	0,160	0,160	0,162	0,165	0,168	0,170	0,170	0,169	0,167	0,164	0,162	0,160	<b>0,165</b>
PCM panel: mean power (W)	64,7	60,8	52,5	41,2	33,4	27	27,3	36,5	44,5	53,5	62,3	62,8	<b>47,2</b>
PCM panel: total energy gen. (KWh)	48,1	40,8	39,0	29,6	24,9	19,4	20,3	27,2	32,0	39,8	44,9	46,7	<b><u>412,8</u></b>

COX'S BAZAR													
LAT(°)   LONG(°)	21.45   92.97												
Optimum tilt (°)	27												
Month	Jan	Feb	Mar	Apr	May	Jun	Jul	Aug	Sep	Oct	Nov	Dec	TOTAL YEAR
mean ambient Temperature (°C)	20,8	22,6	26,3	28,5	29	27,8	27,6	27,2	27,5	27,7	25,5	21,8	<b>26,0</b>
total incident rad. (KWh/m <sup>2</sup> )	182,3	168,5	194,4	182,5	166,0	127,6	116,5	130,0	141,8	173,6	170,2	179,0	<b>1932,5</b>
mean wind speed (m/s)	1,6	1,8	1,9	2,4	3,1	2,7	3,1	2,7	2,3	1,6	0,9	1,2	<b>2,1</b>
St. panel: mean cell Temp. (°C)	29,5	31,5	35,7	37,7	37	34,4	33,2	33,5	34,8	36,4	34,5	30,7	<b>34,1</b>
St. panel: mean theoretical eff.	0,162	0,161	0,158	0,156	0,157	0,159	0,159	0,159	0,158	0,157	0,159	0,161	<b>0,159</b>
Standard panel: mean power (W)	48,3	48,9	50,2	48,7	43,4	35,1	31,5	34,9	38,6	44,9	45,6	47,2	<b>43,1</b>
St. panel: total energy gen. (KWh)	36,0	32,8	37,3	35,1	32,3	25,3	23,4	25,9	27,8	33,4	32,8	35,1	<b>377,2</b>
Fins panel: mean cell Temp. (°C)	26,5	28,5	32,5	34,6	34,4	32,2	31,3	31,4	32,3	33,4	31,3	27,6	<b>31,3</b>
Fins panel: mean theoretical eff.	0,164	0,163	0,160	0,159	0,159	0,160	0,161	0,161	0,160	0,159	0,161	0,163	<b>0,161</b>
Fins panel: mean power (W)	50,3	50,9	52,3	50,6	44,9	36,1	32,2	35,8	39,9	46,7	47,6	49,2	<b>44,7</b>
Fins panel: total energy gen. (KWh)	37,4	34,2	38,9	36,4	33,4	26,0	24,0	26,7	28,7	34,7	34,3	36,6	<b>391,4</b>
PCM panel: mean cell Temp. (°C)	31,3	33,5	37,8	39,6	38,2	35,6	33,9	34,6	36,2	38,2	36,7	32,7	<b>35,7</b>
PCM panel: mean theoretical eff.	0,161	0,159	0,156	0,155	0,156	0,158	0,159	0,159	0,157	0,156	0,157	0,160	<b>0,158</b>
PCM panel: mean power (W)	48,6	49,3	50,8	49,4	43,9	35,4	31,6	35	39	45,5	46,2	47,5	<b>43,5</b>
PCM panel: total energy gen. (KWh)	36,2	33,1	37,8	35,5	32,7	25,5	23,5	26,1	28,1	33,8	33,2	35,3	<b>380,8</b>

HARARE													
LAT(°)   LONG(°)	-18.18   31.5												
Optimum tilt (°)	18												
Month	Jan	Feb	Mar	Apr	May	Jun	Jul	Aug	Sep	Oct	Nov	Dec	TOTAL YEAR
mean ambient Temperature (°C)	20,8	20,9	21,3	18,9	16,7	14,6	14,3	15,8	19,7	21,2	21,7	21,1	<b>18,9</b>
total incident rad. (KWh/m <sup>2</sup> )	157,3	143,7	177,9	167,3	169,6	157,7	172,2	182,2	200,8	199,9	181,2	156,4	<b>2066,4</b>
mean wind speed (m/s)	2,3	2,7	3,3	3,4	3,4	2,8	3,5	3,7	4,2	4,5	3,7	3,7	<b>3,4</b>
St. panel: mean cell Temp. (°C)	28,9	28,8	30,1	27,3	24,8	22,2	22,3	24,3	29,4	30,7	30,8	28,8	<b>27,4</b>
St. panel: mean theoretical eff.	0,162	0,162	0,162	0,163	0,165	0,167	0,167	0,166	0,162	0,161	0,161	0,162	<b>0,163</b>
Standard panel: mean power (W)	42,8	43,1	47,5	46,5	46	44,7	47,3	49,2	54,7	52,6	49,8	42,5	<b>47,2</b>
St. panel: total energy gen. (KWh)	31,8	29,0	35,3	33,4	34,2	32,2	35,2	36,6	39,4	39,2	35,9	31,6	<b>413,7</b>
Fins panel: mean cell Temp. (°C)	26,1	26,1	27,1	24,5	22,1	19,7	19,6	21,4	26,2	27,5	27,8	26,2	<b>24,5</b>
Fins panel: mean theoretical eff.	0,164	0,164	0,164	0,165	0,167	0,169	0,169	0,167	0,164	0,163	0,163	0,164	<b>0,165</b>
Fins panel: mean power (W)	44,1	44,5	49,3	48,2	47,7	46,3	49	51,2	57,1	54,8	51,7	43,8	<b>49,0</b>
Fins panel: total energy gen. (KWh)	32,8	29,9	36,6	34,7	35,5	33,3	36,5	38,1	41,1	40,8	37,2	32,6	<b>429,2</b>
PCM panel: mean cell Temp. (°C)	30,3	30,1	31,6	28,8	26,3	23,7	23,7	25,8	31,2	32,3	32,5	30	<b>28,9</b>
PCM panel: mean theoretical eff.	0,161	0,162	0,161	0,162	0,164	0,166	0,166	0,164	0,161	0,160	0,160	0,162	<b>0,162</b>
PCM panel: mean power (W)	42,8	43,2	47,7	46,6	46	44,7	47,2	49,3	55,1	53,1	50,1	42,5	<b>47,4</b>
PCM panel: total energy gen. (KWh)	31,8	29,0	35,5	33,6	34,2	32,2	35,1	36,7	39,7	39,5	36,1	31,6	<b>415,0</b>



JIMMA													
LAT(°)   LONG(°)	8.68   37.84												
Optimum tilt (°)	14												
Month	Jan	Feb	Mar	Apr	May	Jun	Jul	Aug	Sep	Oct	Nov	Dec	TOTAL YEAR
mean ambient Temperature (°C)	17,2	18,8	19,4	19,4	19,2	18,5	17,6	17,5	17,9	18,7	17,2	17,2	<b>18,2</b>
total incident rad. (KWh/m <sup>2</sup> )	186,8	168,5	185,9	161,4	157,0	140,5	129,8	138,1	148,6	168,2	187,3	183,9	<b>1956,0</b>
mean wind speed (m/s)	0,5	1,2	0,6	0,8	1	0,7	0,5	0,5	0,9	0,8	0,4	0,3	<b>0,7</b>
St. panel: mean cell Temp. (°C)	27,1	28,6	29,2	28,3	27,6	26,3	24,6	24,9	25,9	27,5	27,4	27	<b>27,0</b>
St. panel: mean theoretical eff.	0,164	0,163	0,162	0,163	0,163	0,164	0,165	0,165	0,164	0,163	0,163	0,164	<b>0,164</b>
Standard panel: mean power (W)	49,3	48,9	48,8	44,5	42,2	39,6	35,9	37,9	41,6	44,8	51	48,6	<b>44,4</b>
St. panel: total energy gen. (KWh)	36,7	32,9	36,3	32,0	31,4	28,5	26,7	28,2	30,0	33,4	36,7	36,2	<b>388,9</b>
Fins panel: mean cell Temp. (°C)	23,7	25,2	25,8	25,2	24,7	23,5	22,2	22,3	23,1	24,4	23,8	23,6	<b>24,0</b>
Fins panel: mean theoretical eff.	0,166	0,165	0,164	0,165	0,165	0,166	0,167	0,167	0,166	0,165	0,166	0,166	<b>0,166</b>
Fins panel: mean power (W)	51,6	51,2	51,1	46,3	43,8	41	37	39,2	43,2	46,7	53,4	50,8	<b>46,3</b>
Fins panel: total energy gen. (KWh)	38,4	34,4	38,0	33,3	32,6	29,5	27,5	29,2	31,1	34,7	38,5	37,8	<b>405,0</b>
PCM panel: mean cell Temp. (°C)	29,3	30,8	31,3	30,2	29,2	27,8	26	26,3	27,5	29,4	29,7	29,2	<b>28,9</b>
PCM panel: mean theoretical eff.	0,162	0,161	0,161	0,161	0,162	0,163	0,164	0,164	0,163	0,162	0,162	0,162	<b>0,162</b>
PCM panel: mean power (W)	49,8	49,5	49,3	44,7	42,4	39,6	35,9	37,9	41,7	45,1	51,5	49	<b>44,7</b>
PCM panel: total energy gen. (KWh)	37,1	33,2	36,7	32,2	31,5	28,5	26,7	28,2	30,0	33,5	37,1	36,5	<b>391,2</b>

KUCHING													
LAT(°)   LONG(°)	2.55   110.33												
Optimum tilt (°)	1												
Month	Jan	Feb	Mar	Apr	May	Jun	Jul	Aug	Sep	Oct	Nov	Dec	TOTAL YEAR
mean ambient Temperature (°C)	25,4	25,8	26,1	26,6	26,7	27	26,5	26,4	26,3	26	25,8	25,5	<b>26,2</b>
total incident rad. (KWh/m <sup>2</sup> )	115,5	110,5	130,2	128,4	139,5	129,9	134,5	139,5	131,9	135,1	125,5	117,0	<b>1537,6</b>
mean wind speed (m/s)	1	0,8	1,1	0,8	1,1	1	0,9	1,3	1,2	1	0,8	1,1	<b>1,0</b>
St. panel: mean cell Temp. (°C)	31,9	32,7	33,4	34,1	34,6	34,7	34,1	34,3	33,9	33,5	33	32	<b>33,5</b>
St. panel: mean theoretical eff.	0,160	0,160	0,159	0,159	0,159	0,158	0,159	0,159	0,159	0,159	0,160	0,160	<b>0,159</b>
Standard panel: mean power (W)	30,9	32,6	34,5	35	36,6	35,3	35,5	36,6	35,9	35,6	34,3	31,2	<b>34,5</b>
St. panel: total energy gen. (KWh)	23,0	21,9	25,7	25,2	27,2	25,4	26,4	27,2	25,8	26,5	24,7	23,2	<b>302,3</b>
Fins panel: mean cell Temp. (°C)	29,6	30,2	30,8	31,5	31,8	32	31,4	31,5	31,2	30,9	30,5	29,7	<b>30,9</b>
Fins panel: mean theoretical eff.	0,162	0,161	0,161	0,161	0,160	0,160	0,161	0,161	0,161	0,161	0,161	0,162	<b>0,161</b>
Fins panel: mean power (W)	31,9	33,7	35,7	36,2	37,9	36,5	36,7	37,9	37,2	36,9	35,5	32,2	<b>35,7</b>
Fins panel: total energy gen. (KWh)	23,7	22,6	26,6	26,1	28,2	26,3	27,3	28,2	26,8	27,5	25,6	24,0	<b>312,9</b>
PCM panel: mean cell Temp. (°C)	33,4	34,3	35,1	35,9	36,4	36,5	35,9	36,1	35,8	35,3	34,7	33,5	<b>35,2</b>
PCM panel: mean theoretical eff.	0,159	0,159	0,158	0,158	0,157	0,157	0,158	0,157	0,158	0,158	0,158	0,159	<b>0,158</b>
PCM panel: mean power (W)	31,1	32,8	34,8	35,3	37	35,7	35,8	37	36,2	35,9	34,6	31,4	<b>34,8</b>
PCM panel: total energy gen. (KWh)	23,1	22,0	25,9	25,4	27,5	25,7	26,7	27,5	26,1	26,7	24,9	23,4	<b>305,0</b>

LAS VEGAS													
LAT(°)   LONG(°)	36.11   -115.83												
Optimum tilt (°)	34												
Month	Jan	Feb	Mar	Apr	May	Jun	Jul	Aug	Sep	Oct	Nov	Dec	TOTAL YEAR
mean ambient Temperature (°C)	7,8	9,3	12,9	19,4	24,8	30,2	33,1	31,5	27,5	19,6	13,1	8,3	<b>19,8</b>
total incident rad. (KWh/m <sup>2</sup> )	144,7	150,5	186,6	215,1	220,7	215,3	221,1	224,5	215,0	195,0	170,8	146,7	<b>2306,1</b>
mean wind speed (m/s)	3,1	4,7	5,4	5,9	6	5,5	4,1	4,4	3,6	3,8	3,8	3,3	<b>4,5</b>
St. panel: mean cell Temp. (°C)	14,2	16,3	20,4	28,3	33,8	39,6	43,2	41,5	37,8	28,3	20,7	14,8	<b>28,2</b>
St. panel: mean theoretical eff.	0,172	0,171	0,168	0,163	0,159	0,155	0,153	0,154	0,156	0,163	0,168	0,172	<b>0,163</b>
Standard panel: mean power (W)	41,2	46,8	52	59,8	57,8	56,8	55,2	56,4	56,2	52	48,7	41,4	<b>52,0</b>
St. panel: total energy gen. (KWh)	30,7	31,5	38,7	43,0	43,0	40,9	41,1	42,0	40,5	38,7	35,1	30,8	<b>455,9</b>
Fins panel: mean cell Temp. (°C)	12	14	18	25,6	31	36,7	39,9	38,3	34,4	25,4	18,2	12,6	<b>25,5</b>
Fins panel: mean theoretical eff.	0,174	0,172	0,170	0,165	0,161	0,157	0,155	0,156	0,159	0,165	0,170	0,173	<b>0,165</b>
Fins panel: mean power (W)	42,6	48,4	53,6	61,8	59,8	58,8	57,4	58,7	58,8	54	50,4	42,8	<b>53,9</b>
Fins panel: total energy gen. (KWh)	31,7	32,5	39,9	44,5	44,5	42,3	42,7	43,7	42,3	40,2	36,3	31,9	<b>472,5</b>
PCM panel: mean cell Temp. (°C)	15,1	17,2	21,3	29,4	34,8	40,4	43,9	42,5	39,2	29,6	21,8	15,8	<b>29,3</b>
PCM panel: mean theoretical eff.	0,172	0,170	0,168	0,162	0,158	0,155	0,152	0,153	0,155	0,162	0,167	0,171	<b>0,162</b>
PCM panel: mean power (W)	41,1	46,7	51,8	59,9	58,4	57,6	56,1	57,4	57,1	52,3	48,6	41,3	<b>52,4</b>
PCM panel: total energy gen. (KWh)	30,6	31,4	38,5	43,1	43,4	41,5	41,8	42,7	41,1	38,9	35,0	30,8	<b>458,9</b>

MANAUS													
LAT(°)   LONG(°)	-3.88   -60.97												
Optimum tilt (°)	5												
Month	Jan	Feb	Mar	Apr	May	Jun	Jul	Aug	Sep	Oct	Nov	Dec	TOTAL YEAR
mean ambient Temperature (°C)	25,9	25,8	26,4	26,5	26,5	26,4	26,7	27,7	27,9	27,8	27,2	26,6	<b>26,8</b>
total incident rad. (KWh/m <sup>2</sup> )	129,9	120,8	138,3	134,9	133,2	138,0	161,5	168,4	168,0	168,9	143,8	141,2	<b>1747,0</b>
mean wind speed (m/s)	1	1,2	1,2	1	0,7	1,3	0,7	0,9	0,9	1	0,9	1,1	<b>1,0</b>
St. panel: mean cell Temp. (°C)	33,1	33,2	34,1	34,3	33,9	34,3	35,6	37	37,4	37,1	35,5	34,5	<b>35,0</b>
St. panel: mean theoretical eff.	0,160	0,159	0,159	0,159	0,159	0,159	0,158	0,157	0,157	0,157	0,158	0,159	<b>0,158</b>
Standard panel: mean power (W)	34,5	35,4	36,3	36,7	35,1	37,5	41,9	43,3	44,5	43,3	38,6	37	<b>38,7</b>
St. panel: total energy gen. (KWh)	25,7	23,8	27,0	26,4	26,1	27,0	31,2	32,2	32,0	32,2	27,8	27,5	<b>339,0</b>
Fins panel: mean cell Temp. (°C)	30,5	30,6	31,4	31,5	31,3	31,5	32,5	33,7	34,1	33,8	32,5	31,7	<b>32,1</b>
Fins panel: mean theoretical eff.	0,161	0,161	0,161	0,161	0,161	0,161	0,160	0,159	0,159	0,159	0,160	0,160	<b>0,160</b>
Fins panel: mean power (W)	35,70 0	36,70 0	37,70 0	38,10 0	36,40 0	38,90 0	43,70 0	45,20 0	46,50 0	45,30 0	40,20 0	38,40 0	<b>40,2</b>
Fins panel: total energy gen. (KWh)	26,6	24,7	28,1	27,4	27,1	28,0	32,5	33,7	33,5	33,7	28,9	28,6	<b>352,7</b>
PCM panel: mean cell Temp. (°C)	34,8	34,9	36	36,1	35,7	36,2	37,8	39,2	39,7	39,4	37,4	36,4	<b>37,0</b>
PCM panel: mean theoretical eff.	0,158	0,158	0,158	0,157	0,158	0,157	0,156	0,155	0,155	0,155	0,157	0,157	<b>0,157</b>
PCM panel: mean power (W)	34,7	35,7	36,7	37	35,4	37,8	42,4	43,9	45,1	44	39,1	37,4	<b>39,1</b>
PCM panel: total energy gen. (KWh)	25,8	24,0	27,3	26,6	26,3	27,2	31,6	32,7	32,5	32,7	28,1	27,8	<b>342,8</b>

<b>MOMBASA</b>													
LAT(°)   LONG(°)	-4.96   40.67												
Optimum tilt (°)	2												
Month	Jan	Feb	Mar	Apr	May	Jun	Jul	Aug	Sep	Oct	Nov	Dec	TOTAL YEAR
mean ambient Temperature (°C)	26,8	27	28,1	26,9	26	24,9	23,7	24,1	24,6	25,7	26,2	26,9	<b>25,9</b>
total incident rad. (KWh/m <sup>2</sup> )	178,0	168,5	186,8	160,0	140,8	141,5	144,7	160,7	171,7	181,5	173,6	169,1	<b>1977,0</b>
mean wind speed (m/s)	3,6	3,9	3	3,2	4,2	4,3	3,4	3,6	4	3	2,7	3,1	<b>3,5</b>
St. panel: mean cell Temp. (°C)	36,5	37,1	38,3	36	33,8	32,9	31,6	32,8	34,1	35,5	35,9	36,2	<b>35,1</b>
St. panel: mean theoretical eff.	0,157	0,157	0,156	0,158	0,159	0,160	0,161	0,160	0,159	0,158	0,158	0,157	<b>0,158</b>
Standard panel: mean power (W)	45,8	47,7	47,4	42,8	37	38,6	38,4	42,3	46,1	46,9	46,2	43,7	<b>43,6</b>
St. panel: total energy gen. (KWh)	34,1	32,0	35,3	30,8	27,6	27,8	28,6	31,5	33,2	34,9	33,3	32,5	<b>381,6</b>
Fins panel: mean cell Temp. (°C)	33	33,5	34,6	32,8	31	30,1	28,8	29,7	30,8	32	32,5	32,9	<b>31,8</b>
Fins panel: mean theoretical eff.	0,160	0,159	0,158	0,160	0,161	0,162	0,162	0,162	0,161	0,160	0,160	0,160	<b>0,160</b>
Fins panel: mean power (W)	47,9	49,9	49,7	44,6	38,4	40,1	39,9	44,1	48,2	49	48,3	45,6	<b>45,5</b>
Fins panel: total energy gen. (KWh)	35,6	33,6	37,0	32,1	28,6	28,9	29,7	32,8	34,7	36,5	34,8	33,9	<b>398,2</b>
PCM panel: mean cell Temp. (°C)	38,8	39,5	40,6	38,1	35,6	34,8	33,4	34,8	36,4	38	38,3	38,5	<b>37,2</b>
PCM panel: mean theoretical eff.	0,156	0,155	0,154	0,156	0,158	0,158	0,159	0,158	0,157	0,156	0,156	0,156	<b>0,157</b>
PCM panel: mean power (W)	46,4	48,4	48,2	43,3	37,4	38,9	38,6	42,6	46,6	47,4	46,9	44,3	<b>44,1</b>
PCM panel: total energy gen. (KWh)	34,5	32,5	35,9	31,2	27,8	28,0	28,8	31,7	33,5	35,3	33,7	33,0	<b>385,9</b>

OSLO													
LAT(°)   LONG(°)	60.91   11.76												
Optimum tilt (°)	36												
Month	Jan	Feb	Mar	Apr	May	Jun	Jul	Aug	Sep	Oct	Nov	Dec	TOTAL YEAR
mean ambient Temperature (°C)	-3,8	-0,9	0,9	4,6	11,9	14,7	17,5	16,6	11	6,7	1,8	-1,6	<b>6,6</b>
total incident rad. (KWh/m <sup>2</sup> )	17,8	31,2	77,2	107,1	161,3	164,8	161,8	127,8	77,7	47,5	19,1	9,2	<b>1002,5</b>
mean wind speed (m/s)	1,2	2	2,1	2,6	2,3	2,8	2,5	2,3	2,6	2,7	1,4	3	<b>2,3</b>
St. panel: mean cell Temp. (°C)	-3,9	0,1	4	9,2	19,2	22,3	24,9	22,4	14,5	8,3	1,8	-2,1	<b>10,1</b>
St. panel: mean theoretical eff.	0,185	0,182	0,179	0,176	0,169	0,167	0,165	0,167	0,172	0,176	0,181	0,183	<b>0,175</b>
Standard panel: mean power (W)	5,7	10,8	23,4	32,8	45,5	48	45	35,9	23,4	14,3	6,1	2,9	<b>24,5</b>
St. panel: total energy gen. (KWh)	4,2	7,3	17,4	23,7	33,9	34,6	33,5	26,7	16,9	10,6	4,4	2,2	<b><u>215,2</u></b>
Fins panel: mean cell Temp. (°C)	-3,9	-0,2	3	7,8	16,8	19,9	22,5	20,5	13,4	7,8	1,8	-2	<b>9,0</b>
Fins panel: mean theoretical eff.	0,185	0,182	0,180	0,177	0,171	0,168	0,167	0,168	0,173	0,177	0,181	0,183	<b>0,176</b>
Fins panel: mean power (W)	5,7	10,9	23,9	33,6	46,8	49,2	46,2	36,8	23,9	14,5	6,2	3	<b>25,1</b>
Fins panel: total energy gen. (KWh)	4,3	7,4	17,8	24,2	34,8	35,4	34,4	27,4	17,2	10,8	4,5	2,2	<b><u>220,2</u></b>
PCM panel: mean cell Temp. (°C)	-3,8	0,4	4,5	9,9	20,2	23,2	25,9	23,2	14,9	8,6	2	-2,1	<b>10,6</b>
PCM panel: mean theoretical eff.	0,184	0,182	0,179	0,175	0,168	0,166	0,164	0,166	0,172	0,176	0,181	0,183	<b>0,175</b>
PCM panel: mean power (W)	5,7	10,8	23,4	32,8	45,3	47,8	44,9	35,8	23,4	14,3	6,1	3	<b>24,4</b>
PCM panel: total energy gen. (KWh)	4,2	7,3	17,4	23,6	33,7	34,4	33,4	26,7	16,9	10,6	4,4	2,2	<b><u>214,8</u></b>

OSNABRÜCK													
LAT(°)   LONG(°)	52.27   8.5												
Optimum tilt (°)	36												
Month	Jan	Feb	Mar	Apr	May	Jun	Jul	Aug	Sep	Oct	Nov	Dec	TOTAL YEAR
mean ambient Temperature (°C)	2,4	3,2	6,2	10	13,8	16,6	18,4	18,3	14,8	10,8	6,3	2,6	<b>10,3</b>
total incident rad. (KWh/m <sup>2</sup> )	34,8	52,5	101,6	115,3	139,9	132,6	160,7	126,6	117,8	77,1	45,1	22,1	<b>1126,1</b>
mean wind speed (m/s)	3,7	3,7	3,8	3,4	3,2	3	3,1	3,1	2,4	2,5	2,6	3,1	<b>3,1</b>
St. panel: mean cell Temp. (°C)	3,3	5,3	10,3	14,9	19,8	22,7	25,5	23,9	20,1	14	7,8	2,9	<b>14,2</b>
St. panel: mean theoretical eff.	0,180	0,178	0,175	0,172	0,169	0,167	0,165	0,166	0,168	0,172	0,177	0,180	<b>0,172</b>
Standard panel: mean power (W)	10,8	17,6	29,9	34,6	39,8	38,4	44,5	35,4	34	22,4	14	6,9	<b>27,4</b>
St. panel: total energy gen. (KWh)	8,1	11,8	22,2	24,9	29,6	27,6	33,1	26,4	24,5	16,7	10,1	5,1	<b><u>240,1</u></b>
Fins panel: mean cell Temp. (°C)	3	4,6	9	13,4	17,9	20,7	23,3	22,1	18,4	13	7,3	2,7	<b>13,0</b>
Fins panel: mean theoretical eff.	0,180	0,179	0,176	0,173	0,170	0,168	0,166	0,167	0,169	0,173	0,177	0,180	<b>0,173</b>
Fins panel: mean power (W)	11	17,9	30,6	35,3	40,7	39,3	45,7	36,2	34,9	22,9	14,2	6,9	<b>28,0</b>
Fins panel: total energy gen. (KWh)	8,2	12,1	22,7	25,4	30,3	28,3	34,0	27,0	25,2	17,0	10,2	5,2	<b><u>245,5</u></b>
PCM panel: mean cell Temp. (°C)	3,5	5,6	10,9	15,5	20,5	23,4	26,4	24,6	20,9	14,5	8,1	3	<b>14,7</b>
PCM panel: mean theoretical eff.	0,180	0,178	0,175	0,171	0,168	0,166	0,164	0,165	0,168	0,172	0,176	0,180	<b>0,172</b>
PCM panel: mean power (W)	10,8	17,6	29,8	34,6	39,7	38,4	44,5	35,4	34	22,4	14	6,9	<b>27,3</b>
PCM panel: total energy gen. (KWh)	8,1	11,8	22,2	24,9	29,6	27,6	33,1	26,3	24,5	16,7	10,1	5,1	<b><u>240,0</u></b>

RIAD													
LAT(°)   LONG(°)	25.77   47.74												
Optimum tilt (°)	23												
Month	Jan	Feb	Mar	Apr	May	Jun	Jul	Aug	Sep	Oct	Nov	Dec	TOTAL YEAR
mean ambient Temperature (°C)	14	16,7	20,3	25,9	32,1	35,2	36,2	36,4	33	27,6	21,6	14,9	<b>26,2</b>
total incident rad. (KWh/m <sup>2</sup> )	168,0	165,8	193,3	191,9	215,3	220,9	225,7	225,8	218,9	217,7	174,9	142,6	<b>2360,7</b>
mean wind speed (m/s)	3	3	3,6	3,6	3	3,7	4,3	3,5	2,5	2,2	1,1	2,8	<b>3,0</b>
St. panel: mean cell Temp. (°C)	21,6	25,3	29,1	35,3	42,8	46,2	46,7	47,6	44,3	38,2	30,6	21,5	<b>35,8</b>
St. panel: mean theoretical eff.	0,167	0,165	0,162	0,158	0,153	0,151	0,150	0,150	0,152	0,156	0,161	0,167	<b>0,158</b>
Standard panel: mean power (W)	46,3	49,5	51,4	51,2	53,8	56,1	55,2	54,6	55,3	54,8	47,1	39,3	<b>51,2</b>
St. panel: total energy gen. (KWh)	34,5	33,3	38,2	36,8	40,0	40,4	41,1	40,6	39,8	40,8	33,9	29,2	<b>448,7</b>
Fins panel: mean cell Temp. (°C)	19,1	22,4	26,2	32,1	39,2	42,6	43,4	43,9	40,5	34,6	27,5	19,3	<b>32,6</b>
Fins panel: mean theoretical eff.	0,169	0,167	0,164	0,160	0,155	0,153	0,153	0,152	0,155	0,158	0,163	0,169	<b>0,160</b>
Fins panel: mean power (W)	48	51,6	53,5	53,4	56,3	58,7	57,7	57,3	58,2	57,6	49,3	40,7	<b>53,5</b>
Fins panel: total energy gen. (KWh)	35,7	34,7	39,8	38,4	41,9	42,3	42,9	42,6	41,9	42,9	35,5	30,3	<b>468,9</b>
PCM panel: mean cell Temp. (°C)	22,9	26,8	30,7	36,9	43,8	46,7	46,9	47,5	45,7	40,4	32,9	22,7	<b>37,0</b>
PCM panel: mean theoretical eff.	0,166	0,164	0,161	0,157	0,152	0,150	0,150	0,150	0,151	0,155	0,160	0,167	<b>0,157</b>
PCM panel: mean power (W)	46,2	49,6	51,6	51,8	54,7	57,1	56,3	55,7	56,4	55,7	47,6	39,3	<b>51,8</b>
PCM panel: total energy gen. (KWh)	34,4	33,3	38,4	37,3	40,7	41,1	41,9	41,4	40,6	41,5	34,3	29,2	<b>454,1</b>



SEVILLA													
LAT(°)   LONG(°)	37.38   -6.3												
Optimum tilt (°)	31												
Month	Jan	Feb	Mar	Apr	May	Jun	Jul	Aug	Sep	Oct	Nov	Dec	TOTAL YEAR
mean ambient Temperature (°C)	10,4	11,7	15,1	16,1	19,8	24,1	27,4	26,5	24,5	19,5	13,7	11,5	<b>18,4</b>
total incident rad. (KWh/m <sup>2</sup> )	112,1	123,8	175,0	170,7	209,4	203,0	223,5	217,8	180,9	146,1	108,3	101,0	<b>1971,5</b>
mean wind speed (m/s)	2,2	2,2	2,6	2,9	3,4	2,9	2,9	2,6	2,1	2,4	3,3	2,6	<b>2,7</b>
St. panel: mean cell Temp. (°C)	15,3	17,8	23	24	29,1	33,9	38	36,8	33,6	26,1	18,4	15,7	<b>26,0</b>
St. panel: mean theoretical eff.	0,172	0,170	0,166	0,166	0,162	0,159	0,156	0,157	0,159	0,164	0,169	0,171	<b>0,164</b>
Standard panel: mean power (W)	32	38,4	47,5	47,9	55,8	54,6	56,8	55,5	48,1	39,4	31,4	28,9	<b>44,7</b>
St. panel: total energy gen. (KWh)	23,8	25,8	35,3	34,5	41,5	39,3	42,3	41,3	34,6	29,3	22,6	21,5	<b>391,8</b>
Fins panel: mean cell Temp. (°C)	13,7	15,8	20,4	21,4	26	30,6	34,5	33,4	30,5	23,9	16,9	14,4	<b>23,5</b>
Fins panel: mean theoretical eff.	0,173	0,171	0,168	0,167	0,164	0,161	0,159	0,159	0,161	0,166	0,170	0,172	<b>0,166</b>
Fins panel: mean power (W)	32,9	39,6	49,3	49,6	57,9	56,7	59,2	57,9	50,2	40,8	32,3	29,6	<b>46,3</b>
Fins panel: total energy gen. (KWh)	24,5	26,6	36,7	35,7	43,0	40,8	44,1	43,1	36,1	30,3	23,3	22,0	<b>406,3</b>
PCM panel: mean cell Temp. (°C)	16,2	18,8	24,3	25,1	30,3	35,1	39,1	38,1	35	27,2	19,2	16,5	<b>27,1</b>
PCM panel: mean theoretical eff.	0,171	0,169	0,165	0,165	0,161	0,158	0,155	0,156	0,158	0,164	0,169	0,171	<b>0,164</b>
PCM panel: mean power (W)	32	38,3	47,6	48,1	56,1	55,1	57,7	56,4	48,9	39,6	31,4	28,9	<b>45,0</b>
PCM panel: total energy gen. (KWh)	23,8	25,8	35,4	34,6	41,7	39,7	42,9	41,9	35,2	29,5	22,6	21,5	<b>394,5</b>

## Annex 3. Detailed economic results for all the locations and PV panel options

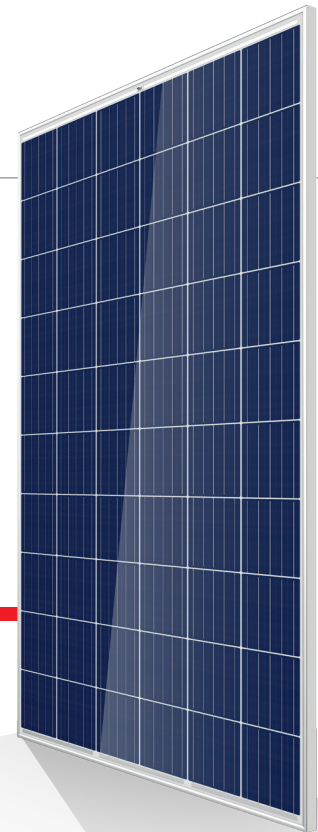
ALICE SPRINGS									
	Annual power generation (KWh)			Annual installation cost (€)			Electricity cost (€/KWh)		
	Min	Mean	Max	Min	Mean	Max	Min	Mean	Max
Standard panel	411.3	419.7	428.1	15.9	30.8	45.6	0.037	0.073	0.111
	-	0%	-						
Fins-cooled panel	430.1	438.9	447.7	24.1	51.0	77.8	0.054	0.116	0.181
	-	+4.6%	-						
PCM-cooled panel	415.5	424.0	432.5	26.5	58.7	90.8	0.061	0.138	0.219
	-	+1.0%	-						
ANTOFAGASTA									
	Annual power generation (KWh)			Annual installation cost (€)			Electricity cost (€/KWh)		
	Min	Mean	Max	Min	Mean	Max	Min	Mean	Max
Standard panel	400.5	408.7	416.9	15.9	30.8	45.6	0.038	0.075	0.114
	-	0%	-						
Fins-cooled panel	416.0	424.5	433.0	24.1	51.0	77.8	0.056	0.120	0.187
	-	+3.9%	-						
PCM-cooled panel	399.5	407.7	415.9	26.5	58.7	90.8	0.064	0.144	0.227
	-	-0.2%	-						
BOLOGNA									
	Annual power generation (KWh)			Annual installation cost (€)			Electricity cost (€/KWh)		
	Min	Mean	Max	Min	Mean	Max	Min	Mean	Max
Standard panel	223.2	227.8	232.4	15.9	30.8	45.6	0.068	0.135	0.204
	-	0%	-						
Fins-cooled panel	229.6	234.3	239.0	24.1	51.0	77.8	0.101	0.218	0.339
	-	+2.9%	-						
PCM-cooled panel	223.9	228.5	233.1	26.5	58.7	90.8	0.114	0.257	0.406
	-	0.3%	-						
CAPE TOWN									
	Annual power generation (KWh)			Annual installation cost (€)			Electricity cost (€/KWh)		
	Min	Mean	Max	Min	Mean	Max	Min	Mean	Max
Standard panel	366.0	373.5	381.0	15.9	30.8	45.6	0.042	0.082	0.125
	-	0%	-						
Fins-cooled panel	378.9	386.6	394.3	24.1	51.0	77.8	0.061	0.132	0.205
	-	+3.5%	-						
PCM-cooled panel	366.5	374.0	381.5	26.5	58.7	90.8	0.069	0.157	0.248
	-	+0.1%	-						
COX'S BAZAR									
	Annual power generation (KWh)			Annual installation cost (€)			Electricity cost (€/KWh)		
	Min	Mean	Max	Min	Mean	Max	Min	Mean	Max
Standard panel	334.9	341.7	348.5	15.9	30.8	45.6	0.046	0.090	0.136
	-	0%	-						
Fins-cooled panel	347.5	354.6	361.7	24.1	51.0	77.8	0.067	0.144	0.224
	-	+3.8%	-						
PCM-cooled panel	338.1	345.0	351.9	26.5	58.7	90.8	0.075	0.170	0.269
	-	+1.0%	-						

<b>HARARE</b>									
	Annual power generation (KWh)			Annual installation cost (€)			Electricity cost (€/KWh)		
	Min	Mean	Max	Min	Mean	Max	Min	Mean	Max
Standard panel	367.3	374.8	382.3	15.9	30.8	45.6	0.042	0.082	0.124
	-	0%	-						
Fins-cooled panel	381.1	388.9	396.7	24.1	51.0	77.8	0.061	0.131	0.204
	-	+3.8%	-						
PCM-cooled panel	368.5	376.0	383.5	26.5	58.7	90.8	0.069	0.156	0.246
	-	+0.3%	-						
<b>JIMMA</b>									
	Annual power generation (KWh)			Annual installation cost (€)			Electricity cost (€/KWh)		
	Min	Mean	Max	Min	Mean	Max	Min	Mean	Max
Standard panel	345.3	352.3	359.3	15.9	30.8	45.6	0.044	0.087	0.132
	-	0%	-						
Fins-cooled panel	359.6	366.9	374.2	24.1	51.0	77.8	0.064	0.139	0.216
	-	+4.1%	-						
PCM-cooled panel	347.3	354.4	361.5	26.5	58.7	90.8	0.073	0.166	0.261
	-	+0.6%	-						
<b>KUCHING</b>									
	Annual power generation (KWh)			Annual installation cost (€)			Electricity cost (€/KWh)		
	Min	Mean	Max	Min	Mean	Max	Min	Mean	Max
Standard panel	268.4	273.9	279.4	15.9	30.8	45.6	0.057	0.112	0.170
	-	0%	-						
Fins-cooled panel	277.8	283.5	289.2	24.1	51.0	77.8	0.083	0.180	0.280
	-	+3.5%	-						
PCM-cooled panel	270.8	276.3	281.8	26.5	58.7	90.8	0.094	0.212	0.335
	-	+0.9%	-						
<b>LAS VEGAS</b>									
	Annual power generation (KWh)			Annual installation cost (€)			Electricity cost (€/KWh)		
	Min	Mean	Max	Min	Mean	Max	Min	Mean	Max
Standard panel	404.7	413.0	421.3	15.9	30.8	45.6	0.038	0.075	0.113
	-	0%	-						
Fins-cooled panel	419.5	428.1	436.7	24.1	51.0	77.8	0.055	0.119	0.185
	-	+3.7%	-						
PCM-cooled panel	407.5	415.8	424.1	26.5	58.7	90.8	0.062	0.141	0.223
	-	+0.7%	-						
<b>MANAUS</b>									
	Annual power generation (KWh)			Annual installation cost (€)			Electricity cost (€/KWh)		
	Min	Mean	Max	Min	Mean	Max	Min	Mean	Max
Standard panel	301.0	307.1	313.2	15.9	30.8	45.6	0.051	0.100	0.151
	-	0%	-						
Fins-cooled panel	313.1	319.5	325.9	24.1	51.0	77.8	0.074	0.160	0.248
	-	4.0%	-						
PCM-cooled panel	304.4	310.6	316.8	26.5	58.7	90.8	0.084	0.189	0.298
	-	1.1%	-						

<b>MOMBASA</b>									
	Annual power generation (KWh)			Annual installation cost (€)			Electricity cost (€/KWh)		
	Min	Mean	Max	Min	Mean	Max	Min	Mean	Max
Standard panel	338.8	345.7	352.6	15.9	30.8	45.6	0.045	0.089	0.135
	-	0%	-						
Fins-cooled panel	353.6	360.8	368.0	24.1	51.0	77.8	0.065	0.141	0.220
	-	+4.4%	-						
PCM-cooled panel	342.6	349.6	356.6	26.5	58.7	90.8	0.074	0.168	0.265
	-	+1.1%	-						
<b>OSLO</b>									
	Annual power generation (KWh)			Annual installation cost (€)			Electricity cost (€/KWh)		
	Min	Mean	Max	Min	Mean	Max	Min	Mean	Max
Standard panel	191.1	195.0	198.9	15.9	30.8	45.6	0.080	0.158	0.239
	-	0%	-						
Fins-cooled panel	195.5	199.5	203.5	24.1	51.0	77.8	0.118	0.256	0.398
	-	2.3%	-						
PCM-cooled panel	190.7	194.6	198.5	26.5	58.7	90.8	0.134	0.302	0.476
	-	-0.2%	-						
<b>OSNABRÜCK</b>									
	Annual power generation (KWh)			Annual installation cost (€)			Electricity cost (€/KWh)		
	Min	Mean	Max	Min	Mean	Max	Min	Mean	Max
Standard panel	213.2	217.5	221.9	15.9	30.8	45.6	0.072	0.142	0.214
	-	0%	-						
Fins-cooled panel	218.0	222.4	226.8	24.1	51.0	77.8	0.106	0.229	0.357
	-	+2.3%	-						
PCM-cooled panel	213.1	217.4	221.7	26.5	58.7	90.8	0.120	0.270	0.426
	-	-0.1%	-						
<b>RIAD</b>									
	Annual power generation (KWh)			Annual installation cost (€)			Electricity cost (€/KWh)		
	Min	Mean	Max	Min	Mean	Max	Min	Mean	Max
Standard panel	398.4	406.5	414.6	15.9	30.8	45.6	0.038	0.076	0.114
	-	0%	-						
Fins-cooled panel	416.3	424.8	433.3	24.1	51.0	77.8	0.056	0.120	0.187
	-	+4.5%	-						
PCM-cooled panel	403.2	411.4	419.6	26.5	58.7	90.8	0.063	0.143	0.225
	-	+1.2%	-						
<b>SEVILLA</b>									
	Annual power generation (KWh)			Annual installation cost (€)			Electricity cost (€/KWh)		
	Min	Mean	Max	Min	Mean	Max	Min	Mean	Max
Standard panel	347.9	355.0	362.1	15.9	30.8	45.6	0.044	0.087	0.131
	-	0%	-						
Fins-cooled panel	360.7	368.1	375.5	24.1	51.0	77.8	0.064	0.139	0.216
	-	+3.7%	-						
PCM-cooled panel	350.3	357.4	364.5	26.5	58.7	90.8	0.073	0.164	0.259
	-	+0.7%	-						



## **Annex 4. TSM-PD05 datasheet**



# THE Honey MODULE

## TSM-PD05

**60 CELL**  
MULTICRYSTALLINE MODULE

**255–270W**  
POWER OUTPUT RANGE

**16.5%**  
MAXIMUM EFFICIENCY

**0/+5W**  
POSITIVE POWER TOLERANCE

**TRINA SOLAR: A STRONG AND RELIABLE PARTNER**

As a leading global manufacturer of next generation photovoltaic products, Trina Solar is committed to building mutually beneficial alliances with installers, developers, distributors and technological partners as the backbone of our shared goal to drive Smart Energy Together. Thanks to an extensive sales and service network with local expert teams throughout Europe, Trina Solar is perfectly positioned to support your needs. With Trina Solar as your strong, bankable partner you can rest assured knowing that you've made the right choice.

[www.trinasolar.com](http://www.trinasolar.com)



**Excellent low light performance on cloudy days, mornings and evenings**

- Advanced surface texturing
- Back surface field
- Selective emitter



**Maximize Limited Space**

- 60-cell module power output up to 270W
- Up to 165 W/m<sup>2</sup> power density



**Highly reliable due to stringent quality control**

- All modules have to pass electroluminescence (EL) inspection
- Over 30 in-house tests (UV, TC, HF, and many more)
- In-house testing goes well beyond certification requirements
- PID resistant
- 1000 V UL/1000V IEC certified

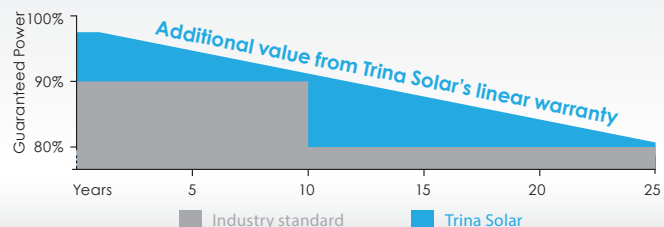


**Certified to withstand challenging environmental conditions**

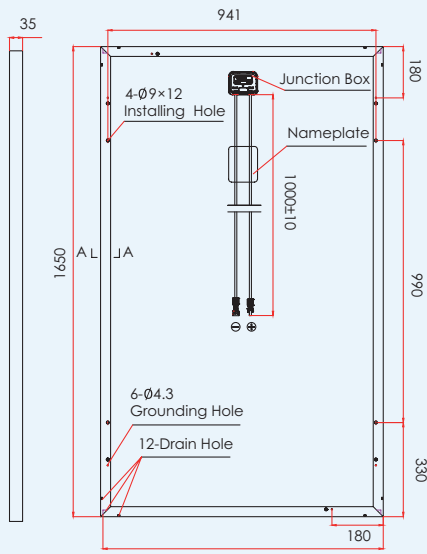
- 130 km/h wind load (2400 Pa)
- 900 kg snow load per module (5400 Pa)
- 35 mm hail stones at 97 km/h
- Ammonia resistance
- Salt mist resistance
- resistance to sand and dust abrasion

**LINEAR PERFORMANCE WARRANTY**

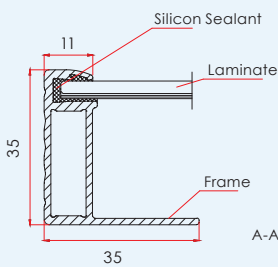
10 Year Product Warranty • 25 Year Linear Power Warranty



**DIMENSIONS OF PV MODULE TSM-PD05**  
(unit:mm)

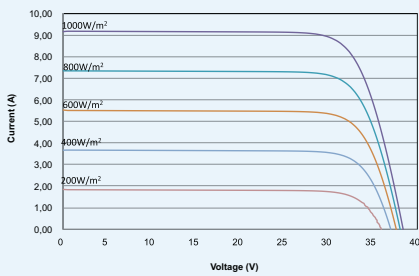


Back View

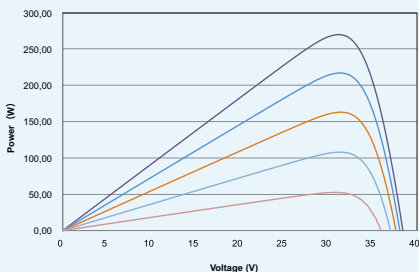


A-A

**I-V CURVES OF PV MODULE (270W)**



**P-V CURVES OF PV MODULE (270W)**



**CERTIFICATION**

IEC61215/EN61215  
IEC61730/EN61730  
IEC 627162 PfG 1917/05.11  
IEC 61701  
DIN EN 60068-2-68 LC2  
MCS BRE PV0183

ELECTRICAL DATA @ STC	TSM-255 PD05	TSM-260 PD05	TSM-265 PD05	TSM-270 PD05
Peak Power Watts- $P_{MAX}$ (Wp)*	255	260	265	270
Power Output Tolerance- $P_{MAX}$ (W)	0/+5	0/+5	0/+5	0/+5
Maximum Power Voltage- $V_{MPP}$ (V)	30.5	30.6	30.8	30.9
Maximum Power Current- $I_{MPP}$ (A)	8.37	8.50	8.61	8.73
Open Circuit Voltage- $V_{OC}$ (V)	38.1	38.2	38.3	38.4
Short Circuit Current- $I_{SC}$ (A)	8.88	9.00	9.10	9.18
Module Efficiency $\eta_m$ (%)	15.6	15.9	16.2	16.5

STC: Irradiance 1000 W/m<sup>2</sup>, Cell Temperature 25°C, Air Mass AM1.5  
\* Measuring tolerance: ±3%

ELECTRICAL DATA @ NOCT	TSM-255 PD05	TSM-260 PD05	TSM-265 PD05	TSM-270 PD05
Maximum Power- $P_{MAX}$ (Wp)	189	193	197	200
Maximum Power Voltage- $U_{MPP}$ (V)	28.2	28.4	28.6	28.7
Maximum Power Current- $I_{MPP}$ (A)	6.71	6.81	6.89	6.97
Open Circuit Voltage- $U_{OC}$ (V)	35.3	35.4	35.5	35.5
Short Circuit Current- $I_{SC}$ (A)	7.17	7.27	7.35	7.41

NOCT: Irradiance at 800 W/m<sup>2</sup>, Ambient Temperature 20°C, Wind Speed 1 m/s.

**MECHANICAL DATA**

Solar Cells	Multicrystalline 156 × 156 mm (6 inches)
Cell Orientation	60 cells (6 × 10)
Module Dimensions	1650 × 992 × 35 mm (65.0 × 39.1 × 1.38 inches)
Weight	18.6 kg
Glass	High Transparency, Anti-Reflective, AR Coated and Heat Tempered Solar Glass - 3.2 mm (0.13 inches)
Backsheet	White
Frame	Silver Anodized Aluminium Alloy
J-Box	IP 67 rated or IP 68 rated
Cables	Photovoltaic Technology Cable 4.0mm <sup>2</sup> (0.006 inches <sup>2</sup> ), 1000 mm (39.4 inches)
Connector	MC4 Compatible

**TEMPERATURE RATINGS**

Nominal Operating Cell Temperature (NOCT)	44°C (±2K)
Temperature Coefficient of $P_{MAX}$	- 0.41%/K
Temperature Coefficient of $V_{OC}$	- 0.32%/K
Temperature Coefficient of $I_{SC}$	0.05%/K

**MAXIMUM RATINGS**

Operational Temperature	-40 to +85°C
Maximum System Voltage	1000V DC (IEC) 1000V DC (UL)
Max Series Fuse Rating	15A
Mechanical Load	5400 Pa
Wind Load	2400 Pa

**WARRANTY**

10 year Product Workmanship Warranty

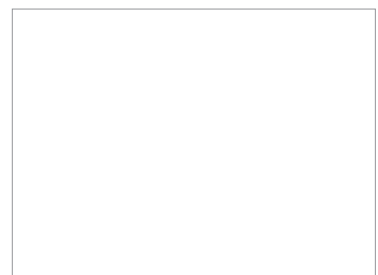
25 year Linear Performance Warranty

(Please refer to product warranty for details)

**PACKAGING CONFIGURATION**

Modules per box: 30 pieces

Modules per 40' container: 840 pieces



TSM\_EN\_2016\_B



## **Annex 5. RT44HC datasheet**

## RT44HC

RUBITHERM® RT is a pure PCM, this heat storage material utilising the processes of phase change between solid and liquid (melting and congealing) to store and release large quantities of thermal energy at nearly constant temperature. The RUBITHERM® phase change materials (PCM's) provide a very effective means for storing heat and cold, even when limited volumes and low differences in operating temperature are applicable.

We look forward to discussing your particular questions, needs and interests with you.

Properties for RT-line:

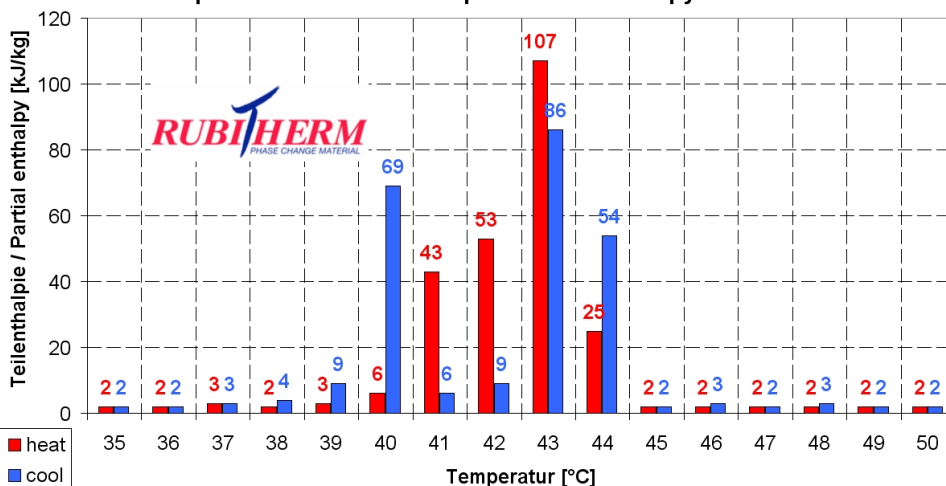
- high thermal energy storage capacity
- heat storage and release take place at relatively constant temperatures
- no supercooling effect, chemically inert
- long life product, with stable performance through the phase change cycles
- melting temperature range between -9 °C and 100 °C available



### The most important data:

	Typical Values	
<b>Melting area</b>	<b>41-44</b>	[°C]
	main peak: 43	
<b>Congealing area</b>	<b>44-40</b>	[°C]
	main peak: 43	
<b>Heat storage capacity ± 7,5%</b>	<b>250</b>	[kJ/kg]*
Combination of latent and sensible heat in a temperatur range of 35°C to 50°C.	<b>70</b>	[Wh/kg]*
<b>Specific heat capacity</b>	<b>2</b>	[kJ/kg·K]
<b>Density solid</b> at 25 °C	<b>0,8</b>	[kg/l]
<b>Density liquid</b> at 80 °C	<b>0,7</b>	[kg/l]
<b>Heat conductivity (both phases)</b>	<b>0,2</b>	[W/(m·K)]
<b>Volume expansion</b>	<b>12,5</b>	[%]
<b>Flash point</b>	<b>&gt;180</b>	[°C]
<b>Max. operation temperature</b>	<b>70</b>	[°C]

Beispiel: RT44HC Teilenthalpie / Partial enthalpy distribution



Rubitherm Technologies GmbH  
 Imhoffweg 6  
 D-12307 Berlin  
 Tel: +49 (30) 7109622-0  
 Fax: +49 (30) 7109622-22  
 E-Mail: info@rubitherm.com  
 Internet: www.rubitherm.com

The product information given is a non-binding planning aid, subject to technical changes without notice. Version: 06.08.2018

\*Measured with 3-layer-calorimeter.

## **Annex 6. Simulation code**



```
[A,opt_tilt,mean_ang_wind]=read_xlsx_sim(Book,lat,long);

angle=opt_tilt; % Optimal panel tilt for the location

%% SIMULATION FOR EVERY MONTH
%%
for month=1:12

if month==1
    day_0=1; % First day of the month
    day_f=31; % Last day of the month
else
    day_0=sum(days_month(1:(month-1)))+1; % First day of the month
    day_f=sum(days_month(1:(month))); % Last day of the month
end

t_amb_mean_month(month)=mean(A((day_0-1)*24+1:(day_f*24),1)); % [°C] Mean ambient
Temperature of the month
g_month(month)=sum(A((day_0-1)*24+1:(day_f*24),2)); % [W/m^2] Total
incident radiation of the month
wind_mean_month(month)=mean(A((day_0-1)*24+1:(day_f*24),3)); % [m/s] Mean wind
speed of the month

%% SIMULATION FOR EVERY DAY OF THE MONTH
%%
for day=day_0:day_f

disp(location_txt);
disp(strcat(int2str(day-day_0+1), '/', int2str(month)));

t_amb_mean_day(day)=mean(A((24*(day-1)+1):(24*day),1)); % [°C] Mean ambient
Temperature of the day
g_day(day)=sum(A((24*(day-1)+1):(24*day),2)); % [W/m^2] Total incident
radiation of the day
wind_mean_day(day)=mean(A((24*(day-1)+1):(24*day),3)); % [m/s] Mean wind speed of
the day

sim_step=0.5; % [s] sim_step: time step for the
simulation
time_data_v=0:3600:3600*24; % [s] time_data_v: time vector for the data
time_sim_v=0:sim_step:3600*24; % [s] time_sim_v: time vector for the simulation

t_amb_data=A((24*(day-1)+1):(24*day+1),1)+273.15; % [°C] t_amb_data:
available data of the ambient Temperature
g_data=A((24*(day-1)+1):(24*day+1),2); % [W/m^2] g_data: available data
of the radiation
wind_data=A((24*(day-1)+1):(24*day+1),3); % [m/s] wind_data: available
data of the wind speed

t_amb=interp1(time_data_v,t_amb_data,time_sim_v,'pchip'); % [°C] t_amb:
interpolation of the ambient Temperature for the simulation step
g=interp1(time_data_v,g_data,time_sim_v,'pchip'); % [W/m^2] g:
interpolation of the radiation for the simulation step
wind=interp1(time_data_v,wind_data,time_sim_v,'pchip'); % [m/s] wind:
interpolation of the wind speed for the simulation step
```

```
if day==1
    t_0_st=zeros(1,7);
    t_0_fins=zeros(1,7);
    t_0_pcm=zeros(1,7);

    t_0_st(1,:)=t_amb(1);
    t_0_fins(1,:)=t_amb(1);
    t_0_pcm(1,:)=t_amb(1);
else
    t_0_st=t_f_st;
    t_0_fins=t_f_fins;
    t_0_pcm=t_f_pcm;
end

%% Day simulation for standard panel
%%
[Wh_standard_day(day),t_cell_standard_mean_day(day),t_f_st]=standard_panel(sim_step,
time_sim_v,t_amb,g,wind,angle,c_vis,c_k,c_pr,c_dens,t_0_st,mean_ang_wind);

% [W] Mean day power for standard panel
power_standard_mean_day(day)=Wh_standard_day(day)/24;

% [-] Mean day theoretical efficiency for standard panel
eff_standard_mean_day(day)=0.165*(1-0.0041*(t_cell_standard_mean_day(day)-25-273.15));

%% Day simulation for fins panel
%%
[Wh_fins_day(day),t_cell_fins_mean_day(day),t_f_fins]=fins_panel(sim_step,time_sim_v,
t_amb,g,wind,angle,c_vis,c_k,c_pr,c_dens,t_0_fins,mean_ang_wind);

% [W] Mean day power for fins panel
power_fins_mean_day(day)=Wh_fins_day(day)/24;

% [-] Mean day theoretical efficiency for fins panel
eff_fins_mean_day(day)=0.165*(1-0.0041*(t_cell_fins_mean_day(day)-25-273.15));

%% Day simulation for PCM panel
%%
[Wh_pcm_day(day),t_cell_pcm_mean_day(day),t_f_pcm]=pcm_panel(sim_step,time_sim_v,
t_amb,g,wind,angle,c_vis,c_k,c_pr,c_dens,t_0_pcm,mean_ang_wind);

% [W] Mean day power for PCM panel
power_pcm_mean_day(day)=Wh_pcm_day(day)/24;

% [-] Mean day theoretical efficiency for PCM panel
eff_pcm_mean_day(day)=0.165*(1-0.0041*(t_cell_pcm_mean_day(day)-25-273.15));

clearvars t_amb g wind t_amb_data g_data wind_data;

end

Wh_standard_month(month)=sum(Wh_standard_day(day_0:day_f)); % [Wh] Total month
generation of energy for standard panel
Wh_fins_month(month)=sum(Wh_fins_day(day_0:day_f)); % [Wh] Total month
generation of energy for fins panel
```

```
generation of energy for fins panel
Wh_pcm_month(month)=sum(Wh_pcm_day(day_0:day_f)); % [Wh] Total month
generation of energy for PCM panel

eff_standard_mean_month(month)=mean(eff_standard_mean_day(day_0:day_f)); % [-] Mean
month theoretical efficiency for standard panel
eff_fins_mean_month(month)=mean(eff_fins_mean_day(day_0:day_f)); % [-] Mean
month theoretical efficiency for fins panel
eff_pcm_mean_month(month)=mean(eff_pcm_mean_day(day_0:day_f)); % [-] Mean
month theoretical efficiency for PCM panel

power_standard_mean_month(month)=mean(power_standard_mean_day(day_0:day_f)); % [W]
Mean month power for standard panel
power_fins_mean_month(month)=mean(power_fins_mean_day(day_0:day_f)); % [W]
Mean month power for fins panel
power_pcm_mean_month(month)=mean(power_pcm_mean_day(day_0:day_f)); % [W]
Mean month power for PCM panel

t_cell_standard_mean_month(month)=mean(t_cell_standard_mean_day(day_0:day_f)); %
[°C] Mean month cell Temperature standard panel
t_cell_fins_mean_month(month)=mean(t_cell_fins_mean_day(day_0:day_f)); %
[°C] Mean month cell Temperature for fins panel
t_cell_pcm_mean_month(month)=mean(t_cell_pcm_mean_day(day_0:day_f)); %
[°C] Mean month cell Temperature for PCM panel

end

%% WRITE OUTPUT .XLSX FILE
%%
%>>> Monthly results
disp('WRITING EXCEL MONTHLY OUTPUT...');

xlswrite('SIMULATION OUTPUT.xlsx',opt_tilt,1,strcat('B',int2str(8+(loc-1)*21)));

xlswrite('SIMULATION OUTPUT.xlsx',round(t_amb_mean_month,1),1,strcat('B',int2str(10+
(loc-1)*21)));
xlswrite('SIMULATION OUTPUT.xlsx',round(g_month,1),1,strcat('B',int2str(11+(loc-1)
*21)));
xlswrite('SIMULATION OUTPUT.xlsx',round(wind_mean_month,1),1,strcat('B',int2str(12+
(loc-1)*21)));

xlswrite('SIMULATION OUTPUT.xlsx',round(t_cell_standard_mean_month-273.15,1),1,strcat
('B',int2str(13+(loc-1)*21)));
xlswrite('SIMULATION OUTPUT.xlsx',round(eff_standard_mean_month,3),1,strcat('B',
int2str(14+(loc-1)*21)));
xlswrite('SIMULATION OUTPUT.xlsx',round(power_standard_mean_month,1),1,strcat('B',
int2str(15+(loc-1)*21)));
xlswrite('SIMULATION OUTPUT.xlsx',round(Wh_standard_month,1),1,strcat('B',int2str(16+
(loc-1)*21)));

xlswrite('SIMULATION OUTPUT.xlsx',round(t_cell_fins_mean_month-273.15,1),1,strcat('B',
int2str(17+(loc-1)*21)));
xlswrite('SIMULATION OUTPUT.xlsx',round(eff_fins_mean_month,3),1,strcat('B',int2str
(18+(loc-1)*21)));
```

```
xlswrite('SIMULATION OUTPUT.xlsx',round(power_fins_mean_month,1),1,strcat('B',int2str
(19+(loc-1)*21)));
xlswrite('SIMULATION OUTPUT.xlsx',round(Wh_fins_month,1),1,strcat('B',int2str(20+(loc-
1)*21)));

xlswrite('SIMULATION OUTPUT.xlsx',round(t_cell_pcm_mean_month-273.15,1),1,strcat('B',
int2str(21+(loc-1)*21)));
xlswrite('SIMULATION OUTPUT.xlsx',round(eff_pcm_mean_month,3),1,strcat('B',int2str(22+
(loc-1)*21)));
xlswrite('SIMULATION OUTPUT.xlsx',round(power_pcm_mean_month,1),1,strcat('B',int2str
(23+(loc-1)*21)));
xlswrite('SIMULATION OUTPUT.xlsx',round(Wh_pcm_month,1),1,strcat('B',int2str(24+(loc-
1)*21)));

%>>> Daily results
disp('WRITING EXCEL DAILY OUTPUT...');

xlswrite('DAILY RESULTS.xlsx',round(t_amb_mean_day,1),loc+1,'E4');
xlswrite('DAILY RESULTS.xlsx',round(g_day,1),loc+1,'F4');
xlswrite('DAILY RESULTS.xlsx',round(wind_mean_day,1),loc+1,'G4');

xlswrite('DAILY RESULTS.xlsx',round(t_cell_standard_mean_day-273.15,1),loc+1,'H4');
xlswrite('DAILY RESULTS.xlsx',round(eff_standard_mean_day,3),loc+1,'I4');
xlswrite('DAILY RESULTS.xlsx',round(power_standard_mean_day,1),loc+1,'J4');
xlswrite('DAILY RESULTS.xlsx',round(Wh_standard_day,1),loc+1,'K4');

xlswrite('DAILY RESULTS.xlsx',round(t_cell_fins_mean_day-273.15,1),loc+1,'L4');
xlswrite('DAILY RESULTS.xlsx',round(eff_fins_mean_day,3),loc+1,'M4');
xlswrite('DAILY RESULTS.xlsx',round(power_fins_mean_day,1),loc+1,'N4');
xlswrite('DAILY RESULTS.xlsx',round(Wh_fins_day,1),loc+1,'O4');

xlswrite('DAILY RESULTS.xlsx',round(t_cell_pcm_mean_day-273.15,1),loc+1,'P4');
xlswrite('DAILY RESULTS.xlsx',round(eff_pcm_mean_day,3),loc+1,'Q4');
xlswrite('DAILY RESULTS.xlsx',round(power_pcm_mean_day,1),loc+1,'R4');
xlswrite('DAILY RESULTS.xlsx',round(Wh_pcm_day,1),loc+1,'S4');
```

end

```

function [Wh_pcm_day_1,t_cell_pcm_mean_day_1,t_f_pcm]=pcm_panel(sim_step,time_sim_v,
t_amb,g,wind,angle,c_vis,c_k,c_pr,c_dens,t_0_pcm,mean_ang_wind)

%% Model scheme
%%
%% AMB: AMBIANCE
%% SG: SOLAR GLASS
%% CELL: SOLAR CELLS
%% BACK: BACK INSULATION
%% conv: convection
%% cond: conduction
%% rad: radiation
%%
%%
%% Q_rad_c=g*(abs_sg+trans_sg-ref_cell)----|
%% Q_rad_sg=g*a*(abs_sg+trans_sg-ref_cell)----|
%% Qsky----|
%% [AMB]---<R_conv_sg_amb>---[SG_AMB]---<R_cond_sg/2>---[SG]---<R_cond_sg/2>---[CELL]
-----
%%
%% ...---<R_cond_back/2>---[BACK]---<R_cond_back/2>---<R_cond_gap>---[BACK_PCM]---
<R_conv_back_amb>---[AMB]
%%
%% Q_pcm-----|
%%
%% Fisical parameters
%%
[a,p,l,a_cells,a_sil,th_sg,m_sg,cp_sg,k_sg,emis_sg,th_c,m_c,cp_c,k_c,...
th_back,m_back,cp_back,k_back,th_fin,l_fin,z_fin,th_fin,n_fin,m_fin,...
cp_fin,k_fin,a_cover,dens_pcm,cp_pcm,k_pcm,sigma,lg_prf,w_prf_h,...
w_prf_v,th_prf,n_prf,k_al,cp_al,dens_al,abs_glass,abs_Cells,a_abs]
=fisical_param();

%% PCM model variables
%%
n_horiz=6; n_vert=6; % Number of horizontal and vertical nodes for the PCM-profiles
Temperature calculation
[PHASE,MASS,TEMP,ENERGY,RESIST_H,RESIST_V,energy_melt,energy_solid,m_profiles]
=PCM_variables(n_vert,n_horiz,time_sim_v,t_amb,w_prf_h,w_prf_v,lg_prf,n_prf,th_prf,
k_pcm,k_al,dens_al,dens_pcm);

%% Simulation variables
%%
t_sg_amb=zeros(1,length(time_sim_v)); t_sg_amb(1)=t_0_pcm(1); % [K] Solar Glass
Ambiance Temperature
t_sg=zeros(1,length(time_sim_v)); t_sg(1)=t_0_pcm(2); % [K] Solar Glass
Temperature
t_cell=zeros(1,length(time_sim_v)); t_cell(1)=t_0_pcm(3); % [K] Cell
Temperature
t_back=zeros(1,length(time_sim_v)); t_back(1)=t_0_pcm(4); % [K] Back
insulation Temperature
t_back_amb=zeros(1,length(time_sim_v)); t_back_amb(1)=t_0_pcm(5); % [K] Back
insulation - Ambiance Temperature
t_fins=zeros(1,length(time_sim_v)); t_fins(1)=t_0_pcm(6); % [K] Fins

```

```

Temperature
t_back_pcm=zeros(1,length(time_sim_v)); t_back_pcm(1)=t_0_pcm(7); % [K] Back PCM
Temperature
h_top=zeros(1,length(time_sim_v)); % [W/K*m^2]
Convection coefficient of the top surface
h_back=zeros(1,length(time_sim_v)); % [W/K*m^2]
Convection coefficient of the back surface

eff=zeros(1,length(time_sim_v)); % [-] Teoretic
efficiency of the cell
power=zeros(1,length(time_sim_v)); % [W] Output
power of the module
Wh=zeros(1,length(time_sim_v)); % [Wh]Total
energy generated by the module

%% Conductive thermal resistances
%%
R_cond_sg=th_sg/(k_sg*a); % [K/W] conductive thermal resistance of the
solar glass
R_cond_back=th_back/(a*k_back); % [K/W] conductive thermal resistance of the back
insulation

for i=1:(length(time_sim_v)-1)
%% SOLAR GLASS (SG)
%%
%>>> [W] Q_solar_rad_sg: radiation heat absorbed in the glass
Q_solar_rad_sg=g(i)*a_abs*abs_glass;

%>>> [W] Q_rad_sg_sky: radiation heat from the sky
t_sky=0.0552*t_amb(i)^1.5; % [K] Temperature of the sky
Q_rad_sg_sky=sigma*emis_sg*(t_sg_amb(i)^2+t_sky^2)*(t_sg_amb(i)+t_sky)*(t_sg_amb
(i)-t_sky);

%>>> [W] Q_cond_sg: heat flux due to conduction between solar glass and solar
cells
Q_cond_sg=(t_sg(i)-t_cell(i))/(R_cond_sg/2);

%>>> [W] Q_conv_sg: convective heat flux between solar glass and ambiance
top=1; back=0; % Convection on the top: there are forced convection due to the
wind
% [W/K*m^2] h_top: convective coefficient on the top of the panel
[h_top(i)]=inclined_plane_conv(t_sg_amb(i),t_amb(i),wind(i),1,top,back,angle,
c_vis,c_k,c_pr,c_dens,mean_ang_wind);
R_conv_sg=1/(h_top(i)*a); % [K/W] convective thermal resistance between the
solar glass and the ambiance
Q_conv_sg=(t_sg(i)-t_amb(i))/(R_conv_sg+(R_cond_sg/2));

%>>> [K] t_sg(i+1): temperature of the (middle) solar glass at the 'i+1' step
t_sg(i+1)=(Q_solar_rad_sg-Q_cond_sg-Q_conv_sg-Q_rad_sg_sky)*sim_step/(m_sg*cp_sg)
+t_sg(i); % [K] Temperature for the next step

%>>> [K] t_sg_amb(i+1): temperature of the solar glass surface at the 'i+1' step
t_sg_amb(i+1)=t_sg(i+1)+(Q_solar_rad_sg-Q_conv_sg-Q_rad_sg_sky)*(R_cond_sg/2);

```

```

%% CELLS (C)
%%
%>>> [W] Q_solar_rad_c: radiation heat absorbed in the CELLS
Q_solar_rad_c=g(i)*a_abs*a_cells*abs_Cells;

%>>> [W] power(i+1): fraction of the solar radiation that turns into electrical
power
eff(i+1)=0.165*(1-0.0041*(t_cell(i)-25-273.15)); % [-] Teoretic efficiency of the
cell
power(i+1)=g(i)*eff(i)*a_sil*a_cells;

%>>> [W] Q_cond_back: heat flux due to conduction between cells and back
insulation
Q_cond_back=(t_cell(i)-t_back(i))/R_cond_back;

%>>> [K] t_c(i+1): temperature of the cells at the 'i+1' step
t_cell(i+1)=(Q_solar_rad_c+Q_cond_sg-Q_cond_back-power(i))*sim_step/(m_c*cp_c)
+t_cell(i);

%% BACK INSULATION
%%
fins=0; pcm=1;
if (fins==0)&&(pcm==0) % Standard panel
%>>> [W] Q_conv_back: heat flux due to convection with the ambiance
top=0; back=1; % Convection on the back: only free convection (no
wind)
[h_back(i)]=inclined_plane_conv(t_back_amb(i),t_amb(i),wind(i),1,top,back,
angle,c_vis,c_k,c_pr,c_dens,mean_ang_wind);
R_conv_back=1/(h*a); % [K/W] convective thermal resistance between the back
insulation and the ambiance
Q_conv_back=(t_back(i)-t_amb(i))/(R_conv_back+(R_cond_back/2));

%>>> [K] t_back(i+1): temperature of the (middle) back insulation at the 'i+1'
step
t_back(i+1)=(Q_cond_back-Q_conv_back)*sim_step/(m_back*cp_back)+t_back(i);

%>>> [K] t_back_amb(i+1): temperature of the back surface at the 'i+1' step
t_back_amb(i+1)=t_back(i+1)-Q_conv_back*(R_cond_back/2);
else
if pcm==1 % PCM panel
% [K/W] R_cond_gap: conductive thermal resistance due to the air gap
between the back insulation and the PCM profiles
k_air=24.12+0.07225*(t_back(i)-273.15); % [W/m*K] thermal conductivity of
the air at the back insulation Temperature
R_cond_gap=0.002/(k_air*(10^-3)*a);

% [W] Q_cond_profiles: heat flux due to conduction between the back
insulation and the PCM profiles
Q_cond_profiles=(t_back(i)-t_back_pcm(i))/(R_cond_back/2+R_cond_gap);

%>>> [K] t_back(i+1): temperature of the (middle) back insulation at the
'i+1' step
t_back(i+1)=(Q_cond_back-Q_cond_profiles)*sim_step/(m_back*cp_back)+t_back
(i);

```

```

end
if fins==1 % Fins panel
% [K/W] R_cond_gap: conductive thermal resistance due to the air gap
between the back insulation and the 'L' fins
k_air=24.12+0.07225*(t_back(i)-273.15); % [W/m*K] thermal conductivity of
the air at the back insulation Temperature
R_cond_gap=0.000/(k_air*(10^-3)*a);

%>>> [W] Q_cond_fins: heat flux due to conduction between the back
insulation and the fins
Q_cond_fins=(t_back(i)-t_fins(i))/(R_cond_back/2+R_cond_gap);

%>>> [K] t_back(i+1): temperature of the (middle) back insulation at the
'i+1' step
t_back(i+1)=(Q_cond_back-Q_cond_fins)*sim_step/(m_back*cp_back)+t_back(i);
% [K] Temperature for the next step
end
end

%% PCM
%%
% ENERGY: matrix for the stored energy of each PCM mass element in the full
melting
% interval (35 - 50 °C): 35.0°C-->energy=0 // 50.99°C-->256(KJ/Kg)*mass
ENERGY(:,i+1)=ENERGY(:,i); % Initial value for 'i+1' step

% PHASE: phase of each PCM mass element
% 0: fluid, 1: phase change, 2: solid, 3: aluminum
PHASE(i+1)=PHASE(i); % Initial value for 'i+1' step

%>>> [W] Q_H: horizontal heat flow in the PCM profile matrix
Q_H=zeros(n_vert-2,n_horiz-1);
for y=1:n_vert-2
for x=1:n_horiz-1
Q_H(y,x)=(TEMP(y+1,x,i)-TEMP(y+1,x+1,i))/RESIST_H(y,x);
end
end

%>>> [W] Q_V: vertical heat flow in the PCM profile matrix
Q_V=zeros(n_vert-1,n_horiz);
for y=1:n_vert-1
for x=1:n_horiz
Q_V(y,x)=(TEMP(y,x,i)-TEMP(y+1,x,i))/RESIST_V(y,x);
end
end

%>>> [W] Q_pcm: total heat exchange between the aluminum profiles and the PCM
(Heat entering the aluminum profiles)
Q_pcm=sum(Q_V(n_vert-1,2:n_horiz-1))+sum(Q_V(1,2:n_horiz-1))+sum(Q_H(1:n_vert-2,
n_horiz-1))-sum(Q_H(1:n_vert-2,1));

% [K/W] R_conv_back_pcm: convective thermal resistance between the back and the
ambiance
top=0; back=1; % Convection on the back: only free convection (no wind)
[h_back(i)]=inclined_plane_conv(t_back_pcm(i),t_amb(i),wind(i),1,top,back,angle,

```

```

c_vis,c_k,c_pr,c_dens,mean_ang_wind);
R_conv_back_pcm=1/(h_back(i)*a);

%>>> [W] Q_conv_back_pcm: convective heat at the back of the panel
Q_conv_back_pcm=(t_back_pcm(i)-t_amb(i))/R_conv_back_pcm;

%>>> [K] t_back_pcm(i+1): temperature of the PCM-aluminum profiles at the 'i+1' step
% (it is considered the same Temperature in all the volume of the aluminum profiles)
t_back_pcm(i+1)=(Q_cond_profiles+Q_pcm-Q_conv_back_pcm)*sim_step/(m_profiles*cp_al)+t_back_pcm(i);

TEMP(1,:,i+1)=t_back_pcm(i+1); % First row of the Temperature matrix: aluminum top cover
TEMP(n_vert,:,i+1)=t_back_pcm(i+1); % Last row of the Temperature matrix: aluminum back cover

%>>> Temperature calculation of all the differential mass elements of the PCM
for y=2:n_vert-1 % y: vertical nodes (rows of the matrix)
TEMP(y,1,i+1)=t_back_pcm(i+1); % Left side of the aluminum profile
TEMP(y,n_horiz,i+1)=t_back_pcm(i+1); % Right side of the aluminum profile
for x=2:(n_horiz-1) % x: horizontal nodes (columns of the matrix)
if (TEMP(y,x,i)>(273.15+40)) && (TEMP(y,x,i)<(273.15+45)) % 40-45 °C: PCM phase change interval (1)
PHASE(y,x,i+1)=1;
else if (TEMP(y,x,i)<(273.15+40)) % <40 °C: PCM solid (0)
PHASE(y,x,i+1)=0;
else % >45 °C: PCM liquid (2)
PHASE(y,x,i+1)=2;
end
end

Q_net=Q_V(y-1,x)-Q_V(y,x)+Q_H(y-1,x-1)-Q_H(y-1,x); % [W] Q_net: net heat in the (x-1,y) mass element

if (TEMP(y,x,i)>(273.15+35)) && (TEMP(y,x,i)<(273.15+51)) % 35-51 °C: interval where the PCM heat capacity is not constant (melting-solidification)
ENERGY(y,x,i+1)=Q_net*sim_step+ENERGY(y,x,i); % [J=W*s] Net energy in mass element for the 35-51°C interval
if ENERGY(y,x,i+1)>(sum(energy_melt(2,:))*MASS(y-1,x)) % If the net energy exceed the upper limit of the 35-51°C interval
ENERGY(y,x,i+1)=sum(energy_melt(2,:))*MASS(y-1,x);
TEMP(y,x,i+1)=Q_net*sim_step/(MASS(y-1,x)*cp_pcm)+TEMP(y,x,i); % [K] Temperature in the mass element (>51°C)
else if ENERGY(y,x,i+1)<0 % If the net energy is below the lower limit of the 35-51°C interval
ENERGY(y,x,i+1)=0;
TEMP(y,x,i+1)=Q_net*sim_step/(MASS(y-1,x)*cp_pcm)+TEMP(y,x,i);
end
end
i);

```

```
end
```

```

else % The net energy is in the 35-51°C interval
% Energy interpolation in the 35-51°C
if Q_net>0 % Heat flow entering the PCM: melting process
ind=find((energy_melt(3,:)*MASS(y-1,x))>ENERGY(y,x,i+1));
end
else % Heat flow out the PCM: solidification
ind=find((energy_solid(3,:)*MASS(y-1,x))>ENERGY(y,x,i+1));
end
if ENERGY(y,x,i+1)>(energy_melt(3,length(energy_melt))*MASS(y-1,x))
ind=length(energy_melt)+1;
end
if Q_net>0 % Melting process
% Temperature of the (x,y) mass element
TEMP(y,x,i+1)=273.15+energy_melt(1,ind-1)+((ENERGY(y,x,i+1)-energy_melt(3,ind-1)*MASS(y-1,x))/(energy_melt(2,ind-1)*MASS(y-1,x)));
end
if Q_net<0 % Solidification process
% Temperature of the (x,y) mass element
TEMP(y,x,i+1)=273.15+energy_solid(1,ind-1)+((ENERGY(y,x,i+1)-energy_solid(3,ind-1)*MASS(y-1,x))/(energy_solid(2,ind-1)*MASS(y-1,x)));
end
end
else % Temperature out of the 35-51°C interval
TEMP(y,x,i+1)=Q_net*sim_step/(MASS(y-1,x)*cp_pcm)+TEMP(y,x,i);
if (TEMP(y,x,i+1)>(273.15+35)) && (TEMP(y,x,i+1)<(273.15+51)) % If the temperature at the 'i+1' step is in the 35-51°C interval
if Q_net>0
ENERGY(y,x,i+1)=MASS(y-1,x)*cp_pcm*(TEMP(y,x,i+1)-(273.15+35));
end
if Q_net<0
ENERGY(y,x,i+1)=energy_solid(3,length(energy_solid))*MASS(y-1,x)*cp_pcm*(TEMP(y,x,i+1)-(273.15+51));
end
end
end
end

% Generation of Energy (Wh) according to the simulation
%
Wh(i+1)=power(i)*(sim_step/3600)+Wh(i);

end

t_f_pcm=[t_sg_amb(i+1) t_sg(i+1) t_cell(i+1) t_back(i+1) t_back_amb(i+1) t_fins(i+1) t_back_pcm(i+1)];

Wh_pcm_day_1=Wh(length(Wh));
t_cell_pcm_mean_day_1=mean(t_cell);

```

```

function [Wh_fins_day_1,t_cell_fins_mean_day_1,t_f_fins]=fins_panel(sim_step,time_sim_v,t_amb,g,wind,angle,c_vis,c_k,c_pr,c_dens,t_0_fins,mean_ang_wind)

% Model scheme
%%
% AMB: AMBIANCE
% SG: SOLAR GLASS
% CELL: SOLAR CELLS
% BACK: BACK INSULATION
% conv: convection
% cond: conduction
% rad: radiation
%
%
% Q_rad_c=g*a_eff*trans_sg_amb_c----|
% Q_rad_sg=g*a*(abs_sg+trans_sg_ref_cell)----|
% Qsky----|
% [AMB]---<R_conv_sg_amb---[SG_AMB]---<R_cond_sg/2---[SG]---<R_cond_sg/2---[CELL]
-----
% ...---<R_cond_back/2---[BACK]---<R_cond_back/2---<R_cond_gap---[FINS]---|
<R_conv_fins>---|---[AMB]
|
% |---
<R_conv_cover>---|

% Fisical parameters
%%
[a,p,l,a_cells,a_sil,th_sg,m_sg,cp_sg,k_sg,emis_sg,th_c,m_c,cp_c,k_c,...
th_back,m_back,cp_back,k_back,th_fin,l_fin,z_fin,th_fin,n_fin,m_fin,...
cp_fin,k_fin,a_cover,dens_pcm,cp_pcm,k_pcm,sigma,lg_prf,w_prf_h,...
w_prf_v,th_prf,n_prf,k_al,cp_al,dens_al,abs_glass,abs_Cells,a_abs]
=fisical_param();

% Simulation variables
%%
t_sg_amb=zeros(1,length(time_sim_v)); t_sg_amb(1)=t_0_fins(1); % [K] Solar Glass
- Ambiance Temperature
t_sg=zeros(1,length(time_sim_v)); t_sg(1)=t_0_fins(2); % [K] Solar Glass
Temperature
t_cell=zeros(1,length(time_sim_v)); t_cell(1)=t_0_fins(3); % [K] Cell
Temperature
t_back=zeros(1,length(time_sim_v)); t_back(1)=t_0_fins(4); % [K] Back
insulation Temperature
t_back_amb=zeros(1,length(time_sim_v)); t_back_amb(1)=t_0_fins(5); % [K] Back
insulation - Ambiance Temperature
t_fins=zeros(1,length(time_sim_v)); t_fins(1)=t_0_fins(6); % [K] Fins
Temperature
t_back_pcm=zeros(1,length(time_sim_v)); t_back_pcm(1)=t_0_fins(7); % [K] Back PCM
Temperature

h_top=zeros(1,length(time_sim_v)); % [W/K-m^2]

```



```

Convection coefficient of the top surface
h_back=zeros(1,length(time_sim_v)); % [W/K*m^2] ✓
Convection coefficient of the back surface

eff=zeros(1,length(time_sim_v)); % [-] Theoretic ✓
efficiency of the cell
power=zeros(1,length(time_sim_v)); % [W] Output ✓
power of the module
Wh=zeros(1,length(time_sim_v)); % [Wh] Total ✓
energy generated by the module

%% Conductive thermal resistances
%%
R_cond_sg=th_sg/(k_sg*a); % [K/W] conductive thermal resistance of the ✓
solar glass
R_cond_back=th_back/(a*k_back); % [K/W] conductive thermal resistance of the back ✓
insulation

for i=1:(length(time_sim_v)-1)

    %% SOLAR GLASS (SG)
    %%
    %>>> [W] Q_solar_rad_sg: radiation heat absorbed in the glass
    Q_solar_rad_sg=g(i)*a_amb*abs_glass;

    %>>> [W] Q_rad_sg_sky: radiation heat from the sky
    t_sky=0.052*t_amb(i)^1.5; % [K] Temperature of the sky
    Q_rad_sg_sky=sigma*emis_sg*(t_sg_amb(i)^2+t_sky^2)*(t_sg_amb(i)+t_sky)*(t_sg_amb(i)-t_sky);

    %>>> [W] Q_cond_sg: heat flux due to conduction between solar glass and solar ✓
    cells
    Q_cond_sg=(t_sg(i)-t_cell(i))/(R_cond_sg/2);

    %>>> [W] Q_conv_sg: convective heat flux between solar glass and ambience
    top=1; back=0; % Convection on the top: there are forced convection due to the ✓
    wind
    % [W/K*m^2] h_top: convective coefficient on the top of the panel
    [h_top(i)]=inclined_plane_conv(t_sg_amb(i),t_amb(i),wind(i),1,top,back,angle, ✓
    c_vis,c_k,c_pr,c_dens,mean_ang_wind);
    R_conv_sg=1/(h_top(i)*a); % [K/W] convective thermal resistance between the ✓
    solar glass and the ambience
    Q_conv_sg=(t_sg(i)-t_amb(i))/(R_conv_sg+(R_cond_sg/2));

    %>>> [K] t_sg(i+1): temperature of the (middle) solar glass at the 'i+1' step
    t_sg(i+1)=(Q_solar_rad_sg-Q_cond_sg-Q_conv_sg-Q_rad_sg_sky)*sim_step/(m_sg*cp_sg) ✓
    +t_sg(i); % [K] Temperature for the next step

    %>>> [K] t_sg_amb(i+1): temperature of the solar glass surface at the 'i+1' step
    t_sg_amb(i+1)=t_sg(i+1)+(Q_solar_rad_sg-Q_conv_sg-Q_rad_sg_sky)*(R_cond_sg/2);

    %% CELLS (C)
    %%
    %>>> [W] Q_solar_rad_c: radiation heat absorbed in the CELLS
    Q_solar_rad_c=g(i)*a_amb*a_cells*abs_Cells;

```

```

    %>>> [W] power(i+1): fraction of the solar radiation that turns into electrical ✓
    power
    eff(i+1)=0.165*(1-0.0041*(t_cell(i)-25-273.15)); % [-] Theoretic efficiency of the ✓
    cell
    power(i+1)=g(i)*eff(i)*a*a_sil*a_cells;

    %>>> [W] Q_cond_back: heat flux due to conduction between cells and back ✓
    insulation
    Q_cond_back=(t_cell(i)-t_back(i))/R_cond_back;

    %>>> [K] t_c(i+1): temperature of the cells at the 'i+1' step
    t_cell(i+1)=(Q_solar_rad_c+Q_cond_sg-Q_cond_back-power(i))*sim_step/(m_c*cp_c) ✓
    +t_cell(i);

    %% BACK INSULATION
    %%
    fins=1; pcm=0;
    if (fins==0) && (pcm==0) % Standard panel
    %>>> [W] Q_conv_back: heat flux due to convection with the ambience
    top=0; back=1; % Convection on the back: only free convection (no ✓
    wind)
    [h_back(i)]=inclined_plane_conv(t_back_amb(i),t_amb(i),wind(i),1,top,back, ✓
    angle,c_vis,c_k,c_pr,c_dens,mean_ang_wind);
    R_conv_back=1/(h*a); % [K/W] convective thermal resistance between the back ✓
    insulation and the ambience
    Q_conv_back=(t_back(i)-t_amb(i))/(R_conv_back+(R_cond_back/2));

    %>>> [K] t_back(i+1): temperature of the (middle) back insulation at the 'i+1' ✓
    step
    t_back(i+1)=(Q_cond_back-Q_conv_back)*sim_step/(m_back*cp_back)+t_back(i);

    %>>> [K] t_back_amb(i+1): temperature of the back surface at the 'i+1' step
    t_back_amb(i+1)=t_back(i+1)-Q_conv_back*(R_cond_back/2);
    else
    if pcm==1 % PCM panel
    % [K/W] R_cond_gap: conductive thermal resistance due to the air gap ✓
    between the back insulation and the PCM profiles
    k_air=24.12+0.07225*(t_back(i)-273.15); % [W/m*K] thermal conductivity of ✓
    the air at the back insulation Temperature
    R_cond_gap=0.002/(k_air*(10^-3)*a);

    % [W] Q_cond_profiles: heat flux due to conduction between the back ✓
    insulation and the PCM profiles
    Q_cond_profiles=(t_back(i)-t_back_pcm(i))/(R_cond_back/2+R_cond_gap);

    %>>> [K] t_back(i+1): temperature of the (middle) back insulation at the ✓
    'i+1' step
    t_back(i+1)=(Q_cond_back-Q_cond_profiles)*sim_step/(m_back*cp_back)+t_back ✓
    (i);
    end
    if fins==1 % Fins panel
    % [K/W] R_cond_gap: conductive thermal resistance due to the air gap ✓
    between the back insulation and the 'L' fins
    k_air=24.12+0.07225*(t_back(i)-273.15); % [W/m*K] thermal conductivity of ✓

```

```

the air at the back insulation Temperature
R_cond_gap=0.002/(k_air*(10^-3)*a);

%>>> [W] Q_cond_fins: heat flux due to conduction between the back ✓
insulation and the fins
Q_cond_fins=(t_back(i)-t_fins(i))/(R_cond_back/2+R_cond_gap);

%>>> [K] t_back(i+1): temperature of the (middle) back insulation at the ✓
'i+1' step
t_back(i+1)=(Q_cond_back-Q_cond_fins)*sim_step/(m_back*cp_back)+t_back(i); ✓
[K] Temperature for the next step
end

%% COOLING FINNS
%%
%>>> [W/K*m^2] h_back: Convective coefficient on the back of the panel
top=0; back=1; % Convection on the back: only free convection (no wind)
[h_back(i)]=inclined_plane_conv(t_fins(i),t_amb(i),wind(i),1,top,back,angle,c_vis, ✓
c_k,c_pr,c_dens,mean_ang_wind); ✓
% [W/m^2/K] Convection coefficient for the back of the panel

%>>> [K/W] R_conv_cover: convective thermal Resistance on the gaps between the fins
R_conv_cover=1/(h_back(i)*(a_cover-n_fin*th_fin*z_fin));

%>>> [K/W] R_conv_cover: convective thermal Resistance of the cooling fins
m=sqrt(2*(th_fin+z_fin)*h_back(i)/((th_fin*z_fin)*k_fin)); % Auxiliar parameter ✓
for the convective thermal Resistance of the fins
R_conv_fins=1/(n_fin*k_fin*z_fin*th_fin*m*tanh(m*l_fin));

%>>> [K/W] R_eq: convective global thermal Resistance on the back of the fins panel
R_eq=(R_conv_cover*R_conv_fins)/(R_conv_cover+R_conv_fins);

%>>> [W] Q_conv_fin: convective heat flux on the back of the fins panel
Q_conv_fin=(t_fins(i)-t_amb(i))/R_eq; % [W] Heat flux due to ✓
convection with the ambience

%>>> [K] t_fins: Temperature of the aluminum 'L' fins
t_fins(i+1)=(Q_cond_fins-Q_conv_fin)*sim_step/((a_cover*th_fin*dens_al+m_fin) ✓
*cp_al)+t_fins(i);

%% Generation of Energy (Wh) according to the simulation
%%
Wh(i+1)=power(i)*(sim_step/3600)+Wh(i);

end

t_f_fins=[t_sg_amb(i+1) t_sg(i+1) t_cell(i+1) t_back(i+1) t_back_amb(i+1) t_fins(i+1) ✓
t_back_pcm(i+1)];

Wh_fins_day_1=Wh(length(Wh));
t_cell_fins_mean_day_1=mean(t_cell);

end

```

```

function [Wh_pcm_day_1,t_cell_pcm_mean_day_1,t_f_pcm]=pcm_panel(sim_step,time_sim_v, ✓
t_amb,g,wind,angle,c_vis,c_k,c_pr,c_dens,t_0_pcm,mean_ang_wind)

%% Model scheme
%%
% AMB: AMBIANCE
% SG: SOLAR GLASS
% CELL: SOLAR CELLS
% BACK: BACK INSULATION
% conv: convection
% cond: conduction
% rad: radiation
%
%
% Q_rad_c=g*a*(abs_sg+trans_sg*ref_cell)----|
% Q_sky----|
% [AMB]---<R_conv_sg_amb---<[SG_AMB]---<R_cond_sg/2---<[SG]---<R_cond_sg/2---<[CELL] ✓
-----
% ...---<R_cond_back/2---<[BACK]---<R_cond_back/2---<R_cond_gap---<[BACK_PCM]--- ✓
<R_conv_back_amb---<[AMB]
% Q_pcm-----|

%% Fisical parameters
%%
[a,p,l,a_cells,a_sil,th_sg,m_sg,cp_sg,k_sg,emis_sg,th_c,m_c,cp_c,c_k,...
th_back,m_back,cp_back,k_back,th_fin,l_fin,z_fin,th_fin,n_fin,m_fin,...
cp_fin,k_fin,a_cover,dens_pcm,cp_pcm,k_pcm,sigma,lg_prf,w_prf_h,...
w_prf_v,th_prf,n_prf,k_al,cp_al,dens_al,abs_glass,abs_Cells,a_amb] ✓
=fisical_param();

%% PCM model variables
%%
n_horiz=6; n_vert=6; % Number of horizontal and vertical nodes for the PCM-profiles ✓
Temperature calculation
[PHASE,MASS,TEMP,ENERGY,RESIST_H,RESIST_V,energy_melt,energy_solid,m_profiles] ✓
=PCM_variables(n_vert,n_horiz,time_sim_v,t_amb,w_prf_h,w_prf_v,lg_prf,n_prf,th_prf, ✓
k_pcm,k_al,dens_al,dens_pcm);

%% Simulation variables
%%
t_sg_amb=zeros(1,length(time_sim_v)); t_sg_amb(1)=t_0_pcm(1); % [K] Solar Glass ✓
Ambiance Temperature
t_sg=zeros(1,length(time_sim_v)); t_sg(1)=t_0_pcm(2); % [K] Solar Glass ✓
Temperature
t_cell=zeros(1,length(time_sim_v)); t_cell(1)=t_0_pcm(3); % [K] Cell ✓
Temperature
t_back=zeros(1,length(time_sim_v)); t_back(1)=t_0_pcm(4); % [K] Back ✓
insulation Temperature
t_back_amb=zeros(1,length(time_sim_v)); t_back_amb(1)=t_0_pcm(5); % [K] Back ✓
insulation - Ambiance Temperature
t_fins=zeros(1,length(time_sim_v)); t_fins(1)=t_0_pcm(6); % [K] Fins ✓

```



```

Temperature
t_back_pcm=zeros(1,length(time_sim_v)); t_back_pcm(1)=t_0_pcm(7); % [K] Back PCM
Temperature

h_top=zeros(1,length(time_sim_v)); % [W/K*m^2]
Convection coefficient of the top surface
h_back=zeros(1,length(time_sim_v)); % [W/K*m^2]
Convection coefficient of the back surface

eff=zeros(1,length(time_sim_v)); % [-] Theoretic
efficiency of the cell
power=zeros(1,length(time_sim_v)); % [W] Output
power of the module
Wh=zeros(1,length(time_sim_v)); % [Wh] Total
energy generated by the module

%% Conductive thermal resistances
%%
R_cond_sg=th_sg/(k_sg*a); % [K/W] conductive thermal resistance of the
solar glass
R_cond_back=th_back/(a*k_back); % [K/W] conductive thermal resistance of the back
insulation

for i=1:(length(time_sim_v)-1)

    %% SOLAR GLASS (SG)
    %%
    >>> [W] Q_solar_rad_sg: radiation heat absorbed in the glass
    Q_solar_rad_sg=g(i)*a_abs*a_sil*a_cells;

    >>> [W] Q_rad_sg_sky: radiation heat from the sky
    t_sky=0.0552*t_amb(i)^1.5; % [K] Temperature of the sky
    Q_rad_sg_sky=sigma*emis_sg*(t_sg_amb(i)^2+t_sky^2)*(t_sg_amb(i)+t_sky)*(t_sg_amb
(i)-t_sky);

    >>> [W] Q_cond_sg: heat flux due to conduction between solar glass and solar
cells
    Q_cond_sg=(t_sg(i)-t_cell(i))/(R_cond_sg/2);

    >>> [W] Q_conv_sg: convective heat flux between solar glass and ambience
    top=1; back=0; % Convection on the top: there are forced convection due to the
wind
    % [W/K*m^2] h_top: convective coefficient on the top of the panel
    [h_top(i)]=inclined_plane_conv(t_sg_amb(i),t_amb(i),wind(i),1,top,back,angle,
c_vis,c_k,c_pr,c_dens,mean_ang_wind);
    R_conv_sg=1/(h_top(i)*a); % [K/W] convective thermal resistance between the
solar glass and the ambience
    Q_conv_sg=(t_sg(i)-t_amb(i))/(R_conv_sg+(R_cond_sg/2));

    >>> [K] t_sg(i+1): temperature of the (middle) solar glass at the 'i+1' step
    t_sg(i+1)=(Q_solar_rad_sg-Q_cond_sg-Q_conv_sg-Q_rad_sg_sky)*sim_step/(m_sg*cp_sg)
+t_sg(i); % [K] Temperature for the next step

    >>> [K] t_sg_amb(i+1): temperature of the solar glass surface at the 'i+1' step
    t_sg_amb(i+1)=t_sg(i+1)+(Q_solar_rad_sg-Q_conv_sg-Q_rad_sg_sky)*(R_cond_sg/2);

```

```

%% CELLS (C)
%%
>>> [W] Q_solar_rad_c: radiation heat absorbed in the CELLS
Q_solar_rad_c=g(i)*a_abs*a_cells*a_cells;

>>> [W] power(i+1): fraction of the solar radiation that turns into electrical
power
eff(i+1)=0.165*(1-0.0041*(t_cell(i)-25-273.15)); % [-] Theoretic efficiency of the
cell
power(i+1)=g(i)*eff(i)*a_sil*a_cells;

>>> [W] Q_cond_back: heat flux due to conduction between cells and back
insulation
Q_cond_back=(t_cell(i)-t_back(i))/R_cond_back;

>>> [K] t_c(i+1): temperature of the cells at the 'i+1' step
t_cell(i+1)=(Q_solar_rad_c+Q_cond_sg-Q_cond_back-power(i))*sim_step/(m_c*cp_c)
+t_cell(i);

%% BACK INSULATION
%%
fins=0; pcm=1;
if (fins==0) && (pcm==0) % Standard panel
    >>> [W] Q_conv_back: heat flux due to convection with the ambience
    top=0; back=1; % Convection on the back: only free convection (no
wind)
    [h_back(i)]=inclined_plane_conv(t_back_amb(i),t_amb(i),wind(i),1,top,back,
angle,c_vis,c_k,c_pr,c_dens,mean_ang_wind);
    R_conv_back=1/(h*a); % [K/W] convective thermal resistance between the back
insulation and the ambience
    Q_conv_back=(t_back(i)-t_amb(i))/(R_conv_back+(R_cond_back/2));

    >>> [K] t_back(i+1): temperature of the (middle) back insulation at the 'i+1'
step
    t_back(i+1)=(Q_cond_back-Q_conv_back)*sim_step/(m_back*cp_back)+t_back(i);

    >>> [K] t_back_amb(i+1): temperature of the back surface at the 'i+1' step
    t_back_amb(i+1)=t_back(i+1)-Q_conv_back*(R_cond_back/2);
else
    if pcm==1 % PCM panel
        % [K/W] R_cond_gap: conductive thermal resistance due to the air gap
between the back insulation and the PCM profiles
        k_air=24.12+0.07225*(t_back(i)-273.15); % [W/m*K] thermal conductivity of
the air at the back insulation Temperature
        R_cond_gap=0.002/(k_air*(10^-3)^a);

        % [W] Q_cond_profiles: heat flux due to conduction between the back
insulation and the PCM profiles
        Q_cond_profiles=(t_back(i)-t_back_pcm(i))/(R_cond_back/2+R_cond_gap);

        >>> [K] t_back(i+1): temperature of the (middle) back insulation at the
'i+1' step
        t_back(i+1)=(Q_cond_back-Q_cond_profiles)*sim_step/(m_back*cp_back)+t_back
(i);

```

```

end
if fins==1 % Fins panel
    % [K/W] R_cond_gap: conductive thermal resistance due to the air gap
between the back insulation and the 'L' fins
    k_air=24.12+0.07225*(t_back(i)-273.15); % [W/m*K] thermal conductivity of
the air at the back insulation Temperature
    R_cond_gap=0.002/(k_air*(10^-3)^a);

    >>> [W] Q_cond_fins: heat flux due to conduction between the back
insulation and the fins
    Q_cond_fins=(t_back(i)-t_fins(i))/(R_cond_back/2+R_cond_gap);

    >>> [K] t_back(i+1): temperature of the (middle) back insulation at the
'i+1' step
    t_back(i+1)=(Q_cond_back-Q_cond_fins)*sim_step/(m_back*cp_back)+t_back(i);
% [K] Temperature for the next step
end
end
%% PCM
%%
% ENERGY: matrix for the stored energy of each PCM mass element in the full
melting
% interval (35 - 50 °C): 35.0°C-->energy=0 // 50.99°C-->256(KJ/Kg)*mass
ENERGY(:,i+1)=ENERGY(:,i); % Initial value for 'i+1' step

% PHASE: phase of each PCM mass element
% 0: fluid, 1: phase change, 2: solid, 3: aluminum
PHASE(i+1)=PHASE(i); % Initial value for 'i+1' step

>>> [W] Q_H: horizontal heat flow in the PCM profile matrix
Q_H=zeros(n_vert-2,n_horiz-1);
for y=1:n_vert-2
    for x=1:n_horiz-1
        Q_H(y,x)=(TEMP(y+1,x,1)-TEMP(y+1,x+1,1))/RESIST_H(y,x);
    end
end

>>> [W] Q_V: vertical heat flow in the PCM profile matrix
Q_V=zeros(n_vert-1,n_horiz);
for y=1:n_vert-1
    for x=1:n_horiz
        Q_V(y,x)=(TEMP(y,x,1)-TEMP(y+1,x,1))/RESIST_V(y,x);
    end
end

>>> [W] Q_pcm: total heat exchange between the aluminum profiles and the PCM
(Heat entering the aluminum profiles)
Q_pcm=sum(Q_V(n_vert-1,2:n_horiz-1))-sum(Q_V(1,2:n_horiz-1))+sum(Q_H(1:n_vert-2,
n_horiz-1))-sum(Q_H(1:n_vert-2,1));

% [K/W] R_conv_back_pcm: convective thermal resistance between the back and the
ambience
top=0; back=1; % Convection on the back: only free convection (no wind)
[h_back(i)]=inclined_plane_conv(t_back_pcm(i),t_amb(i),wind(i),1,top,back,angle,

```

```

c_vis,c_k,c_pr,c_dens,mean_ang_wind);
R_conv_back_pcm=1/(h_back(i)*a);

>>> [W] Q_conv_back_pcm: convective heat at the back of the panel
Q_conv_back_pcm=(t_back_pcm(i)-t_amb(i))/R_conv_back_pcm;

>>> [K] t_back_pcm(i+1): temperature of the PCM-aluminum profiles at the 'i+1'
step
% (it is considered the same Temperature in all the volume of the aluminum
profiles)
t_back_pcm(i+1)=(Q_cond_profiles+Q_cond_pcm-Q_conv_back_pcm)*sim_step/
(m_profiles*cp_al)+t_back_pcm(i);

TEMP(1,:,i+1)=t_back_pcm(i+1); % First row of the Temperature matrix: aluminum
top cover
TEMP(n_vert,:,i+1)=t_back_pcm(i+1); % Last row of the Temperature matrix: aluminum
back cover

>>> Temperature calculation of all the differential mass elements of the PCM
for y=2:n_vert-1 % y: vertical nodes (rows of the matrix)
    TEMP(y,1,i+1)=t_back_pcm(i+1); % Left side of the aluminum
profile
    TEMP(y,n_horiz,i+1)=t_back_pcm(i+1); % Right side of the aluminum
profile
    for x=2:(n_horiz-1) % x: horizontal nodes (columns of the matrix)
        if (TEMP(y,x,i)>(273.15+40)) && (TEMP(y,x,i)<(273.15+45)) % 40-45 °C: PCM
phase change interval (1)
            PHASE(y,x,i+1)=1;
        else if (TEMP(y,x,i)<(273.15+40)) % <40 °C: PCM
solid (0)
            PHASE(y,x,i+1)=0;
        else
            PHASE(y,x,i+1)=2; % >45 °C: PCM
liquid (2)
        end
    end
    Q_net=Q_V(y-1,x)-Q_V(y,x)+Q_H(y-1,x)-Q_H(y,x); % [W] Q_net: net
heat in the (x-1,y) mass element
    if (TEMP(y,x,i)>(273.15+35)) && (TEMP(y,x,i)<(273.15+51)) % 35-51 °C:
interval where the PCM heat capacity is not constant (melting-solidification)
        ENERGY(y,x,i+1)=Q_net*sim_step+ENERGY(y,x,i); % [J=W*s] Net
energy in mass element for the 35-51°C interval
        if ENERGY(y,x,i+1)>(sum(energy_melt(2,:))*MASS(y-1,x)) % If the net
energy exceed the upper limit of the 35-51°C interval
            ENERGY(y,x,i+1)=sum(energy_melt(2,:))*MASS(y-1,x);
        else
            TEMP(y,x,i+1)=Q_net*sim_step/(MASS(y-1,x)*cp_pcm)+TEMP(y,x,i); %
[K] Temperature in the mass element (>51°C)
        else if ENERGY(y,x,i+1)<0 % If the net energy is below the lower
limit of the 35-51°C interval
            ENERGY(y,x,i+1)=0;
            TEMP(y,x,i+1)=Q_net*sim_step/(MASS(y-1,x)*cp_pcm)+TEMP(y,x,
i);

```

```

else % The net energy is in the 35-51°C interval
% Energy interpolation in the 35-51°C
if Q_net>0 % Heat flow entering the PCM: melting process
ind=find((energy_melt(3,:)*MASS(y-1,x))>ENERGY(y,x,i+1),
);
else % Heat flow out the PCM: solidification
ind=find((energy_solid(3,:)*MASS(y-1,x))>ENERGY(y,x,i+1),
);
end
if ENERGY(y,x,i+1)>(energy_melt(3,length(energy_melt))*MASS(y-
1,x))
ind=length(energy_melt)+1;
end
if Q_net>0 % Melting process
% Temperature of the (x,y) mass element
TEMP(y,x,i+1)=273.15+energy_melt(1,ind-1)+(ENERGY(y,x,
i+1)-energy_melt(3,ind-1)*MASS(y-1,x))/(energy_melt(2,ind-1)*MASS(y-1,x));
end
if Q_net<0 % Solidification process
% Temperature of the (x,y) mass element
TEMP(y,x,i+1)=273.15+energy_solid(1,ind-1)+(ENERGY(y,x,
i+1)-energy_solid(3,ind-1)*MASS(y-1,x))/(energy_solid(2,ind-1)*MASS(y-1,x));
end
end
else % Temperature out of the 35-51°C interval
TEMP(y,x,i+1)=Q_net*sim_step/(MASS(y-1,x)*cp_pcm)+TEMP(y,x,i);
if (TEMP(y,x,i+1)>(273.15+35))&&(TEMP(y,x,i+1)<(273.15+51)) % If
the temperature at the 'i+1' step is in the 35-51°C interval
if Q_net>0
ENERGY(y,x,i+1)=MASS(y-1,x)*cp_pcm*(TEMP(y,x,i+1)-(273.15
+35));
end
if Q_net<0
ENERGY(y,x,i+1)=energy_solid(3,length(energy_solid))+MASS(y-1,
x)*cp_pcm*(TEMP(y,x,i+1)-(273.15+51));
end
end
end
end
% Generation of Energy (Wh) according to the simulation
%
Wh(i+1)=power(i)*(sim_step/3600)+Wh(i);
end
t_f_pcm=[t_sg_amb(i+1) t_sg(i+1) t_cell(i+1) t_back(i+1) t_back_amb(i+1) t_fins(i+1)
t_back_pcm(i+1)];
Wh_pcm_day_1=Wh(length(Wh));
t_cell_pcm_mean_day_1=mean(t_cell);

```

end

```

function [Wh_pcm_day_1,t_cell_pcm_mean_day_1,t_f_pcm]=pcm_panel(sim_step,time_sim_v,
t_amb,g,wind,angle,c_vis,c_k,c_pr,c_dens,t_0_pcm,mean_ang_wind)
% Model scheme
%
% AMB: AMBIANCE
% SG: SOLAR GLASS
% CELL: SOLAR CELLS
% BACK: BACK INSULATION
% conv: convection
% cond: conduction
% rad: radiation
%
% Q_rad_c=g*a_eff*trans_sg*abs_c----|
% Q_rad_sg=g*a*(abs_sg+trans_sg*ref_cell)----|
% Qsky----|
% [AMB]---<R_conv_sg_amb---[SG_AMB]---<R_cond_sg/2---[SG]---<R_cond_sg/2---[CELL]
%
% ---<R_cond_back/2---[BACK]---<R_cond_back/2---<R_cond_gap---[BACK_PCM]---
<R_conv_back_amb---[AMB]
%
% Q_pcm-----|
%
% Fisical parameters
%
[a,p,l,a_cells,a_sil,th_sg,m_sg,cp_sg,k_sg,emis_sg,th_c,m_c,cp_c,k_c,...
th_back,m_back,cp_back,k_back,th_fin,l_fin,z_fin,th_fin,n_fin,m_fin,...
cp_fin,k_fin,a_cover,dens_pcm,cp_pcm,k_pcm,sigma,lg_prf,w_prf_h,...
w_prf_v,th_prf,n_prf,k_al,cp_al,dens_al,abs_glass,abs_Cells,a_abs]
=fisical_param();
% PCM model variables
n
n_horiz=6; n_vert=6; % Number of horizontal and vertical nodes for the PCM-profiles
Temperature calculation
[PHASE,MASS,TEMP,ENERGY,RESIST_H,RESIST_V,energy_melt,energy_solid,m_profiles]
=PCM_variables(n_vert,n_horiz,time_sim_v,t_amb,w_prf_h,w_prf_v,lg_prf,n_prf,th_prf,
k_pcm,k_al,dens_al,dens_pcm);
% Simulation variables
%
t_sg_amb=zeros(1,length(time_sim_v)); t_sg_amb(1)=t_0_pcm(1); % [K] Solar Glass
Ambiance Temperature
t_sg=zeros(1,length(time_sim_v)); t_sg(1)=t_0_pcm(2); % [K] Solar Glass
Temperature
t_cell=zeros(1,length(time_sim_v)); t_cell(1)=t_0_pcm(3); % [K] Cell
Temperature
t_back=zeros(1,length(time_sim_v)); t_back(1)=t_0_pcm(4); % [K] Back
insulation Temperature
t_back_amb=zeros(1,length(time_sim_v)); t_back_amb(1)=t_0_pcm(5); % [K] Back
insulation - Ambiance Temperature
t_fins=zeros(1,length(time_sim_v)); t_fins(1)=t_0_pcm(6); % [K] Fins

```

```

Temperature
t_back_pcm=zeros(1,length(time_sim_v)); t_back_pcm(1)=t_0_pcm(7); % [K] Back PCM
Temperature
h_top=zeros(1,length(time_sim_v)); % [W/K·m²]
Convection coefficient of the top surface
h_back=zeros(1,length(time_sim_v)); % [W/K·m²]
Convection coefficient of the back surface
eff=zeros(1,length(time_sim_v)); % [-] Theoretic
efficiency of the cell
power=zeros(1,length(time_sim_v)); % [W] Output
power of the module
Wh=zeros(1,length(time_sim_v)); % [Wh] Total
energy generated by the module
% Conductive thermal resistances
%
R_cond_sg=th_sg/(k_sg*a); % [K/W] conductive thermal resistance of the
solar glass
R_cond_back=th_back/(a*k_back); % [K/W] conductive thermal resistance of the back
insulation
for i=1:(length(time_sim_v)-1)
% SOLAR GLASS (SG)
%
%>>> [W] Q_solar_rad_sg: radiation heat absorbed in the glass
Q_solar_rad_sg=g(i)*a_abs*abs_glass;
%>>> [W] Q_rad_sg_sky: radiation heat from the sky
t_sky=0.0552*t_amb(i)^1.5; % [K] Temperature of the sky
Q_rad_sg_sky=sigma*emis_sg*(t_sg_amb(i)^2+t_sky^2)*(t_sg_amb(i)+t_sky)*(t_sg_amb
(i)-t_sky);
%>>> [W] Q_cond_sg: heat flux due to conduction between solar glass and solar
cells
Q_cond_sg=(t_sg(i)-t_cell(i))/(R_cond_sg/2);
%>>> [W] Q_conv_sg: convective heat flux between solar glass and ambiance
top=1; back=0; % Convection on the top: there are forced convection due to the
wind
% [W/K·m²] h_top: convective coefficient on the top of the panel
[h_top(i)]=inclined_plane_conv(t_sg_amb(i),t_amb(i),wind(i),1,top,back,angle,
c_vis,c_k,c_pr,c_dens,mean_ang_wind);
R_conv_sg=1/(h_top(i)*a); % [K/W] convective thermal resistance between the
solar glass and the ambiance
Q_conv_sg=(t_sg(i)-t_amb(i))/(R_conv_sg+(R_cond_sg/2));
%>>> [K] t_sg(i+1): temperature of the (middle) solar glass at the 'i+1' step
t_sg(i+1)=(Q_solar_rad_sg-Q_cond_sg-Q_conv_sg-Q_rad_sg_sky)*sim_step/(m_sg*cp_sg)
+t_sg(i); % [K] Temperature for the next step
%>>> [K] t_sg_amb(i+1): temperature of the solar glass surface at the 'i+1' step
t_sg_amb(i+1)=t_sg(i+1)+(Q_solar_rad_sg-Q_conv_sg-Q_rad_sg_sky)*(R_cond_sg/2);

```

```

%% CELLS (C)
%%
%>>> [W] Q_solar_rad_c: radiation heat absorbed in the CELLS
Q_solar_rad_c=g(i)*a_amb*a_cells*abs_Cells;

%>>> [W] power(i+1): fraction of the solar radiation that turns into electrical
power
eff(i+1)=0.165*(1-0.0041*(t_cell(i)-25-273.15)); % [-] Teoretic efficiency of the
cell
power(i+1)=g(i)*eff(i)*a_sil*a_cells;

%>>> [W] Q_cond_back: heat flux due to conduction between cells and back
insulation
Q_cond_back=(t_cell(i)-t_back(i))/R_cond_back;

%>>> [K] t_c(i+1): temperature of the cells at the 'i+1' step
t_cell(i+1)=(Q_solar_rad_c+Q_cond_sg-Q_cond_back-power(i))*sim_step/(m_c*cp_c)
+t_cell(i);

%% BACK INSULATION
%%
fins=0; pcm=1;
if (fins==0)&&(pcm==0) % Standard panel
%>>> [W] Q_conv_back: heat flux due to convection with the ambiance
top=0; back=1; % Convection on the back: only free convection (no
wind)
[h_back(i)]=inclined_plane_conv(t_back_amb(i),t_amb(i),wind(i),l,top,back,
angle,c_vis,c_k,c_pr,c_dens,mean_ang_wind);
R_conv_back=1/(h*a); % [K/W] convective thermal resistance between the back
insulation and the ambiance
Q_conv_back=(t_back(i)-t_amb(i))/(R_conv_back+(R_cond_back/2));

%>>> [K] t_back(i+1): temperature of the (middle) back insulation at the 'i+1'
step
t_back(i+1)=(Q_cond_back-Q_conv_back)*sim_step/(m_back*cp_back)+t_back(i);

%>>> [K] t_back_amb(i+1): temperature of the back surface at the 'i+1' step
t_back_amb(i+1)=t_back(i+1)-Q_conv_back*(R_cond_back/2);
else
if pcm==1 % PCM panel
% [K/W] R_cond_gap: conductive thermal resistance due to the air gap
between the back insulation and the PCM profiles
k_air=24.12+0.07225*(t_back(i)-273.15); % [W/m·K] thermal conductivity of
the air at the back insulation Temperature
R_cond_gap=0.002/(k_air*(10^-3)*a);

% [W] Q_cond_profiles: heat flux due to conduction between the back
insulation and the PCM profiles
Q_cond_profiles=(t_back(i)-t_back_pcm(i))/(R_cond_back/2+R_cond_gap);

%>>> [K] t_back(i+1): temperature of the (middle) back insulation at the
'i+1' step
t_back(i+1)=(Q_cond_back-Q_cond_profiles)*sim_step/(m_back*cp_back)+t_back
(i);

```

```

end
if fins==1 % Fins panel
% [K/W] R_cond_gap: conductive thermal resistance due to the air gap
between the back insulation and the 'L' fins
k_air=24.12+0.07225*(t_back(i)-273.15); % [W/m·K] thermal conductivity of
the air at the back insulation Temperature
R_cond_gap=0.000/(k_air*(10^-3)*a);

%>>> [W] Q_cond_fins: heat flux due to conduction between the back
insulation and the fins
Q_cond_fins=(t_back(i)-t_fins(i))/(R_cond_back/2+R_cond_gap);

%>>> [K] t_back(i+1): temperature of the (middle) back insulation at the
'i+1' step
t_back(i+1)=(Q_cond_back-Q_cond_fins)*sim_step/(m_back*cp_back)+t_back(i);
% [K] Temperature for the next step
end

%% PCM
%%
% ENERGY: matrix for the stored energy of each PCM mass element in the full
melting
% interval (35 - 50 °C): 35.0°C-->energy=0 // 50.99°C-->256(KJ/Kg)*mass
ENERGY(:,i+1)=ENERGY(:,i); % Initial value for 'i+1' step

% PHASE: phase of each PCM mass element
% 0: fluid, 1: phase change, 2: solid, 3: aluminum
PHASE(i+1)=PHASE(i); % Initial value for 'i+1' step

%>>> [W] Q_H: horizontal heat flow in the PCM profile matrix
Q_H=zeros(n_vert-2,n_horiz-1);
for y=1:n_vert-2
for x=1:n_horiz-1
Q_H(y,x)=(TEMP(y+1,x,i)-TEMP(y+1,x+1,i))/RESIST_H(y,x);
end
end

%>>> [W] Q_V: vertical heat flow in the PCM profile matrix
Q_V=zeros(n_vert-1,n_horiz);
for y=1:n_vert-1
for x=1:n_horiz
Q_V(y,x)=(TEMP(y,x,i)-TEMP(y+1,x,i))/RESIST_V(y,x);
end
end

%>>> [W] Q_pcm: total heat exchange between the aluminum profiles and the PCM
(Heat entering the aluminum profiles)
Q_pcm=sum(Q_V(n_vert-1,2:n_horiz-1))-sum(Q_V(1,2:n_horiz-1))+sum(Q_H(1:n_vert-2,
n_horiz-1))-sum(Q_H(1:n_vert-2,1));

% [K/W] R_conv_back_pcm: convective thermal resistance between the back and the
ambiance
top=0; back=1; % Convection on the back: only free convection (no wind)
[h_back(i)]=inclined_plane_conv(t_back_pcm(i),t_amb(i),wind(i),l,top,back,angle,

```

```

c_vis,c_k,c_pr,c_dens,mean_ang_wind);
R_conv_back_pcm=1/(h_back(i)*a);

%>>> [W] Q_conv_back_pcm: convective heat at the back of the panel
Q_conv_back_pcm=(t_back_pcm(i)-t_amb(i))/R_conv_back_pcm;

%>>> [K] t_back_pcm(i+1): temperature of the PCM-aluminum profiles at the 'i+1'
step
% (it is considered the same Temperature in all the volume of the aluminum
profiles)
t_back_pcm(i+1)=(Q_cond_profiles+Q_pcm-Q_conv_back_pcm)*sim_step/
(m_profiles*cp_al)+t_back_pcm(i);

TEMP(1,:i+1)=t_back_pcm(i+1); % First row of the Temperature matrix: aluminum
back cover
TEMP(n_vert,:i+1)=t_back_pcm(i+1); % Last row of the Temperature matrix: aluminum
back cover

%>>> Temperature calculation of all the differential mass elements of the PCM
for y=2:n_vert-1 % y: vertical nodes (rows of the matrix)
TEMP(y,1,i+1)=t_back_pcm(i+1); % Left side of the aluminum
profile
TEMP(y,n_horiz,i+1)=t_back_pcm(i+1); % Right side of the aluminum
profile
for x=2:(n_horiz-1) % x: horizontal nodes (columns of the matrix)
if (TEMP(y,x,i)>(273.15+40))&&(TEMP(y,x,i)<(273.15+45)) % 40-45 °C: PCM
phase change interval (1)
PHASE(y,x,i+1)=1;
else if (TEMP(y,x,i)<(273.15+40)) % <40 °C: PCM
solid (0)
PHASE(y,x,i+1)=0;
else
PHASE(y,x,i+1)=2; % >45 °C: PCM
liquid (2)
end
end

Q_neto=Q_V(y-1,x)-Q_V(y,x)+Q_H(y-1,x-1)-Q_H(y-1,x); % [W] Q_neto: net
heat in the (x-1,y) mass element

if (TEMP(y,x,i)>(273.15+35))&&(TEMP(y,x,i)<(273.15+51)) % 35-51 °C:
interval where the PCM heat capacity is not constant (melting-solidification)
ENERGY(y,x,i+1)=Q_neto*sim_step+ENERGY(y,x,i); % [J=W*s] Net
energy in mass element for the 35-51°C interval
if ENERGY(y,x,i+1)>(sum(energy_melt(2,:))*MASS(y-1,x)) % If the net
energy exceed the upper limit of the 35-51°C interval
ENERGY(y,x,i+1)=sum(energy_melt(2,:))*MASS(y-1,x);
TEMP(y,x,i+1)=Q_neto*sim_step/(MASS(y-1,x)*cp_pcm)+TEMP(y,x,i); %
[K] Temperature in the mass element (>51°C)
else if ENERGY(y,x,i+1)<0 % If the net energy is below the lower
limit of the 35-51°C interval
ENERGY(y,x,i+1)=0;
TEMP(y,x,i+1)=Q_neto*sim_step/(MASS(y-1,x)*cp_pcm)+TEMP(y,x,
i);

```

```

else % The net energy is in the 35-51°C interval
% Energy interpolation in the 35-51°C
if Q_neto>0 % Heat flow entering the PCM: melting process
ind=find((energy_melt(3,:)*MASS(y-1,x))>ENERGY(y,x,i+1),
1);
process
else % Heat flow out the PCM: solidification
ind=find((energy_solid(3,:)*MASS(y-1,x))>ENERGY(y,x,i+1),
1);
end
if ENERGY(y,x,i+1)>(energy_melt(3,length(energy_melt))*MASS(y-
1,x))
ind=length(energy_melt)+1;
end
if Q_neto>0 % Melting process
% Temperature of the (x,y) mass element
TEMP(y,x,i+1)=273.15+energy_melt(1,ind-1)+((ENERGY(y,x,
i+1)-energy_melt(3,ind-1)*MASS(y-1,x))/(energy_melt(2,ind-1)*MASS(y-1,x));
end
if Q_neto<0 % Solidification process
% Temperature of the (x,y) mass element
TEMP(y,x,i+1)=273.15+energy_solid(1,ind-1)+((ENERGY(y,x,
i+1)-energy_solid(3,ind-1)*MASS(y-1,x))/(energy_solid(2,ind-1)*MASS(y-1,x));
end
end
else % Temperature out of the 35-51°C interval
TEMP(y,x,i+1)=Q_neto*sim_step/(MASS(y-1,x)*cp_pcm)+TEMP(y,x,i);
if (TEMP(y,x,i+1)>(273.15+35))&&(TEMP(y,x,i+1)<(273.15+51)) % If
the temperature at the 'i+1' step is in the 35-51°C interval
if Q_neto>0
ENERGY(y,x,i+1)=MASS(y-1,x)*cp_pcm*(TEMP(y,x,i+1)-(273.15
+35));
end
if Q_neto<0
ENERGY(y,x,i+1)=energy_solid(3,length(energy_solid))*MASS(y-1,
x)*cp_pcm*(TEMP(y,x,i+1)-(273.15+51));
end
end
end

%>>> Generation of Energy (Wh) according to the simulation
%%
Wh(i+1)=power(i)*(sim_step/3600)+Wh(i);

end

t_f_pcm=[t_sg_amb(i+1) t_sg(i+1) t_cell(i+1) t_back(i+1) t_back_amb(i+1) t_fins(i+1)
t_back_pcm(i+1)];

Wh_pcm_day_1=Wh(length(Wh));
t_cell_pcm_mean_day_1=mean(t_cell);

```

end

```

n_fin=56; % [-] Number of fins installed in the panel
m_fin=n_fin*dens_al*th_fin*z_fin*(w_fin+l_fin-th_fin); % [Kg] Total mass of the
fins
cp_fin=cp_al; % [J/Kg/K] Specific heat value of the
(aluminum) fins
k_fin=k_al; % [W/m/K] Conductivity of the (aluminum) fin
a_cover=n_fin*w_fin*z_fin; % [m^2] Area covered by the fins

%>>> PCM
dens_pcm=800; % [Kg/m^3] Density of the PCM
cp_pcm=2000; % [J/Kg/K] Specific heat capacity of the PCM
k_pcm=0.2; % [W/m^2/K] Conductivity of the PCM

%>>> Profiles PCM
lg_prf=1.355; % [m] Length of the PCM profiles
w_prf_h=0.025; % [m] Horizontal width of the PCM profiles section
w_prf_v=0.025; % [m] Vertical width of the PCM profiles section
th_prf=0.002; % [m] Thickness of the PCM profiles section
n_prf=34; % [-] Number of PCM profiles

%>>> Radiation absorbed by glass and by PC cells

% row 1: wavelength interval, row 2: transmissivity, row 3: absorptivity, row 4:
reflectivity
glass=[0 320 2200; 0 0.9 0; 0.975 0.075 0; 0.025 0.025 1];
EVA=[0 370 1700 2250; 0 0.97 0.85 0; 0 0 0 0; 1 0.03 0.15 1];
Silicon=[0 250 400 1100; 0 0 0 0.30; 0.65 0.65 0.80 0.20; 0.35 0.35 0.20 0.50];
Aluminum=[0 200; 0 0; 1 0.20; 0 0.80];

% Equivalent absorption of the PV cells, according to the properties of the Silicon
and the Aluminum
Cells=zeros(4,5);
Cells(1,:)= [0 200 250 400 1100];
for i=1:5
    ind_Sil=find(Silicon(1,:)<=Cells(1,i));
    ind_Al=find(Aluminum(1,:)<=Cells(1,i));
    Cells(2,i)=a_sil*Silicon(2,ind_Sil(end))+(1-a_sil)*Aluminum(2,ind_Al(end));
    Cells(3,i)=a_sil*Silicon(3,ind_Sil(end))+(1-a_sil)*Aluminum(3,ind_Al(end));
    Cells(4,i)=a_sil*Silicon(4,ind_Sil(end))+(1-a_sil)*Aluminum(4,ind_Al(end));
end

% Calculation of the absorptivity of glass and cells, considering the whole path of
the incoming radiation
[abs_glass,abs_Cells]=abs_trans_ref(glass,EVA,Cells);

```

```

function [a,p,l,a_cells,a_sil,th_sg,m_sg,cp_sg,k_sg,emis_sg,th_c,m_c,cp_c,k_c,th_back,
m_back,cp_back,k_back,w_fin,l_fin,z_fin,th_fin,n_fin,m_fin,cp_fin,k_fin,a_cover,
dens_pcm,cp_pcm,k_pcm,sigma,lg_prf,w_prf_h,w_prf_v,th_prf,n_prf,k_al,cp_al,dens_al,
abs_glass,abs_Cells,a_abs]=fisical_param()

%>>> [W/m^2/K^4] Stefan-Boltzmann constant
sigma=5.67e-8;

%>>> Aluminum
k_al=235; % [W/m/K] Conductivity of the Aluminum
cp_al=897; % [J/Kg/K] Specific heat capacity of the Aluminum
dens_al=2700; % [Kg/m^3] Density of the Aluminum

%>>> Silicon
dens_si=2336; % [Kg/m^3] Density of the Silicon
k_si=150; % [W/m/K] Conductivity of the Silicon
cp_si=703; % [J/Kg/K] Specific heat capacity of the Silicon

%>>> Module
a=1.650*0.992; % [m^2] Surface of the module
p=0.992*2+1.65*2; % [m] Perimeter of the module
l=4*a/p; % [m] characteristic lenght for Reynolds equation
a_cells=0.9; % [-] Area of the pannel covered by cells/total area of the
pannel
a_sil=0.9; % [-] Area of the cell covered by silicon/total area of the
cell

%>>> Solar glass
th_sg=0.0032; % [m] Thickness of the solar glass
m_sg=2500*a*th_sg; % [Kg] Mass of the solar glass
cp_sg=837; % [J/Kg/K] Specific heat capacity of the solar glass
k_sg=0.9; % [W/m/K] Conductivity of the solar glass
emis_sg=0.13; % [-] Emissivity of the solar glass
a_abs=(a-0.011*2*(1.65+0.992)); % [-] Area of the panel which receive radiation
(subtracting the area coverd by the frame)

%>>> Silicon cells and aluminum conductors
th_c=0.0005; % [m] Thickness of the cells
m_c=(dens_si*a_sil+dens_al*(1-a_sil))*a*a_cells*th_c; % [Kg] Mass of the cell
cp_c=cp_si*a_sil+cp_al*(1-a_sil); % [J/Kg/K] heat capacity of
the cell
k_c=a_sil*k_si+(1-a_sil)*k_al; % [W/m/K] Conductivity of the
cell element

%>>> Back insulation
th_back=0.00038; % [m] Thickness of the insulation
m_back=1380*a*th_back; % [Kg] Mass of the insulation
cp_back=1050; % [J/Kg/K] Specific heat value of the insulation
k_back=0.2; % [W/m/K] Conductivity of the insulation

%>>> Cooling fins
th_fin=0.003; % [m] Thickness of the fin
l_fin=0.035-th_fin; % [m] Length of the fin
w_fin=0.025; % [m] Width of the L aluminum profile
z_fin=0.922; % [m] Length of the L aluminum profile

```

```

function [v,k,Pr,dens]=dry_air(T,c_vis,c_k,c_dens,c_pr)

v=(c_vis(1)*(T^4)+c_vis(2)*(T^3)+c_vis(3)*(T^2)+c_vis(4)*T+c_vis(5))*10^-6;
k=(c_k(1)*(T^4)+c_k(2)*(T^3)+c_k(3)*(T^2)+c_k(4)*T+c_k(5))*10^-3;
Pr=c_pr(1)*(T^4)+c_pr(2)*(T^3)+c_pr(3)*(T^2)+c_pr(4)*T+c_pr(5);
dens=c_dens(1)*(T^4)+c_dens(2)*(T^3)+c_dens(3)*(T^2)+c_dens(4)*T+c_dens(5);

end

```

```

function [PHASE,MASS,TEMP,ENERGY,RESIST_H,RESIST_V,energy_melt,energy_solid,
m_profiles]=PCM_variables(n_vert,n_horiz,time_sim_v,t_amb,w_prf_h,w_prf_v,lg_prf,
n_prf,th_prf,k_pcm,k_al,dens_al,dens_pcm)

PHASE=zeros(n_vert,n_horiz,length(time_sim_v)); %0: fluid, 1: phase change, 2:
solid, 3: aluminum
MASS=zeros(n_vert-2,n_horiz);
TEMP=zeros(n_vert,n_horiz,length(time_sim_v));
ENERGY=zeros(n_vert,n_horiz,length(time_sim_v));
RESIST_H=zeros(n_vert-2,n_horiz-1);
RESIST_V=zeros(n_vert-1,n_horiz);

energy_melt=[35,36,37,38,39,40,41,42,43,44,45,46,47,48,49,50;
2,2,3,2,3,6,43,53,107,25,2,2,2,2,2,2;
0,2,4,7,9,12,18,61,114,221,246,248,250,252,254,256];
energy_melt(2:3,:)=energy_melt(2:3,:)*1000;
energy_solid=[35,36,37,38,39,40,41,42,43,44,45,46,47,48,49,50;
2,2,3,4,9,69,6,9,86,54,2,3,2,3,2,2;
0,2,4,7,11,20,89,95,104,190,244,246,249,251,254,256];
energy_solid(2:3,:)=energy_solid(2:3,:)*1000;

PHASE(:,1)=3;
PHASE(:,n_horiz)=3;
PHASE(1,:)=3;
PHASE(n_horiz,:)=3;

TEMP(:,1)=t_amb(1);

RESIST_H(:,:)=((w_prf_h-th_prf*2)/(n_horiz-2))/((w_prf_v-th_prf*2)/(n_vert-2))*
*lg_prf*n_prf*k_pcm);
RESIST_H(:,1)=RESIST_H(:,1)/2;
RESIST_H(:,n_horiz-1)=RESIST_H(:,n_horiz-1)/2;

RESIST_V(:,:)=((w_prf_v-th_prf*2)/(n_vert-2))/((w_prf_h-th_prf*2)/(n_horiz-2))*
*lg_prf*n_prf*k_pcm);
RESIST_V(:,1)=((w_prf_v-th_prf*2)/(n_vert-2))/((n_prf*th_prf*lg_prf)*k_al);
RESIST_V(:,n_horiz)=((w_prf_v-th_prf*2)/(n_vert-2))/((n_prf*th_prf*lg_prf)*k_al);
RESIST_V(1,:)=RESIST_V(1,:)/2;
RESIST_V(n_vert-1,:)=RESIST_V(n_vert-1,:)/2;

MASS(:,:)=dens_pcm*((w_prf_h-th_prf*2)*(w_prf_v-th_prf*2))/((n_horiz-2)*(n_vert-2))*
*lg_prf*n_prf;
MASS(:,1)=dens_al*((w_prf_v-th_prf)/(n_vert-2))*th_prf*lg_prf*n_prf;
MASS(:,n_horiz)=dens_al*((w_prf_v-th_prf)/(n_vert-2))*th_prf*lg_prf*n_prf;

% [Kg] m_profile: total mass of the aluminum profiles
m_profiles=n_prf*lg_prf*((w_prf_h*w_prf_v)-((w_prf_h-2*th_prf)*(w_prf_v-2*th_prf)))*
*dens_al;

end

```

```

function [abs_glass,abs_Sil]=abs_trans_ref(glass,EVA,Silicon)

Tsun=5778; % [K] Sun Temperature

fracc_rad=zeros(2,60);
aux=0;
for i=1:40
    aux=aux+200;
    fracc_rad(1,i)=aux;
end
for i=41:60
    aux=aux+500;
    fracc_rad(1,i)=aux;
end
fracc_rad(1,49:60)=[13000 14000 15000 16000 18000 20000 25000 30000 40000 50000 75000
100000];

fracc_rad(2,:)=[0 0 0 0 0 0.002 0.007 0.020 0.039 0.067 0.101 0.140 0.183 0.228 0.273
0.318 0.362 0.404 0.443 0.481 0.516 0.549 0.579 0.608 0.634 0.659 0.680 0.701 0.720
0.738 0.754 0.769 0.783 0.796 0.808 0.819 0.830 0.839 0.848 0.856 0.874 0.890 0.903
0.914 0.924 0.932 0.940 0.945 0.955 0.963 0.970 0.974 0.981 0.986 0.992 0.995 0.998
0.999 1 1];

% row 1: wavelength interval, row 2: transmissivity, row 3: absorptivity, row 4:
reflectivity
glass=[0 320 2200; 0 0.9 0; 0.975 0.075 0; 0.025 0.025 1];
EVA=[0 370 1700 2250; 0 0.97 0.85 0; 0 0 0; 1 0.03 0.15 1];
Silicon=[0 250 400 1100; 0 0 0 0; 0 0.45 0.65 0.55; 0 0.55 0.35 0.45];

%>>> Transmissivity glass+EVA / Total incident radiation

wl=sort([glass(1,:) EVA(1,:)]);
wl_1(1)=wl(1); ind=2;
for i=2:length(wl)
    if ~(wl(i)==wl(i-1))
        wl_1(ind)=wl(i);
        ind=ind+1;
    end
end
clearvars wl;
wl=wl_1;
clearvars ind wl_1;

fr_rad=interp1(fracc_rad(1,:),fracc_rad(2,:),wl(2)*Tsun/1000,'pchip');
trans_glass=glass(2,1)*EVA(2,1)*fr_rad;
for i=2:(length(wl))
    u=find(glass(1,:)<=wl(i));
    v=find(EVA(1,:)<=wl(i));
    if isempty(u)
        u=length(glass(1,:));
    end
    if isempty(v)
        v=length(EVA(1,:));
    end
    if i==length(wl)
        fr_rad=interp1(fracc_rad(1,:),fracc_rad(2,:),wl(i)*Tsun/1000,'pchip');
    else
        fr_rad=interp1(fracc_rad(1,:),fracc_rad(2,:),wl(i+1)*Tsun/1000,'pchip')-interp1
(fracc_rad(1,:),fracc_rad(2,:),wl(i)*Tsun/1000,'pchip');
    end
    abs_glass=abs_glass+glass(3,u(end))*fr_rad;
end
clearvars u v w;

%>>> Absorptivity glass from Silicon reflected radiation / Total incident radiation

wl=sort([glass(1,:) EVA(1,:) Silicon(1,:)]);
wl_1(1)=wl(1); ind=2;
for i=2:length(wl)
    if ~(wl(i)==wl(i-1))

```

```

        fr_rad=interp1(fracc_rad(1,:),fracc_rad(2,:),wl(i)*Tsun/1000,'pchip');
    else
        fr_rad=interp1(fracc_rad(1,:),fracc_rad(2,:),wl(i+1)*Tsun/1000,'pchip')-interp1
(fracc_rad(1,:),fracc_rad(2,:),wl(i)*Tsun/1000,'pchip');
    end
    trans_glass=trans_glass+glass(2,u(end))*EVA(2,v(end))*fr_rad;
end
clearvars u v;

%>>> Reflectivity glass+EVA / Total incident radiation

wl=sort([glass(1,:) EVA(1,:)]);
wl_1(1)=wl(1); ind=2;
for i=2:length(wl)
    if ~(wl(i)==wl(i-1))
        wl_1(ind)=wl(i);
        ind=ind+1;
    end
end
clearvars wl;
wl=wl_1;
clearvars ind wl_1;

fr_rad=interp1(fracc_rad(1,:),fracc_rad(2,:),wl(2)*Tsun/1000,'pchip');
reflect_glass=(glass(4,1)+glass(2,1)*EVA(4,1))*fr_rad;
for i=2:(length(wl))
    u=find(glass(1,:)<=wl(i));
    v=find(EVA(1,:)<=wl(i));
    if isempty(u)
        u=length(glass(1,:));
    end
    if isempty(v)
        v=length(EVA(1,:));
    end
    if i==length(wl)
        fr_rad=interp1(fracc_rad(1,:),fracc_rad(2,:),wl(i)*Tsun/1000,'pchip');
    else
        fr_rad=interp1(fracc_rad(1,:),fracc_rad(2,:),wl(i+1)*Tsun/1000,'pchip')-interp1
(fracc_rad(1,:),fracc_rad(2,:),wl(i)*Tsun/1000,'pchip');
    end
    reflect_glass=reflect_glass+(glass(4,u(end))+glass(2,u(end))*EVA(4,v(end)))*fr_rad;
end
clearvars u v;

%>>> Absorptivity glass / Total incident radiation

wl=glass(1,:);

fr_rad=interp1(fracc_rad(1,:),fracc_rad(2,:),wl(2)*Tsun/1000,'pchip');
abs_glass=glass(3,1)*fr_rad;
for i=2:(length(wl))
    u=find(glass(1,:)<=wl(i));
    if isempty(u)
        u=length(glass(1,:));
    end
end

```

```

    if i==length(wl)
        fr_rad=interp1(fracc_rad(1,:),fracc_rad(2,:),wl(i)*Tsun/1000,'pchip');
    else
        fr_rad=interp1(fracc_rad(1,:),fracc_rad(2,:),wl(i+1)*Tsun/1000,'pchip')-interp1
(fracc_rad(1,:),fracc_rad(2,:),wl(i)*Tsun/1000,'pchip');
    end
    abs_glass=abs_glass+glass(3,u(end))*fr_rad;
end
clearvars u;

%>>> Absorptivity Silicon / Total incident radiation

wl=sort([glass(1,:) EVA(1,:) Silicon(1,:)]);
wl_1(1)=wl(1); ind=2;
for i=2:length(wl)
    if ~(wl(i)==wl(i-1))
        wl_1(ind)=wl(i);
        ind=ind+1;
    end
end
clearvars wl;
wl=wl_1;
clearvars ind wl_1;

fr_rad=interp1(fracc_rad(1,:),fracc_rad(2,:),wl(2)*Tsun/1000,'pchip');
abs_Sil=glass(2,1)*EVA(2,1)*Silicon(3,1)*fr_rad;
for i=2:(length(wl))
    u=find(glass(1,:)<=wl(i));
    v=find(EVA(1,:)<=wl(i));
    w=find(Silicon(1,:)<=wl(i));
    if isempty(u)
        u=length(glass(1,:));
    end
    if isempty(v)
        v=length(EVA(1,:));
    end
    if isempty(w)
        w=length(Silicon(1,:));
    end
    if i==length(wl)
        fr_rad=interp1(fracc_rad(1,:),fracc_rad(2,:),wl(i)*Tsun/1000,'pchip');
    else
        fr_rad=interp1(fracc_rad(1,:),fracc_rad(2,:),wl(i+1)*Tsun/1000,'pchip')-interp1
(fracc_rad(1,:),fracc_rad(2,:),wl(i)*Tsun/1000,'pchip');
    end
    abs_Sil=abs_Sil+glass(2,u(end))*EVA(2,v(end))*Silicon(3,w(end))*fr_rad;
end
clearvars u v w;

%>>> Absorptivity glass from Silicon reflected radiation / Total incident radiation

wl=sort([glass(1,:) EVA(1,:) Silicon(1,:)]);
wl_1(1)=wl(1); ind=2;
for i=2:length(wl)
    if ~(wl(i)==wl(i-1))

```

```

    wl_1(ind)=wl(i);
    ind=ind+1;
end
clearvars wl;
wl=wl_1;
clearvars ind wl_1;

fr_rad=interp1(fracc_rad(1,:),fracc_rad(2,:),wl(2)*Tsun/1000,'pchip');
abs_glass_ref=glass(2,1)*EVA(2,1)*Silicon(4,1)*glass(3,1)*fr_rad;
for i=2:(length(wl))
    u=find(glass(1,:)<=wl(i));
    v=find(EVA(1,:)<=wl(i));
    w=find(Silicon(1,:)<=wl(i));
    if isempty(u)
        u=length(glass(1,:));
    end
    if isempty(v)
        v=length(EVA(1,:));
    end
    if isempty(w)
        w=length(Silicon(1,:));
    end
    if i==length(wl)
        fr_rad=1-interp1(fracc_rad(1,:),fracc_rad(2,:),wl(i)*Tsun/1000,'pchip');
    else
        fr_rad=interp1(fracc_rad(1,:),fracc_rad(2,:),wl(i+1)*Tsun/1000,'pchip')-interp1(
(fracc_rad(1,:),fracc_rad(2,:),wl(i)*Tsun/1000,'pchip');
    end
    abs_glass_ref=abs_glass_ref+glass(2,u(end))*EVA(2,v(end))*Silicon(4,w(end))*glass(
(3,u(end))*fr_rad;
end
abs_glass=abs_glass+abs_glass_ref;
clearvars u v w;

end

```

```

function [h]=inclined_plane_conv(T_w,T_amb,v_wind,l,top,back,angle,c_vis,c_k,c_pr,
c_dens,mean_ang_wind)

    angle=90-angle;
    T=(T_w+T_amb)/2-273.15;
    [vis,k,pr,dens]=dry_air(T,c_vis,c_k,c_dens,c_pr); % Air properties

    beta=1/T_amb; % coefficient
for calculations
    gr=9.81*beta*abs(T_w-T_amb)^(1/3)/(vis^2); % Grashof number
    ra=gr*pr; % Rayleigh
number
    fpr=((1+(0.492/pr)^(9/16)))^(-16/9)); % function for
prandtl number
    rac=10*(8.9-0.00178*angle*1.82); % critical
Rayleigh number
    if ra>rac
        nu_free=0.56*(rac*cos(angle*pi/180))^(1/4)+0.13*(ra^(1/3)-rac^(1/3)); %
Nusselt number for free convection
    else
        nu_free=(0.825+0.387*((ra*cos(angle*pi/180)*fpr)^(1/6)))^2; % free
convection on the back of the panel
    end
    if top==1
        re=(l/2)*1*v_wind/vis; % [-] Reynolds number
    end
    if back==1
        re=0; % [-] Reynolds number
    end
    m=(90-mean_ang_wind)/(90+mean_ang_wind); % Coefficients for caclcuations,
dependent on the angle
    Af=(1+m)^(-0.5)*(1+1.36*m^0.88)/(1+m^0.99);
    nu_forz=Af*1.2*(re*pr)^0.5; % Nusselt number for forced convection
    nu=(nu_forz^3+nu_free^3)^(1/3); % Nusselt number for superimposed
forced and free convection
    h=real(nu*k/l); % [W/m^2/K] Convection coefficient for
the front of the panel

end

```

```

function mean_ang_wind=mean_ang_horz_wind_panel(angle)

%>>> Module tilt
ang_mod=angle;

%>>> Integration step
int_step=0.01;
%>>> Horizontal wind angle interval for the integration
ang_horiz=pi/2:int_step:3*pi/2;

%>>> [Horizontal wind - Top plane of the module] angle
ang_wind_panel=zeros(1,length(ang_horiz));

%>>> Calculation of the mean [Horizontal wind - Top plane of the module] angle by
discrete integration
mean_ang_wind=0;
for i=1:length(ang_horiz)
    ang_wind_panel(i)=(180/pi)*(acos(cos(ang_horiz(i))*sin(ang_mod*pi/180))-pi/2);
    mean_ang_wind=mean_ang_wind+int_step*ang_wind_panel(i);
end
mean_ang_wind=(1/pi)*mean_ang_wind;

end

```

```

function [Wh_pcm_day_1,t_cell_pcm_mean_day_1,t_f_pcm]=pcm_panel(sim_step,time_sim_v,
T_amb,g,wind,angle,c_vis,c_k,c_pr,c_dens,t_0_pcm,mean_ang_wind)

%% Model scheme
%%
% AMB: AMBIANCE
% SG: SOLAR GLASS
% CELL: SOLAR CELLS
% BACK: BACK INSULATION
% conv: convection
% cond: conduction
% rad: radiation
%
%
% Q_rad_c=g*a_eff*trans_sg*abs_c-----|
% Q_rad_sg=g*a*(abs_sg+trans_sg*ref_cell)----|
% Qsky-----|
% [AMB]---<R_conv_sg_amb>---[SG_AMB]---<R_cond_sg/2>---[SG]---<R_cond_sg/2>---[CELL]
-----
%
% ...---<R_cond_back/2>---[BACK]---<R_cond_back/2>---<R_cond_gap>---[BACK_PCM]---
<R_conv_back_amb>---[AMB]
%
% Q_pcm-----|
%
%% Fisical parameters
%%
[a,p,l,a_cells,a_sil,th_sg,m_sg,cp_sg,k_sg,emis_sg,th_c,m_c,cp_c,k_c,...
th_back,m_back,cp_back,k_back,th_fin,l_fin,z_fin,th_fin,n_fin,m_fin,...
cp_fin,k_fin,a_cover,dens_pcm,cp_pcm,k_pcm,sigma,lg_prf,w_prf_h,...
w_prf_v,th_prf,n_prf,k_al,cp_al,dens_al,abs_glass,abs_Cells,a_abs]
=fisical_param();

%% PCM model variables
%%
n_horiz=6; n_vert=6; % Number of horizontal and vertical nodes for the PCM-profiles
Temperature calculation
[PHASE,MASS,TEMP,ENERGY,RESIST_H,RESIST_V,energy_melt,energy_solid,m_profiles]
=PCM_variables(n_vert,n_horiz,time_sim_v,T_amb,w_prf_h,w_prf_v,lg_prf,n_prf,th_prf,
k_pcm,k_al,dens_al,dens_pcm);

%% Simulation variables
%%
t_sg_amb=zeros(1,length(time_sim_v)); t_sg_amb(1)=t_0_pcm(1); % [K] Solar Glass -
Ambiance Temperature
t_sg=zeros(1,length(time_sim_v)); t_sg(1)=t_0_pcm(2); % [K] Solar Glass
Temperature
t_cell=zeros(1,length(time_sim_v)); t_cell(1)=t_0_pcm(3); % [K] Cell
Temperature
t_back=zeros(1,length(time_sim_v)); t_back(1)=t_0_pcm(4); % [K] Back
insulation Temperature
t_back_amb=zeros(1,length(time_sim_v)); t_back_amb(1)=t_0_pcm(5); % [K] Back
insulation - Ambiance Temperature
t_fins=zeros(1,length(time_sim_v)); t_fins(1)=t_0_pcm(6); % [K] Fins

```



```

Temperature
t_back_pcm=zeros(1,length(time_sim_v)); t_back_pcm(1)=t_0_pcm(7); % [K] Back PCM
Temperature

h_top=zeros(1,length(time_sim_v)); % [W/K*m^2]
Convection coefficient of the top surface
h_back=zeros(1,length(time_sim_v)); % [W/K*m^2]
Convection coefficient of the back surface

eff=zeros(1,length(time_sim_v)); % [-] Theoretic
efficiency of the cell
power=zeros(1,length(time_sim_v)); % [W] Output
power of the module
Wh=zeros(1,length(time_sim_v)); % [Wh] Total
energy generated by the module

%% Conductive thermal resistances
%%
R_cond_sg=th_sg/(k_sg*a); % [K/W] conductive thermal resistance of the
solar glass
R_cond_back=th_back/(a*k_back); % [K/W] conductive thermal resistance of the back
insulation

for i=1:(length(time_sim_v)-1)

    %% SOLAR GLASS (SG)
    %%
    >>> [W] Q_solar_rad_sg: radiation heat absorbed in the glass
    Q_solar_rad_sg=g(i)*a_abs*abs_glass;

    >>> [W] Q_rad_sg_sky: radiation heat from the sky
    t_sky=0.0552*t_amb(i)^1.5; % [K] Temperature of the sky
    Q_rad_sg_sky=sigma*emis_sg*(t_sg_amb(i)^2+t_sky^2)*(t_sg_amb(i)+t_sky)*(t_sg_amb
(i)-t_sky);

    >>> [W] Q_cond_sg: heat flux due to conduction between solar glass and solar
cells
    Q_cond_sg=(t_sg(i)-t_cell(i))/(R_cond_sg/2);

    >>> [W] Q_conv_sg: convective heat flux between solar glass and ambience
    top=1; back=0; % Convection on the top: there are forced convection due to the
wind
    % [W/K*m^2] h_top: convective coefficient on the top of the panel
    [h_top(i)]=inclined_plane_conv(t_sg_amb(i),t_amb(i),wind(i),1,top,back,angle,
c_vis,c_k,c_pr,c_dens,mean_ang_wind);
    R_conv_sg=1/(h_top(i)*a); % [K/W] convective thermal resistance between the
solar glass and the ambience
    Q_conv_sg=(t_sg(i)-t_amb(i))/(R_conv_sg+(R_cond_sg/2));

    >>> [K] t_sg(i+1): temperature of the (middle) solar glass at the 'i+1' step
    t_sg(i+1)=(Q_solar_rad_sg-Q_cond_sg-Q_conv_sg-Q_rad_sg_sky)*sim_step/(m_sg*cp_sg)
+t_sg(i); % [K] Temperature for the next step

    >>> [K] t_sg_amb(i+1): temperature of the solar glass surface at the 'i+1' step
    t_sg_amb(i+1)=t_sg(i+1)+(Q_solar_rad_sg-Q_conv_sg-Q_rad_sg_sky)*(R_cond_sg/2);

```

```

%% CELLS (C)
%%
>>> [W] Q_solar_rad_c: radiation heat absorbed in the CELLS
Q_solar_rad_c=g(i)*a_abs*a_cells*abs_cells;

>>> [W] power(i+1): fraction of the solar radiation that turns into electrical
power
eff(i+1)=0.165*(1-0.0041*(t_cell(i)-25-273.15)); % [-] Theoretic efficiency of the
cell
power(i+1)=g(i)*eff(i)*a_sil*a_cells;

>>> [W] Q_cond_back: heat flux due to conduction between cells and back
insulation
Q_cond_back=(t_cell(i)-t_back(i))/R_cond_back;

>>> [K] t_c(i+1): temperature of the cells at the 'i+1' step
t_cell(i+1)=(Q_solar_rad_c+Q_cond_sg-Q_cond_back-power(i))*sim_step/(m_c*cp_c)
+t_cell(i);

%% BACK INSULATION
%%
fins=0; pcm=1;
if (fins==0) && (pcm==0) % Standard panel
    >>> [W] Q_conv_back: heat flux due to convection with the ambience
    top=0; back=1; % Convection on the back: only free convection (no
wind)
    [h_back(i)]=inclined_plane_conv(t_back_amb(i),t_amb(i),wind(i),1,top,back,
angle,c_vis,c_k,c_pr,c_dens,mean_ang_wind);
    R_conv_back=1/(h*a); % [K/W] convective thermal resistance between the back
insulation and the ambience
    Q_conv_back=(t_back(i)-t_amb(i))/(R_conv_back+(R_cond_back/2));

    >>> [K] t_back(i+1): temperature of the (middle) back insulation at the 'i+1'
step
    t_back(i+1)=(Q_cond_back-Q_conv_back)*sim_step/(m_back*cp_back)+t_back(i);

    >>> [K] t_back_amb(i+1): temperature of the back surface at the 'i+1' step
    t_back_amb(i+1)=t_back(i+1)-Q_conv_back*(R_cond_back/2);
else
    if pcm==1 % PCM panel
        % [K/W] R_cond_gap: conductive thermal resistance due to the air gap
between the back insulation and the PCM profiles
        k_air=24.12+0.07225*(t_back(i)-273.15); % [W/m*K] thermal conductivity of
the air at the back insulation Temperature
        R_cond_gap=0.002/(k_air*(10^-3)*a);

        % [W] Q_cond_profiles: heat flux due to conduction between the back
insulation and the PCM profiles
        Q_cond_profiles=(t_back(i)-t_back_pcm(i))/(R_cond_back/2+R_cond_gap);

        >>> [K] t_back(i+1): temperature of the (middle) back insulation at the
'i+1' step
        t_back(i+1)=(Q_cond_back-Q_cond_profiles)*sim_step/(m_back*cp_back)+t_back
(i);

```

```

end
if fins==1 % Fins panel
    % [K/W] R_cond_gap: conductive thermal resistance due to the air gap
between the back insulation and the 'L' fins
    k_air=24.12+0.07225*(t_back(i)-273.15); % [W/m*K] thermal conductivity of
the air at the back insulation Temperature
    R_cond_gap=0.002/(k_air*(10^-3)*a);

    >>> [W] Q_cond_fins: heat flux due to conduction between the back
insulation and the fins
    Q_cond_fins=(t_back(i)-t_fins(i))/(R_cond_back/2+R_cond_gap);

    >>> [K] t_back(i+1): temperature of the (middle) back insulation at the
'i+1' step
    t_back(i+1)=(Q_cond_back-Q_cond_fins)*sim_step/(m_back*cp_back)+t_back(i);
% [K] Temperature for the next step
end
end

%% PCM
%%
% ENERGY: matrix for the stored energy of each PCM mass element in the full
melting
% interval (35 - 50 °C): 35.0°C-->energy=0 // 50.99°C-->256(KJ/Kg)*mass
ENERGY(:,i+1)=ENERGY(:,i); % Initial value for 'i+1' step

% PHASE: phase of each PCM mass element
% 0: fluid, 1: phase change, 2: solid, 3: aluminum
PHASE(i+1)=PHASE(i); % Initial value for 'i+1' step

>>> [W] Q_H: horizontal heat flow in the PCM profile matrix
Q_H=zeros(n_vert-2,n_horiz-1);
for y=1:n_vert-2
    for x=1:n_horiz-1
        Q_H(y,x)=(TEMP(y+1,x,1)-TEMP(y+1,x+1,1))/RESIST_H(y,x);
    end
end

>>> [W] Q_V: vertical heat flow in the PCM profile matrix
Q_V=zeros(n_vert-1,n_horiz);
for y=1:n_vert-1
    for x=1:n_horiz
        Q_V(y,x)=(TEMP(y,x,1)-TEMP(y+1,x,1))/RESIST_V(y,x);
    end
end

>>> [W] Q_pcm: total heat exchange between the aluminum profiles and the PCM
(Heat entering the aluminum profiles)
Q_pcm=sum(Q_V(n_vert-1,2:n_horiz-1))-sum(Q_V(1,2:n_horiz-1))+sum(Q_H(1:n_vert-2,
n_horiz-1))-sum(Q_H(1:n_vert-2,1));

% [K/W] R_conv_back_pcm: convective thermal resistance between the back and the
ambience
top=0; back=1; % Convection on the back: only free convection (no wind)
[h_back(i)]=inclined_plane_conv(t_back_pcm(i),t_amb(i),wind(i),1,top,back,angle,

```

```

c_vis,c_k,c_pr,c_dens,mean_ang_wind);
R_conv_back_pcm=1/(h_back(i)*a);

>>> [W] Q_conv_back_pcm: convective heat at the back of the panel
Q_conv_back_pcm=(t_back_pcm(i)-t_amb(i))/R_conv_back_pcm;

>>> [K] t_back_pcm(i+1): temperature of the PCM-aluminum profiles at the 'i+1'
step
% (it is considered the same Temperature in all the volume of the aluminum
profiles)
t_back_pcm(i+1)=(Q_cond_profiles+Q_cond_pcm-Q_conv_back_pcm)*sim_step/
(m_profiles*cp_al)+t_back_pcm(i);

TEMP(1,:,i+1)=t_back_pcm(i+1); % First row of the Temperature matrix: aluminum
top cover
TEMP(n_vert,:,i+1)=t_back_pcm(i+1); % Last row of the Temperature matrix: aluminum
back cover

>>> Temperature calculation of all the differential mass elements of the PCM
for y=2:n_vert-1 % y: vertical nodes (rows of the matrix)
    TEMP(y,1,i+1)=t_back_pcm(i+1); % Left side of the aluminum
profile
    TEMP(y,n_horiz,i+1)=t_back_pcm(i+1); % Right side of the aluminum
profile
    for x=2:(n_horiz-1) % x: horizontal nodes (columns of the matrix)
        if (TEMP(y,x,i)>(273.15+40)) && (TEMP(y,x,i)<(273.15+45)) % 40-45 °C: PCM
phase change interval (1)
            PHASE(y,x,i+1)=1;
        else if (TEMP(y,x,i)<(273.15+40)) % <40 °C: PCM
solid (0)
            PHASE(y,x,i+1)=0;
        else
            PHASE(y,x,i+1)=2; % >45 °C: PCM
liquid (2)
        end
    end

    Q_net=Q_V(y-1,x)-Q_V(y,x)+Q_H(y-1,x-1)-Q_H(y-1,x); % [W] Q_net: net
heat in the (x-1,y) mass element

    if (TEMP(y,x,i)>(273.15+35)) && (TEMP(y,x,i)<(273.15+51)) % 35-51 °C:
interval where the PCM heat capacity is not constant (melting-solidification)
        ENERGY(y,x,i+1)=Q_net*sim_step+ENERGY(y,x,i); % [J=W*s] Net
energy in mass element for the 35-51°C interval
        if ENERGY(y,x,i+1)>(sum(energy_melt(2,:))*MASS(y-1,x)) % If the net
energy exceed the upper limit of the 35-51°C interval
            ENERGY(y,x,i+1)=sum(energy_melt(2,:))*MASS(y-1,x);
        else
            TEMP(y,x,i+1)=Q_net*sim_step/(MASS(y-1,x)*cp_pcm)+TEMP(y,x,i); %
[K] Temperature in the mass element (>51°C)
        else if ENERGY(y,x,i+1)<0 % If the net energy is below the lower
limit of the 35-51°C interval
            ENERGY(y,x,i+1)=0;
            TEMP(y,x,i+1)=Q_net*sim_step/(MASS(y-1,x)*cp_pcm)+TEMP(y,x,
i);

```

```

else % The net energy is in the 35-51°C interval
% Energy interpolation in the 35-51°C
if Q_net>0 % Heat flow entering the PCM: melting process
ind=find((energy_melt(3,:)*MASS(y-1,x))>ENERGY(y,x,i+1),
);
else % Heat flow out the PCM: solidification
ind=find((energy_solid(3,:)*MASS(y-1,x))>ENERGY(y,x,i+1),
);
end
if ENERGY(y,x,i+1)>(energy_melt(3,length(energy_melt))*MASS(y-
1,x))
ind=length(energy_melt)+1;
end
if Q_net>0 % Melting process
% Temperature of the (x,y) mass element
TEMP(y,x,i+1)=273.15+energy_melt(1,ind-1)+((ENERGY(y,x,
i+1)-energy_melt(3,ind-1)*MASS(y-1,x))/(energy_melt(2,ind-1)*MASS(y-1,x));
end
if Q_net<0 % Solidification process
% Temperature of the (x,y) mass element
TEMP(y,x,i+1)=273.15+energy_solid(1,ind-1)+((ENERGY(y,x,
i+1)-energy_solid(3,ind-1)*MASS(y-1,x))/(energy_solid(2,ind-1)*MASS(y-1,x));
end
end
else % Temperature out of the 35-51°C interval
TEMP(y,x,i+1)=Q_net*sim_step/(MASS(y-1,x)*cp_pcm)+TEMP(y,x,i);
if (TEMP(y,x,i+1)>(273.15+35))&&(TEMP(y,x,i+1)<(273.15+51)) % If
the temperature at the 'i+1' step is in the 35-51°C interval
if Q_net>0
ENERGY(y,x,i+1)=MASS(y-1,x)*cp_pcm*(TEMP(y,x,i+1)-(273.15
+35));
end
if Q_net<0
ENERGY(y,x,i+1)=energy_solid(3,length(energy_solid))+MASS(y-1,
x)*cp_pcm*(TEMP(y,x,i+1)-(273.15+51));
end
end
end
end
% Generation of Energy (Wh) according to the simulation
%
Wh(i+1)=power(i)*(sim_step/3600)+Wh(i);
end
t_f_pcm=[t_sg_amb(i+1) t_sg(i+1) t_cell(i+1) t_back(i+1) t_back_amb(i+1) t_fins(i+1)
t_back_pcm(i+1)];
Wh_pcm_day_1=Wh(length(Wh));
t_cell_pcm_mean_day_1=mean(t_cell);

```

end

```

function [Wh_pcm_day_1,t_cell_pcm_mean_day_1,t_f_pcm]=pcm_panel(sim_step,time_sim_v,
t_amb,g,wind,angle,c_vis,c_k,c_pr,c_dens,t_0_pcm,mean_ang_wind)
% Model scheme
%
% AMB: AMBIANCE
% SG: SOLAR GLASS
% CELL: SOLAR CELLS
% BACK: BACK INSULATION
% conv: convection
% cond: conduction
% rad: radiation
%
% Q_rad_c=g*a_eff*trans_sg*abs_c----|
% Q_rad_sg=g*a*(abs_sg+trans_sg*ref_cell)----|
% Qsky----|
% [AMB]---<R_conv_sg_amb---[SG_AMB]---<R_cond_sg/2---[SG]---<R_cond_sg/2---[CELL]
%
% ---<R_cond_back/2---[BACK]---<R_cond_back/2---<R_cond_gap---[BACK_PCM]---
<R_conv_back_amb---[AMB]
%
% Q_pcm-----|
%
% Fisical parameters
%
[a,p,l,a_cells,a_sil,th_sg,m_sg,cp_sg,k_sg,emis_sg,th_c,m_c,cp_c,k_c,...
th_back,m_back,cp_back,k_back,th_fin,l_fin,z_fin,th_fin,n_fin,m_fin,...
cp_fin,k_fin,a_cover,dens_pcm,cp_pcm,k_pcm,sigma,lg_prf,w_prf_h,...
w_prf_v,th_prf,n_prf,k_al,cp_al,dens_al,abs_glass,abs_Cells,a_abs]
=fisical_param();
% PCM model variables
%
n_horiz=6; n_vert=6; % Number of horizontal and vertical nodes for the PCM-profiles
Temperature calculation
[PHASE,MASS,TEMP,ENERGY,RESIST_H,RESIST_V,energy_melt,energy_solid,m_profiles]
=PCM_variables(n_vert,n_horiz,time_sim_v,t_amb,w_prf_h,w_prf_v,lg_prf,n_prf,th_prf,
k_pcm,k_al,dens_al,dens_pcm);
% Simulation variables
%
t_sg_amb=zeros(1,length(time_sim_v)); t_sg_amb(1)=t_0_pcm(1); % [K] Solar Glass
Ambiance Temperature
t_sg=zeros(1,length(time_sim_v)); t_sg(1)=t_0_pcm(2); % [K] Solar Glass
Temperature
t_cell=zeros(1,length(time_sim_v)); t_cell(1)=t_0_pcm(3); % [K] Cell
Temperature
t_back=zeros(1,length(time_sim_v)); t_back(1)=t_0_pcm(4); % [K] Back
insulation Temperature
t_back_amb=zeros(1,length(time_sim_v)); t_back_amb(1)=t_0_pcm(5); % [K] Back
insulation - Ambiance Temperature
t_fins=zeros(1,length(time_sim_v)); t_fins(1)=t_0_pcm(6); % [K] Fins

```

```

Temperature
t_back_pcm=zeros(1,length(time_sim_v)); t_back_pcm(1)=t_0_pcm(7); % [K] Back PCM
Temperature
h_top=zeros(1,length(time_sim_v)); % [W/K·m²]
Convection coefficient of the top surface
h_back=zeros(1,length(time_sim_v)); % [W/K·m²]
Convection coefficient of the back surface
eff=zeros(1,length(time_sim_v)); % [-] Theoretic
efficiency of the cell
power=zeros(1,length(time_sim_v)); % [W] Output
power of the module
Wh=zeros(1,length(time_sim_v)); % [Wh] Total
energy generated by the module
% Conductive thermal resistances
%
R_cond_sg=th_sg/(k_sg*a); % [K/W] conductive thermal resistance of the
solar glass
R_cond_back=th_back/(a*k_back); % [K/W] conductive thermal resistance of the back
insulation
for i=1:(length(time_sim_v)-1)
% SOLAR GLASS (SG)
%
%>>> [W] Q_solar_rad_sg: radiation heat absorbed in the glass
Q_solar_rad_sg=g(i)*a_abs*abs_glass;
%>>> [W] Q_rad_sg_sky: radiation heat from the sky
t_sky=0.0552*t_amb(i)^1.5; % [K] Temperature of the sky
Q_rad_sg_sky=sigma*emis_sg*(t_sg_amb(i)^2+t_sky^2)*(t_sg_amb(i)+t_sky)*(t_sg_amb
(i)-t_sky);
%>>> [W] Q_cond_sg: heat flux due to conduction between solar glass and solar
cells
Q_cond_sg=(t_sg(i)-t_cell(i))/(R_cond_sg/2);
%>>> [W] Q_conv_sg: convective heat flux between solar glass and ambiance
top=1; back=0; % Convection on the top: there are forced convection due to the
wind
% [W/K·m²] h_top: convective coefficient on the top of the panel
[h_top(i)]=inclined_plane_conv(t_sg_amb(i),t_amb(i),wind(i),1,top,back,angle,
c_vis,c_k,c_pr,c_dens,mean_ang_wind);
R_conv_sg=1/(h_top(i)*a); % [K/W] convective thermal resistance between the
solar glass and the ambiance
Q_conv_sg=(t_sg(i)-t_amb(i))/(R_conv_sg+(R_cond_sg/2));
%>>> [K] t_sg(i+1): temperature of the (middle) solar glass at the 'i+1' step
t_sg(i+1)=(Q_solar_rad_sg-Q_cond_sg-Q_conv_sg-Q_rad_sg_sky)*sim_step/(m_sg*cp_sg)
+t_sg(i); % [K] Temperature for the next step
%>>> [K] t_sg_amb(i+1): temperature of the solar glass surface at the 'i+1' step
t_sg_amb(i+1)=t_sg(i+1)+(Q_solar_rad_sg-Q_conv_sg-Q_rad_sg_sky)*(R_cond_sg/2);

```



```

%% CELLS (C)
%%
%>>> [W] Q_solar_rad_c: radiation heat absorbed in the CELLS
Q_solar_rad_c=g(i)*a_amb*a_cells*abs_Cells;

%>>> [W] power(i+1): fraction of the solar radiation that turns into electrical
power
eff(i+1)=0.165*(1-0.0041*(t_cell(i)-25-273.15)); % [-] Teoretic efficiency of the
cell
power(i+1)=g(i)*eff(i)*a_sil*a_cells;

%>>> [W] Q_cond_back: heat flux due to conduction between cells and back
insulation
Q_cond_back=(t_cell(i)-t_back(i))/R_cond_back;

%>>> [K] t_c(i+1): temperature of the cells at the 'i+1' step
t_cell(i+1)=(Q_solar_rad_c+Q_cond_sg-Q_cond_back-power(i))*sim_step/(m_c*cp_c)
+t_cell(i);

%% BACK INSULATION
%%
fins=0; pcm=1;
if (fins==0)&&(pcm==0) % Standard panel
%>>> [W] Q_conv_back: heat flux due to convection with the ambiance
top=0; back=1; % Convection on the back: only free convection (no
wind)
[h_back(i)]=inclined_plane_conv(t_back_amb(i),t_amb(i),wind(i),l,top,back,
angle,c_vis,c_k,c_pr,c_dens,mean_ang_wind);
R_conv_back=1/(h*a); % [K/W] convective thermal resistance between the back
insulation and the ambiance
Q_conv_back=(t_back(i)-t_amb(i))/(R_conv_back+(R_cond_back/2));

%>>> [K] t_back(i+1): temperature of the (middle) back insulation at the 'i+1'
step
t_back(i+1)=(Q_cond_back-Q_conv_back)*sim_step/(m_back*cp_back)+t_back(i);

%>>> [K] t_back_amb(i+1): temperature of the back surface at the 'i+1' step
t_back_amb(i+1)=t_back(i+1)-Q_conv_back*(R_cond_back/2);
else
if pcm==1 % PCM panel
% [K/W] R_cond_gap: conductive thermal resistance due to the air gap
between the back insulation and the PCM profiles
k_air=24.12+0.07225*(t_back(i)-273.15); % [W/m·K] thermal conductivity of
the air at the back insulation Temperature
R_cond_gap=0.002/(k_air*(10^-3)*a);

% [W] Q_cond_profiles: heat flux due to conduction between the back
insulation and the PCM profiles
Q_cond_profiles=(t_back(i)-t_back_pcm(i))/(R_cond_back/2+R_cond_gap);

%>>> [K] t_back(i+1): temperature of the (middle) back insulation at the
'i+1' step
t_back(i+1)=(Q_cond_back-Q_cond_profiles)*sim_step/(m_back*cp_back)+t_back
(i);

```

```

end
if fins==1 % Fins panel
% [K/W] R_cond_gap: conductive thermal resistance due to the air gap
between the back insulation and the 'L' fins
k_air=24.12+0.07225*(t_back(i)-273.15); % [W/m·K] thermal conductivity of
the air at the back insulation Temperature
R_cond_gap=0.000/(k_air*(10^-3)*a);

%>>> [W] Q_cond_fins: heat flux due to conduction between the back
insulation and the fins
Q_cond_fins=(t_back(i)-t_fins(i))/(R_cond_back/2+R_cond_gap);

%>>> [K] t_back(i+1): temperature of the (middle) back insulation at the
'i+1' step
t_back(i+1)=(Q_cond_back-Q_cond_fins)*sim_step/(m_back*cp_back)+t_back(i);
% [K] Temperature for the next step
end

%% PCM
%%
% ENERGY: matrix for the stored energy of each PCM mass element in the full
melting
% interval (35 - 50 °C): 35.0°C-->energy=0 // 50.99°C-->256(KJ/Kg)*mass
ENERGY(:,i+1)=ENERGY(:,i); % Initial value for 'i+1' step

% PHASE: phase of each PCM mass element
% 0: fluid, 1: phase change, 2: solid, 3: aluminum
PHASE(i+1)=PHASE(i); % Initial value for 'i+1' step

%>>> [W] Q_H: horizontal heat flow in the PCM profile matrix
Q_H=zeros(n_vert-2,n_horiz-1);
for y=1:n_vert-2
for x=1:n_horiz-1
Q_H(y,x)=(TEMP(y+1,x,i)-TEMP(y+1,x+1,i))/RESIST_H(y,x);
end
end

%>>> [W] Q_V: vertical heat flow in the PCM profile matrix
Q_V=zeros(n_vert-1,n_horiz);
for y=1:n_vert-1
for x=1:n_horiz
Q_V(y,x)=(TEMP(y,x,i)-TEMP(y+1,x,i))/RESIST_V(y,x);
end
end

%>>> [W] Q_pcm: total heat exchange between the aluminum profiles and the PCM
(Heat entering the aluminum profiles)
Q_pcm=sum(Q_V(n_vert-1,2:n_horiz-1))+sum(Q_H(1:n_vert-2,
n_horiz-1))-sum(Q_H(1:n_vert-2,1));

% [K/W] R_conv_back_pcm: convective thermal resistance between the back and the
ambiance
top=0; back=1; % Convection on the back: only free convection (no wind)
[h_back(i)]=inclined_plane_conv(t_back_pcm(i),t_amb(i),wind(i),l,top,back,angle,

```

```

c_vis,c_k,c_pr,c_dens,mean_ang_wind);
R_conv_back_pcm=1/(h_back(i)*a);

%>>> [W] Q_conv_back_pcm: convective heat at the back of the panel
Q_conv_back_pcm=(t_back_pcm(i)-t_amb(i))/R_conv_back_pcm;

%>>> [K] t_back_pcm(i+1): temperature of the PCM-aluminum profiles at the 'i+1'
step
% (it is considered the same Temperature in all the volume of the aluminum
profiles)
t_back_pcm(i+1)=(Q_cond_profiles+Q_pcm-Q_conv_back_pcm)*sim_step/
(m_profiles*cp_al)+t_back_pcm(i);

TEMP(1,:i+1)=t_back_pcm(i+1); % First row of the Temperature matrix: aluminum
back cover
TEMP(n_vert,:i+1)=t_back_pcm(i+1); % Last row of the Temperature matrix: aluminum
back cover

%>>> Temperature calculation of all the differential mass elements of the PCM
for y=2:n_vert-1 % y: vertical nodes (rows of the matrix)
TEMP(y,1,i+1)=t_back_pcm(i+1); % Left side of the aluminum
profile
TEMP(y,n_horiz,i+1)=t_back_pcm(i+1); % Right side of the aluminum
profile
for x=2:(n_horiz-1) % x: horizontal nodes (columns of the matrix)
if (TEMP(y,x,i)>(273.15+40))&&(TEMP(y,x,i)<(273.15+45)) % 40-45 °C: PCM
phase change interval (1)
PHASE(y,x,i+1)=1;
else if (TEMP(y,x,i)<(273.15+40)) % <40 °C: PCM
solid (0)
PHASE(y,x,i+1)=0;
else
PHASE(y,x,i+1)=2; % >45 °C: PCM
liquid (2)
end
end

Q_net=Q_V(y-1,x)-Q_V(y,x)+Q_H(y-1,x)-Q_H(y,x); % [W] Q_net: net
heat in the (x-1,y) mass element

if (TEMP(y,x,i)>(273.15+35))&&(TEMP(y,x,i)<(273.15+51)) % 35-51 °C:
interval where the PCM heat capacity is not constant (melting-solidification)
ENERGY(y,x,i+1)=Q_net*sim_step+ENERGY(y,x,i); % [J=W*s] Net
energy in mass element for the 35-51°C interval
if ENERGY(y,x,i+1)>(sum(energy_melt(2,:))*MASS(y-1,x)) % If the net
energy exceed the upper limit of the 35-51°C interval
ENERGY(y,x,i+1)=sum(energy_melt(2,:))*MASS(y-1,x);
TEMP(y,x,i+1)=Q_net*sim_step/(MASS(y-1,x)*cp_pcm)+TEMP(y,x,i); %
[K] Temperature in the mass element (>51°C)
else if ENERGY(y,x,i+1)<0 % If the net energy is below the lower
limit of the 35-51°C interval
ENERGY(y,x,i+1)=0;
TEMP(y,x,i+1)=Q_net*sim_step/(MASS(y-1,x)*cp_pcm)+TEMP(y,x,
i);

```

```

else % The net energy is in the 35-51°C interval
% Energy interpolation in the 35-51°C
if Q_net>0 % Heat flow entering the PCM: melting process
ind=find((energy_melt(3,:)*MASS(y-1,x))>ENERGY(y,x,i+1),
1);
process
else % Heat flow out the PCM: solidification
ind=find((energy_solid(3,:)*MASS(y-1,x))>ENERGY(y,x,i+1),
1);
end
if ENERGY(y,x,i+1)>(energy_melt(3,length(energy_melt))*MASS(y-
1,x))
ind=length(energy_melt)+1;
end
if Q_net>0 % Melting process
% Temperature of the (x,y) mass element
TEMP(y,x,i+1)=273.15+energy_melt(1,ind-1)+((ENERGY(y,x,
i+1)-energy_melt(3,ind-1)*MASS(y-1,x))/(energy_melt(2,ind-1)*MASS(y-1,x));
end
if Q_net<0 % Solidification process
% Temperature of the (x,y) mass element
TEMP(y,x,i+1)=273.15+energy_solid(1,ind-1)+((ENERGY(y,x,
i+1)-energy_solid(3,ind-1)*MASS(y-1,x))/(energy_solid(2,ind-1)*MASS(y-1,x));
end
end
else % Temperature out of the 35-51°C interval
TEMP(y,x,i+1)=Q_net*sim_step/(MASS(y-1,x)*cp_pcm)+TEMP(y,x,i);
if (TEMP(y,x,i+1)>(273.15+35))&&(TEMP(y,x,i+1)<(273.15+51)) % If
the temperature at the 'i+1' step is in the 35-51°C interval
if Q_net>0
ENERGY(y,x,i+1)=MASS(y-1,x)*cp_pcm*(TEMP(y,x,i+1)-(273.15
+35));
end
if Q_net<0
ENERGY(y,x,i+1)=energy_solid(3,length(energy_solid))*MASS(y-1,
x)*cp_pcm*(TEMP(y,x,i+1)-(273.15+51));
end
end
end

%>>> Generation of Energy (Wh) according to the simulation
%>>>
Wh(i+1)=power(i)*(sim_step/3600)+Wh(i);

end

t_f_pcm=[t_sg_amb(i+1) t_sg(i+1) t_cell(i+1) t_back(i+1) t_back_amb(i+1) t_fins(i+1)
t_back_pcm(i+1)];

Wh_pcm_day_1=Wh(length(Wh));
t_cell_pcm_mean_day_1=mean(t_cell);

```

end